LEABHARLANN CHOLÁISTE NA TRÍONÓIDE, BAILE ÁTHA CLIATH | TRINITY COLLEGE LIBRARY DUBLIN
Ollscoil Átha Cliath | The University of Dublin

Terms and Conditions of Use of Digitised Theses from Trinity College Library Dublin

Copyright statement

All material supplied by Trinity College Library is protected by copyright (under the Copyright and Related Rights Act, 2000 as amended) and other relevant Intellectual Property Rights. By accessing and using a Digitised Thesis from Trinity College Library you acknowledge that all Intellectual Property Rights in any Works supplied are the sole and exclusive property of the copyright and/or other IPR holder. Specific copyright holders may not be explicitly identified. Use of materials from other sources within a thesis should not be construed as a claim over them.

A non-exclusive, non-transferable licence is hereby granted to those using or reproducing, in whole or in part, the material for valid purposes, providing the copyright owners are acknowledged using the normal conventions. Where specific permission to use material is required, this is identified and such permission must be sought from the copyright holder or agency cited.

Liability statement

By using a Digitised Thesis, I accept that Trinity College Dublin bears no legal responsibility for the accuracy, legality or comprehensiveness of materials contained within the thesis, and that Trinity College Dublin accepts no liability for indirect, consequential, or incidental, damages or losses arising from use of the thesis for whatever reason. Information located in a thesis may be subject to specific use constraints, details of which may not be explicitly described. It is the responsibility of potential and actual users to be aware of such constraints and to abide by them. By making use of material from a digitised thesis, you accept these copyright and disclaimer provisions. Where it is brought to the attention of Trinity College Library that there may be a breach of copyright or other restraint, it is the policy to withdraw or take down access to a thesis while the issue is being resolved.

Access Agreement

By using a Digitised Thesis from Trinity College Library you are bound by the following Terms & Conditions. Please read them carefully.

I have read and I understand the following statement: All material supplied via a Digitised Thesis from Trinity College Library is protected by copyright and other intellectual property rights, and duplication or sale of all or part of any of a thesis is not permitted, except that material may be duplicated by you for your research use or for educational purposes in electronic or print form providing the copyright owners are acknowledged using the normal conventions. You must obtain permission for any other use. Electronic or print copies may not be offered, whether for sale or otherwise to anyone. This copy has been supplied on the understanding that it is copyright material and that no quotation from the thesis may be published without proper acknowledgement.

The Mechanistic Characterisation of Misfolding Proteins in Disease and Cancer Therapy

A dissertation submitted to the University of Dublin

for the degree of Doctor of Philosophy

by

Níal Harte

Under the supervision of:

Dr. Kenneth Hun Mok

2015

Department of Biochemistry and Immunology,

Trinity Biomedical Sciences Institute

TRINITY COLLEGE
2 9 JUL 2015
LIBRARY DUBLIN

Thesis 10616

DECLARATION

I hereby certify that this report represents the sole work of the author except where stated and has not been submitted in whole or in part to any other university or institution as part of a degree or other qualification.

I agree to deposit this thesis in the University's open access institutional repository or allow the library to do so on my behalf, subject to Irish Copyright Legislation and Trinity College Library conditions of use and acknowledgement

Níal Harte

School of Biochemistry and Immunology
University of Dublin, Trinity College
October 2014

ABSTRACT

Protein folding is a highly ordered and governed event which results in the production of native peptide structures capable of carrying out a myriad of functions and processes within the cell. Failure to produce fully folded proteins was thought to result in toxic entities which have been associated with numerous degenerative disorders such as Alzheimer's disease. Despite significant advances, the molecular identity of the cytotoxic species populated during *in vivo* amyloid formation crucial for the understanding of neurodegenerative and other systemic amyloidosis is yet to be revealed. Importantly not all protein misfolding has a negative outcome. Recently it has been shown that a number of specific proteins maintain the ability to bind oleic acid while in a partially unfolded state and in this conformation, these complexes have shown remarkable selectivity towards tumour cells in both *in vitro* and *in vivo* experiments. Here we investigate the negative and positive consequences of protein folding. We have generated several protein-fatty acid complexes which selectively target tumour cells for destruction. These complexes are taken up in larger quantities into tumour cells when compared to healthy cells and also elicit an apoptotic cell death pathway. We demonstrated that BAMLET reduces tumour volume and prolongs survival in a murine melanoma model and is effective through both subcutaneous and intraperitoneal injection routes. Interestingly BAMLET in combination with the TLR agonist R848 resulted in improved survival and tumour regression when compared to single treatments and displayed prolonged protection even after a tumour re-challenge which may be due to its ability to activate a Th2 cell mediated immune response. As a negative consequence of protein folding we engineered oligomers and amyloid fibrils from innocuous hen lysozyme through a combined and optimized ultrafiltration/ultracentrifugation method and have characterized the assemblies with various optical spectroscopic techniques and atomic force microscopy. We find that both oligomers and fibrils display cytotoxic capabilities towards cultured cells *in vitro*, with oligomers producing elevated levels of cellular injury towards undifferentiated PC12 cells. Furthermore, dual flow cytometry staining experiments demonstrate that the oligomers and mature fibrils induce divergent cellular death pathways. Also, we find that oligomers but not sonicated mature fibrils inhibit hippocampal long-term potentiation (a form of synaptic plasticity implicated in learning and memory) *in vivo*.

In conclusion we show that proteins which are not in fully native folds can have negative and positive consequences in relation to certain diseases. When combined with oleic acid some proteins can selectively destroy tumour cells both *in vitro* and *in vivo*. Conversely, proteins in aggregated states can induce neuronal cell death *in vitro* and inhibit LTP *in vivo*. This work highlights the diverse nature of proteins and demonstrates how simple changes in the overall structure can have detrimental or positive effects on cells.

This thesis is dedicated to my mother and father, Patricia and Patrick Harte,

Without whose support, encouragement, and continued patience this work would not have been possible.

ACKNOWLEDGEMENTS

First and foremost I would like to thank Dr. Ken Mok for all his support throughout this PhD. I can still remember reading your gracious and thoughtful reply to my first letter to you and thinking that I would like to work in your lab. Four years later it has been a privilege to work under your guidance and mentorship. You have always supported any experimental ideas which I may have suggested and have always offered me advice on what I could do to improve my work. I feel that I have grown as a scientist and a person under your watch and for that I am extremely grateful.

I would also like to thank Dr. Derek Nolan for all his support and guidance throughout my PhD. Not only have you helped me with work related issues but you have always been a source of sage wisdom and advice and for that I am truly grateful. Your genuine interest in students' wellbeing and your open door policy sets you apart as an exceptional mentor.

I would like to thank everyone past and present from the Mok lab; Soyoung (my cell culture mentor), Louise (see you in a few days), Yeon, and of course Yongjing, my science sister, thank you for all the help throughout.

Of course I will have to give an extra special thanks to Kate, Kim, and Sandra. Kate, my work wife, so much banter and laughs had, what can I say. You were ever present in my working day (mainly because you sit behind me) and were always there for a chat. You are truly one of a kind. Kimbo Slice, the girliest girl I know, you opened up my eyes to a world of many things that men should know about like shellacs and weddings (you're the one my mates blame). Last but not least, Sandra thank you for all the laughs shared over beers and lunches (long may it continue) and your general help in the whole science area was a big help, more than you know.

Big thank you to all the other mates and acquaintances I have made along my scientific travels. Trev (the only man or woman to ever make Sue jealous), Conor McGregor, sorry I mean Chris, Dan, Nick, Rob, Laura B, Stephen Q, Fernando, Ronan, Alan (all the footy lads really). Conor Finley, you legend, thanks for all the help. Big BIGGG thank you to all my reading room and 5th floor chums; Jenni (ah so many good stories), Andy, Darren (remember all I've taught you protégé), Laura, Niki, Úna, Ray, Rosy, Simon, Natalie, Paul, Ryan,

Nicoleta, Lois, Emily, Matteo. You guys have been brilliant to get to know and I have never hated coming into work because there was always good fun to be had. One of the great things I have gotten from this PhD is the chance to meet and make so many good friends and it is something that I am very grateful for (there I said it now, that's the only time you guys are getting this level of emotion).

Special thanks to Lydia, Neil Marshall, and Igor for the collaborations we had together and all the hard work you did.

The people behind the scenes, FACS Barry, Gavin, Liam, Noel, Mary-Pat of course, thank you.

Big thanks to all my non-work related mates, not that they even know what I do. All the lads from Lucan (not going to name everyone to save space), and the lads from Maynooth, especially my country brother Shane.

It's not science related but I guess I should thank the Big Man himself…Arsene Wenger. Thank you for allowing me know what it feels like to get so close to glory and happiness only to have it ripped out of my grasp. But I hold the faith. Maybe next year.

Huge thanks to my family for all their support. My brothers Ciaran (my science shadow) and Darragh and my Dad. And of course my mother who has been a constant source of encouragement, guidance, love, and fun throughout my life. I owe everything I have to you guys (which isn't much…yet). Special thank you to my 2nd family the Boylans and to my two very special Nans (and granddad as well), love you all.

Finally to Sue who has been my rock for the last the last 4 years and more. I'm going to keep this relatively non-sappy as I have a rep in work but I don't know where or in what general physical state I would be in without your support and love. You have been there for me when I have needed to vent, needed help with work and life, and you have always guided and encouraged me in the right direction. More than anyone I would not have got here without you.

Ohhh, and Moe. Nearly forgot. My furry compadre gets me through the day.

PUBLICATIONS

•**Harte NP**, Klyubin I, McCarthy et al. Amyloid Oligomers and Mature Fibrils Prepared from an Innocuous Protein Cause Diverging Cellular Death Mechanisms: A PC12 Comparative Cytotoxicity Assay. Under review JBC

•Xie Y, Min S, **Harte NP**, Kirk H et al. Electrostatic interactions play an essential role in the binding of oleic acid with α-lactalbumin in the HAMLET-like complex: a study using charge-specific chemical modifications. Proteins. 2013 81(1):1-17.

•Min S, Meehan J, Sullivan LM, **Harte NP** et al. Alternatively folded proteins with unexpected beneficial functions. Biochemical Society Transactions. 2012 40(4):746-51.

PRESENTATIONS AT CONFERENCES

- "A Mechanistic Characterisation of Misfolded/Alternatively-Folded Proteins in Disease and Cancer Therapy".

  - December 2012, 3rd Annual HAMLET Conference, Lund University, Sweden.

  - October 2012, Scientists, Technologists and Artists Generating Exploration Symposium, CRANN, Trinity College, Dublin.

- "Neurotoxic Amyloid Oligomers and Fibrils Generated from Non-Disease-Related Proteins: Apoptosis and Necrosis in PC12 Cells from Hen Egg White Lysozyme"
  - July 2012, EUROMAR 2012 conference, University College Dublin, Dublin.

  - December 2011, IASBS Annual Meeting 2011, National University of Maynooth, Kildare.

Table of Contents

1. Introduction 1

1.1. Protein Folding 2

1.1.1. The Protein Folding Landscape *2*

1.1.2. The Molten Globule State of Proteins *5*

1.2. Protein Misfolding 8

1.2.1. Protein Misfolding and Disease *10*

1.2.2. The Development and Structure of Amyloid Fibrils *12*

1.2.3. Improper Protein Conformation and Degenerative Disorders *14*

1.2.4. Beneficial Protein Misfolding *20*

1.3. Cancer 21

1.3.1. Mechanisms of Cancer *21*

1.3.2. Cancer Metastasis and Immunological Avoidance *23*

1.3.3. Apoptotic Cell Death in Cancer Cells *26*

1.4. Protein Selective Cytotoxicity in Cancer: The HAMLET Case 28

1.4.1. HAMLET: A Complex of α-LA and OA with Antimicrobial Effects *29*

1.4.2. HAMLET Mechanisms of Action *30*

1.4.3. Potential of HAMLET as a Future Treatment for Cancer. *35*

1.4.4. HAMLET has Shown Success in Both in vivo and in vitro Studies *36*

1.5. Alternative P-FA Complexes 37

1.5.1. The Formation of HAMLET *38*

1.5.2. Cytotoxic Component of P-FA Complexes *39*

1.5.3. Cytotoxic Capabilities of FAs *41*

1.6. Hypothesis and Aim 42

2. Materials & Methods 44

2.1. Reagents 45

2.1.1. Cell Culture Medium 45
2.1.2. Thioflavin T (ThT) Buffer Solution 45
2.1.3. ThT Stock Solution 45
2.1.4. ThT Working Solution 45
2.1.5. CR Buffer Solution 45
2.1.6. CR Working Solution 46
2.1.7. CR Birefringence Solution 46
2.1.8. 1-anilinonaphthalene-8-sulfonic acid (ANS) Buffer 46
2.1.9. 1X Annexin Binding Buffer 46
2.1.10. PI Working Solution 46
2.1.11. Tris Buffer A 46
2.1.12. Tris Buffer B 46
2.1.13. TEM 2X Fixing Solution 47
2.1.14. 10 mM Biotin Solution 47
2.1.15. 2X Laemmli Buffer 47
2.1.16. 4X Sample buffer 47
2.1.17. 8% Resolving Gel 48
2.1.18. 15% Resolving Gel 48
2.1.19. 5% Stacking Gel 48
2.1.20. Running Buffer 49
2.1.21. Transfer Buffer 49
2.1.22. TBS-T 49
2.1.23. 5% Non-Fat Milk/TBS-T 49
2.1.24. Immunofluorescence Blocking Buffer 49
2.1.25. Immunofluorescence Antibody Blocking Buffer 50
2.1.26. CD3 Antibody Solution 50

2.1.27. EDTA (200 μM) *50*

2.1.28. ELISA Developing Solution *50*

2.1.29. ELISA Washing Buffer *50*

2.1.30. ELISA Blocking Buffer *50*

2.1.31. ELISA Stopping Solution *50*

2.1.32. Phosphate Citrate Buffer *50*

2.1.33. Phosphate Buffered Saline (PBS) 10X *51*

2.1.34. MACS Buffer *51*

2.2. Cell Culture 52

2.2.1. U2OS and B16 Cell subculture *52*

2.2.2. PC12 Subculture *53*

2.3. Cell Counts 53

2.4. Cytotoxicity Assay 54

2.5. Alamar Blue Cell Viability Assay 54

2.6. Ion Exchange Chromatography (IEC) 56

2.7. Dialysis 57

2.8. Freeze Drying 57

2.9. HEWL Aggregation 58

2.10. HEWL Separation 58

2.11. ThT Assay 61

2.12. CR Spectroscopic Analysis 61

2.13. CR Birefringence 61

2.14. ANS Binding 62

2.15. Flow Cytometry 62

2.16. Apoptotic/Necrotic/Healthy Cells Detection Kit 63

2.17. AFM Imaging 63

2.18. Sonication 64
2.19. *In vivo* Electrophysiology 64
2.20. *In vivo* Tumour Studies 65
2.21. Mice 66
2.22. Western Blotting 67
2.22.1. Protein Extraction 67
2.22.2. Protein Concentration 67
2.22.3. Sodium Dodecyl Sulfate-Polyacrylamide Gel Electrophoresis (SDS-PAGE) 68
2.22.4. Western Blot Analysis 68
2.23. Transmission Electron Microscopy (TEM) 69
2.24. Biotinylation of Protein 70
2.25. Immunofluorescence 70
2.26. $CD4^+$ T Cell Stimulation 71
2.26.1. Isolation of Spleen Cells 71
2.26.2. Magnetic-Activated Cell Sorting (MACS) $CD4^+$ T Cell Isolation 71
2.26.3. $CD4^+$ T Cell Differentiation 72
2.27. Enzyme-linked Immunosorbent Assay (ELISA) 73
2.27.1. Standard Cytokine ELISA 73
2.28. Data and Statistical Analysis 74
3. *In Vitro* Investigation into the Structural and Mechanistic Properties of P-FA Complexes 75
3.1. Introduction 76
3.2. Results 83
3.2.1. HAMLET Significantly Reduces Viability in Cancer Cells When Compared to Differentiated Cells in vitro. 83

3.2.2. BAMLET Significantly Reduces Viability in Cancer Cells When Compared to Differentiated Cells in vitro 87

3.2.3. TEM of BAMLET Treated U2OS Suggests that OA Accumulates Within the Cell 90

3.2.4. The AMb-OA Complex Significantly Reduces Viability in Cancer Cells when Compared to Differentiated Cells in vitro 92

3.2.5. The β-LG-OA Complex Significantly Reduces Viability in Cancer Cells When Compared to Differentiated Cells in vitro. 95

3.2.6. The Cyto-c-OA Complex Significantly Reduces Viability in Cancer Cells When Compared to Differentiated Cells in vitro. 98

3.2.7. The Mb-OA Complex Significantly Reduces Viability in Cancer Cells When Compared to Differentiated Cells in vitro 101

3.2.8. The Ub-OA Complex Significantly Reduces Viability in Cancer Cells When Compared to Differentiated Cells in vitro 104

3.2.9. Non-OA Complexes are Not Cytotoxic Towards Cells 107

3.2.10. Biotinylated P-FA Complexes are Taken up in Larger Qualities into Tumour Cells 110

3.2.11. P-FA Complexes do not Display Signs of Aggregation 115

3.2.12. ThT Fluorescence of P-FA Complexes 116

3.2.13. CR Spectroscopic and Birefringence Assays Using P-FA complexes Display no Signs of Aggregation 118

3.2.14. P-FA Complexes Induce an Apoptotic Death Pathway in Cells 121

3.2.15. Flow Cytometry Analysis of PC12$^{undiff/diff}$ Cells Treated with P-FA Complexes Show That They Induce an Apoptotic Cell Death Pathway 122

3.2.16. PARP Cleavage of PC12$^{undiff/diff}$ Cells Suggests a Role for Apoptosis in Response to P-FA Complexes 126

3.2.17. Apoptotic/Necrotic/Healthy Cell Detection Kit Shows that PC12 Cells Trigger Apoptosis 128

3.3. Discussion 133

3.3.1. P-FA Complexes Generated from Novel Proteins Display Tumouricidal Cytotoxicity *133*

3.3.2. Examination of P-FA Complexes Reveals that they are not fully Aggregated *136*

3.3.3. P-FA Complexes Activate an Apoptotic Cell Death Response *137*

4. The Mechanistic and Immunological Effects of BAMLET using an *in vivo* Murine Melanoma Model 140

4.1. Introduction 141

4.2. Results 149

4.2.1. BAMLET Kills Mouse Melanoma B16 Cells in vitro *149*

4.2.2. FCS inhibits BAMLETs ability to destroy B16 cells in vitro *151*

4.2.3. BAMLET Induces an Apoptotic Cell Death Pathway in B16 Cells in vitro *154*

4.2.4. BAMLET Prolonged Survival in a Mouse B16 Melanoma Model and Administration Route of BAMLET did not affect its Efficacy *157*

4.2.6. BAMLET in Combination with the TLR 7/8 Agonist R848 Decreases Murine Melanoma Volume and Prolongs Survival after a Tumour Re-challenge *162*

4.2.7. Effect of BAMLET on $CD4^+$ T cell Differentiation *166*

4.3. Discussion 177

4.3.1. BAMLET Elicits an Apoptotic Cell Death Pathway in B16 Cells *177*

4.3.2. BAMLET Induces B16 Cell Death in vitro in the Presence of FCS *178*

4.3.3. BAMLET Efficacy in vivo is not Dependent on Route of Administration *179*

4.3.4. BAMLET Reduces Tumour Growth in Combination with R848 ..... *180*

4.3.5. BAMLET may Activate a Humoral Immune Response *182*

5. Isolation and Characterisation of Amyloid Oligomers, Sonicated Fibrils, and Mature Fibrils Prepared from an Innocuous Protein 188

5.1. Introduction 189

5.2. Results 195

5.2.1. HEWL Aggregation was Examined using ThT and ANS *195*

5.2.2. CR Binds Amyloid Fibrils *198*

5.2.3. AFM Imaging of Amyloid Aggregates *202*

5.2.4. TEM of Hen Egg White Lysozyme at Different States of Aggregation *205*

5.2.5. Separated HEWL Aggregates are Cytotoxic to PC12$^{undiff/diff}$ Cells *207*

5.2.6. Oligomers and Fibrils are Cytotoxic to the Human Osteosarcoma Cell Line U2OS. *209*

5.2.7. HEWL Oligomers, Sonicated Fibrils, and Mature Fibrils Induce Cellular Death via Secondary Necrotic and Apoptotic Pathways *212*

5.2.8. PARP Cleavage of PC12$^{undiff/diff}$ Cells Treated with HEWL Fractions Suggests that cells die via an Apoptotic Mechanism *215*

5.2.9. TEM Imaging of U2OS Cells Treated With HEWL Oligomers and Fibrils *217*

5.2.10. HEWL Oligomers but not Sonicated or Mature Fibrillar Fragments Inhibit Hippocampal LTP in vivo *220*

5.3. Discussion 222

5.3.1. Native HEWL can be Engineered into Distinct Amyloid Fractions *222*

5.3.2. HEWL Aggregates Induce Cell Death *223*

5.3.3. HEWL Oligomers, Sonicated Fibrils and Mature Fibrils Induce Cell Death via Apoptotic and Secondary Necrotic Pathways *225*

5.3.4. HEWL Oligomers but not Sonicated Fibrils Inhibit LTP in vivo *225*

6. General Discussion 228

6.1. Future Directions 241

7. References 242

LIST OF FIGURES

Figure 1.1 Schematic representation of energy landscape for protein folding. 4
Figure 1.2 Normal events governing protein folding and misfolding. 12
Figure 1.3 The Hallmarks of Cancer and Targeted Therapeutics 23
Figure 1.4 Structural changes of cells undergoing necrosis or apoptosis. 28
Figure 1.5 Schematic diagram of the HAMLET formation through the binding of OA. 29
Figure 1.6 Flow chart of the production of HAMLET using IEC 39
Figure 2.1 Salt gradient used to elute P-FA complexes. 57
Figure 2.2 Schematic representation of process used to separate HEWL fractions. 59
Figure 3.1 Effects of NGF treatment on cultured PC12 cells 84
Figure 3.2 The preparation of the HAMLET by IEC on an OA-conditioned exchange column. 85
Figure 3.3 Dosage–response viability curve for HAMLET tested on PC12 and U2OS cells using an Alamar Blue assay 86
Figure 3.4 The preparation of the BAMLET by IEC on an OA-conditioned exchange column. 88
Figure 3.5 Dosage–response curve for BAMLET tested on PC12 and U2OS cells. 89
Figure 3.6 TEM of U2OS cells treated with BAMLET. 91
Figure 3.7 The preparation of the AMb-OA by IEC on an OA-conditioned exchange column. 93
Figure 3.8 Dosage–response viability curve for AMb-OA tested on PC12 and U2OS cells using an Alamar Blue assay 94
Figure 3.9 The preparation of the β-LG-OA by IEC on an OA-conditioned exchange column. 96
Figure 3.10 Dosage–response viability curve for β-LG-OA tested on PC12 and U2OS cells 97
Figure 3.11 The preparation of the Cyto-*c*-OA by IEC on an OA-conditioned exchange column. 99
Figure 3.12 Dosage–response viability curve for Cyto-*c*-OA tested on PC12 and U2OS cells using Alamar Blue assay 100

Figure 3.13 The preparation of the Mb-OA by IEC on an OA-conditioned exchange column. 102
Figure 3.14 Dosage–response viability curve for Mb-OA tested on PC12 and U2OS cells using Alamar Blue assay..... 103
Figure 3.15 The preparation of the Ub-OA by IEC on an OA-conditioned exchange column. 105
Figure 3.16 Dosage–response viability curve for Ub-OA tested on PC12 and U2OS cells. 106
Figure 3.17 Cell lines treated with 0.1 mg/ml of native protein 108
Figure 3.18 $PC12^{undiff/diff}$ cells without biotinylated P-FA complexes 112
Figure 3.19 Uptake of biotinylated P-FA complexes in $PC12^{undiff}$ cells 113
Figure 3.20 Uptake of biotinylated of P-FA complexes in $PC12^{diff}$ cells..... 114
Figure 3.21 ThT fluorescence of P-FA complexes 117
Figure 3.22 CR binding to P-FA complexes..... 119
Figure 3.23 CR displays no birefringence upon mixing with P-FA complexes 120
Figure 3.24 $PC12^{undiff}$ cells treated with P-FA complexes induce apoptosis..... 124
Figure 3.25 $PC12^{diff}$ cells treated with P-FA complexes induce apoptosis 125
Figure 3.26 Western blot analysis of PARP cleavage in $PC12^{undiff/diff}$ cells..... 127
Figure 3.27 Immunofluorescence of $PC12^{undiff}$ cells with single dyes and a combination of dyes in the absence of P-FA complexes 129
Figure 3.28 Immunofluorescence of $PC12^{diff}$ cells with single dyes and a combination of dyes in the absence of P-FA complexes..... 130
Figure 3.29 Immunofluorescence showing cell death in $PC12^{undiff}$ cells 131
Figure 3.30 Immunofluorescence showing cell death in $PC12^{diff}$ cells 132
Figure 4.1 B16 cells treated with BAMLET in heat inactivated FCS 150
Figure 4.2 B16 cells treated with BAMLET in the presence of FCS 152
Figure 4.3 B16 cells treated with BAMLET activate an apoptotic cell death pathway 155
Figure 4.4 Immunofluorescence images of B16 cells stained with apoptotic/necrotic/healthy cells detection kit 156
Figure 4.5 Schematic representation of how C57/BL mice were grouped for treatment. ..159
Figure 4.6 Mice treated with BAMLET via SC and i.p show a decreased average tumour volume (mm^3) and increased survival compared to control. 160

Figure 4.7 Mice treated with the combination of BAMLET 0.7 mM and R848 show the greatest reduction in tumour size and increase in survival..... 164
Figure 4.8 Mice re-challenged with B16 tumours show delayed growth in treated groups. 165
Figure 4.9 . BAMLET blocks IL-2 production in $CD4^+$ T cells 168
Figure 4.10 BAMLET increases IL-10 production in Th1 cells 170
Figure 4.11 BAMLET caused an increase IL-17 in Th17 cells 172
Figure 4.12 BAMLET increases the secretion of TNF-α in Th0 cells. 174
Figure 4.13 BAMLET reduces IFN-γ levels in both Th0 and Th17 176
Figure 5.1 The process of amyloid formation. 191
Figure 5.2 Fluorescence emission spectra of ThT in the presence HEWL protein..... 196
Figure 5.3 Interaction of HEWL oligomers and mature fibrils with the hydrophobic dye ANS. 197
Figure 5.4 CR binds mature amyloid fibrils *in vitro* 199
Figure 5.5 CR amyloid binding to amyloid fibril..... 200
Figure 5.6 CR absorbance spectra of lysozyme separated fractions. 201
Figure 5.7 AFM of amyloid fibrils at different stages of aggregation 203
Figure 5.8 AFM imaging, z-height, and 3-dimensional representation of lysozyme fibril. 204
Figure 5.9 TEM of different stages of HEWL aggregation 206
Figure 5.10 Viability results for PC12 cell lines treated with HEWL fractions 208
Figure 5.11 U2OS cells treated with HEWL separated fractions 210
Figure 5.12 Death pathway of $PC12^{undiff}$ cells treated with HEWL aggregates was assessed using Annexin V-FITC/PI and flow cytometry..... 213
Figure 5.13 Death pathway of $PC12^{diff}$ cells treated with HEWL aggregates was assessed using Annexin V-FITC/PI and flow cytometry..... 214
Figure 5.14 Western blot analysis of PARP cleavage in $PC12^{undiff/diff}$ cells..... 216
Figure 5.15 TEM of U2OS cells treated with oligomers 218
Figure 5.16 TEM of U2OS cells treated with mature fibrils..... 219
Figure 5.17 HEWL oligomers but not fibrillar fragments inhibit hippocampal LTP *in vivo* 221

LIST OF TABLES

Table 1.1 Proteins that can form equilibrium MG states 7
Table 1.2 List of the prominent amyloid related disorders and the proteins involved 16
Table 2.1 P-FA Concentration Table for U2OS and $PC12^{diff}$ Cells. 55
Table 2.2 P-FA Concentration Table for $PC12^{undiff}$ Cells 55
Table 2.3 Concentration table for U2OS and $PC12^{diff}$ Cells treated with HEWL aggregates. 60
Table 2.4 Concentration table for $PC12^{undiff}$ Cells treated with HEWL aggregates. 60
Table 2.5 Antibodies used in Western blotting 69
Table 2.6 Antibody concentrations and reagents used in ELISA 74
Table 3.1 Proteins used to form P-FA complexes using IEC 82
Table 3.2 LC_{50} values (in mg/ml and molarity) for P-FA samples on cell lines 109
Table 3.3 List of concentrations used for biotinylation 111
Table 3.4 P-FA concentrations used for flow cytometry and immunofluorescence mg/ml and (μM) 123
Table 4.1 Concentrations of BAMLET used for treatment of B16 cells *in vitro*. Values given in mg/ml and (μM) 149
Table 4.2 LC_{50} values for B16 cells treated with BAMLET in media with (+) or without (-) heat inactivated FCS. 153
Table 4.3 Average tumour volume for mice at 11, 21, 28 days post inoculation. 161
Table 4.4 Average (given in pg/ml) of IL-2 secretion levels in $CD4^+$ T cells 167
Table 4.5 Average (given in pg/ml) of IL-10 secretion levels in $CD4^+$ T cells 169
Table 4.6 Average (given in pg/ml) of IL-17 secretion levels in $CD4^+$ T cells 171
Table 4.7 Average (given in pg/ml) of TNF-α secretion levels in $CD4^+$ T cells 173
Table 4.8 Average (given in ng/ml) of IFN-γ secretion levels in $CD4^+$ T cells 175
Table 5.1 LC_{50} values (μM) of amyloid oligomers, fibrils, and sonicated fibrils on PC $12^{undiff/diff}$ cells. 211

LIST OF ABBREVIATIONS

α-LA	α-Lactalbumin
β-LG	β-Lactoglobulin
β-LG-OA	β-Lactoglobulin-Oleic Acid
Aβ	β-Amyloid
ACS	American Cancer Society
AD	Alzheimer's disease
ALL	Acute Lymphoblastic Leukemia
AFM	Atomic Force Microscopy
AFT	Activating Transcription Factor
AMb	Apomyoglobin
AMb-OA	Apomyoglobin-OA
ANOVA	Analysis of Variance
ANS	1-anilinonaphthalene-8-sulfonic acid
Apaf-1	Apoptosis Activating Factor 1
APP	Amyloid Precursor Protein
ATP	Adenosine Triphosphate
BAMLET	Bovine α-Lactalbumin Made Lethal to Tumour Cells
BCA	Bicinchoninic Acid
BFA	Brefeldin A
BSA	Bovine Serum Albumin
CA1	Cornu Ammonis 1
CD	Cluster of Differentiation
CFTR	CF Transmembrane Conductance regulator
CJD	Creutzfeldt-Jakob Disease
CR	Congo Red
Cyto-*c*	Cytochrome *c*
Cyto-*c*-OA	Cytochrome *c*-Oleic Acid
DAMP	Danger-Associated Molecular Pattern
DAPI	4',6-Diamidino-2-Phenylindole
DCs	Dendritic Cells
DEAE	Diethylaminoethyl
DMEM	Dulbecco's Modified Eagle's Medium
DMSO	Dimethyl Sulfoxide
DTT	Dithiothreitol
ECM	Extracellular Matrix
EDTA	Ethlyenediaminetetraacetic Acid
ELISA	Enzyme-Linked Immunosorbent Assay
ELOA	Equine Lysozyme Oleic Acid
ETC	Electron Transport Chain
EPR	Electron Paramagnetic Resonance
ER	Endoplasmic Reticulem
ERK	Extracellular Signal-Regulated Kinases
EPSP	Excitatory Postsynaptic Potentials
FA	Fatty Acid
FACS	Fluorescence-Activated Cell Sorting

FAP	Familial Amyloid Polyneuropathy
FCS	Foetal Calf Serum
FDA	United States Food and Drug Administration
FF	Fast Flow
HAMLET	Human α-Lactalbumin Made Lethal to Tumour Cells
HDAC	Histone Deacetylases
HDI	Histone Deacetylase Inhibitors
HEWL	Hen Egg White Lysozyme
HFS	High Frequency Stimulation
HK	Hexokinase
HPLC	High Performance Liquid Chromatography
HPV	Human Papillomavirus
HRP	Horseradish Peroxidise
HSP	Heat Shock Protein
i.c.v	Intracerebroventricular
IEC	Ion Exchange Chromatography
IFN	Interferon
Ig	Immunoglobulin
IL	Interleukin
i.p	Interperitoneal
IPD	Intrinsically Disordered Protein
IRK1	Inositol Requiring Kinase 1
kDa	Kilodalton
LC_{50}	Lethal Concentration 50%
LPS	Lipopolysaccharide
LTP	Long Term Potentiation
MACS	Magnetic-Activated Cell Sorting
MAL	Multimeric Alpha-Lactalbumin
Mb	Myoglobin
Mb-OA	Myoglobin-OA
MDR	Multi-Drug Resistance
MG	Molten Globule
MG-OA	Molten Globule-Oleic Acid
MHC	Major Histocompatibility Complex
mRNA	Messenger Ribonucleic Acid
mTOR	Mammalian Target Of Rapamycin
NAP	Nucleosome Assembly Protein
NGF	Nerve Growth Factor
NHS	*N*-Hydroxysuccinimide
NK	Natural Killer
NMR	Nuclear Magnetic Resonance
OA	Oleic Acid
PAGE	Polyacrylamide Gel Electrophoresis
PAMP	Pathogen-Associated Molecular Pattern
PARP	Poly (ADP-ribose) Polymerase
PRR	Pattern-Recognition Receptor
PBS	Phosphate Buffer Solution

PC12	Pheochromocytoma 12
$PC12^{diff}$	Differentiated Pheochromocytoma 12
$PC12^{undiff}$	Undifferentiated Pheochromocytoma 12
PCD	Protein Conformational Disorders
PD	Parkinson's Disease
PERK	(PKR)-like Endoplasmic Reticulum Kinase
P-FA	Protein-Fatty Acid
pI	Isoelectric Point
PI	Propidium Iodide
PMA	Phorbol Myristate Acetate
PrP	Prion Protein
PS	Phosphatidylserine
PSEN	Presenilin
PVDF	Polyvinylidene Difluoride
RB1	Retinoblastoma Protein 1
RIPK	Receptor Interacting Protein Kinase
ROS	Reactive Oxygen Species
rpm	Revolutions Per Minute
RPMI	Roswell Park Memorial Institute Medium
RT	Room Temperature
SC	Subcutaneous
SDS	Sodium Dodecyl Sulfate
SEM	Standard Error of the Mean
shRNA	Small Hairpin RNA
SO	Sodium Oleate
TBS	Tris Buffer Solution
TEM	Transmission Electron Microscopy
Th	T-Helper
ThT	Thioflavin T
TLR	Toll Like Receptor
TNF	Tumour Necrosis Factor
Treg	Regulatory T
TSE	Transmissible Spongiform Encephalopathy
U2OS	Human Osteosarcoma Cells
Ub	Ubiquitin
UGGT	(UDP)-Glucose:Glycoprotein Glucosyltransferase
Ub-OA	Ubiquitin-Oleic Acid
UPP	Ubiquitin Protease Pathway
UPR	Unfolded Protein Response
UV	Ultraviolet

1. Introduction

1.1. Protein Folding

1.1.1. The Protein Folding Landscape

The central dogma of molecular biology, with particular emphasis on protein folding, is that DNA is transcribed into mRNA via the ribosome, resulting in the production of functional protein molecules comprised of polypeptide chains of amino acids (Groppo and Richter, 2009). Christian Anfinsen's pioneering work in the 1950's established a new paradigm regarding protein folding by discovering that the totality of interatomic interactions governed by the amino acid sequence determines the proteins native conformation. He also specified that in order for this to happen the Gibbs free energy for folding must be at its lowest (Anfinsen, 1973).

Self-assembly of proteins is one of the defining characteristics of all living systems and as such must be carried out with precision and fidelity however, due to the intricacy of this event coupled with various other biological processes occurring simultaneously within the cell, protein misfolding can occur. Given the importance of proteins to an organism's very existence, protein misfolding and subsequently proteins which lose the ability to remain correctly folded, can lead to a wide variety of pathological conditions (Dobson, 2003). In an optimal system there would be an ideal balance between protein synthesis, maturation, and degradation. In eukaryotic cells protein folding predominately occurs within the cytosol of the cell or in the endoplasmic reticulum (ER) (Sitia and Braakman, 2003). Protein folding can occur in a very short space of time: *in vitro* studies have shown that small proteins can fold in seconds or less (Calamini *et al.*, 2012). Couple the speed of assembly with the total bulk of proteins within a living organism (~100,000 different protein types) (Dobson, 2001) and it becomes apparent that the cell faces a monstrous task in trying to correctly regulate protein folding.

The sheer number of possible protein conformations that can arise from a peptide chain is substantial and makes protein folding particularly difficult to manage efficiently. In an *in vivo* system within the host, the potential amount of conformations would take too long to analyse individually, therefore an alternative mechanism must be employed (Ptitsyn, 1991). This puzzle was first noted by Cyrus Levinthal in 1968 and has subsequently become known as 'Levinthal's paradox'. Levinthal postulated that it is impossible for a polypeptide chain to

explore the entire conformational space in order to find its native state (Zwanzig *et al.*, 1992). Therefore a type of search algorithm must be employed whereby the protein chain does not search all possible conformations but instead forms fluctuating embryos of secondary structure regions which in turn collapse and are adjusted to a unique native structure (Ptitsyn, 1991). In recent years a new view has emerged regarding protein folding, one which describes the process in terms of a funnel shaped energy landscape whereby the funnel represents a strong energy drive to the native energy minimum (Dill *et al.*, 2007, Dinner *et al.*, 2000, Dobson, 2003). Instead of a stepwise process of interactions between specific partially unfolded states, the peptide chain employs a stochastic search mechanism of multiple accessible conformations, represented in Figure 1.1. In order to find its lowest energy structure the polypeptide chain uses a method of trial and error to anaylse the strength of interactions between the residues. In general, native like interactions are more stable and so will persist longer than the non-native forms. Given the right shape, protein molecules need only sample a small fraction of all possible conformations during the transitional period from random coil to a native structure (Zhuravlev and Papoian, 2010).

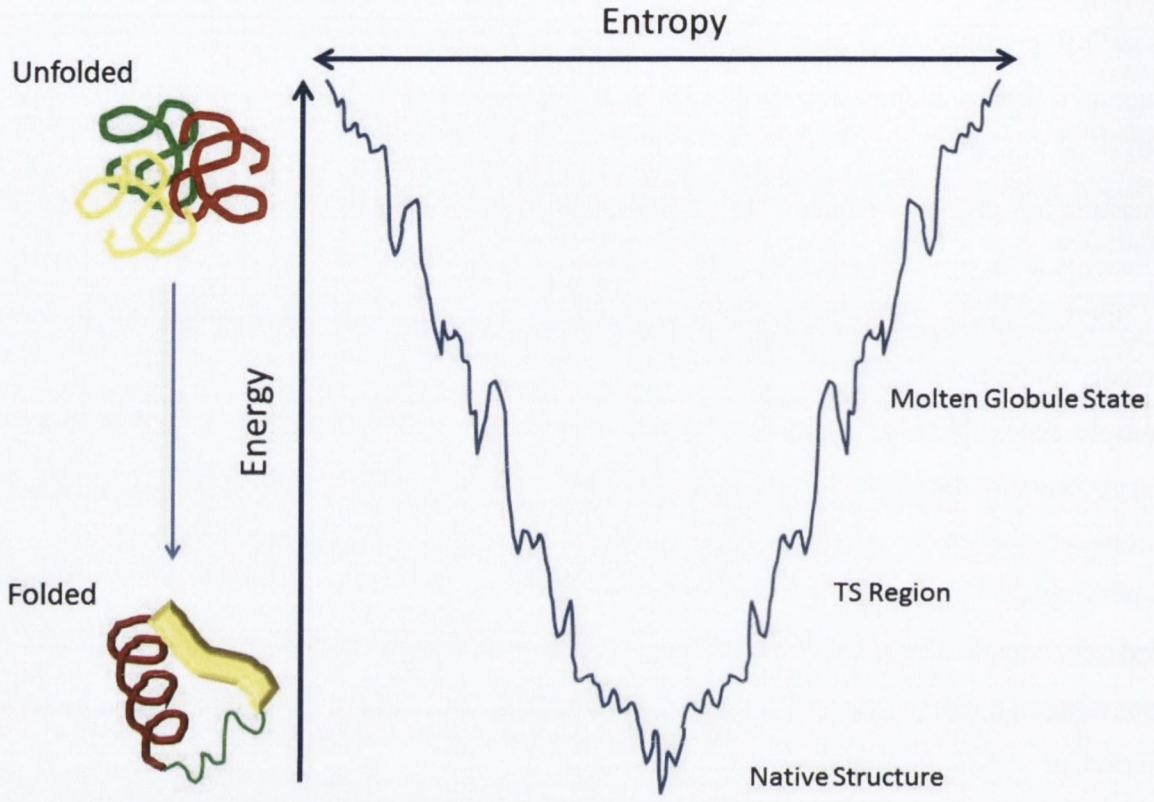

Figure 1.1 Schematic representation of energy landscape for protein folding.

Folding path taken by simplified protein. Native conformation is achieved via surface funnelling of a multitude of denatured states. Folding occurs through the progressive organization of structures as they pass through the funnel shaped folding landscape. Adapted from Dobson, 2004.

1.1.2. The Molten Globule State of Proteins

The native state of a protein is one that is usually associated with the correct folding of the polypeptide chains, leading to the formation of a compact globular macromolecule which possesses a highly rigid and ordered structure (Cabrita *et al.*, 2010). Over the past 50 years since Anfinsen's experiments the view on protein folding has changed dramatically. It was assumed that the transition from ordered native protein to denatured protein was a one-step event in which a protein became completely non-functional once it had left its globular conformation. The compact native structure which confers such rigidity and definition to the proteins structure has allowed for the 3D structure of many proteins to be analysed via X-ray crystallography, nuclear magnetic resonance (NMR), theoretical modeling, and cryoelectron microscopy (Berman *et al.*, 2000). The idea that proteins could only remain functional while in a fully ordered compact globular structure has changed with the recent discovery that many partially or completely disordered proteins obtain the ability to function whilst in these states (Dunker *et al.*, 2008b, Dyson and Wright, 2005, Tompa, 2005). The main criteria for all proteins is that they become folded in such a way as to allow them to carry out a specific function and the fact that many disordered proteins possess this characteristic means that they must in their own right be classed as native proteins (Dunker *et al.*, 2008a). It has been proposed by Dunker *et al*, that proteins exist in a trinity of structures; the ordered 3D state, the molten globule (MG), and the random coil (Dunker *et al.*, 2001). Collectively, any protein which has become unfolded is often referred to as an intrinsically disordered protein (IDP). Using bioinformatics coupled with data mining, thousands of natively disordered proteins in eukaryotes, archaea and bacteria have been revealed and approximately 35-51% of all proteins are disordered in eukaryotic organisms (Dunker *et al.*, 2002). Prior to the discovery of random coils, which are proteins whose amino acids are randomly aligned in a monomer conformation, MG proteins were thought to be the only collapsed disordered molecules (Dunker *et al.*, 2008b). MG proteins were first described in the early 1980's (Ohgushi and Wada, 1983b) and subsequently much work has been carried out to further understand their role as an intermediate protein folding entity (Redfield, 1999). The structure of the MG is a perfect example of the importance of flexibility in protein structure and fully illustrates that protein conformation is not as ridged and unforgiving as earlier believed. MG proteins possess some features of native structure and are often said to have native-like structure

however they lack global tertiary structure in that their side chain packing is looser and they also have a dramatic increase in the mobility of loops and at the end of their chains. It is these features which render this protein an intermediate between fully native and unfolded states (Vassilenko and Uversky, 2002, Uversky and Dunker, 2010). The MG can be further subdivided into pre-MG, which is a less compact state than the MG but more compact than the unfolded state (Uversky and Ptitsyn, 1994). The MG state of protein folding is driven by hydrophobic collapse and cannot form a stable structure due to the inability to produce tight side chain packing however, the pre-MG formation is likely driven due to water being a poor solvent for polypeptides. In this condition the protein remains very unstable, has the propensity to aggregate, and remains in a more hydrophobic state than normal. The MG state can be induced by lowering pH values, increasing ionic strength conditions, or by the removal of a co-factor (Regan, 2003). Many proteins possess the ability to form equilibrium MG forms and are outlined in Table 1.1. In this state these proteins often retain functionality despite being partially folded. These proteins are involved in a plethora of duties from facilitating in the translocation of proteins across membranes (Bychkova *et al.*, 1988), to interacting with chaperone molecules (Martin *et al.*, 1991) and ligands (Gunasekaran and Nussinov, 2007).

Table 1.1 Proteins that can form equilibrium MG states

Protein	pI	Reference
Human α-lactalbumin	4.7	Kuwajima 1996. *FASEB J* 10(1): 102-109.
Bovine α-lactalbumin	4.8	Gast *et al.* 1998. *Protein Sci* 7(9): 2004-2011.
Equine lysozyme	8.41	Mizuguchi *et al.* 1998. *J Mol Biol* 283(1): 265-277.
Bovine carbonic anhydrase B	6.4	Wong and Tanford. *J. Biol. Chem.* 1973 Dec 25;248(24):8518-23
B-lactamase (penicillinase) S. Aureus	9.52	Robson and Pain. *Biochem J.* 1976 May 1; 155(2):331-44
Diphtheria Toxin fragment A	5.06	Dumont and Richards. *J Biol Chem.* 1988 Feb 5;263(4):2087-97
Mouse dihydrofolate reductase	8.58	Eilers and Schatz. *Nature.* 1986 Jul 17-23;322(6076):228-32
Human apomyoglobin	7.29	Hughson and Baldwin. *Biochemistry.* 1989 May 16;28(10):4415-22
E.coli apocytochrome b-562	5.38	Feng *et al. Biochemistry.* 1991 Aug 6;30(31):7711-7
E.coli chaperone protein dnaK	4.83	Palleros *et al. J Biol Chem.* 1992 Mar 15;267(8):5279-85
Human brain-derived neurotrophic factor	9.59	Philo *et al. Biochemistry.* 1993 Oct 12;32(40):10812-8
E.coli (K12) Aspartate amino transferase	5.54	Herold and Kirschner. *Biochemistry.* 1990 Feb 20;29(7):1907-13
Horse cytochrome *c*	9.59	Jeng *et al. Biochemistry.* 1990 Nov 20;29(46):10433-7
Bovine β-lactoglobulin	4.83	Ptitsyn OB et al. FEBS Lett. 1990 Mar 12;262(1):20-4
***E.coli* RNase H1**	4.43	Dabora and Marqusee. *Protein Sci.* 1994 Sep; 3(9):1401-8
Yeast phosphoglycerate kinase	7.09	Watson *et al. EMBO J.* **1** (12): 1635–40
Interleukin 4	9.26	Redfield *et al. Nat Struct Biol.* 1994 Jan;1(1):23-9
Ubiquitin	6.56	Harding *et al. Biochemistry.* 1991 Mar 26;30(12):3120-8

1.2. Protein Misfolding

In eukaryotes protein folding occurs in either the cytosol or the ER (Hebert and Molinari, 2007). To ensure that the integrity of the protein is not compromised the folding process is constantly monitored and augmented through the dynamic integration of cellular signals and environmental factors (Hetz, 2012). The protein folding milieu contains a number of auxiliary proteins which aid and facilitate the correct structural assembly of these molecules (Hartl, 1996) such as molecular heat shock protein (HSP) chaperones.

The HSP-70 molecule has a molecular mass of 70 kDa and is divided into two separate domains, one of which mediates adenosine triphosphate (ATP) binding while the other binds to the protein substrate (Mayer and Bukau, 2005). The substrate binding cleft within the HSP-70 molecule binds to hydrophobic residues on polypeptide chains, often sections related to partially unfolded proteins in a non-native conformation, and sequesters the partially or completely unfolded protein resulting in the cessation of aggregation (Fink, 1999). The chaperone can also repeatedly bind and release the unfolded molecule in an effort to get it to naturally refold into its native state (Szilágyi *et al.*, 2007). The HSP-60 protein family is often referred to as the chaperonin family and can be extended to include GroEL and TCP-1 ring complex families. The HSP-60 chaperone binds to partially folded intermediates and thus directly facilitates folding (Fink, 1999).

There are also several other HSP molecules that work to correctly amend protein misfolds, such as the HSP-90 chaperone which is involved in mending late stage protein misfolding and stimulating signal transduction systems. Another such molecule, the HSP-100 chaperone can unfold even stably folded proteins (Saibil, 2008). Beneficial as these structural coordinators are they are not essential as folding can occur in their absence, which further strengthens the hypothesis that the code for folding is contained within the amino acid sequence itself, a paradigm first championed by Anfinsen in the 1970's (Anfinsen, 1973). In addition to providing sequestration to assist the folding of proteins, HSP's also have a role in the innate and adaptive immune systems, stimulating the maturation of dendritic cells (DCs) as well as promoting antigen presentation by major histocompatibility complex (MHC) class I molecules (Li *et al.*, 2002, Tsan and Gao, 2009).

The ER also contains a number of regulatory mechanisms that track and facilitate the formation of native protein structures. The ER is a membrane enclosed multifunctional cellular organelle that is found ubiquitously in eukaryotic cells. The functions of the ER are multiple and broad, and include storage of Ca^{2+} and the synthesis of lipids and sterols. The primary role of the ER is as a site for the synthesis and folding of secretory and membrane proteins which collectively account for a significant proportion of all proteins produced by mammalian cells (Lin *et al.*, 2008). Physiological ER stress such as protein production overload or even pathological stresses such as that caused by the presence of mutated proteins can lead to the activation of a series of complementary adaptive mechanisms collectively termed the unfolded protein response (UPR) (Hetz, 2012, Lin *et al.*, 2008). The ER acts as a reservoir for a number of molecules involved in protein folding. As mentioned previously, chaperone molecules (with the exception of HSP-10, HSP-60, and HSP-104) are stored here and facilitate the folding process. Additionally, folding enzymes such as calnexin and calreticulin are also present at this location (Schroder, 2008).

Any irreversible stress detected by the cell results in the immediate elicitation of the UPR, ensuring that these rogue protein molecules are targeted for elimination via apoptosis (Hetz, 2012). The UPR is initiated when unfolded proteins are tightly bound to recognition molecules, specifically BiP and (UDP)-glucose:glycoprotein glucosyltransferase (UGGT). These recognition factors which work in sync with various chaperone molecules maintain the unfolded protein in its disruptive state long enough for the activation of three ER resident transcription proteins; the inositol requiring kinase 1 (IRK1), activating transcription factor 6 (AFT6), and double-stranded RNA-activated protein kinase (PKR)-like endoplasmic reticulum kinase (PERK). Once activated these signals promote an unfolded protein signal across the membrane of the ER, resulting in Ca^{2+} release and the activation of apoptotic-signaling pathways which leads to the destruction of the cell and consequently the unfolded protein (Schroder and Kaufman, 2005).

In addition to the UPR and its various chaperone mediated, apoptotic inducing pathways, the cell can also utilise a multisubunit enzyme known as the proteasome. This 2.4 kDa multifunctional ATP-dependent proteolytic complex, sometimes referred to as the 26S proteasome, is expressed in the cytoplasm and nucleus of all eukaryotic cells. The proteasome has a key role in cell cycle regulation and cell survival and its primary function as a molecule

is to degrade proteins (Kisselev and Goldberg, 2001). In order for a protein to be processed by the proteasome it must be first tagged with a small peptide fraction of ubiquitin (Ub). This event occurs repeatedly until the targeted protein becomes polyubiquitinated, that is it contains numerous ubiquitin molecules covalently bound, which flags the protein for destruction by the proteasome (Figure 1.2) (Pickart, 2001). This process is known as the Ub-protease pathway (UPP) (Roos-Mattjus and Sistonen, 2004). Five or more Ub molecules attached to the targeted protein is sufficient for the complex to recognise it and process it for degradation. Ub is removed and the protein is linearised prior to it being translocated to the central core of the proteasome where it is digested to peptides. These peptides are further broken down to amino acids by peptidases present in the cytoplasm or used in antigen presentation (Lecker *et al.*, 2006).

1.2.1. Protein Misfolding and Disease

The term 'misfolded protein' is generally reserved for proteins who have adopted incomplete or incorrect overall protein structures. Regardless of the numerous mechanisms employed to counteract such a phenomenon, misfolded proteins are extremely common with approximately 30% of all synthesized polypeptides being tagged for rapid degradation (Yewdell, 2005). Although the presence of folding facilitators such as chaperones are beneficial to the process of protein assembly it should be noted that these molecular chaperones are only capable of mitigating the occurrence of misfolded proteins and do not provide steric information for correct folding structures. As such these helper molecules do not function as direct coordinators of protein self-assemble but rather as facilitators of the process by increasing the efficiency (Ellis and Hartl, 1999).

These elaborate systems employed by the host work remarkably well considering the burden of protein related issues that can arise when a polypeptide molecule is folding. Despite the rigorous checkpoints in place rogue misfolded proteins can escape the regulatory mechanisms utilised by the cell (Lee and Yu, 2005). These incorrectly folded proteins have been associated with numerous neurological and systemic diseases (Soto, 2003) and collectively these disorders are often referred to as protein conformational disorders (PCD) or amyloidoses (Calamini *et al.*, 2012, Lee and Yu, 2005).

PCDs are generally defined as a disease which is "caused by inherited or acquired modification in protein structure" and can encompass a wide range of categories. These disorders can be dominantly inherited or can be induced, which is often the case with prion related diseases (Kopito and Ron, 2000). PCDs can arise from both loss and gain-of-function. α1-antitrypsin is normally produced by the liver and is important in neutralizing elastin, a neutrophil protease that can be harmful to connective tissue. In the case of α1-antitrypsin deficiency, defective production of the misfolded α1-antitrypsin is retained rather than secreted and can lead to the onset of emphysema due to a failure to protect the lungs from proteolysis by elastase (Lomas and Carrell, 2002). A large section of PCDs (in particular misfolded diseases) act through a gain-of–function mechanism. Most protein misfolding diseases are related to a specific group of peptides and proteins which have been converted from a soluble functional state into well-defined proteinaceous fibrillar aggregates known as amyloid fibrils (Chiti and Dobson, 2006).

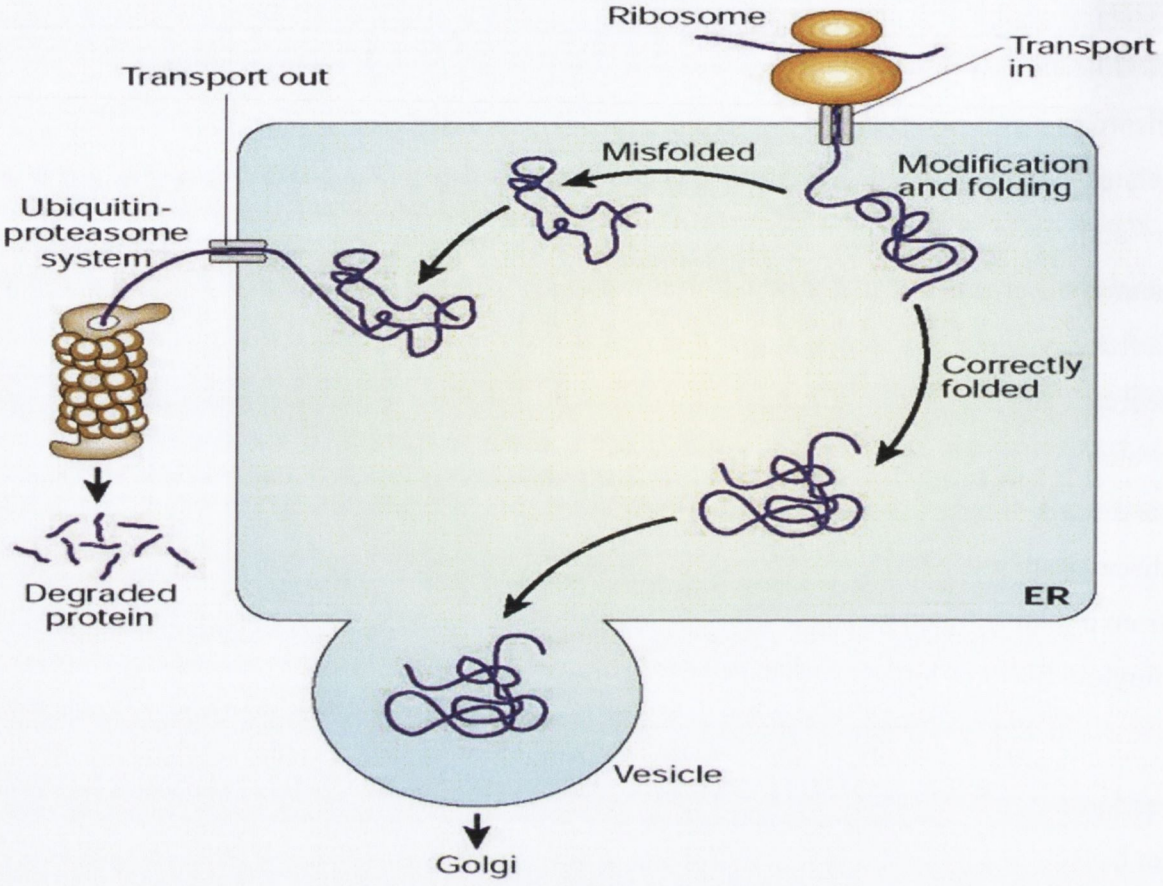

Figure 1.2 Normal events governing protein folding and misfolding.

In protein folding newly synthesised proteins are translocated to the ER where with the help of chaperone molecules (not shown) the 3D structural protein molecule is formed. The correctly folded molecules are then shuttled to the Golgi complex where they are released into the extracellular environment. In the event of protein misfolding, incorrectly folded proteins are tagged for ubiquitination and degraded by the Ub-proteasome system Dobson, 2003.

1.2.2. The Development and Structure of Amyloid Fibrils

The onset and progression of neurodegenerative disorders is for the most part a consequence of the formation and propagation of amyloid protein aggregates. Amyloid fibrils have long been associated with these diseases however, their true cytotoxic role is still a topic of debate (Selkoe, 2003). The formation of amyloid fibrils is a multistep process which begins with a

native protein and ends with an insoluble amyloid fibril. The process has numerous intermediate developmental stages such as the formation of monomers, oligomers, protofiliments, and full mature fibrils or filaments. Each stage in this process has been rigorously investigated in order to identify and characterise the true biologically toxic species involved (Murphy, 2007). Although it was originally thought that the mature amyloid fibrils were the cytotoxic component involved in the pathology of these degenerative diseases, recent evidence suggests that the more soluble, intermediate oligomeric species may play a bigger role in actual toxicity (Chiti and Dobson, 2006). There is a growing need to identify the true toxic component involved with these disorders as compounds which sequester different stages of the development process (Walsh *et al.*, 2005, Klein *et al.*, 2001) may prove to be of therapeutic interest.

Monomers are considered to be relatively innocuous in relation to the pathology of degenerative diseases (Chiti and Dobson, 2006). Monomers themselves are generally disordered and likened to a random coil. In Huntington's disease the monomeric form of the polyQ protein involved in the progression of the disease can adopt a linear, extended and unstructured configuration (Hoffner and Djian, 2014). In the case of β-amyloid (Aβ), the key protein involved in Alzheimer's disease (AD), the disordered Aβ monomers form into helical regions during the formation of fibrillar Aβ (Fezoui and Teplow, 2002). Monomers appear to be the first stage in the formation of full length amyloid fibrils, and although generally disordered, are capable of developing into oligomers (Hoffner and Djian, 2014).

Oligomers are soluble globular aggregates which appear as small spherical beads when visualised using atomic force microscopy (AFM). They generally have well defined α-helical structure but lack a well-defined secondary structure, which becomes more structured and pronounced the more the oligomers convert into fibrils (Apetri *et al.*, 2006). The sizes of different oligomeric species vary depending on the original protein. Small diffusible Aβ oligomers were found to be globular in shape ranging from 4.8-5.7 nm in length. These oligomeric species were also found to have a mass of between 17 and 42 kDa (Lambert *et al.*, 1998). Subsequent examination of the Parkinson's disease (PD) protein α-synuclein revealed that these spheroidal oligomers contain 47% α-helical secondary structure and were approximately 2-6 nm in height (Apetri *et al.*, 2006) and ~40 kDa in size (Kayed *et al.*, 2003). Oligomers can be divided further into the spherical 'classic' oligomer structures or linear

strings known as protofibrils (Dubnovitsky *et al.*, 2013) which are structural epitopes of oligomers and also mechanistically similar (Kayed *et al.*, 2003).

Fibrils are insoluble, straight, generally unbranching (in rare cases branching can occur) (Andersen *et al.*, 2009) structures which are around 10 nm in diameter and of indeterminate length. The generic structure of these amyloid bodies has been examined extensively using a variety of techniques including electron microscopy (Shirahama and Cohen, 1967), electron paramagnetic resonance (EPR), and solid state NMR (Tycko, 2003). They are comprised of two or more protofilaments arranged together in a helical manner (Makin and Serpell, 2005). The protofilaments themselves are 2.5-3.5 nm β-sheet rich structures which make up the bulk of the fibril (Murphy, 2007). The cross-β structure is comprised of parallel and antiparallel β-strands which are hydrogen bonded into sheets which run parallel to the fibrillar axis in a twisted manner. These protofilaments arrange laterally around a hollow center to form fibrils which are anywhere in length from hundreds of nanometers to tens of micrometers (Xu *et al.*, 2007, Wetzel, 2002).

Fibrils stain with Congo Red (CR) dye, which can be observed using microscopic birefringence (Puchtler *et al.*, 1962) or ultraviolet (UV)-Vis spectrometry (Klunk *et al.*, 1989). In the case of Aβ, fibrils are formed when 5-6 filaments wrap together yielding an unbranched fibrillar structure which can reach lengths of 1 μm or more (Murphy, 2007). The formation of Aβ fibrils is thought to be the end stage result of the amyloid cascade hypothesis in which the Aβ protein uncoils to reveal monomers, which proceed the formation of Aβ soluble oligomers, which then subsequently result in the formation of fully formed Aβ fibrils that join together to form amyloid deposits or plaques (Karran *et al.*, 2011). Many other proteins have demonstrated the ability to form amyloid fibrils it has been suggested that any protein has the propensity to form amyloid fibrils under specific conditions (Krebs *et al.*, 2000).

1.2.3. Improper Protein Conformation and Degenerative Disorders

The failure of specific proteins to correctly fold and adopt a native structure has led to the emergence of a vast range of human diseases (Chiti and Dobson, 2006). An arsenal of different, unrelated proteins are involved in the development of these disorders such as the

catabolic enzyme β-glucocerebrosidase in Gaucher's disease (Chen and Wang, 2008) or the CF transmembrane conductance regulator (CFTR) found in patients with cystic fibrosis (Storey and Wald, 2008), to name but a few. The core domain of human p53 has relatively low intrinsic thermodynamic stability which allows for rapid transition between unfolded and folded states. This instability has been linked with the susceptibility of p53 to mutate, and in the progression of some cancers (Joerger and Fersht, 2010).

As mentioned previously, amyloid fibrils have been implicated in a plethora of degenerative diseases which affect a variety of peripheral tissues along with the central nervous system (Falk *et al.*, 1997). These diseases, generally termed amyloidosis (Pepys, 2006), include disorders such as transmissible spongiform encephalopathy (TSE) (Lu *et al.*, 2007), Creutzfeldt-Jakob disease (CJD), type 2 diabetes mellitus, as well as the better known neurodegenerative disorders AD and PD (Majumdar *et al.*, 2011, Dobson, 2001, Maji *et al.*, 2009, Lansbury and Lashuel, 2006). These clinical disorders are primarily characterized by the presence of intracellular (aggresome, inclusion body) and extracellular (plaque) fibrillar deposits (Stefani, 2004).

To date, at least 25 different proteins have been recognized as causative agents of amyloid diseases (see Table 1.2 for several examples) including Aβ with AD, α-synuclein with PD, prion protein (PrP) with the spongiform encephalopathies, and islet amyloid polypeptide (IAPP) with diabetes type 2 (Eisenberg and Jucker, 2012). However, recent evidence suggests that this phenomenon is not unique to this small group of proteins and that this ability to aggregate may be a generic property of possibly all polypeptide chains under specific denaturing conditions (Krebs *et al.*, 2000, Gharibyan *et al.*, 2007). Numerous *in vitro* experiments have demonstrated the effects of various denaturing conditions on a large repertoire of innocuous proteins (Fändrich *et al.*, 2003, Bouchard *et al.*, 2000, Mishra *et al.*, 2007, Vieira *et al.*, 2007) with one of the first being hen egg white lysozyme (HEWL) (Krebs *et al.*, 2000). Although the human derivative of this enzyme has previously been identified as a main contributor to hereditary non-neuropathic systemic amyloidosis, wild type HEWL has no pathogenic capabilities (Pepys *et al.*, 1993). *In vitro* aggregation of this protein at acidic pH and elevated temperatures makes HEWL a very useful model to study protein misfolding and disease.

Table 1.2 List of the prominent amyloid related disorders and the proteins involved

Clinical syndrome	Fibril Component
Alzheimer's disease	Aβ peptides (1–40, 1–41, 1–42, 1–43); Tau
Spongiform encephalopathies	Prion protein (full-length or fragments)
Parkinson's disease	α-synuclein (wild type or mutant)
Fronto-temporal dementias	Tau (wild type or mutant)
Familial Danish dementia	ADan peptide
Familial British dementia	ABri peptide
Amyotrophic lateral sclerosis	Superoxide dismutase (wild type or mutant)
Dentatorubro-pallido-Luysian atrophy	Atrophin 1 (polyQ expansion)
Huntington's disease	Huntingtin (polyQ expansion)
Cerebellar ataxias	Ataxins (polyQ expansion)
Kennedy disease	Androgen receptor (polyQ expansion)
Primary systemic amyloidosis	Ig light chains (full-length or fragments)
Secondary systemic amyloidosis	Serum amyloid A (fragments)
Familial Mediterranean fever	Serum amyloid A (fragments)
Senile systemic amyloidosis	Transthyretin (wild-type or fragments)
Hemodialysis-related amyloidosis	β2-microglobulin
Familial amyloid polyneuropathy III	Apolipoprotein A-1 (fragments)
Type II diabetes	Pro-islet amyloid polypeptide (fragments)
Medullary carcinoma of the thyroid	Procalcitonin (full-length or fragment)
Lysozyme systemic amyloidosis	Lysozyme (full-length, mutant)
Insulin-related amyloid	Insulin (full-length)
Fibrinogen a-chain amyloidosis	Fibrinogen (a-chain variants and fragments)

1.2.3.1. Cellular cytotoxity of oligomers and fibrils

Despite the advancements in the field of protein aggregation and disease pathology very little is known about the exact mechanisms surrounding their formation and cytotoxicity. Although generated from one original peptide or protein, amyloid oligomers and fibrils are distinctively different in structure and as such carry different cellular functions (Glabe, 2006). Oligomers generated from widely varying primary sequences bound to a conformation dependent antibody which recognizes a common epitope on amyloid oligomers and not monomers or fibrils, suggesting that oligomers share a common structure. This common structure suggests that oligomers would interact with cells in a generic manner and may possess the same primary mechanism of toxicity in diseases (Kayed *et al.*, 2003). There is now wide agreement on the role played by amyloid oligomers in neurotoxicity however, the mechanisms through which they induce neuronal cell dysfunction and cell death are not fully understood. Ca^{2+} homeostasis dysregulation is one of the better understood mechanisms by which oligomers interact and injure cells. The Ca^{2+} concentration gradient is tightly regulated by Ca^{2+} ions in neuronal cells (Simons, 1988), an imbalance of which can be detrimental to the cell. It has been shown that Aβ destabilizes neuronal Ca^{2+} homeostasis and by doing so renders neurons more vulnerable to environmental insults (Mattson *et al.*, 1992). It has also been suggested that oligomers form non-selective Ca^{2+}-permeable pores which alter the internal and external concentrations of cellular Ca^{2+} (Nelson *et al.*, 1993). Lipid rafts have also been involved in the pathophysiology of diseases associated with protein misfolding. The high level of mature neuronal plasma membrane may sensitize the cell membranes against amyloid proteins and could increase their vulnerability with regards to cytotoxic attack (Malchiodi-Albedi *et al.*, 2011).

It is thought that amyloid fibrils interact with the cell membrane however, unlike oligomers this interaction does not affect the Ca^{2+} integrity. Instead fibrillar binding to cell membranes results in structural reorganization of the membrane and aggregation of membrane rafts. In addition Sup35p fibrils bind to cell surface receptors and induce apoptosis through the stimulation of the cell surface death receptor Fas, which triggers caspase-8 activation (Bucciantini *et al.*, 2012).

1.2.3.2. The oligomer versus fibril hypothesis

Despite the fact that amyloidoses have been known of for many years, the true cytotoxic components involved in the pathology of these diseases is still not fully understood. This lack of understanding has led to the emergence of the oligomer versus fibril hypothesis of cellular cytotoxicity (Vieira *et al.*, 2007). As mentioned previously, it was originally thought that mature amyloid fibrils were the main cytotoxic components in relation to the pathogenicity observed in amyloidosis (Gustavsson *et al.*, 1991, Lorenzo and Yankner, 1994, Lorenzo and Yankner, 1996). Amyloidosis has been known for more than 150 years however, it wasn't until 1984 that the first amyloid protein specifically responsible for human disease was isolated from the tissue of an AD patient (Glenner and Wong, 1984). The presence of amyloid deposits or plaques is a key feature of amyloidosis. Early histopathological findings demonstrated that large amyloid aggregates were present in extracellular deposits or in intracellular inclusions which were later designated amyloid plaques (Maloy *et al.*, 1981, Ishii and Haga, 1984, Cras *et al.*, 1991). This conclusion made sense as these plaques were generally found in locations were the aforementioned disease appeared to affect. For example patients with AD generally present with amyloid plaques on sections of the brain associated with memory and cognitive functionality (Armstrong, 2009) ergo it was hypothesized that there must be a direct correlation between the presence of these senile plaques and tangles, and the pathology of the disease. When examined closely these plaques contained independent fibrils that appear to form a solid structure in a mesh like fashion (Merz *et al.*, 1983). In addition various studies involving animal models (Kohno *et al.*, 1997, Shimada *et al.*, 1989) and cell lines (Yankner *et al.*, 1990, Kowall *et al.*, 1991, Iversen *et al.*, 1995) provided evidence which supported the idea that there was a significant correlation between disease state and mature fibril cytotoxicity (Hardy and Higgins, 1992).

However, despite the level of supportive experimental data, the 'fibril hypothesis' does not explain several fundamental pathological and clinical aspects of numerous degenerative disorders. A key argument has been that the quantity of amyloid present in these plaques does not correlate to the level of neurodegeneration in diseases (Sakudo and Ikuta, 2009). Research has shown that amyloid plaque burden in AD patients has no correlation with the severity of the disease (Rowe *et al.*, 2010, Katzman *et al.*, 1988). Furthermore in prion disorders the amount and distribution of PrP^{Sc} deposits is not always in direct correlation with the

progression and severity of the disease. Patients with sporadic CJD sometimes show the complete absence of plaques despite the advanced stage of their disease (Budka, 2003). Another study examined nerve tissue biopsies from patients suffering from familial amyloid polyneuropathy (FAP). These biopsies contained non-fibrillar aggregates which were negative for CR birefringence (Sousa *et al.*, 2001) suggesting a role for some other proteinaceous species in the pathology of the disease.

In light of these experiments and numerous others a new target emerged which could account for the toxicity observed in these types of diseases, the soluble amyloid oligomer, a prefibrillar, post monomer aggregate. Recent studies have provided leverage to this new 'oligomer hypotheses' with many human amyloid diseases found to be linked to these aggregate bodies (Iuchi *et al.*, 2003, Klein *et al.*, 2001, Kim *et al.*, 2003, Reixach *et al.*, 2004, Oddo *et al.*, 2006). In the case of AD, soluble Aβ oligomers have been shown to be directly responsible for neuronal cell death (Querfurth and Laferla, 2010), inhibiting long term potentiation (LTP) response *in vivo* (Wang *et al.*, 2002) thus effecting long term memory, and increased oligomer burden has even been shown to directly correlate to the progression and severity of the disease (Mclean *et al.*, 1999). The growth in literature surrounding the role of oligomers in neurodegenerative disease pathology has coincided with increasing levels of controversy surrounding mature fibrils in these disorders. It has been suggested that in some circumstances fibrils possess no toxic capabilities at all (Giannakopoulos *et al.*, 2003, Reixach *et al.*, 2004, Vieira *et al.*, 2007, Bucciantini *et al.*, 2002). Others suggest that the fibril may have a protective role to play, in that fibrillization would be an effective way for the cell to sequester potentially harmful protofibrils and oligomers (Lansbury, 1999). The formation of fibrillar plaques may be an end stage event of amyloid formation representing an evolutionary protection mechanism which attempts to stem the toxic effects of oligomeric species (Rottkamp *et al.*, 2002). Despite these theories there is still a substantial body of recent experimental evidence which fully demonstrates that amyloid fibrils are capable of causing cellular death in numerous situations (Pike *et al.*, 1991, Cohen *et al.*, 2006, Yoshiike *et al.*, 2007, Mossuto *et al.*, 2010, Xue *et al.*, 2009, Xue *et al.*, 2010). The true cytotoxic component involved in these extremely damaging and life treating diseases therefore is still to be fully elucidated.

1.2.4. Beneficial Protein Misfolding

While aggregation due to protein misfolding is responsible for the pathogenicity observed in several disorders it should be noted that the dysfunctional assembly of peptides does not always carry a negative consequence. Indeed the very formation of a MG may be classified as a protein folding anomaly yet we know that in this conformation various proteins can carry out dutiful functions such as those seen with α-lactalbumin (α-LA) (Permyakov and Berliner, 2000). Recently misfolded proteins have been shown to display new and uncharacterized properties which were previously unknown and act as an additional function to what was already known about them. When in complex with oleic acid (OA) several beneficial misfolded proteins have been shown to exhibit cytotoxicity towards tumour cells both *in vitro* and *in vivo* in addition to the normal housekeeping activities which they also provide (Håkansson *et al.*, 1995, Wilhelm *et al.*, 2009, Nakamura *et al.*, 2013).

Prion proteins have also been shown to contain beneficial properties in addition to the more commonly known detrimental consequences of their formation. Prions are a unique form of protein aggregation in that they are infectious agents capable of converting functional polypeptides into the nonfunctional prion forms (Chien *et al.*, 2004). There are three genetic criteria which need to be followed in order to establish whether an infectious agent is indeed a prion and not a virus or plasmid: (i) prion strains can reappear spontaneously at low frequency in cured cells, (ii) overexpression of the infectious protein increases the frequency of the prion phenotype, and (iii) a unique relationship exists between the prion state and mutation rate in the gene of the protein whereby a prion state may only be maintained in cells which express the gene of a specific protein (Krzewska and Melki, 2007). One particular prion which possesses a beneficial characteristic in the prion state is the *S. cerevisiae* yeast protein Sup35p. Sup35p is essential in translation termination and plays a key role in facilitating the read-through of stop codons (Chien *et al.*, 2004). Aggregation of the Sup35p protein to an amyloid state results in the formation of the prion [PSI^+] which renders the majority of Sup35p proteins nonfunctional and results in the increase of nonsense suppression levels (Alberti *et al.*, 2009). Despite this pernicious effect it is postulated that [PSI^+] may be beneficial towards the host. Polymorphisms to the Sup35p (M) domain lead to variations within the species which produce barriers to prion transmission (Bateman and Wickner, 2012). Furthermore, variations produced by [PSI^+] provide the means to produce

hidden genetic variation which can in turn lead to the acquisition of new heritable phenotypes. These new phenotypes can be exploited by the yeast cells allowing them to thrive in conditions that would normally be inhospitable (True and Lindquist, 2000).

1.3. Cancer

Multicellular organisms require cell proliferation in order to meet the requirements demanded of them for events such as embryogenesis, growth, adult tissue formation, and organ formation, to name but a few. The overall function of proliferation is to ensure the correct and identical reproduction of chromosomal DNA and thus preserve genetic information. The DNA of every eukaryotic cell is under continuous attack by various agents seeking to disrupt or damage its base pair integrity. If the DNA is damaged the cell can halt progression and remedy the problem or it can target that cell for apoptotic destruction (Kastan and Bartek, 2004). To do this the cell needs a mechanism to screen and identify DNA damage in a highly specific and effective way. Therefore the cell has developed a chain of checkpoints which temporarily stop progression through the cell cycle until the previous processes such as DNA replication and mitosis are assessed and deemed satisfactory (Hartwell and Weinert, 1989). On rare occasions cells gain the ability to deviate from the norm and continuously divide despite these regulatory mechanisms. These cells are known as cancer cells.

1.3.1. Mechanisms of Cancer

On a basic level cancer is a disease that arises when cells lose the ability to govern their rates of proliferation, subsequently resulting in the production of masses of cells all programmed to continuously divide (Lobo *et al.*, 2007). Originally, virtually all cancers were thought to acquire the same six 'classic' hallmarks which allow it to be deemed a true cancer (Hanahan and Weinberg, 2000). In more recent times these hallmarks have had additions made and we now see as much as ten true hallmarks of cancer. Each tumour promoting feature represented is targeted with unique and tailored therapies (outlined in Figure 1.3). The diverse nature of tumour cells and the numerous mechanisms they can employ to avoid detection, destruction,

and promote tumour growth and metastasis is the key reason this disease is so difficult to treat. Despite this there has been an increase in the emergence of new classes of drugs which specifically target different tumour promoting hallmarks allowing for better treatment of patients worldwide (Hanahan and Weinberg, 2011). On a global scale, cancer is responsible for every one in eight deaths and by the year 2020, an estimated 10.1 million people will die of a cancer related illness (Siegel *et al.*, 2013). As an umbrella term, cancer encompasses more than 100 distinct diseases associated with a plethora of epidemiological variables and risk factors and can affect almost every cell in the body (Stratton *et al.*, 2009). Under normal conditions any cell presenting abnormal DNA (a fundamental characteristic of every neoplasm) would be targeted for cell cycle arrest, chromatin remolding, DNA repair, or destruction via apoptosis (Kastan and Bartek, 2004). All cancers allow for the existence of an abundance of cells however, it is not as simplistic as this. In order to achieve this, cells must be programmed in such a way as to avoid or ignore signals designed to tell the cell to adhere, differentiate, or die (Rivoltini *et al.*, 2005).

In the tumour cell environment these regulators for optimal cell proliferation are weakened or switched off and 'tricked' into allowing cells to continuously divide to the point of tumour formation and metastasis (Whiteside, 2009). A number of key regulatory genes are activated or deactivated in response to cellular stresses. As mentioned previously, DNA damage can illicit cell cycle arrest or apoptosis however, other events such as hypoxia, mitotic spindle damage, and nitric oxide production can all trigger similar responses (Jin and Levine, 2001). The tumour suppressor gene p53 is one such molecule activated in response to such events and results in the activation of two separate apoptotic pathways, intrinsic and extrinsic (Haupt *et al.*, 2003). This transcription factor is vital for the stress management of eukaryotic cells and is upregulated via upstream p53 mediators, including protein kinases and Sumo-1 (Jin and Levine, 2001). p53 is imperative for the prevention of cancer however, its function is reminiscent of a double edged sword. On one hand it is vital in destroying damaged cells which may act as precursors for tumour cells. On the other hand, mutations to p53 have been detected in nearly all tumour types and are estimated to be involved in approximately 50% of all cancers, bestowing onto p53 the honour of being the most commonly mutated gene in human malignant cancers (Amundson *et al.*, 1998).

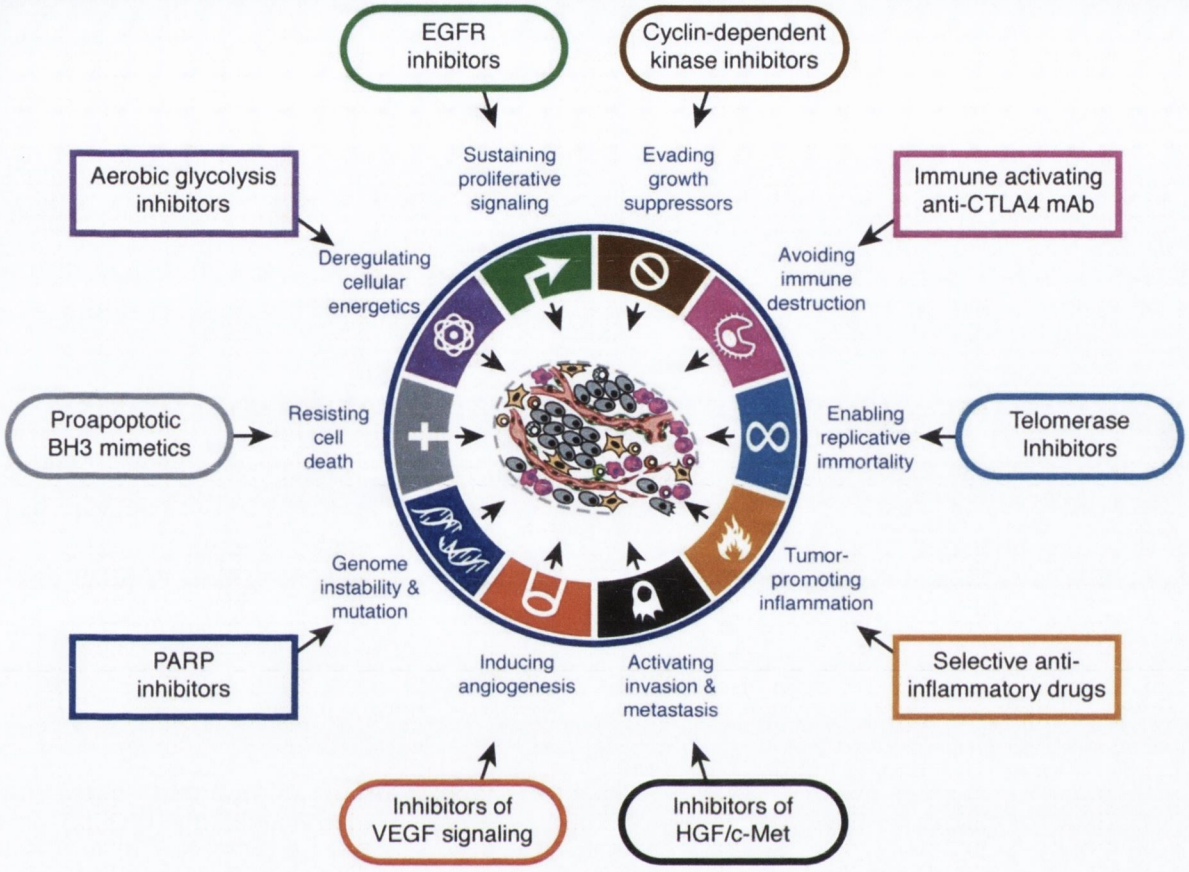

Figure 1.3 The hallmarks of cancer and targeted therapeutics

This figure highlights the six 'classic' characteristic features that a tumour cell can take on in order to survive and metastasize. These are apoptotic evasion, angiogenesis, sustained proliferation and growth, and the ability to invade neighboring cells and organs. In addition emerging aspects of cancer have also been added which include avoiding immune detection, promoting inflammation, genome instability/mutations, and deregulating cellular energetics. For each hallmark, specific drugs are designed to inhibit or circumvent the events occurring (Hanahan and Weinberg, 2011).

1.3.2. Cancer Metastasis and Immunological Avoidance

The role of a normal functioning immune system is to target and destroy pathogens before they have a chance to harm and spread through the body. Loss of immunological competence

may increase the likelihood of tumour progression within an organism. Individuals with lower natural killer (NK) cell activity have been shown to be at higher risk of developing cancer (Strayer *et al.*, 1986). The hosts' immune system is capable of mounting a combative response targeted at cancer cells as is evident by the presence of pre-existing antitumour cellular responses and tumour associated antigens in affected patients (Whiteside, 2010). Irrespective of the immunological competency of the host, tumour progression is a common feature of many cancers due to the ability of metastatic cells to evade the labyrinth of detection and destruction mechanisms employed by the immune system (Whiteside, 2009).

Tumours are generally classified as benign, where the tumour is non-invasive and can be removed through surgery, or malignant, where they can invade tissues and organs not directly located at the site of the tumour mass. Malignant cells not only invade neighbouring tissues but can also pervade the circulatory system, from where they can access distant organs and form secondary tumours (Mareel and Leroy, 2003). The progression from a single transformed cell to a mass of metastatic cells takes place over a subsequent period of time and is the end result of numerous genetic alterations occurring within the host species. As the tumour cells grow and divide they are initially recognized by the hosts' immune system and targeted for elimination. These cells are subsequently replaced by genetic tumour cell variants which are resistant to immune intervention. These new genetic variants give rise to a heterogeneous population of malignant cells which are responsible for the spread of the tumour. This lethal game of cat and mouse is reiterated for a prolonged period of time, the immune system attempting to restrict tumour growth while genetic modifications help the tumour cells avoid consequential elimination. The resulting tumour cell is resistant to immune effector cells and capable of producing tumour masses of cells with identical qualities (Whiteside, 2010).

Some tumour cells are able to suppress various aspects of the immune system which allows cancer to progress. One of the most extensively studied genes in tumour biology due to its facilitatory role in tumour progression is p53. Under normal circumstances p53 is activated in response to cellular stress. It is also stimulated as a riposte to oncogene expression (Schuler and Green, 2001) and plays a vital role in tumour suppression due to its ability to target cells for apoptosis (Bellamy, 1997). Loss of function mutations to this gene can therefore have a detrimental effect on the host as they allow cells to continuously divide and expand

(Amundson *et al.*, 1998). Due to the prevalence of nonfunctioning p53 in tumour progression, efforts to target this gene therapeutically have increased dramatically in recent years (Di Agostino *et al.*, 2008).

Despite huge advancements in our understanding of the biology of tumour cells, cancer targeted treatments still remain at an unacceptably low level in terms of efficacy. In fact, therapies which actually fully cure cancers are a scarcity in modern tumour medicine (Mukherjee, 2010). Presently there are three areas of therapy which have been the main strategies used to treat patients with cancer. From early in cancers history, up to present day, solid tumours have primarily been treated with surgery. In addition, the discovery of X-rays at the end of the nineteenth century added great weight in the battle to fight cancer and could be used jointly with surgery (Devita and Chu, 2008). In the mid 1940's, a pediatric pathologist named Sidney Farber demonstrated that aminopterin (a folic acid antagonist) could provide temporary remission for children with acute lymphoblastic leukemia (ALL), and so ushered in the dawn of chemotherapeutic drugs for the treatment of malignant cancers (Miller, 2006). More recently newer theories have emerged which have proved very successful in particular cancers. Antibody based therapy has become an established and highly successful treatment for patients with hematological malignancies and solid tumours (Scott *et al.*, 2012). Targeted therapies, where drugs are designed to interfere with specific molecular targets are also becoming popular. The use of imatinib mesylate (Gleevec), a drug which inhibits mutant kinases, has shown clinical progress in the treatment of chronic myeloid leukemia (Sawyers, 2004).

Despite the recent success of some of these treatments there are still major challenges in cancer therapy which are: (1) tumour initiating cells need to be identified and targeted in order to achieve complete remission, (2) the discovery of robust biomarkers for the prediction of therapeutic responses to a given therapy, and (3) the selective targeting of tumour cells for destruction (Pavet *et al.*, 2011). Perhaps the greatest problem with current treatments such as chemotherapy and radiation in particular is that they lack specificity for cancer cells. The holy grail of cancer therapy is to destroy tumour cells and tumour cells only while not harming other localized and non-localized cells. Tumour cells do display specific markers that could be isolated and identified by targeted drug therapy. Monoclonal antibodies can

target specific receptors on tumour cells however, their high molecular weight acts as a major drawback in this treatment (Shadidi and Sioud, 2003).

Even with the increasing repertoire of drugs available to treat cancer patients, drug resistance is still a major concern. Chemotherapy destroys many tumour cells but leaves behind a number of drug-resistant cells which can initiate tumour growth again, but this time with cells that are resistant to the previously used therapy (Gottesman, 2002). Key events involved in this process include altered membrane transport involving the P-glycoprotein product of the multidrug resistance (MDR) gene, altered expression of drug-metabolising enzymes, altered target enzyme, and increased drug degradation and drug inactivation. Currently the use of combinational drug therapies are being exploited more and more to overcome this problem (Luqmani, 2005).

1.3.3. Apoptotic Cell Death in Cancer Cells

In general, there are three morphologically different pathways of cell death, each of which is highly efficient and regulated. Necrotic cell death is often referred to as passive cell death and can arise from environmental perturbations resulting in the release of cellular inflammatory contents. Necrosis is also referred to as oncosis, as the term necrosis can sometimes be used to describe the sum of the cellular changes that have resulted in the death of the cell, regardless of the pre-lethal stage (Fink and Cookson, 2005). Necrosis, or oncosis, is characterised by the rupture of the plasma membrane following rapid cytoplasmic swelling (Krysko *et al.*, 2008).

In contrast to oncosis, apoptosis, or programmed cell death, is a more regulated and 'cleaner' method of cell death (Figure 1.4). The process itself is tightly ordered and controlled by numerous intracellular signals and caspases (Elmore, 2007). Cells undergoing apoptotic cell death display characteristic morphological changes including cell shrinkage, plasma membrane blebbing, karyorrhexis, chromatin condensation, and the formation of apoptotic bodies (Krysko *et al.*, 2008).

Although cell death is typically discussed dichotomously as either apoptosis or necrosis, other cell death mechanisms do exist that act distinctively from these main two. Autophagy

is similar to apoptosis but differs in the presentation of cellular material for degradation. In apoptosis, the cell is broken up into extracellular apoptotic bodies which compartmentalize the internal cellular contents (Elmore, 2007), which are subsequently destroyed by the body however, in autophagy the cellular components are degraded inside the dying cell itself in autophagic vacuoles (Fink and Cookson, 2005).

Recently, necroptosis has emerged as another alternative mechanism of cell death. As the name implies, necroptosis appears to bridge the two distinctly different pathways of necrosis and apoptosis, and can be regarded as a more controlled and regulated form of necrotic cell death which is dependent on receptor-interacting protein kinase 1 and 3 (RIPK1 and RIPK3) (Linkermann and Green, 2014). The activation of tumour necrosis factor (TNF)-α, stimulates TNF-α receptor 1 which subsequently leads to the formation of a complex of ubiquinated RIPK1 and RIPK3 and the induction of necroptosis (Christofferson and Yuan, 2010).

From a medical standpoint, and in particular in terms of therapy, a drug that induces apoptosis is far more desirable than one that activates necrosis (Gerl and Vaux, 2005). Due to the membrane damage and subsequent porous nature of the external cell structure incurred during necrosis, the cytosolic constituents spill out into the extracellular milieu and may provoke an inflammatory response from the host, unlike apoptosis where all the internal components are tightly and selectively packaged for destruction via macrophages (Proskuryakov *et al.*, 2003). Although the end stage of inflammation is usually favourable, it can have negative consequences on the host. Inflammation has been shown to be involved in the progression of certain cancers (De Martel and Franceschi, 2009) and can even negatively influence post-operative outcomes in particular cancer patients (Doyle *et al.*, 2010).

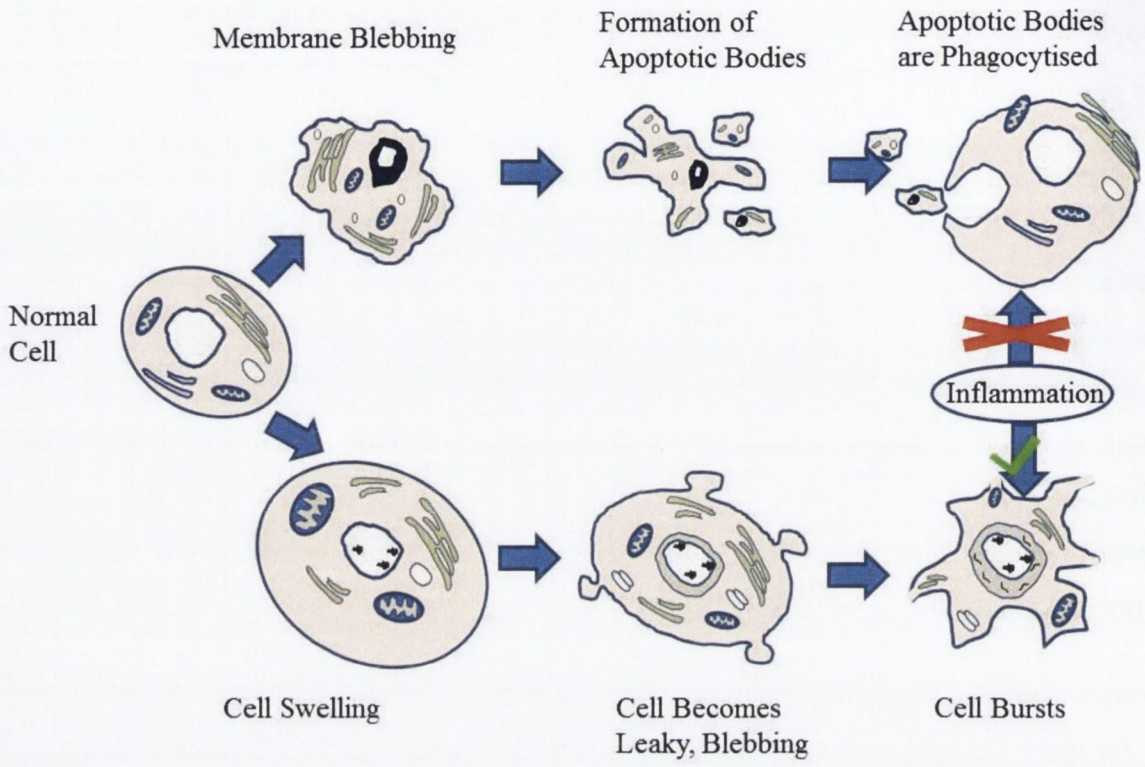

Figure 1.4 Structural changes of cells undergoing necrosis or apoptosis.

In the event of apoptotic cell death cells display cellular shrinking and membrane blebbing, karyorrhexis and eventually the formation of membrane-bound apoptotic bodies that contain organelles, cytosol, and nuclear fragments which are phagocytosed. Necrotic cells swell to a large size forcing them to become leaky and finally lyse, releasing their contents into the surrounding tissue. The process of apoptosis is a cleaner method of cell death and does not stimulate inflammation whereas necrotic cells induce an inflammatory response. Adapted from Van Cruchten and Van Den Broeck, 2002.

1.4. Protein Selective Cytotoxicity in Cancer: The HAMLET Case

Recently proteins have emerged as an unlikely answer to the problem of tumour cell specific targeting. Exogenous administration of viral-derived proteins have been shown to selectively induce death in tumour cells, as was seen with apoptin, which stimulated p53 dependent apoptosis in numerous tumour cell lines (Backendorf *et al.*, 2008). Additionally, a new group of protein-fatty acid (P-FA) complexes have recently emerged and have shown remarkable

selective cytotoxicity towards tumour cells in both *in vitro* and *in vivo* settings. This new class of drug consists of specific proteins with the ability to bind and sequester fatty acids (FA)s such as OA, which enables it to cytotoxically target a large number of tumour cells at a greater frequency than normal healthy cells.

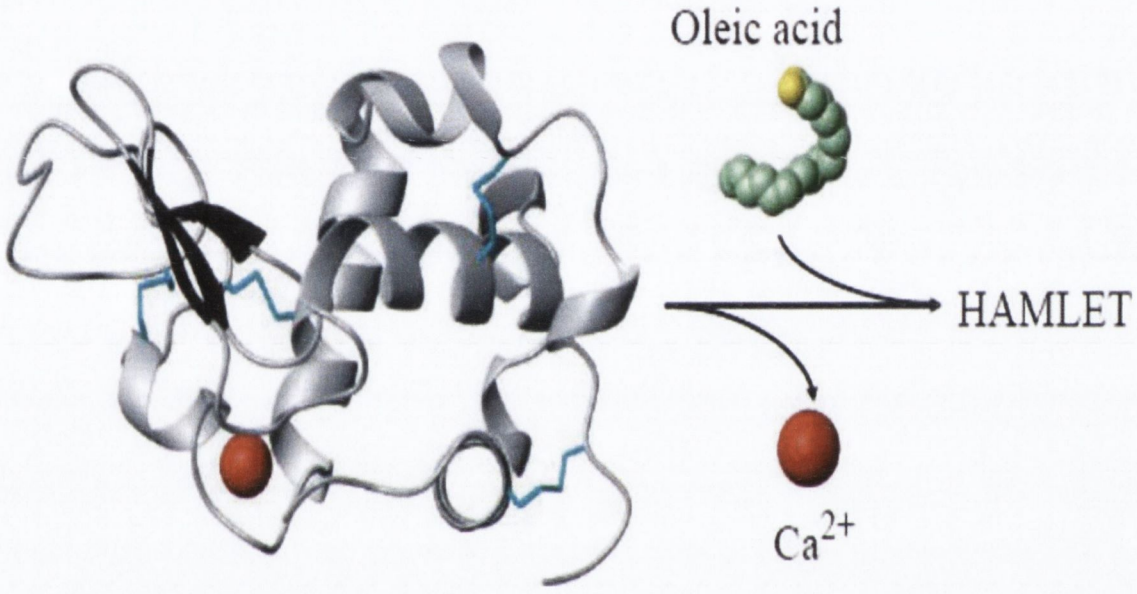

Figure 1.5 Schematic diagram of the HAMLET formation through the binding of OA. Under specific conditions, α-LA enters into a partially unfolded state, upon where it's Ca^{2+} ion dissociates, enabling OA to bind to form the tumouricidal complex known as HAMLET. Taken from Pettersson-Kastberg *et al.*, 2009a.

1.4.1. HAMLET: A Complex of α-LA and OA with Antimicrobial Effects

This new group of P-FA drugs began with the discovery of HAMLET (Human Alpha lactalbumin Made Lethal to Tumour cells). HAMLET (seen in Figure 1.5) is a tumouricidal protein complex of α-LA and OA (Svensson *et al.*, 2000). During an experiment investigating the effects of human breast milk on bacterial adherence in tumour cells, one of the casein fractions was shown to kill the cells via apoptosis. The active component of this complex was later identified as α-LA which had undergone partial unfolding towards a MG state

(Håkansson *et al.*, 1995). α-LA is an acidic milk protein that is involved in numerous interactions throughout the body. In mammary secretory cells, α-LA is one of the two components of lactose synthase which catalyzes the transfer of galactose from UDP-galactose to glucose, forming lactose (Brew *et al.*, 1968). The protein itself is small (14.2 kDa), and processes a single Ca^{2+} binding site which can also bind to Mg^{2+}, Mn^{2+}, and K^{+} (Permyakov and Berliner, 2000). Predominately (excluding rat) α-LA is comprised of 123 amino acid residues, forming two domains, one α-helical and one β-sheet. These domains are stabilised by disulphide bridges and connected by a Ca^{2+} binding loop (Anderson *et al.*, 1997). The α-LA molecule has become a model system for the study of protein folding due to its ability to form a classic MG state. Interestingly, α-LA has been shown to possess dual functionality by also displaying antimicrobial properties. Proteolytic digestion of α-LA by pepsin, trypsin and chemotrypsin resulted in the production of three polypeptide fragments which were active against Gram-positive bacteria (Pellegrini *et al.*, 1999). Studies have shown that breastfeeding reduces the severity and incidence of several infectious diseases such as bacterial meningitis, respiratory tract infection, bacteremia, and diarrhea (Rudan *et al.*, 2008, German *et al.*, 2002) and it has been proposed that HAMLET may be one of the of the contributing factors to this trend (Marks *et al.*, 2012). In bacterial cells treated with HAMLET, cell death was characteristic of apoptosis with mechanistic and morphologic similarities to apoptotic death in tumor cells (Hakansson *et al.*, 2011). Recently HAMLET has shown great potential as a novel antimicrobial adjuvant. Using both sensitive and resistant pneumococcal strains, HAMLET was shown to potentiate the antimicrobial effects of the antibiotics gentamicin, erythromycin and penicillin. HAMLET in combination with gentamicin and penicillin also eradicated pneumococci during nasopharyngeal colonization in a murine model whereas treatments without the P-FA did not, suggesting that HAMLET can potentiate the effect of antibiotics against strains resistant to the same antibiotic (Marks *et al.*, 2012).

1.4.2. HAMLET Mechanisms of Action

What makes HAMLET such a unique and exciting protein is that upon losing its native structure it gains a new and completely separate function which allows a normally innocuous protein to develop into an OA complex capable of selectively targeting tumour cells for

destruction whilst simultaneously leaving normal healthy cells relatively unharmed. HAMLET triggers cell death through a number of independent pathways (Gustafsson et al., 2005, Aits et al., 2009, Düringer et al., 2003).

1.4.2.1. HAMLET targets the nucleus of cells and forms insoluble complexes with histones

Regarding the exact mechanisms of action of HAMLET, it has been shown to interact directly with several intracellular components within tumour cells. One of the first studies probing the mechanistic characteristics of HAMLET found that it interacts with histones within the nucleus of tumour cells (Svensson *et al.*, 1999) and was only able to do so when in complex with OA (Mercer *et al.*, 2011). The interaction of HAMLET and the nucleus was crucial for the induction of DNA fragmentation since inhibition of nuclear uptake saved cells from DNA fragmentation (Düringer *et al.*, 2003).

The nuclear target molecules for HAMLET in cancer cells were identified as the histones H3, H4, H2A and H2B. Using real time confocal microscopy, Alexa-HAMLET was found to accumulate in the nucleus of tumour cells, whilst in normal healthy cells HAMLET translocated to the cytoplasm but did not interfere with the nucleus of the cell (Düringer *et al.*, 2003). Although binding to histones is not a unique feature of molecules, for example the nucleosome assembly protein, NAP-1, also binds to histones H2A + H2B and/or H3 + H4 (Ishimi *et al.*, 1987), this binding is reversible, whereas HAMLET binding is not. The high affinity that HAMLET possesses for these histones and the irreversibility of the interaction therefore blocks rather than promotes the assembly of chromatin thus leading to cell death (Düringer *et al.*, 2003).

Interestingly, when used in combination with histone deacetylase inhibitor (HDI), compounds used to target HDACs (histone deacetylases) which are generally overexpressed in tumour cells and involved in the acetylation/deacetylation of lysine residues in histone tails, HAMLET was shown to increase its cytotoxic effect (Brest *et al.*, 2007), suggesting that therapy involving a combination of HDIs and HAMLET could be a viable option for certain cancer treatments in the future.

1.4.2.2. HAMLET binds to the 20S proteasome.

Using confocal microscopy and co-immunoprecipitation HAMLET was also found to bind to the 20S proteasome (Gustafsson *et al.*, 2009). The proteasome is an integral instrument of cellular quality control and ensures that incorrectly folded proteins are targeted for degradation within the cell (Hilt and Wolf, 1995). Partially unfolded bovine α-LA is degraded *in vitro* by the 20S proteasome (Wenzel and Baumeister, 1995) and so it would be expected that HAMLET would also suffer the same result given its unfolded structure when in complex with FA. Upon treatment with HAMLET, vast amounts of the P-FA complex are permitted to enter the tumour cell and can be found in a variety of cellular locations (Mercer *et al.*, 2011). Despite this HAMLET remains untouched from this homeostatic powerhouse suggesting that the normal mechanisms employed by these cells to digest proteins are ineffectual against HAMLET.

HAMLET directly modified the structure of the α3 subunit which may have abolished proteasomal peptidase activity. The inhibition of proteasomal activity by HAMLET may have a 2-fold effect although which exact mechanism is still unclear. Firstly due to the dysfunctional interaction with HAMLET, the proteasome itself may go into a self-destruct pathway and terminate itself. Secondly, as it has previously been shown that low concentrations of FAs such as oleic and linoleic acid activate the proteasome (Watanabe and Yamada, 1996), the FA co-factor of HAMLET may stimulate the proteasome into action and this inadvertent activation may disturb the proteasomes structure (Gustafsson *et al.*, 2009).

1.4.2.3. HAMLET induces an apoptosis-like cell death response in cells

There is still some uncertainty regarding the exact cell death mechanism (or mechanisms) employed by HAMLET and other P-FA complexes. From the time of its original discovery, multimeric α-LA (MAL) (originally known as MAL at the time of discovery before it was later changed to HAMLET) was shown to induce apoptotic cell death in several mammalian cell lines and immature cells (Håkansson *et al.*, 1995). Numerous studies have thus been carried out investigating the exact mechanisms of cell death in response to HAMLET and have led to some intriguing discoveries. As mentioned, HAMLET induces apoptosis and has been shown to activate caspase-3-like and to a lesser extent caspase-6-like enzymes, enzymes

that are associated with apoptosis. HAMLET has also been shown to bind to mitochondria and cause cytochrome *c* (Cyto-*c*) release (Köhler *et al.*, 1999). Further experiments showed that treatment with HAMLET led to the formation of a permeability transition pore, which caused the release of Cyto-*c* into the cytosol and the possible activation of caspases (Kohler *et al.*, 2001).

Interestingly apoptosis does not seem to be the sole cell death mechanism utilised by the complex. Caspase inhibitors could not rescue cells treated with HAMLET suggesting HAMLET circumvents this integral step in the apoptosis cascade (Hallgren *et al.*, 2006). In addition to p53, another prominently mutated gene involved in tumour progression is the anti-apoptotic family of proteins known as Bcl-2 (Haupt *et al.*, 2003). Deletions or gain of function mutations to p53 as well as Bcl-2 overexpression could not rescue cells treated with HAMLET (Hallgren *et al.*, 2006). The fact that HAMLET kills cells independently of the caspase, p53, or Bcl-2 status of the cell suggests that this P-FA complex is able to successfully circumvent fundamental anti-apoptotic strategies that are employed by many tumour cells to avoid tumour clearance and to allow cancer cell growth. Mutated versions of these genes are often associated with drug resistance observed in patients treated with various chemotherapeutic drugs (Luqmani, 2005) and so HAMLETs ability to avoid this problem makes it a very promising therapeutic for the future.

BAMLET (Bovine α-Lactalbumin Made LEthal to Tumour cells) behaves similarly to its human counterpart also and induces caspase-independent apoptosis-like cell death in cancer cells (Hallgren *et al.*, 2006) and ectopic Bcl-2 expression failed to rescue the tumour cells (Rammer *et al.*, 2010). Furthermore, BAMLET was shown to activate a lysosomal cell death program in cancer cells. After rapid accumulation in the endolysosomal compartment of tumour cells BAMLET induced early leakage of lysosomal cathepsins which were released into the cytosol and are likely to contribute to BAMLET-induced cell death. In this way lysosomal membrane permeabilization may simply be an epiphenomenon of the death process (Rammer *et al.*, 2010).

1.4.2.4. Molecular targets of HAMLET

The broad range of tumour cell toxicity displayed by P-FA complexes in comparison to their ability to harm normal cells suggest that the different phenotype or morphology displayed by tumour cells makes them more sensitive to these proteinaceous complexes. HAMLET has been shown to directly interact with the membranes of cells and in doing so alters the membrane morphology and perturbs its structure resulting in increased membrane fluidity (Mossberg *et al.*, 2010c). The c-Myc oncogene was found to be a molecular target for HAMLET and a potential determinant of the sensitivity displayed by tumour cells to HAMLET (Storm *et al.*, 2011). This transcription factor is involved in promoting cell growth and proliferation, and also inhibiting terminal differentiation of most cell types, while also increasing the cells sensitivity to apoptosis (Pelengaris and Khan, 2003). Using a small hair (sh)-RNA screen, c-Myc was identified as a molecular target of HAMLET. Inhibitory c-Myc shRNAs which resulted in a reduction in c-Myc expression lead to cells becoming more resistant to the lethal effects of HAMLET. In addition to c-Myc, the glycolytic state of tumor cells was defined as a determinant of HAMLET sensitivity as extracellular glucose levels were shown to modulate the sensitivity of tumor cells to HAMLET. Furthermore HAMLET was also shown to bind to the glycolytic enzyme Hexokinase (HK) 1 using a high-content functional protein array and was shown to reduce its activity in cancer cells (Storm *et al.*, 2011). HAMLET binds to tumour cells and interacts with α-actinin-4, a molecule responsible for cell membrane integrity. This interaction causes tumour cells to become detached and increases cell death (Trulsson *et al.*, 2011). Ion channels, which are frequently dysregulated in human cancers (Nilius *et al.*, 2007) are essential in the initiation of HAMLET tumour cell death. HAMLET activates ion fluxes and ion channel inhibitors rescued cells from death (Storm *et al.*, 2013). Although these results suggest that HAMLET specifically interacts with ion channels and molecules located on the plasma membrane, whether this is a unifying feature for all P-FA complexes has yet to be determined.

1.4.2.5. HAMLET induces autophagy in tumour cells

In addition to apoptosis, autophagy has also been suggested as a method for cell death in tumour cells treated with the P-FA complex (Aits *et al.*, 2009). Autophagy is a fundamental and phylogenetically conserved process of self-destruction which takes place within a dying

cell. The process is characterised by several key events, most notably the formation of autophagosomes (double-layered vesicles) which surround intracellular contents which are subsequently delivered to lysosomes (Barth *et al.*, 2010). In mammals the process of autophagy is generally conserved for periods of short term starvation and is employed as a temporary survival mechanism. By degrading nonessential cellular components the cell can continue to survive by utilizing the broken down nutrients which are vital for biosynthetic reactions (Eskelinen, 2005).

Tumour cells treated with HAMLET displayed hallmark signs of autophagic cell death, such as double-membrane-enclosed vesicles, when visualised with TEM. Furthermore, HAMLET caused a significant reduction in mammalian target of rapamycin (mTOR) activity (Aits *et al.*, 2009), a key event responsible for negative regulation of the autophagy (Kim *et al.*, 2011). HAMLET was shown to cause LC3 translocation, a well-established marker of autophagosome formation and also increased the levels of Beclin-1, Atg5 and Atg7 mRNAs and Beclin-1 protein within the cell, all of which are intrinsically involved in the induction of autophagy (Aits *et al.*, 2009). This work is in contrast to previous studies examining the cell death pathways induced by HAMLET. From the time of its discovery, HAMLET has been shown to activate apoptotic cell death (Hakansson *et al.*, 2011, Hallgren *et al.*, 2008) however as has been suggested previously, HAMLET cell death is not dependent on apoptosis, as evident by the ability to kill cells regardless of the p53 and Bcl-2 status of the cells, and its ability to induce macroautophagy which may explain in part the broad tumouricidal effects of HAMLET.

1.4.3. Potential of HAMLET as a Future Treatment for Cancer.

As mentioned previously, standard treatments for cancer involve the use of radiation and chemotherapy which induce apoptosis in localized areas of infected cells. The most serious problems related to these forms of treatment is that they are non-specific and they need to be carefully administered and monitored but will inevitably result in numerous adverse effects such as anemia, fatigue, nausea, vomiting, to name but a few (Lenz, 2012). Another problem associated with these therapies is the cancer cells ability to avoid or evade apoptotic inducing signals activated by these treatments (McConkey *et al.*, 1996). HAMLET could be a potential

alternative to current treatments due to its ability to essentially avoid these problems. An interesting feature of HAMLET is that it is capable of inducing cell death irrespective of the tumour cells p53 and Bcl-2 cellular status. Caspase inhibition and Bcl-2 over-expression had no effect on prolonging cell survival whilst p53 deletions or gain of function mutations did not influence the HAMLET sensitivity of tumour cells (Hallgren *et al.*, 2006). As seen from Figure 1.3 HAMLET currently targets more than one hallmark of cancer. Its ability to target the proto-oncogene c-Myc (Storm *et al.*, 2011) indicates that it could also be used to treat those cancers which promote continued proliferation through the manipulation of growth signals. In addition to this HAMLETs ability to destroy tumour cells regardless of the Bcl-2 content or p53 status (Hallgren *et al.*, 2006) suggests that it could be used to target tumour cells which characteristically resist cell death signals. Furthermore HAMLET also appears to target tumour cells which display irregular cellular energetics as both ion channels (Storm *et al.*, 2013) and the often upregulated HK 1 molecule (Storm *et al.*, 2011) have all been shown to be targets for HAMLET. From this we can see that HAMLETs multifaceted approach to destroying cancers makes it a very diverse and intriguing potential drug candidate.

1.4.4. HAMLET has Shown Success in Both in vivo and in vitro Studies

HAMLET has been shown to induce apoptosis-like death in over 40 tumour cell lines to date, whilst having little effect on the majority of healthy cells tested (Mok *et al.*, 2007). To further demonstrate the selective efficacy of HAMLET in treating cancer, the P-FA complex has also been used in a number of clinical studies. The first experiment which examined HAMLET's potential as a therapeutic drug looked at the efficacy of the protein complex on skin papillomas, a tumour of the skin caused by transformation of keratinocytes via the human papillomavirus (HPV). In this case, HAMLET was topically applied versus a placebo control in a randomized double-blind study involving 40 patients. The lotion was applied for a period of three-weeks, and then 38 of the patients were assessed after 2 years. In the HAMLET treated group, tumour reduction was significantly higher compared with those treated with a placebo and in all cases no adverse effects were registered (Gustafsson *et al.*, 2004).

Bladder cancer has also showed sensitivity towards HAMLET in both murine and human models. C57BL/6 mice with established MB49 bladder tumours received five intravesical HAMLET instillations and the tumour size was measured using histology and live body imaging (Mossberg *et al.*, 2010a). In the human model, a week before scheduled surgery, nine patients received five intravesical instillations of HAMLET daily and again HAMLET was shown to have a cytotoxic effect on these cells (Mossberg *et al.*, 2007). In both models tumour size was decreased when compared to the control groups of just the native protein alone. In the human bladder cancer model, cell shedding dramatically increased over the course of the week when compared to control. In mice, size reduction was accompanied by a delay in the onset of tumour development. Interestingly for both these studies HAMLET was shown to induce apoptosis in tumour cells (Fischer *et al.*, 2004, Mossberg *et al.*, 2007).

Intratumoural administration of HAMLET was shown to prolong survival in a human glioblastoma xenograft model. HAMLET at 0.7 mM (10 mg/ml) was administered to nude rats explanted with a human glioblastoma hourly over a period of 24 h. These rats showed reduced tumour burden and a reduction in the onset of pressure symptoms when compared to a non-treated group (Fischer *et al.*, 2004).

More recently, mice which carry a mutation leading to the development of sporadic human colorectal tumours were used as a model for the development of the human disease. These mice were treated with pre-oral administrations of HAMLET which reduced the tumour burden and prolonged survival when compared to the control (Puthia *et al.*, 2013).

1.5. Alternative P-FA Complexes

HAMLET is the first protein to exhibit not only a well-defined function while in the native fold but also a gain of function while in the partially unfolded state (Pettersson-Kastberg *et al.*, 2009a). Moonlighting proteins such as extracellular signal-regulated kinase (ERK)-2 in humans are macromolecules capable of performing multiple autonomous functions without partitioning these functions into different protein domains (Huberts and Van Der Klei, 2010) but unlike HAMLET-like complexes, they do not undergo partial unfolding to acquire new functionality (Pettersson-Kastberg *et al.*, 2009a).

HAMLET was the first of these tumouricidal assemblies to be identified and since then other P-FA complexes have been shown to display similar efficacy and methodology. BAMLET, the bovine counterpart of HAMLET, has demonstrated almost identical specificity and efficacy towards various tumour cell lines. The complex is formed using calf's milk in exactly the same method as its human equivalent (Rammer *et al.*, 2010, Svensson *et al.*, 2003a). Species variation does not appear to be an issue for the formation of this cytotoxic complex as equine, porcine, and caprine α-LA-FA assemblies can all be formed and display similar efficacy and structural composition to that observed in the original HAMLET complexes (Pettersson *et al.*, 2006). The similar homology and mechanistic properties, the relative simplicity in acquiring, and the comparatively cheaper cost make BAMLET a potentially better option from a cost productive therapeutic aspect, in particular from a laboratory based view, as experiments can be carried out at a fraction of the cost and speed, which is why we predominately utilised this product as an alternative to HAMLET.

1.5.1. The Formation of HAMLET

The P-FA complex is purified by anion exchange chromatography and eluted using a high salt gradient (Svensson *et al.*, 1999). Other attempts at generating the complex have been tested such as direct mixing of OA and α-LA. It was originally suggested that direct mixing of protein and OA was unable to yield a functioning tumouricidal complex (Svensson *et al.*, 2000) however, several groups since then have been able to generate functioning complexes via direct mixing (Tolin *et al.*, 2010, Kamijima *et al.*, 2008). The formation of HAMLET using a column follows a two-step procedure (shown in Figure 1.6). During anion exchange chromatography, the low pH precipitation results in the dissociation of the Ca^{2+} ion, which in turn leads to α-LA entering into a partially unfolded state. While in this apo-conformational state, the protein has increased affinity for the OA molecule (C18:1 9-cis), the binding of which results in the formation of the P-FA complex (Pettersson-Kastberg *et al.*, 2009b). In this complexed state HAMLET is said to be a kinetically trapped conformer in that it has irreversible functionality and is less stable than the native protein alone (Fast *et al.*, 2005).

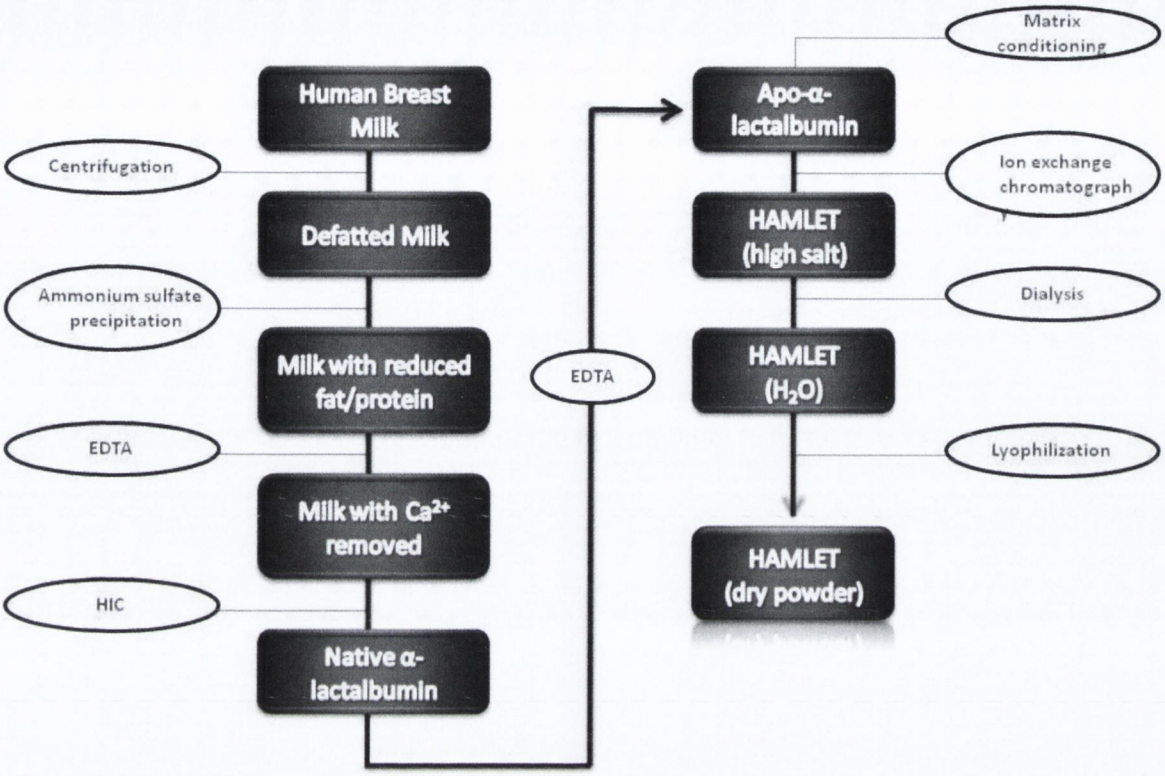

Figure 1.6 Flow chart of the production of HAMLET using IEC.

Under specific conditions, α-LA enters into a partially unfolded state, upon where it's Ca^{2+} ion dissociates, enabling OA to bind to form the tumouricidal complex known as HAMLET. Adapted from Mossberg *et al.*, 2010b.

1.5.2. Cytotoxic Component of P-FA Complexes

One of the key unresolved questions related to these P-FA complexes is regarding their true cytotoxic component. It remains unclear thus far whether the injurious nature of this FA assembly is a result of the proteinaceous component, the OA or whether the two elements act synergistically (Brinkmann *et al.*, 2011a). Despite the initial suggestion that α-LA was the cytotoxic component of this complex, and although still not fully resolved, this idea has changed dramatically in recent years and it is now thought that the FA molecules may be the true toxic entities involved. As mentioned previously α-LA from different species has been

shown to exert cytotoxic effects on malignant cells when in complex with OA (Pettersson *et al.*, 2006). A point of interest that I wanted to address was whether different proteins, under certain conditions, could form similar complexes which would exhibit similar potency and selectivity.

Although different taxa of α-LA have been shown to be cytotoxic, it wasn't until the discovery of equine lysozyme-OA (ELOA) that the idea first emerged that the protein component may not be as important as once thought. Equine lysozyme (EL) is a protein expressed in bacterial cell walls and is involved in the hydrolysis of peptidoglycan residues. This protein can be successfully bound to OA and in this state demonstrates similar cytotoxic effects to HAMLET. EL has close structural homology to both human and bovine α-LA, and similarly can become partially unfolded under denaturing conditions (Wilhelm *et al.*, 2009). Although lysozyme is still structurally similar to α-LA, this complex demonstrated that proteins of different functions could form tumouricidal entities, displaying selective killing.

Since the discovery of ELOA, other P-FA complexes have been generated. Complexes formed from fragments of bovine α-LA obtained via proteolysis, induced apoptosis in Jurkat tumour cells (Tolin *et al.*, 2010). Furthermore, Nielson *et al.*, demonstrated that ELOA interacted with the cell membrane in a similar way as OA alone, yet no membrane interactions were recorded using protein alone leading to the suggestion that the lysozyme acted as a carrier for the OA component (Nielsen *et al.*, 2010). β-lactoglobulin (β-LG) has also been shown to form tumour specific cytotoxic complexes via high performance liquid chromatography (HPLC) with sodium oleate (SO), the salt form of OA. This complex displayed similar properties to BAMLET, in that it induced apoptotic cell death, co-localized in the nucleus, and was less toxic towards healthy cells when compared to tumour cells (Lišková *et al.*, 2011). Serum albumin and the maltose binding protein have also displayed the ability to form a FA complex (Agger and Bro, 2009) while pike parvalbumin, a small globular cytosolic Ca^{2+}-binding protein of the EF-hand superfamily was also shown to make a cytotoxic complex (Permyakov *et al.*, 2012).

The most recent study examining other P-FA complexes used canine milk lysozyme, apo-myoglobin (AMb), and β_2-microglobulin to form HAMLET-like complexes all displaying tumouricidal capabilities (Nakamura *et al.*, 2013). Furthermore in addition to different

unrelated proteins showing the same cytotoxic selectivity against cancer cells, the OA content of P-FA complexes appears to be related to the overall toxicity observed. Increasing the OA content of the P-FA complex has been shown to be directly linked to an increase in injury towards tumour cells (Permyakov *et al.*, 2012). The results over the past years clearly suggest that the protein is not the integral part of this cytotoxic jigsaw and that the only common denominator throughout which enables the complex to acquire cytotoxic properties is the presence of a FA molecule. When not in complex the native proteins are not toxic towards cells as was seen with the disulfide-free *all*-Ala mutant of α-LA, which was able to adopt a MG state yet was not cytotoxic until joined to OA (Pettersson-Kastberg *et al.*, 2009b). The fact that OA possesses cytotoxic capabilities on its own further suggests that the proteins act a carrier for the FA molecules which allows them to circumvent solubility issues and gains them access to cells in large quantities, something that would be otherwise unlikely (Fontana *et al.*, 2013).

1.5.3. Cytotoxic Capabilities of FAs

FAs have long been intrinsically linked to cancer, particularly with regard to dietary intake. Despite the body of work compiled, the true nature of FAs with regards tumours is not fully understood. Eskimos who consume essential FA-rich diets show decreased levels of cancer incidence (Lancet, 1983). Conversely, there is also strong evidence to suggest that a high intake of dietary fats can increase the likelihood of cancer, in particular breast cancer in women (Macrae, 1993). There have been several studies examining the cytotoxic effects of FAs against a variety of malignant cell lines (Begin *et al.*, 1989, Cornelius *et al.*, 1991, Scheim, 2009). Although FA is toxic against cells, the type of cell, the concentrations needed, and the type of FA required for cytotoxicity vary greatly. In non tumour cells such as cytotoxic T lymphocytes, cis-unsaturated FA has been shown to perturb the plasma membrane lipid order resulting in cell death (Anel *et al.*, 1993). This is further supported in other studies (Lima *et al.*, 2002) which also demonstrated that different types of unsaturated fats were toxic towards B-cells as well. FA also induces cell death in Ehrlich ascites tumour cells and melanoma cells (Dymkowska *et al.*, 2004, Andrade *et al.*, 2005). Furthermore, FA has generally been shown to induce cell death through an apoptosis death pathway (Nikolakopoulou *et al.*, 2013, Kaya-Dagistanli *et al.*, 2013, Kant *et al.*, 2012, Artwohl *et al.*, 2009) which is in keeping with what we see in HAMLET and HAMLET-like complexes.

The FA component of P-FA assemblages, OA, has been shown to possess tumouricidal abilities on its own (Cury-Boaventura *et al.*, 2004, Kimura, 2002, Zhu *et al.*, 2005), which makes it an intriguing potential candidate as the true injurious element of these proteinaceous-FA complexes. OA has 18 carbon atoms and one double bond in the carbon-9 position (18:1) and is the most common monoenoic fatty acid in plants and animals. Interaction of OA to the cell membrane can result in changes in membrane fluidity which may in turn lead to changes of membrane protein functions. As suggested previously, the protein moiety does not act as a critical and unique partner in a bioactive OA-complex and acts more as a carrier for the normally insoluble OA. Spolaore *et al.*, demonstrated that the addition of the protein resulted in the dramatic transition of the OA molecule into one that was more water-soluble and smaller in size (Spolaore *et al.*, 2010a). Recent experiments have demonstrated BAMLET became more toxic to malignant cells as the OA content of the complex was increased suggesting that the FA content of the complex may be directly correlated with their ability to kill tumour cells (Brinkmann *et al.*, 2011a).

1.6. Hypothesis and Aim

This work has three hypotheses. Firstly is it possible to engineer novel P-FA complexes which display tumouricidal selectivity similar to HAMLET; secondly can BAMLET attenuate tumour progression in a melanoma model and does it alter the immune system in doing so; and finally can pure oligomers and fibrils be isolated from innocuous HEWL, and do these proteinaceous species differ in their characteristic and mechanistic properties.

The specific aims of the research are as follows:

- Engineer novel P-FA complexes which differ in their protein components and examine their cytotoxic mechanisms on a PC-12 cell model representing differentiated and undifferentiated phenotypes of the same cell.

- Investigate the potential of BAMLET as a single and combinational treatment against melanoma using a murine model, and to establish if it interacts with the immune system.

- To develop and isolate oligomers and mature fibrils from HEWL using a modified separation technique and a battery of characterisation approaches.

- Examine the injurious nature of oligomers and fibrils and determine whether they have an effect on memory and learning.

2. Materials & Methods

2.1. Reagents

All laboratory chemicals and reagents were purchased from Sigma Chemical Company (MO, USA) unless otherwise stated. Solid reagents were weighed using a Classic Plus electronic balance (Mettler Toledo LLC., OH, USA) or a Fisher MH-124 fine electronic balance (Thermo Fisher Scientific Inc., MA, USA). The pH of solutions was measured using a SevenEasy pH metre (Mettler Toledo LLC., OH, USA). Gilson pipettes were used to transfer liquid volumes up to 1ml, Gilson electronic pipette aids (Gilson S.A., France) and disposable Pasteur pipettes (Sarstedt Ltd., Wexford, Ireland) were used for volumes greater than 1 ml.

2.1.1. Cell Culture Medium

Roswell Park Memorial Institute (RPMI) 1640 medium (Lonza, Basel, Switzerland), and Dulbecco's modified Eagle's medium (DMEM) (Lonza, Basel, Switzerland) supplemented with 10% foetal calf serum (FCS) (Invitrogen., CA, USA), 100 mM L-glutamine (Invitrogen., CA, USA), 100 µg/ml penicillin/100 µg/ml streptomycin (Pen/Strep) (Invitrogen., CA, USA).

2.1.2. Thioflavin T (ThT) Buffer Solution

10 mM KH_2PO_4

150 mM NaCl

pH 7.0

2.1.3. ThT Stock Solution

1 ml of ThT buffer solution to 8 mg ThT

2.1.4. ThT Working Solution

1 in 50 dilution of ThT stock solution to ThT Buffer Solution

2.1.5. CR Buffer Solution

5 mM KH_2PO_4

150 mM NaCl

pH 7.4

2.1.6. CR Working Solution

1 ml of CR to 7 mg CR

2.1.7. CR Birefringence Solution

80% ethanol to 20% water solution to which a saturating amount of NaCl was added

Saturating amount of CR added

0.05% sodium azide

2.1.8. 1-anilinonaphthalene-8-sulfonic acid (ANS) Buffer

5 mM Tris buffer

pH 7.4

2.1.9. 1X Annexin Binding Buffer

10.9 mM Hepes

140 mM NaCl

2.5 mM $CaCl^2$

pH 7.4

2.1.10. PI Working Solution

50 µg/ml PI in PBS

2.1.11. Tris Buffer A

10 mM Tris/HCl

pH 8.5

2.1.12. Tris Buffer B

10 mM Tris/HCl

1 M NaCl

pH 8.5

2.1.13. TEM 2X Fixing Solution

10 ml 16% paraformaldehyde

4 ml glutaraldehyde-EM Grade-25%

6 ml 0.666 M HEPES

pH 7.5

2.1.14. 10 mM Biotin Solution

2 mg biotin

590 µl DMSO

2.1.15. 2X Laemmli Buffer

4% SDS

10% 2-mercaptoethanol

20% glycerol

0.125 M Tris HCL

pH 6.8

2.1.16. 4X Sample buffer

0.25 M Tris-HCl pH 6.8,

8% SDS,

30% glycerol,

0.02% Bromophenol Blue

0.3 M DTT

2.1.17. 8% Resolving Gel

4.6 ml H_20

2.7 ml 30% acrylamide mix

2.5 ml 1.5 M Tris (pH 8.8)

100 µl 10% SDS

100 µl 10% ammonium persulfate

6 µl TEMED

2.1.18. 15% Resolving Gel

2.3 ml H_20

5 ml 30% acrylamide/bisacrylamide

2.5 ml 1.5 M Tris (pH 8.8)

100 µl 10% SDS

100 µl 10% ammonium persulfate

4 µl TEMED

2.1.19. 5% Stacking Gel

1.4 ml H_20

330 µl 30% acrylamide/bisacrylamide

250 µl 1 M Tris (pH 6.8)

20 µl 10% SDS

20 µl 10% ammonium persulfate

2 µl TEMED

2.1.20. Running Buffer

25 mM Tris base

190 mM glycine

0.1% SDS

2.1.21. Transfer Buffer

25 mM bicine

25 mM Bis-Tris

1 mM EDTA

50 μM chlorobutanol

1L H_2O

2.1.22. TBS-T

2.42 g Tris base

17.5 g NaCl

2L H_2O

2 mL Tween

2.1.23. 5% Non-Fat Milk/TBS-T

0.5g Marvel milk powder (Cadbury, Birmingham, UK)

10mL TBS-T

2.1.24. Immunofluorescence Blocking Buffer

5% FCS

0.15% Triton X-100

1 L PBS

2.1.25. Immunofluorescence Antibody Blocking Buffer

2% BSA

4% FCS

0.1% Tween

1 L PBS

2.1.26. CD3 Antibody Solution

8.4 µl antiCD3

2.8 ml PBS

2.1.27. EDTA (200 µM)

0.0093 g of EDTA

Dissolved in 50 ml Baxters Water

2.1.28. ELISA Developing Solution

1 OPD tablet dissolved in 25 ml of phosphate citrate buffer

7 µl of hydrogen peroxide H_2O_2

2.1.29. ELISA Washing Buffer

1X PBS

0.2% Tween

2.1.30. ELISA Blocking Buffer

1% w/v Bovine serum albumin (BSA)

Dissolved in 1 X PBS

2.1.31. ELISA Stopping Solution

1 M H_2SO_4

2.1.32. Phosphate Citrate Buffer

10.19 g Anhydrous citric acid

36.69 g $Na_2HPO_4.12H_2O$

Made up in 1 L of dH2O, pH 5

2.1.33. Phosphate Buffered Saline (PBS) 10X

Sodium chloride (NaCl, 1.4 M)

Sodium hydrogen phosphate (Na_2HPO_4, 100 mM)

Potassium dihydrogen phosphate (KH_2PO_4, 18 mM)

Potassium chloride (KCL, 27 mM)

Dissolved in 1 L of dH_20, pH 7

2.1.34. MACS Buffer

2% FCS

5 ml 200 μM EDTA

Made up in 500 ml 1X PBS

2.2. Cell Culture

All cell culture media was purchased from Gibco® and all cell culture plastics were purchased from Starstedt Ltd. (Wexford, Ireland) unless otherwise indicated. Cell culture was carried out in a dedicated cell culture room which was regularly cleaned and sterilised. Cell culture was carried out in a Grade II laminar hood using aseptic technique while wearing a clean lab coat with elasticized cuffs and disposable latex gloves. The cabinet was cleaned with 70% (v/v) ethanol before and after each use and all reagents, media and plastics taken inside the cabinet were also cleaned in this manner. U2OS, a human osteosarcoma cell line expressing wild type p53 and Rb but lacking p16, B16-F10 cells (just referred to as B16 cells), a mouse melanoma cell line, and PC12 cells, a pheochromocytoma cell line of the rat adrenal medulla, were used in this research. U2OS, PC12 and B16 cells were obtained from American Type Culture Collection (VA, USA). U2OS and B16 F10 cells were cultured in DMEM supplemented with 10% fetal calf serum (FCS) (heat inactivated unless otherwise stated), 1% Pen/Strep. Undifferentiated PC12 ($PC12^{undiff}$) cells were cultured in RPMI supplemented with 10% FCS, 1% Pen/Strep. Differentiated PC12 ($PC12^{diff}$) cells were cultured in RPMI supplemented with 1 % FCS, 1% Pen/Strep, and 0.01% nerve growth factor (NGF) (Invitrogen, CA, USA). All cells were cultured at 37°C in humidified incubator under ambient pressure air atmosphere containing 5% CO_2.

2.2.1. U2OS and B16 Cell subculture

Cell lines were examined daily using an inverted phase contrast Nikon microscope (Nikon Corporation, Tokyo, Japan) and subcultured upon reaching 80 – 90% confluency. When cells became sufficiently confluent, growth medium was decanted and cells were washed in phosphate buffered saline (PBS) to remove residual media. Cells were detached using 0.25% trypsin and 0.05% ethlyenediaminetetraacetic acid (EDTA) (Invitrogen, CA, USA) at 37 °C for several mins or until the cells detached from the surface. 10 ml of complete RPMI was then added to inactivate the trypsin and cells were washed by centrifuging them at 1200 revolutions per minute (rpm) using an Eppendorf 5804R Benchtop Centrifuge (Eppendorf, Hamburg, Germany). The media was removed and the pellet was seeded at appropriate densities into new flasks. For cellular assay use, U2OS cells were seeded at a density of $5x10^4$ cells/well in 96 well plates, and $10x10^4$ cells/well when using 12 well plates. B16 cells were

seeded at $1x10^6$ cells/well for use in 96 well plate and at a density of $2x10^5$ cells/well for 12 well plate use.

2.2.2. PC12 Subculture

$PC12^{diff}$ cells were centrifuged at 800 rpm at room temperature (RT) and resuspended in 10 ml of RPMI with no FCS. The cells were resuspended further with a 10 ml syringe (Thermo Fisher Scientific Inc, IL, USA) and 21G needle (Becton, Dickenson and Company., NJ, USA). A new aliquot of cells was prepared using RPMI media supplemented with 1% FCS and 0.01% NGF.). For differentiation to be achieved cells must be grown on collagen coated surfaces. When using 96 well plates, a cell density of $15x10^4$ cells/well was used while for a 12 well plate a cell density of $5x10^5$ cells/well was employed. The media was replenished every 2 days for a period of 8 days or until full differentiation was achieved. For $PC12^{undiff}$ cells, RPMI culture medium, 10% FCS, was replaced every 3 days. Cells were seeded at a density of $1x10^6$ cells/well in 96 and 12 well plates.

2.2.2.1. Collagen coating

Cell culture plates were covered with collagen (Invitrogen, CA, USA) for 24 h at 37°C in a sterile environment. After this time, collagen was removed and plates were washed X2 with 70% ethanol (v/v). Plates were further washed with sterile PBS (X3) and left to air dry in a laminar flow hood. Plates were now ready to be used.

2.3. Cell Counts

Cell counts were performed by diluting cells (1:1 to 1:20) in trypan blue and loading 10 µl of this mixture onto a disposable plastic haemocytometer (Hycor Biomedical, UK). Viable cells which do not stain with trypan blue appear white under a light microscope, whereas dead cells stain blue. Alternatively, in cases where discrimination of live and dead cells was required cell counts were performed in ethidium-bromide/acridine-orange (Sigma-Aldrich) at a 1 in 2 dilution and this mixture was loaded onto a neubauer glass haemocytometer (Hawsley). Using this method viable cells fluoresce green when viewed under a UV fluorescent microscope, while dead cells appear orange. The number of cells per ml was calculated using the following formula:

#cells in central square of haemocytometer x 10^4 x dilution factor = cells/ml

2.4. Cytotoxicity Assay

Immediately prior to experiment aliquots of solutions containing dissolved protein samples were added to dH_2O and applied to cells. P-FA complexes were prepared following guidelines in Table 2.1 and Table 2.2. An initial 10 mg/ml stock of P-FA complex was prepared and dilutions were carried out using dH_2O for assays. For HEWL aggregates, solutions of concentrations varying in the ranges of 20 μM to 300 μM (Table 2.3 and Table 2.4) were used. For cytotoxicity assays clear, flat-bottomed, 96-well plates were used. All cells were treated with a 100 μl solution of containing the proteinaceous component and desired media. Plates were incubated for desired time period at 37°C and cell viability was assessed using an Alamar Blue viability assay.

2.5. Alamar Blue Cell Viability Assay

Alamar Blue (Invitrogen., CA, USA) was used to determine cell viability. 10 μl of Alamar Blue reagent was added to 100 μl of HEWL/cell medium in the 96 well plates. The samples were immediately incubated for 4 h at 37°C in complete darkness. Resazurin, a non-fluorescent indicator dye, is converted to bright red–fluorescent resorufin via the reduction reactions of metabolically active cells. The amount of fluorescence produced is proportional to the number of living cells. Absorbance levels were measured using a SPECTRAmax Gemini XS Microplate Spectrofluorometer (Molecular Devices, CA,USA) (emission 540 nm, excitation 590 nm). Cell viability was expressed as a percentage of fluorescence absorbance in the aggregate-exposed cells in relation to untreated cells (taken as 100%). Each experiment was conducted in triplicate and calculated using Graphpad Prism 5 software.

Table 2.1 P-FA Concentration Table for U2OS and PC12^{diff} Cells.

P-FA Concentration (mg/ml)	P-FA (10mg/ml) (µl)	dH_2O (µl)	DMEM/RPMI (µl)	Total (µl)
0	0	28	322	350
0.01	0.35	27.65	322	350
0.02	0.7	27.3	322	350
0.05	1.75	26.25	322	350
0.08	2.8	25.2	322	350
0.1	3.5	24.5	322	350
0.2	7	21	322	350
0.4	14	14	322	350
0.8	28	0	322	350

Table 2.2 P-FA Concentration Table for PC12^{undiff} Cells

P-FA Concentration (mg/ml)	PFA (10mg/ml) (µl)	dH_2O (µl)	RPMI (µl)	RPMI+Cells (µl)	Total (µl)
0	0	28	147	175	350
0.01	0.35	27.65	147	175	350
0.02	0.7	27.3	147	175	350
0.05	1.75	26.25	147	175	350
0.08	2.8	25.2	147	175	350
0.1	3.5	24.5	147	175	350
0.2	7	21	147	175	350
0.4	14	14	147	175	350
0.8	28	0	147	175	350

2.6. Ion Exchange Chromatography (IEC)

Liquid chromatography or IEC was used to prepare various P-FA complexes and was performed using a Dionex Ultimate 3000 Pump (Thermo Fisher Scientific Inc, IL, USA). Proteins were run on a diethylaminoethonal (DEAE) - Fast Flow (FF) 5ml column (GE Healthcare, Buckinghamshire, UK). The column was first washed with Tris prior to beginning the chromatography procedure, the lines were purged for 1 min to remove any air bubbles and then conditioned by washing them with Tris buffer A at a flow rate 1 ml/min for 30 mins. 224 µl (200 mg) of OA ($C_{18}H_{34}O_2$; 282.5 D) was dissolved in 500 µl of 99.9% ethanol and vortexed for 30 secs. The OA-ethanol solution was then added to 5 ml of Tris buffer A which was then sonicated 30 secs (X10) using a SONOPULS HD2200 (BANDELIN Electronics, Berlin, Germany) (as per Section 2.18) at 4°C. The resulting sonicated sample was filtered through a 0.2 µM filter (Thermo Fisher Scientific Inc, IL, USA) before being loaded to the column at a flow rate of 0.5 mL/min. Once the column is loaded with OA, excess or unbound OA is removed by washing the column using a combination of Tris buffer A and Tris buffer B. The combination of buffers allows for a controlled increase in the salt gradient running through the column which results in the removal of any unbound OA within the column. After this, the lines were washed with Tris buffer A, flow rate 1 mL/min prior to loading with protein solution. A 10 mg/mL protein solution was prepared for each protein sample in 3 mL of Tris buffer A. This solution was vortexed and filtered through a 0.2 µM filter prior to loading. The filtrate was then loaded to the column at a flow rate of 0.5 mL/min. Using an identical program as before, we applied an increasing salt gradient using Tris buffers A and B (Figure 2.1). The chromatogram of the eluent was recorded at UV/Vis wavelength 280 nm. The fractions were identified as being in complex if they were eluted at high salt at approximately 60 mins. Each peak from the chromatogram was collected as a separate sample and stored for dialysis.

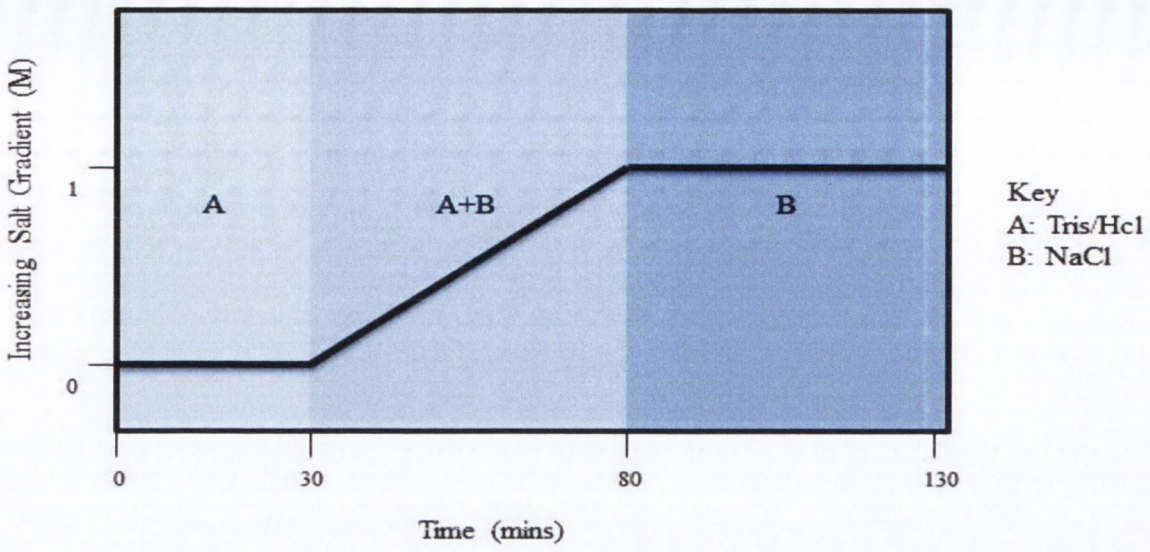

Figure 2.1 Salt gradient used to elute P-FA complexes.

IEC was carried out using DEAE-FF 5 ml columns preconditioned with OA. Complexes were first subjected to Tris buffer with no salt and at 30 mins, 1M NaCl was gradually introduced to elute the complex.

2.7. Dialysis

The fractions collected at approximately 60 mins were dialysed using SnakeSkin dialysis tubing with a 3.5 K molecular weight cut off (Thermo Fisher Scientific Inc, IL, USA). This tubing allows for desalting and buffer exchange to occur between samples which are in a high salt Tris buffer. Each fraction was dialysed for at 4°C for 24 h in 5 L of dH_2O which was changed after 12 h. This allowed for the removal of salt from the Tris buffer and for the removal of any small molecules less than 3.5 K in MW.

2.8. Freeze Drying

Once samples were sufficiently dialysed they were frozen and the water was removed from the solution using a FreeZone 1 L Benchtop Freeze Dry System (Labconc, MO,USA). The solution was lyophilised after reaching temperatures of -50°C leaving a pure protein sample

which contained the complex. The P-FA complex could then be resuspended in the desired buffer and concentration for immediate use when required.

2.9. HEWL Aggregation

Lysozyme was prepared in a dH_2O/HCl solution at pH 2 (protein and dH_2O altered with the addition of 4M HCl buffer). Final solution was amended to yield a final protein concentration of 1 mM (MR of HEWL=14.3 kDa, extinction coefficient = 26.4 at 280 nm for a 1 % (10 mg/ml) lysozyme solution). Aliquots of this mixture were incubated at 65°C for 21 days to allow sufficient fibrillization to occur. Control HEWL was maintained at 4°C for 2 days and displayed no signs of protein aggregation or cytotoxicity

2.10. HEWL Separation

In order to obtain the desired oligomeric and fibrillar fractions of lysozyme, 65°C HEWL aliquots was separated in relation to particle mass (Figure 2.2). 21 day old samples were ultracentrifuged for 1 h at 100,000 g using an Optima TLX Ultracentrifuge (Beckman Coulter Inc, CA, USA). The resulting pellet and supernatant were partitioned in order to obtain individual fractions. The pellet, containing mature amyloid fibrils, was resuspended in dH_2O/HCl, pH 2, to a protein concentration of 1mM. At this point, in order to ascertain sonicated samples, the mature amyloid fibrillar pellet was subjected to ultrasound power for 30 secs periodically for 5 mins. The supernatant was spun down via ultrafiltration, utilizing 100 kDa cutoff filters (Amicon Ultra-4 Centrifugal Filter Devices). The resulting filtrate was further separated by repeating the ultracentrifugation process with 30 kDa cutoff filters. The resulting retentate (>100 kD, <30 kD) constituted the oligomer solution. Both the highly soluble lysozyme oligomers and highly insoluble mature fibrils were diluted to a final concentration of 1 mM for use in cytotoxic assays. All samples were prepared fresh on day of experiments for immediate use.

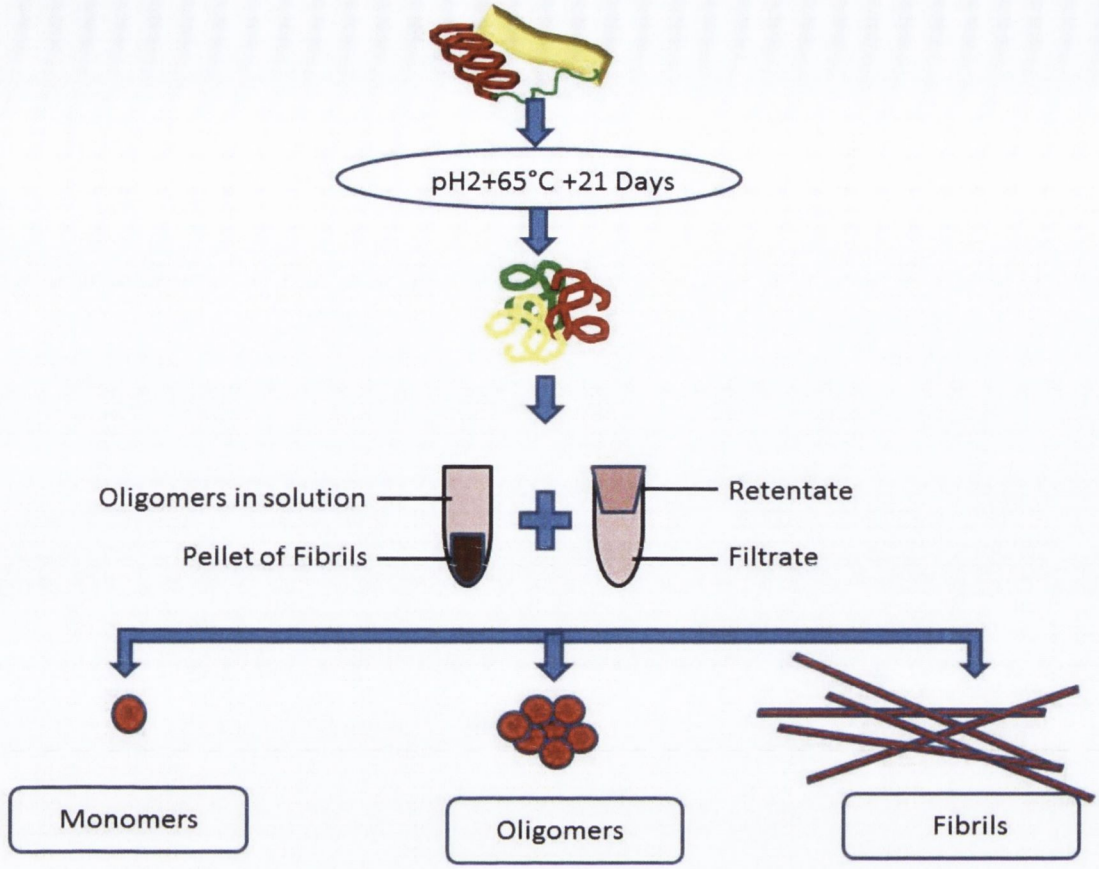

Figure 2.2 Schematic representation of process used to separate HEWL fractions.

HEWL (1 mM) native protein was incubated in pH2 buffer at 65°C for 21 days to allow aggregation to occur. After this time, the sample was separated into different weight based fractions using a combined combination of ultracentrifugation and ultrafiltration. The three resulting fractions, monomers, oligomers, and fibrils were then utilized as required.

Table 2.3 Concentration table for U2OS and PC12^{diff} Cells treated with HEWL aggregates.

Final Concentration (mM)	Aggregates 1mM (µl)	H_2O (µl)	DMEM/RPMI (µl)	Total (µl)
0	0	105	245	350
20	7	98	245	350
40	14	91	245	350
80	28	77	245	350
100	35	70	245	350
200	70	35	245	350
300	105	0	245	350
Control (100)	35	70	245	350

Table 2.4 Concentration table for PC12^{undiff} Cells treated with HEWL aggregates.

Final Concentration (mM)	Aggregates 1mM (µl)	H_2O (µl)	RPMI (µl)	RPMI+Cells (µl)	Total (µl)
0	0	105	70	175	350
20	7	98	70	175	350
40	14	91	70	175	350
80	28	77	70	175	350
100	35	70	70	175	350
200	70	35	70	175	350
300	105	0	70	175	350
Control (100)	35	70	70	175	350

2.11. ThT Assay

The fluorescent dye ThT (Acros Organics, N.V. Belgium) was used to monitor amyloid fibril formation of HEWL over 21 days, and was preformed according to protocol (Khurana *et al.*, 2005). Samples (10 µl) were added to 1 ml of ThT working solution. Samples were immediately mixed and measured using a FP 6200 spectrofluorimeter (JASCO International Co. LTD, Tokyo, Japan). Fluorescence intensity was measured by excitation at 440 nm (slit width 5 nm) and emission 482nm (slit width 5 nm), averaging over 30 secs.

2.12. CR Spectroscopic Analysis

CR-fibril binding was measured using standard protocol (Klunk *et al.*, 1999). CR (Acros Organics, N.V. Belgium) working solution was prepared by combining 7 mg of CR with 1 ml of phosphate buffer. This solution was passed through a 0.2 µM syringe filter (Anachem) immediately prior to use. 10 µl of the HEWL fraction was added to 1 ml phosphate buffer and 5 µl of CR working solution. This mixture was incubated at RT for 30 mins after which time the UV-Vis was measured using a NanoDrop ND-1000 Spectrophotometer between wavelengths 400 nm and 700 nm. A maximal spectral difference at 505 nm is evincive of amyloid fibrils.

2.13. CR Birefringence

CR birefringence is a highly sensitive method for the detection of amyloid fibrils (Puchtler *et al.*, 1962). Solution were prepared and mixed for 5 mins and then filtered through a 0.22 µm filter to remove any excess NaCl and CR. 10 µL of protein sample was air-dried on a glass microscope slide and 200 µl of the CR staining solution was added to each of these slides for 15 secs, before the excess was removed with a lint-free KimWipe. The final stained solution was then allowed to air dry at RT. These slides were analysed using a Nikon Eclipse E400 POL with polarisers crossed at a 90° angle to each other. The presence of a bright apple green colouration within the sample is indicative of amyloid fibrils.

2.14. ANS Binding

The fluorescence emission spectra of ANS with and without protein were recorded on a FP-6200 spectrofluorometer (JASCO International Co. LTD, Tokyo, Japan) at RT using excitation at 390 nm as per (Svensson *et al.*, 2000), emission between 410 nm and 600 nm, with the excitation and emission slits set to 10 nm. The protein (5 μM), the ANS (10 μM) and the ANS buffer were added to a quartz cuvette. The spectrofluorometer was auto zeroed against air and then blanked using the 5 mM Tris buffer. The buffer and ANS were measured and then followed by the buffer, ANS, and the protein. The buffer and ANS measurements were then subtracted to give the final readings.

2.15. Flow Cytometry

The day before analysis, $PC12^{undiff}$ cells were seeded at 10 x 10^5 cells/ml per well in uncoated 12-well suspension plates. $PC12^{diff}$ cells were seeded at 15 x 10^4 in collagen coated wells. For HEWL treated samples, wells were treated with 40 μM oligomer/sonicated fibrils/mature fibril solution and left for 24 h overnight at 37°C. For P-FA treated samples cells were exposed desired complex (see Table 3.4 for concentrations used) and left overnight at 37°C. Following incubation, 1 ml of cells was removed and spun down at 1600 rpm for 5 mins prior to washing (X3) in a 1X annexin binding buffer. Cells were resuspended in 100 μl 1X Annexin binding buffer, stained with 10 μl of anti-Annexin V antibody (IQProducts, Groningen, Netherlands) and left for 15 mins on ice in darkness. Once stained, cells were spun down, washed, and resuspended in 500 μl of 1X Annexin binding buffer. Immediately prior to FACS analysis, cells were treated with 10 μl PI working solution. The different light scattering properties exhibited by apoptotic and necrotic cells were analysed using an Accuri™ C6 FACSCalibur flow fluorocytometer (Becton, Dickenson and Company, NJ, USA). Cell size was determined using forward scatter while cell granularity was identified using side scatter of the laser light. Treated cells were co-stained with Annexin V-fluorescein isothiocyanate (FITC) (green fluorescence), a stain for apoptosis, as well as propidium iodide (PI) (far red fluorescence) which stains for necrotic or non-apoptotic dead cells. The X-axis corresponds to Annexin V staining while the Y-axis is indicative of PI staining. Control samples were prepared using untreated cells with no staining, double stained, and untreated

cells with PI or Annexin V staining only. These control samples were carried out in conjunction with dual staining of treated cells and used to compensate the samples.

2.16. Apoptotic/Necrotic/Healthy Cells Detection Kit

Cell death was also examined using a Live/Dead Detection Kit (PromoKine., Heidelberg, Germany). To induce sufficient levels of cell death for assaying, B16 cells and $PC12^{undiff/diff}$ cells were seeded at 1 x 10^6 cells/ml in 12 well plates and were then treated with P-FA complexes at different concentrations (Table 3.4 for PC12 concentrations and 0.08 mg/ml for B16 cells) and left to incubate for 24 h at 37 °C. After incubation, cells were washed in PBS and then washed again in 1X binding buffer. The cells were then resuspended at 5 x 10^5 cells/ml in 1X binding buffer. 500 µl of cell solution was removed and transferred to an Eppendorf. To this, 5 µl of Annexin V-FITC, 5µl of PI, and 5 µl of 4',6-Diamidino-2-Phenylindole (DAPI) was added and allowed to incubate at RT for 15 mins in the dark. After the incubation period, 20 µl of the solution was removed and added to a poly-L-lysine coated glass slide and covered using a glass cover slip and visulaised using immunofluorescence.

2.17. AFM Imaging

HEWL samples were prepared for t analysis by depositing the fibril suspension onto freshly cleaved mica by spin coating. The spin recipe encompassed a dispersion routine (750 rpm for 45 sec followed by 1000 rpm for 45 sec) allowing the fibril suspension to be spread evenly across the mica surface. Samples were then dried (4000 rpm for 15 sec) to remove any excess solvent. AFM measurements were performed in ambient conditions on an Asylum MFP-3D atomic force microscope (Asylum Research, Santa Barbara). The probe normal spring constant was between 1.2 - 2.0 *N/m* with a tip apex <5 *nm*. High resolution acoustically driven cantilevers (Nanosensors, SSS-FM) operating at a resonance frequency of 60-80 *KHz* in AC-mode were used with a scan resolution of 1024 x 1024 and scan frequency of 0.6 *Hz*. Structures were analyzed using MFP-3D IGOR PRO software.

The spin recipe encompassed a dispersion routine (750 rpm for 45 sec followed by 1000 rpm for 45 sec) allowing the fibril suspension to be spread evenly across the mica surface. Samples were then dried (4000 rpm for 15 sec) to remove any excess solvent. AFM measurements were performed in ambient conditions on an Asylum MFP-3D atomic force

microscope (Asylum Research, Santa Barbara). The probe normal spring constant was between 1.2 - 2.0 *N/m* with a tip apex <5 *nm.* High resolution acoustically driven cantilevers (Nanosensors, SSS-FM) operating at a resonance frequency of 60-80 *KHz* in ac-mode were used with a scan resolution of 1024 x 1024 and scan frequency of 0.6 *Hz*. Structures were analyzed using MFP-3D IGOR PRO software. The AFM were carried out in CRANN in collaboration with Eoin McCarthy and Professor John Boland.

2.18. Sonication

Samples were sonicated using a Bandelin Sonopuls HD2200. OA (MR=280.46 g/mol, density=0.895 g/mol) was resuspended in ethanol (100%) and sonicated for 30 secs at 50% amplitude 15 times. HEWL at 1 mM concentration was sonicated at 40% amplitude at 30 secs increments 15 times. For Western blotting, protein samples were sonicated for 5 secs or until foamy at amplitude power 50%.

2.19. *In vivo* Electrophysiology

In vivo electrophysiology was performed as described previously (Klyubin *et al.*, 2014). Animal experiments were licensed by the Department of Health and Children, Ireland. Adult male Wistar rats were anaesthetized with urethane (1.5 g/kg, i.p.). Single pathway recordings of field excitatory postsynaptic potentials (EPSPs) were made from the stratum radiatum in the Cornu Ammonis (CA1) area of the dorsal hippocampus in response to stimulation of the ipsilateral Schaffer collateral/commissural pathways. Test EPSPs were evoked at a frequency of 0.033 Hz and at a stimulation intensity adjusted to give a EPSP amplitude of 50% of maximum. The high-frequency stimulation (HFS) protocol for inducing LTP consisted of 10 trains of 20 stimuli, inter-stimulus interval 5 ms, inter-train interval 2 sec. The intensity was increased to give an EPSP of 75% of maximum amplitude during the HFS. LTP is expressed as the mean ± standard error of the mean (SEM). % baseline field EPSP amplitude recorded over at least a 30 min baseline period. Similar results were obtained when EPSP slope rather than amplitude was measured.

For statistical analysis, EPSP amplitudes were grouped into 10-min epochs. Standard one-way ANOVA was used to compare the magnitude of LTP between multiple groups followed by post hoc Tukey's tests. Unpaired Student's t-tests were used for 2-group comparisons. A $p<0.05$ was considered statistically significant.

To inject samples into the rat brain a cannula was implanted in the lateral cerebral ventricle (coordinates: 1 mm lateral to the midline and 4 mm below the surface of the dura) just prior to electrode implantation. Injections (15 µl over 10 min) were made via a Hamilton syringe connected to the internal cannula.

In vivo electrophysiology was carried out with the assistance of Dr. Igor Klyubin, and Professor Michael Rowan.

2.20. *In vivo* Tumour Studies

The *in vivo* anti-tumor efficacy of BAMLET and the synthetic toll like receptor 7/8 (TLR7/8) agonist were examined using a B16 melanoma model. B16 cells were injected into C57BL/6 mice at day 0. Typically, cells were cultured to a confluency of 70% and harvested during the log growth phase. Harvested cells were washed 3 times with sterile PBS, counted and the cell concentration adjusted to 2×10^6 cells/ml in sterile PBS. Mice were shaved and 100 µl of the tumour cell suspension was injected subcutaneous (SC) in the right flank. Tumour growth was monitored and tumour size measured every 2-3 days using callipers, measuring width and length of tumours.

For *in vivo* experiments examining the efficacy of BAMLET related to injection route, mice were randomly divided into 5 groups of six mice per cage following tumour induction. BAMLET was prepared on the day of each administration at concentrations of 0.7 mM and 1.5 mM. Mice were given a 100 µl injection via intraperitoneal (i.p) or SC route of either 0.7 mM or 1.5 mM BAMLET. Control mice ($n = 6$) received an SC injection of PBS. Mice were administered BAMLET on days 3, 7, 10, 14 post tumour induction and tumour growth was measured at days 11, 14, 17, 19, 21, 24, 26, and 28 with a sterile vernier calliper.

Work on this section of the project was carried out in conjunction with Dr. Neil Marshall from Professor Kingston Mills lab.

For *in vivo* experiments related to the use of BAMLET as a combination therapy with the TLR7/8 agonist Resiquimod (R848), mice were randomly separated into 5 groups of 7 mice/group. BAMLET was prepared on the experimental day at concentrations of 0.35 mM and 0.7 mM in PBS. R848 was prepared in 10% Dimethyl sulfoxide (DMSO) and added to PBS which was then used to make 0.7 mM BAMLET immediately prior to injection and vortexed to ensure adequate mixing. Mice were given a 100 µl injection via the SC route of either 0.35 mM, 0.7 mM BAMLET or 0.7mM-R848 combination. Mice were administered compounds on days 3, 7, 10, 14 post tumour induction and tumour growth was measured at days 11, 14, 17, 19, 21, 24, 26, and 28 with a sterile vernier calliper. For all mice *in vivo* experiments the long (L) and short (S) axis were recorded and tumour volume (V) was calculated using the following equation.

$V = S^2 \times L/2$

Mice were sacrificed when tumour size exceeded 15mm or tumours became ulcerous.

Work on this section of the project was carried out in conjunction with Lydia Dyck from Professor Kingston Mills lab.

2.21. Mice

Specific pathogen free six to eight week old adult female C57/Black mice were purchased from Harlan laboratories (U.K.). Mice were housed in sterile individually ventilated cages, food and water were provided ad libitum, in accordance with the standard operating procedures set down in SI 17/94 of the European Union. Mice were acclimatised for 1 week before the initiation of any *in vivo* experiments. Animals were killed by CO_2 if found to be in distress (hunching, failure to groom etc.) or if the tumour diameter reached a size greater than 15 mm. Ethical approval was obtained by the BioResources Committee, Trinity College, Dublin.

2.22. Western Blotting

2.22.1. Protein Extraction

PC12^{undiff} cells were seeded at appropriate density immediately prior to treatment. Cells were treated with different P-FA complexes or amyloid fibrils and left to incubate overnight for 24 h. Cells were removed and wells washed with PBS to remove any additional debris. The cell suspension was centrifuged at 800 rpm for 5 mins. The supernatant was removed and the pellet was washed with PBS and centrifuged in identical method. All of the supernatant was removed to yield a pellet. In order to prepare samples for running through the gel the cells were lysed using a 2X laemmli buffer to release individual proteins. 140 µl of a 1:1 dilution of 2X buffer laemmli and PBS was added to each pellet and the sample was sonicated (Bandelin Electronics., Berlin, Germany).

2.22.2. Protein Concentration

Protein quantification was carried out using the commercially available Pierce Bicinchoninic (BCA) Protein Assay Kit (Thermo Fisher Scientific Inc, IL, USA). BCA reacts with the cuprous cation Cu^{+1} (a byproduct of the reduction reaction of Cu^{+2} to Cu^{+1}) to yield a purple-colored reaction product which exhibits a strong absorbance at 562 nm that is nearly linear with increasing protein concentrations over a broad working range. A standard curve was prepared using the supplied stock solution of bovine serum albumin (BSA) (2000 µg/ml) of 1000 µg/ml, 800 µg/ml, 600 µg/ml, 400 µg/ml, 200 µg/ml, 100 µg/ml, 50 µg/ml and 0 µg/ml. Immediately prior to assay, a working solution was prepared by mixing 50 parts BCA Reagent A (Na_2CO_3, $NaHCO_3$, bicinchoninic acid, $Na_2C_4H_4O_6$ (sodium tartrate) in 0.1 M NaOH) with 1 part BCA Reagent B (containing 4% $CuSO_4$). Using a 96-well plate 20 µl of standards and protein were plated in triplicate and 200µl of working solution was added to each. The plate was covered with tinfoil and left for 30 mins at 37°C after which the absorbance was measured at or near 562nm on a plate reader. Concentrations were used to determine final protein concentration to be added to gel wells prior to running. A 4X sample buffer was added to each sample to yield a final protein concentration of 20 µg. The samples were boiled for 2 min in a Stuart block heater (Bibby Scientific Limited, Staffordshire, UK)

at 100°C and dithiothreitol (DTT) was added to each sample to yield a final concentration of 50 mM.

2.22.3. Sodium Dodecyl Sulfate-Polyacrylamide Gel Electrophoresis (SDS-PAGE)

By using the detergent SDS and the reducing agent mercaptoethanol, proteins can be separated based on their molecular size when ran through a polyacrylamide gel. An 8% resolving gel with a 5% stacking gel was used for the separation and prepared immediately prior to use. Using the results obtained from the BCA assay, 25 µg of each protein was added to designated wells. A coloured molecular ladder was also added to allow determination of molecular size. The gel was placed into a running chamber and running buffer was added. The gel was ran for 30 mins at 80 V to allow proteins migrate through the stacking gel, and then for 120 mins at 120 V to allow good separation through the resolving gel. After the run has finished, the stacking gel is removed and the resolving gel is prepared for transferring.

2.22.4. Western Blot Analysis

Bound antibodies were detected using Western blot analysis. After the proteins have been separated using SDS-PAGE, they were blotted from the gel onto a polyvinylidene difluoride (PVDF) (Thermo Fisher Scientific Inc, IL, USA) membrane before been probed with antibodies and visualized. Using the semi-dry transfer method, the gel and 4 sheets of blot paper were placed in transfer buffer for 5 mins. The PVDF membrane was placed in methanol for 20 secs and then transferred to transfer buffer for 5 mins. Using a semi-dry transfer dock 2 sheets of blot paper were placed on the apparatus, followed by the PVDF membrane, the gel, and finally 2 sheets of blot paper. Any remaining bubbles were smoothed out and the transfer sandwich was ran at 10 V for 1 h. After transfer was completed, the PVDF membrane was washed using Tris buffer solution (TBS)-Tween for 5 mins at RT. The membrane was blocked using 5% non-fat milk/TBS-T for 1 hour at RT. The membrane was washed in TBS-Tween 3 times for 5 mins each, and then incubated in the primary antibody, diluted in 5% (w/v) Marvel in TBS-Tween on a shaker overnight at 4 °C. Three further washes for 15 mins each in TBS-Tween were carried out before incubation in horseradish peroxidise (HRP) conjugated secondary antibody (1:2,000 dilution in TBS-Tween) (Dako, Glostrup, Denmark)

for one hour on a shaker at RT. For Poly (ADP-ribose) polymerase (PARP) (eBioscience, Inc, CA, USA), anti-mouse infrared secondary antibody was diluted 1 in 10,000 in 5% Marvel/TBS-Tween/0.01% SDS and the membrane was incubated for 1 h at RT. After incubation, the membrane was removed and washed in TBS-Tween 3 times for 15 mins each. Infrared bound antibodies were visualised using the Odyssey® Infrared Imaging System (LI-COR., NB, USA).

Table 2.5 Antibodies used in Western blotting

Antibody	Supplier	Isotype	Type	Block	Primary Ab
PARP	eBiosciences	Mouse	Polyclonal	5% Marvel 1 hour, RT	1/2,500 o/n, 4°C
β-actin	Calbiochem	Mouse	Monoclonal	5% Marvel 1 hour, RT	1/20,000 1 hour, RT

2.23. Transmission Electron Microscopy (TEM)

U2OS cells were seeded at density of 5 x 10^4 cells per ml in 12 well plates. Cells were treated with 40 μM HEWL oligomer, sonicated fibrils, and mature fibrils and left for 24 h at 37°C. For BAMLET treated samples, cells were treated with 0.05 mg/ml of BAMLET and incubated for 24 h at 37°C. Control cells with no treatment were processed in identical manner to HEWL and BAMLET exposed cells. After treatment cells were trypsinised and centrifuged at 1200 rpm. The supernatant was removed and the pellet was washed in ice cold filtered PBS. The pellet was resuspended in 5 ml filtered PBS and added to 5 ml (2X) fixation solution to yield a final (1X) fixation solution. Incubate cells and fixing solution for 30 mins at RT. After this time, the cells were centrifuge at 1200 rpm, and then washed twice in ice cold filtered PBS. The resulting pellet was resuspended in 500 μl filtered PBS and transferred to an eppendorf tube. The samples were sent to CMA (Center for Microscopy and Analysis) for embedding and processing.

Amyloid fibril samples were visualized using a Jeol 2100 Transmission Electron Microscope operating at 200kv with a Lanthanum Hexaborise emission source. Prior to microscopy, a 1 in 1,000 dilution in buffer was carried out with the HEWL sample and 10 μl of this was deposited onto carbon coated grids. Solution was displaced with 0.5 % glutaraldehyde and

subsequently washed with dH_2O. Sample was stained using uranyl acetate and allowed to air dry before transferring to microscope.

2.24. Biotinylation of Protein

N-Hydroxysuccinimide (NHS)-Biotin (Thermo Fisher Scientific Inc, IL, USA) was used to biotinylate the primary amino groups ($-NH_2$) present in α-LA. For a 10 mg/ml solution of each P-FA complex with a ≥ 12-fold molar excess of biotin was used following the formula;

$$\text{ml protein x } \frac{\text{mg protein}}{\text{ml protein}} \text{ x } \frac{\text{mmol protein}}{\text{mg protein}} \text{ x } \frac{\text{12 mmol Biotin}}{\text{mmol protein}} = \text{mmol Biotin}$$

Using calculations above, appropriate amounts of 10 mM biotin solution were added to each P-FA complex, vortexed, and let incubate at RT for 30 mins immediately prior to treatment of cells. The cells were removed and washed with PBS (X3) to remove excess media.

At this point the cells were either used for Western blot analysis as per Section 2.22 or were prepared for immunofluorescence (Section 2.25).

2.25. Immunofluorescence

The uptake of biotinylated-protein complexes into $PC12^{undiff/diff}$ cells and the cell death mecahnisms employed were monitored using immunofluorescence. For biotinylated cells 25 µl of cells were placed onto poly-L-lysine coated glass slides (Thermo Fisher Scientific Inc., IL, USA) and left to air dry for 30 mins. Once cells had adhered to slide unbound were washed away with PBS (X3). 20 µl of immunofluorescence blocking buffer was placed onto cells and left for 1 h. Cells were washed in PBS (X3) to remove the blocking buffer after time had elapsed. Excess liquid was removed with a KimWipe. 20 µl of a 1/7,500 dilution of Alexa Fluor® 647 Streptavidin (BioLegend., CA, USA) to immunofluorescence antibody blocking buffer solution was added to cells and left to incubate o/n at 4°C. Antibody was removed by washing in PBS (X3). Excess liquid was again removed with a KimWipe and 3

µl of ProLong® Gold Antifade Mountant with DAPI (MolecularProbes., OR, USA) was placed directly onto the cells. A cover slide (VWR International LLC., PA, USA) was carefully lowered onto the mounting media coated cells at a 45° angle and was sealed in place along the edges and kept stored at 4°C in the dark unless being used. For the live/dead assay cells were visualised using a fluorescence microscope using the FITC ($\lambda_{abs}/\lambda_{em}$= 492/514 nm), PI ($\lambda_{abs}/\lambda_{em}$=528/617nm), and DAPI ($\lambda_{abs}/\lambda_{em}$=350/461 nm) filter sets. Green fluorescent plasma membrane staining identifies apoptotic cells, while necrotic cells are identified by red fluorescent nuclear staining. Late apoptotic cells may show green and red staining. For control, DAPI stained cells were treated with singe death stains (Annexin V and PI). All cell nuclei will be stained with DAPI (blue fluorescence). Dead cells may stain more intensely with DAPI than live cells. All immunofluorescence was carried out using a Leica TCS SP8 Confocal Microscope (Leica Microsystems, Athlone, Ireland)

2.26. $CD4^+$ T Cell Stimulation

2.26.1. Isolation of Spleen Cells

48 well plates were coated with CD3 antibody solution the night before the spleens were isolated and allowed to incubate o/n in incubator. The spleens were aseptically removed from mice and placed in RPMI on ice until needed. Spleens were passed through a 40 µm nylon cell strainer (Becton, Dickenson and Company, NJ, USA), and RPMI was added accordingly. The sample was spun down at 1300 rpm for 5 mins at 4°C and resuspended in 20 ml of RPMI. The cells were counted and resuspended to yield a final concentration of 200 x 10^6 cells/ml.

2.26.2. Magnetic-Activated Cell Sorting (MACS) $CD4^+$ T Cell Isolation

2.26.2.1. Magnetic labeling

CD4+ T cells were isolated from mice spleen cells mixture using a MACS $CD4^+$ T Cell Isolation Kit II (Miltenyi Biotec Ltd., Cologne, Germany) as per manufacturer's instructions. After the cells are counted and diluted to give desired concentration, they were spun down at 1300 rpm for 5 mins at 4°C and the supernatant was aspirated off completely. The cells were

resuspended 40 µl of MACS buffer (all calculations in this protocol are worked out for a total cell volume of 10^7 cells). 10 µl of Biotin-Antibody Cocktail (cocktail of biotin conjugated monoclonal antibodies against CD8a, CD11b, CD11c, CD19, CD45R (B220), CD49b (DX5), CD105, Anti-MHC class II, and Ter-119) was then added, vortexed, and placed in 4°C for 10 mins. 30 µl of buffer was added after, the solution was spun down at 1300 rpm for 5 mins at 4°C and supernatant was removed. The cells were resuspended in 60 µl of buffer to which 20 µl of Anti-Biotin MicroBeads (MicroBeads conjugated to monoclonal anti-biotin antibodies (isotype: mouse IgG1)) was added. The cells were mixed and let incubate at 4°C for 15 mins. Cells were spun down at 1300 rpm for 5 mins at 4°C and the total volume was then brought up to 2 ml with buffer.

2.26.2.2. Magnetic separation

LS columns and a MACS separator were used to isolate out $CD4^+$ T cells. LS columns were preconditioned prior to loading with 3 mls of buffer. 1 ml of cells were added at a time and allowed to pass through to a collection tube underneath the LS column. This flow0through represents the unlabeled, enriched $CD4^+$ T cells. The column was washed X3 with buffer and added to the previous collection tube. The flow-through cells were spun at 1300 rpm for 5 mins at 4°C and counted again and resuspended in RPMI to give desired volume of 1.33 x 10^6 cells/ml.

2.26.3. $CD4^+$ T Cell Differentiation

500 µl of the newly isolated $CD4^+$ T cells were added to the CD3 antibody pre-coated wells.

$CD4^+$ T cells subset medium was prepared as follows (per 500 µl total).

- **anti-CD3/ anti-CD28**: 7.5 µl anti-CD 28 + 492.5 µl RPMI
- **Th1**: 7.5 µl anti-CD28 + 2.5 µl IL-12 + 490 µl RPMI
- **Th17**: 7.5 µl anti-CD28 + 1 µl IL-1b +1 µl IL-23 + 490.5 µl RPMI

BAMLET was prepared as follows (per 500 µl total).

- **0.02 mg/ml**: 1 µl (BAMLET 10 mg/ml) + 499 µl RPMI
- **0.05 mg/ml**: 2.5 µl (BAMLET 10 mg/ml) + 497.5 µl RPMI

Cells were left in the incubator at 37°C for 72 h to allow cell differentiation to occur after which time supernatants were removed and analysed as per section 2.27.

2.27. Enzyme-linked Immunosorbent Assay (ELISA)

2.27.1. Standard Cytokine ELISA

ELISA DuoSet assays (R&D Systems, Inc., MN, USA) were used to determine the following cytokine concentrations in mouse $CD4^+$ T cells: interleukin (IL)-2, IL-10, IL-17, TNF-α, and interferon (IFN)-γ (Table 2.5). High-binding 96-well microtiter plates (Greiner Bio-One, NC, USA) were coated over night at 4°C with 50 µl/well of rat anti-mouse capture antibody in coating buffer according to manufacturer's instructions. After washing in 1 X PBS tween, non-specific binding sites were blocked by the addition of 150 µl/well of blocking solution for 2 h at RT. After blocking, plates were washed and 50 µl/well of sample supernatant or serially diluted recombinant cytokine (0-1000 pg/ml) in assay diluent were added to plates and incubated overnight at 4°C. After washing, 50µl of biotinylated goat anti-mouse detection antibody was added per well and incubated for 2 h at RT. Plates were washed again and incubated, in the dark for 20 min, with 50 µl/well of HRP-conjugated streptavidin (Becton, Dickenson and Company., NJ, USA, 1:1000 in assay diluent) followed by washing and addition of 50 µl/well of OPD substrate in phosphate citrate buffer ELISA plates were allowed to develop in the dark for 2-30 min after which, the enzyme reaction was stopped by the addition of 25 µl/well of 1 M H2SO4. The optical density values were determined by measuring absorbance at 492 nm using a microtiter plate reader and cytokine concentrations for supernatant samples were calculated using the standard curve prepared with recombinant mouse cytokine.

Table 2.6 Antibody concentrations and reagents used in ELISA

ELISA	Capture Antibody	Top Standard	Detection Antibody	Reagent Diluent	Blocking Buffer
DuoSet ELISA					
IL-2	1μg/ml	2ng/ml	1 μg/ml	0.05% Tween PBS-	1% BSA in PBS
IL-10	1/180	2μg/ml	1/180	0.1% BSA, 0.05% Tween PBS-	1% BSA in PBS
IL-17A	1/180	1ng/ml	1/180	0.1% BSA, 0.05% Tween PBS-	1% BSA in PBS
TNF-α	1/180	2ng/ml	1/180	0.1% BSA, 0.05% Tween PBS	1% BSA in PBS
IFN-γ	1μg/ml	10ng/ml	1μg/ml	0.05% Tween PBS-	1% BSA in PBS

2.28. Data and Statistical Analysis

Data was analysed using the Prism GraphPad software (GraphPad, CA, USA). Unless otherwise specified, data are expressed as mean ± SEM. SEM is calculated as the standard deviation (SD) of the original sample divided by the square root of the sample size. Paired *t*-test was utilized when comparing two samples. Data analysis was performed by one way analysis of variance (ANOVA), where the number of groups in the experiment was three or more. Survival statistics were calculated using the Kaplan-Meier method. Survival time was measured from the date of first treatment to the date of death or last follow-up. For all statistical analysis, a probability (p) of ≤ 0.05 was considered to represent a significant difference between groups.

3. *In Vitro* Investigation into the Structural and Mechanistic Properties of P-FA Complexes

3.1. Introduction

The discovery of HAMLET opened the door for a new wave of alternatively folded protein molecules which possess dual functionality when in this state. Although HAMLET was the first P-FA complex to display tumouricidal capabilities, there have been a number of new compounds which have been shown to display similar qualities. A key aim of this project was to investigate whether this ability to selectively destroy tumour cells as opposed to healthy cells was an attribute of all alternative P-FA complexes or whether it was just a reserved feature for a select few, and in doing so shed new light on the subject surrounding the true cytotoxic component involved. There has been an increasing level of debate regarding whether the cytotoxic component involved in these complexes is the protein, the FA itself, or even potentially a combination of both.

It is known that different types of FAs such as palmitic, stearic, oleic, land inoleic acid can cause cell death *in vitro* (Martins De Lima *et al.*, 2006, Brinkmann *et al.*, 2011a) and there is also a variety of studies demonstrating that a diet high in FAs can provide protection against certain forms of cancers (Menendez *et al.*, 2005, Menendez *et al.*, 2006, Colomer and Menendez, 2006). It appears that the particular type of FA in complex does not dramatically affect its tumouricidal efficiency, as SO can also be used to generate HAMLET-like complexes when bound to β-LG (Lišková *et al.*, 2011). After testing 14 FAs which differ in their degree of saturation, chain length, cis/trans isomerism, and their ability to make a functional complex it was found that OA is the optimal cofactor in the HAMLET complex (Svensson *et al.*, 2003b).

In contrast to this, α-LA is not cytotoxic towards tumour or differentiated cells (Brinkmann *et al.*, 2011a). When originally discovered, HAMLET was the first example of a protein that exhibits a well-defined function in its native state but which also acquires a new and beneficial function after partial unfolding (Min *et al.*, 2012). Since its discovery other proteins have been shown to exhibit similar functionality and tumour specificity. For example the bovine equivalent, BAMLET, displays similar cytotoxic effects on tumour cells whilst also exhibiting a reduced toxic response towards differentiated cells (Svensson *et al.*, 2003a). Species variation does not affect the ability of the protein to form a tumour killing

complex with OA, as porcine, caprine (Pettersson *et al.*, 2006) and goat (Nakamura *et al.*, 2013) have also been used to form complexes. As α-LAs are highly conserved proteins within species the similarity in results observed from these variations of α-LA are not surprising (Rammer *et al.*, 2010).

EL, although not a direct species variant of α-LA, has close structural homology with that of α-LA and its bovine equivalent (Wilhelm *et al.*, 2009). EL was the first non-LA protein to be engineered into a tumouricidal P-FA complex which displayed the hallmark selectivity that is observed with HAMLET. Using a similar method of IEC and a column preconditioned with OA, the ELOA complex was formed and shown to be partially unfolded and capable of inducing cellular death in PC12 cells (Wilhelm *et al.*, 2009). EL has previously been shown to form amyloid oligomers without OA (Malisauskas *et al.*, 2005). ELOA which was formed using an IEC column preconditioned with OA displays characteristics similar to amyloid oligomers and retained the cytotoxic functionality HAMLET possessed. Using AFM, ELOA was shown to form ring-shaped structures similar to EL oligomers. Also a battery of spectroscopic techniques further demonstrated that this complex was oligomeric as ELOA was bound to CR and caused an increase in ThT. However, the complex did not proceed to the fibrillar state even after prolonged incubation suggesting that the OA stabilizes the complex (Wilhelm *et al.*, 2009). Whether HAMLET/BAMLET remains in a monomeric or oligomeric state remains an area of controversy. Several groups maintain that HAMLET remains in a monomeric conformation under physiological conditions (Mossberg *et al.*, 2010b, Pettersson-Kastberg *et al.*, 2009b). However Sploare *et* al., have shown that BAMLET is in an oligomeric state (Spolaore *et al.*, 2010b) and more recently HAMLET has been shown to exist in three conformations under physiological conditions, the native species, the monomeric complex and the oligomeric species (Nakamura *et al.*, 2013).

Although functionally different proteins, β-LG and α-LA are both the main constitutes of milk, making up nearly 70-80% of total whey protein (Chatterton *et al.*, 2006), and although they possess different structural and functional properties, both can be induced to form cytotoxic assemblies. β-Lactoglobulin-OA (β-LG–OA) complex displays increased potency against human epidermoid larynx carcinoma and *S.pneumoniae* cells when compared to HAMLET (Permyakov *et al.*, 2012). A recent experiment conducted by the Kuwajima group in Japan which runs in parallel to our own work showed that other non-related proteins could

form the tumouricidal complex. AMb and β-microglobulin both formed complexes with OA and exhibited the tumour killing functionality which HAMLET/ BAMLET also display (Nakamura *et al.*, 2013).

A key feature of these P-FA complexes is that they were thought to require a MG protein bound to FA to form a functioning complex. α-LA is the quintessential MG protein and has been extensively studied and examined (Kuwajima, 1989). The unorthodox structure which MG proteins obtain grants them a certain level of flexibility that other normally folded proteins cannot achieve (Ptitsyn, 1995). It is this intermittent folded state which may allow HAMLET/BAMLET and other P-FA complexes to bind or take up FA and form P-FA tumouricidal assemblages. The loss of the Ca^{2+} ions and addition of the OA through column chromatography allows HAMLET to form a tumouricidal complex (Svensson *et al.*, 1999). Despite this theory our group has shown that the electrostatic interactions between the positively-charged basic groups on α-LA and the negatively-charged carboxylate groups on OA molecules play an essential role in the binding of OA to α-LA (Xie *et al.*, 2013). Furthermore β-LG has been shown to complex with OA (Permyakov *et al.*, 2012). Therefore the MG conformation of the protein may not have a paramount role in the formation of a functional P-FA complex.

Myoglobin (Mb), the fundamental intracellular hemoprotein involved in O_2 binding, was the first protein whose atomic resolution was studied using X-ray crystallography. It is a 17kDa globular protein of 152 amino acid residues (Kendrew *et al.*, 1958). This cytoplasmic hemoprotein is located solely in the oxidative skeletal muscle fibers and cardiac myocytes, and acts as short term storage for dioxygen (Ordway and Garry, 2004). Mb is involved in O_2 storage and animals adapted for life with reduced O_2 consumption such as that for deep sea diving mammals have 10-fold higher Mb levels in their skeletal muscle compared with animals that do not experience prolonged apnea (Garry *et al.*, 2000, Noren *et al.*, 2001). In addition to O_2 storage in mammalian tissues, Mb also has a role in buffering intracellular Po_2 (O_2 partial pressure) (Wittenberg and Wittenberg, 2003) and ensures that intracellular O_2 levels remain relatively constant and homogeneous within the body irrespective of O_2 fluctuations caused by increased muscle activity (Richardson *et al.*, 1995, Ordway and Garry, 2004).

The MG protein AMb is structurally very similar to the native (holo) Mb globular protein, as it retains much of its secondary and tertiary conformation (Onufriev *et al.*, 2003). Unfolding and refolding studies have shown that in the presence of acid, AMb undergoes a conformational change to form a MG intermediate state at ~pH 4 (Lin *et al.*, 1994). Further lowering of the pH environment will cause more structural changes until complete unfolding is achieved (Onufriev *et al.*, 2003). In the 'apo' state most proteins retain a hydrophobic core while still maintaining some MG characteristics such as decreased stability and compactness however, NMR studies have shown that while in this state AMb remains reasonably stable (Lin *et al.*, 1994). Recently AMb bound to OA has been shown to form a tumouricidal complex when tested on L1210 cells (Nakamura *et al.*, 2013).

β-LG is the dominant non-casein protein in bovine milk however, it is generally thought of as being absent from human breast milk (Chatterton *et al.*, 2006). β-LG is a globular protein of 18.3kDa mass and possesses low ionic strength and solubility (Madureira *et al.*, 2007). The role of β-LG is still somewhat unclear. Its main role in the body is the digestion of milk fat. Due to its ability to tolerate low pH environments, β-LG can act in the stomach were it binds to released free FAs thus facilitating the digestion process (Madureira *et al.*, 2007). It is known to have an immunological role in developing infants as a transporter of passive immunity and has been shown to have a protective ability against some carcinomas. Orally administered β-LG reduced intestinal tumours in young rats and also increased their anti-cancerous abilities against dimethylhydrazine-induced tumors (Mcintosh *et al.*, 1995). β-LG has also been shown to form tumour specific cytotoxic complexes via IEC yielding a similar tumouricidal complex to HAMLET (Permyakov *et al.*, 2012).

Cyto-*c* is a 13kDa water soluble protein which is located in the inner mitochondrial membrane where it is involved in the electron transport chain (ETC). The ETC is used to drive ATP synthesis, which provides usable energy to all cells. Cyto-*c* functions by accepting and donating electrons during this process and ultimately converts O_2 to H_2O (Ow *et al.*, 2008). Recently it has become apparent that mitochondria can trigger cell death through the release of Cyto-*c* and binds apoptosis activating factor 1 (Apaf-1) which consequently activates procaspase-9 leading to the formation of the apoptosome, an apoptosis promoting multiprotein complex (Borutaite, 2010, Yang *et al.*, 1997). This ability to induce apoptosis within cells has been manipulated by chemotherapeutic drugs, which have been designed to

mimic genotoxic stress conditions, leading to Cyto-*c* release and apoptosis activation (Huber *et al.*, 2011).

Discovered in the mid 1970's, Ub is a 76-residue polypeptide that is remarkably conserved among eukaryotes (Hochstrasser, 2009). This 'ubiquitously' located protein is a multifunctional tool in the body and is involved in histone modification and vesicular trafficking (Nath and Shadan, 2009). It is also responsible for targeting proteins for destruction in the proteasome such as proteins that have become misfolded (Kerscher *et al.*, 2006, Hetz, 2012). Ub mediated destruction of aberrant proteins is involved in numerous intracellular processes such as cell growth and cell-cycle regulation (Nath and Shadan, 2009). Consequentially, irregularities in ubiquinated protein destruction can be a hallmark of several cancers and neurodegenerative related diseases (Kerscher *et al.*, 2006).

P-FA complexes are highly toxic to the majority of tumour cell lines tested and have also shown promising results in *in vivo* experiments (Min *et al.*, 2012). Assessing cell sensitivity to theses complexes has been carried out using unrelated cells of both tumour and non tumour phenotypes (Brinkmann *et al.*, 2011a, Hallgren *et al.*, 2006, Hoque *et al.*, 2013). *In vitro*, it is often difficult to assess the effects of a drug on one particular cell expressing an undifferentiated and differentiated phenotype. The PC12 cell line provides a highly reproducible tumour versus differentiated *in vitro* cell model. In the absence of NGF, these cells typify a normal neoplastic cell line, and exhibit uncontrollable and infinite cell proliferation (Gunning *et al.*, 1981). NGF is normally involved in the development and maintenance of the neural crest origin of several cell lines however, when applied to undifferentiated PC12 cells NGF translocates to the nucleus and binds to nuclear membrane receptors (Yankner and Shooter, 1979). The addition of NGF to PC12 cells causes them to cease cell generation, and exhibit a non-differentiating phenotype which displays neurite growth (Oberdoerster and Rabin, 1999). Therefore PC12 cells provide a reliable assay for studying differences in tumour and healthy cells. By using this model it is possible to analyze the effects of various drugs on a single cell displaying a cancerous phenotype and a normal differentiated phenotype.

For this study we generated novel P-FA complexes using proteins bound to FA molecules. Several of these P-FA complexes have never been engineered or examined prior to this study and represent novel compounds with potential tumouricidal abilities. The mechanistic and selective properties of these newly generated complexes were then examined using a PC12 differentiation model and human U2OS cells.

We have also tested our samples on a U2OS cell line which displays the typical hallmarks of a normal tumour cell. U2OS cells are derived from a human osteosarcoma, a relatively common childhood cancer mainly affecting children and young adults from the ages of 15-29 years.

Table 3.1 Proteins used to form P-FA complexes using IEC

Protein	Molecular Weight (kDa)	Isoelectric Point
Human α-LA	14.2	4.7
Bovine α-LA	14.2	4.8
AMb	17	7.29
β-lactoglobulin	18.3	4.83
Cyto-*c*	13	9.59
Mb	17	7.36
Ub	8.6	6.56

3.2. Results

3.2.1. HAMLET Significantly Reduces Viability in Cancer Cells When Compared to Differentiated Cells in vitro.

HAMLET has been shown by previous groups to selectively target tumour cells for destruction (Svensson *et al.*, 1999, Pettersson *et al.*, 2006, Håkansson *et al.*, 1995) and has a less toxic effect on healthy cells however, it has been shown to target some non-cancer cells for destruction (Brinkmann *et al.*, 2011a). We wanted to establish whether we could observe tumouricidal selective targeting using the same cell line, displaying a tumour and healthy phenotype. For this we used the PC12 differentiation model (Figure 3.1). For further confirmation of the tumouricidal selectivity displayed by these P-FA complexes the human osteosarcoma U2OS cell line was also used. HAMLET was prepared using IEC and the functional complex was eluted at high salt (Figure 3.2). $PC12^{undiff}$ and $PC12^{diff}$ cells were treated with increasing concentrations of HAMLET (Table 2.1 and Table 2.2) and viability was recording using Alamar Blue as per section 2.5. From our results $PC12^{undiff}$ cells treated with HAMLET show a significant decrease in cell viability when compared to that observed in the differentiated cell type (Figure 3.3 (A)). An LC_{50} value of $4.5x10^{-6}$ M (0.064 mg/ml) was obtained for these cancerous cells exposed to this P-FA complex while PC12 cells displaying a differentiated phenotype yielded LC_{50} values of nearly 10-fold higher, at $3.2x10^{-5}$ M (0.45 mg/ml). U2OS cells also gave similar LC_{50} values as those seen in $PC12^{undiff}$ cells of $3.4x10^{-6}$ M (0.048 mg/ml) (Figure 3.3 (B)). These results show that maintaining a differentiated phenotype confers a significant level of resistance for PC12 cells treated with HAMLET. They also confirm the usefulness of the PC12 differentiation model as a method to determine the tumouricidal selectivity of drugs.

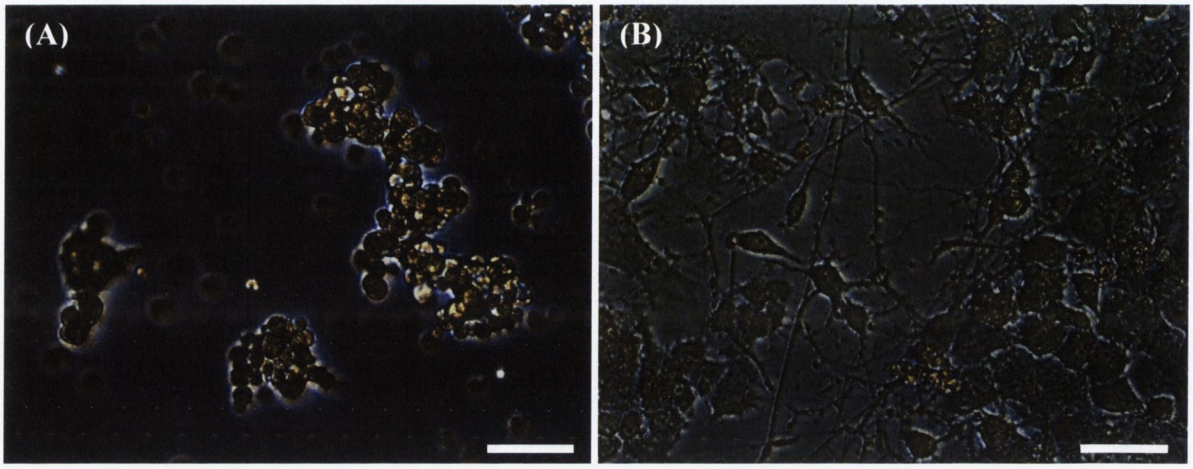

Figure 3.1 Effects of NGF treatment on cultured PC12 cells

Light microscopic image of $PC12^{undiff}$ (A) and 100 ng/ml treated $PC12^{diff}$ cells (B). Cells transform from a suspension state displaying no neurite growth into an adherent phenotype display extensive neurite growth (Scale bar: 100 μm).

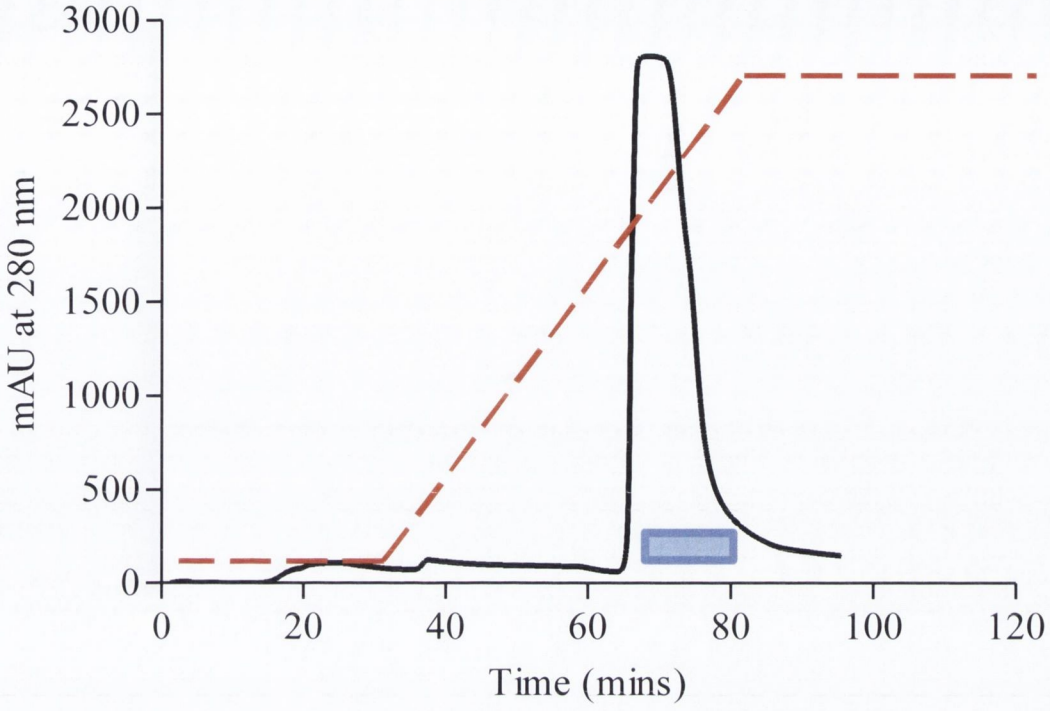

Figure 3.2 The preparation of HAMLET by IEC on an OA-conditioned ion exchange column.

Human α-LA was applied to a DEAE-FF 5 ml column conditioned with OA, and the P-FA complex was eluted with a gradient of 1 M NaCl (dashed red line). The solid blue bar indicates the fractions from the column that were collected for further studies.

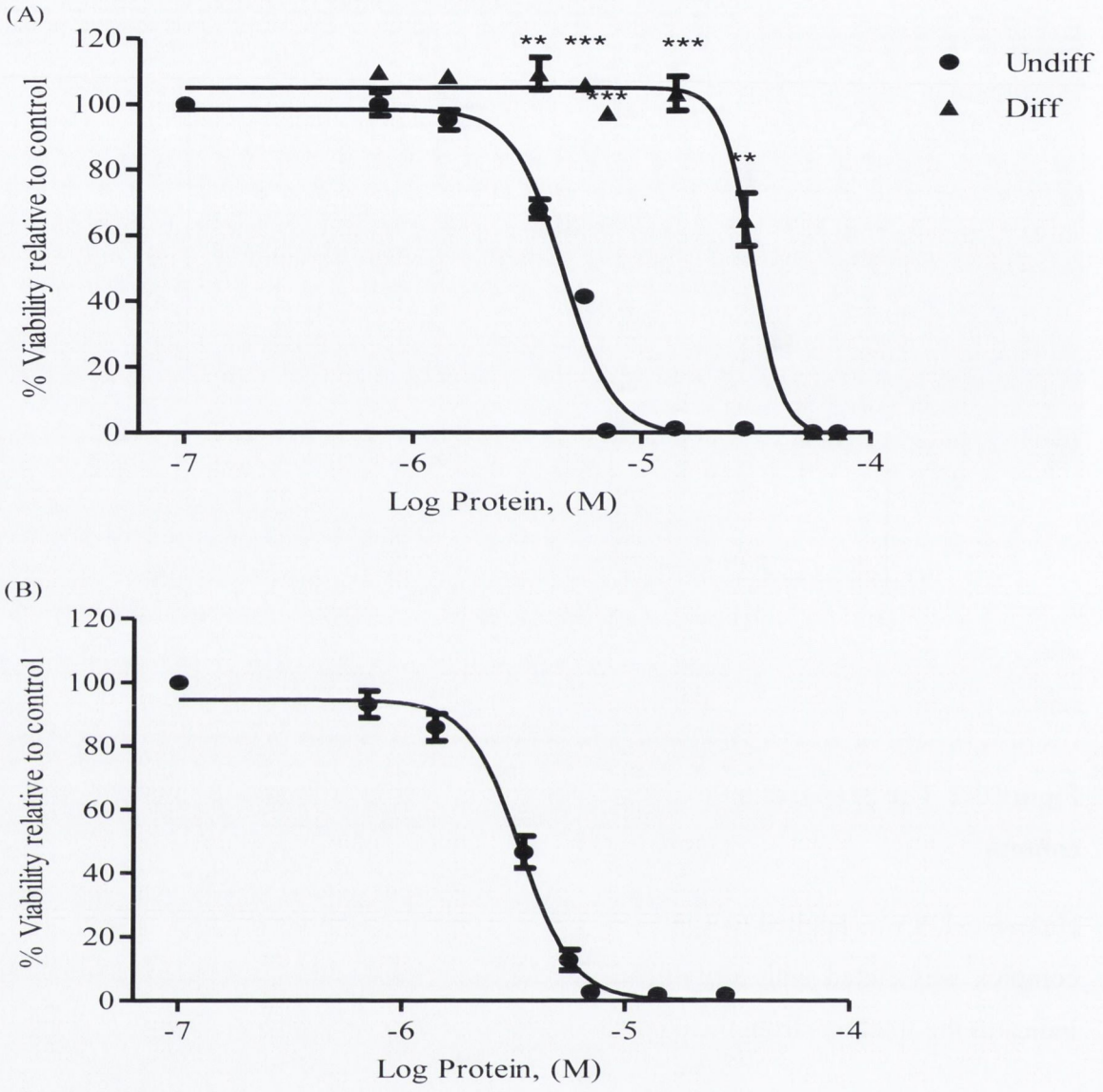

Figure 3.3 Dosage–response viability curve for HAMLET tested on PC12 and U2OS cells using an Alamar Blue assay

Viability results for PC12 cell lines treated with HAMLET (log scale). Undifferentiated and differentiated PC12 cells were exposed to varying concentrations of HAMLET and incubated for 24 h at 37 °C (A). U2OS cells were treated with HAMLET for 24 h at 37°C (B). Viability was calculated as percentage of the untreated control. The values are the means of three experiments with the error bar indicating SEM. $^{*}p < 0.05$, $^{**}p < 0.001$, *** $p < 0.001$ were calculated using GraphPad.

3.2.2. BAMLET Significantly Reduces Viability in Cancer Cells When Compared to Differentiated Cells in vitro.

Having established that the PC12 differentiation model is a robust system to examine the tumouricidal selectivity of HAMLET we then used this method to examine the same properties in BAMLET which was prepared using IEC (Figure 3.4). Cells were treated for 24 h at 37°C with varying concentrations of BAMLET (Table 2.1 and Table 2.2) and assessed using Alamar Blue. Similarly to HAMLET, BAMLET treated undifferentiated and differentiated cells show significant differences in cell viability, with cells of a differential morphology displaying increased resistance against the cytotoxic effects of this P-FA complex (Figure 3.5 (A)). $PC12^{undiff}$ cells yield LC_{50} values of around $3.9x10^{-6}$ M (0.056 mg/ml) while differentiated PC12 cells are considerably less affected with LC_{50} values of around $5.9x10^{-5}$ M (0.84 mg/ml). U2OS cells were treated with BAMLET at identical concentrations as those in the PC12 treated group and resulted in an LC_{50} value of $2.7x10^{-6}$ M (0.038 mg/ml) (Figure 3.5 (B))

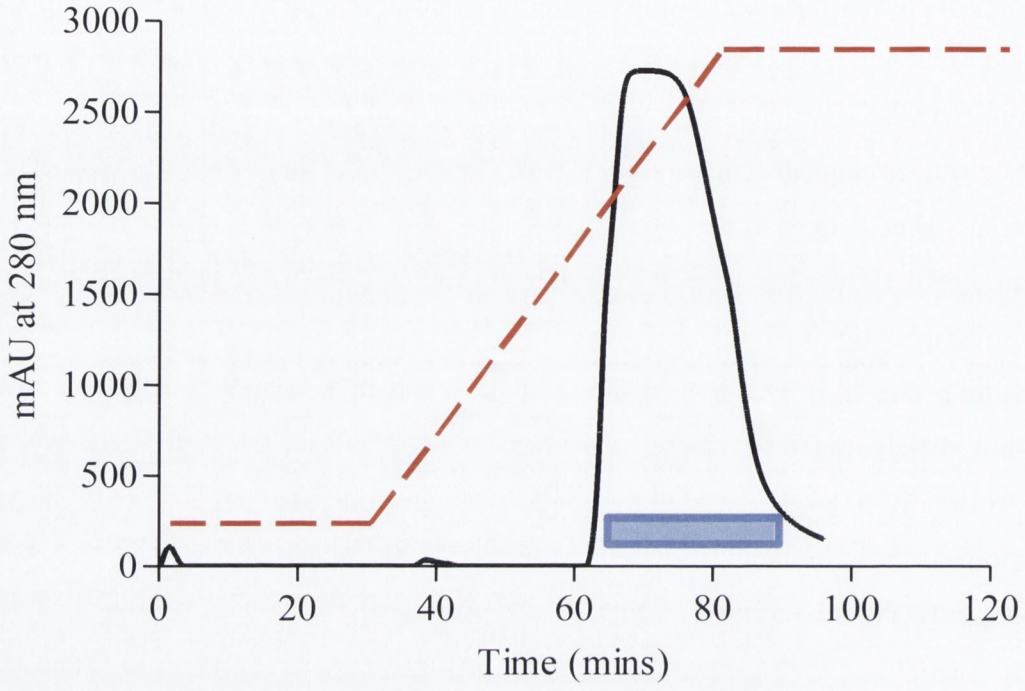

Figure 3.4 The preparation of BAMLET by IEC on an OA-conditioned exchange column.

Bovine α-LA was applied to a DEAE-FF 5 ml column conditioned with OA, and the P-FA complex was eluted with a gradient of 1 M NaCl (dashed red line). The solid blue bar indicates the fractions from the column that were collected for further studies.

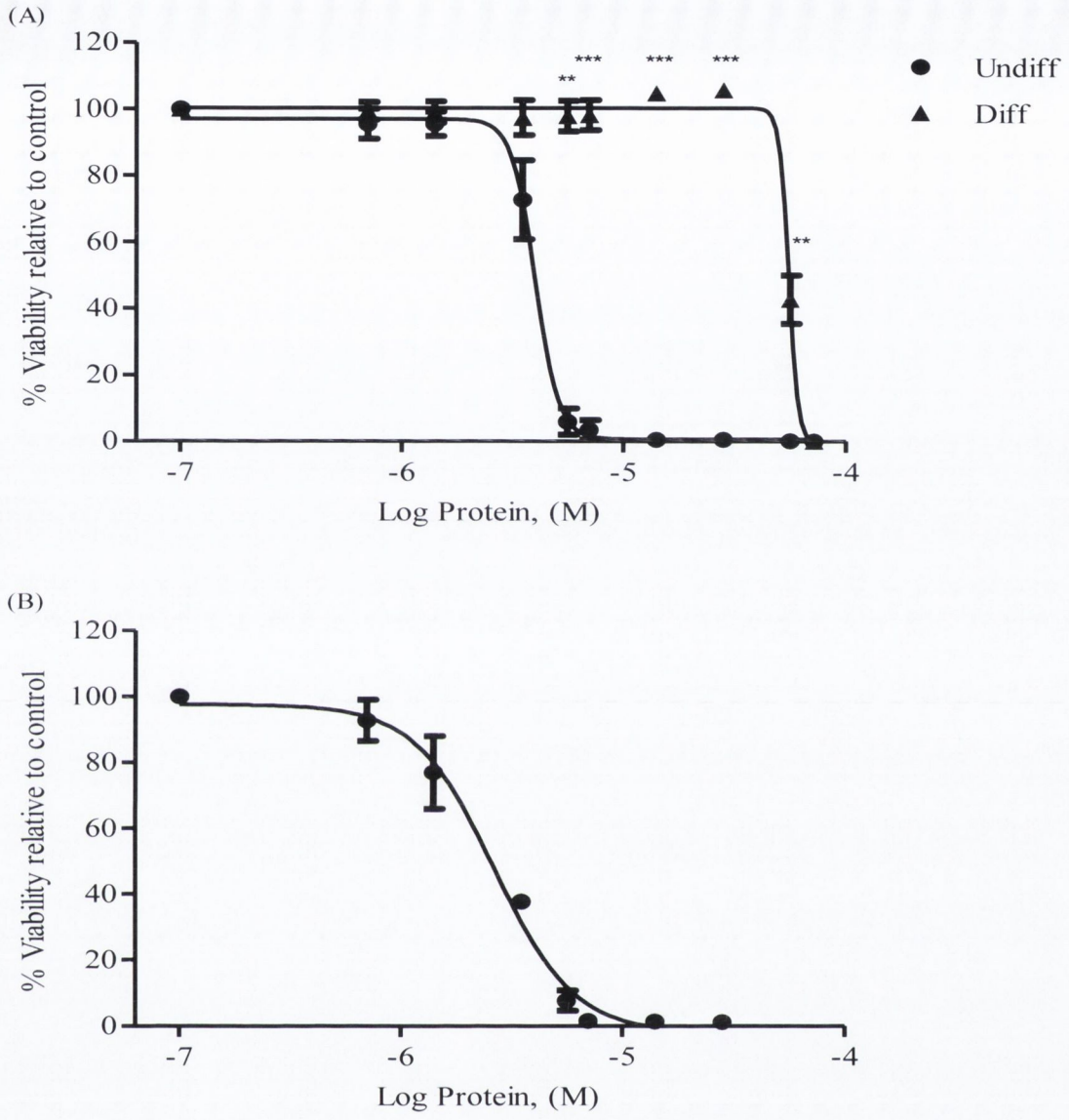

Figure 3.5 Dosage–response curve for BAMLET tested on PC12 and U2OS cells.

PC12 cell lines treated with BAMLET (log scale) and incubated for 24 h at 37 °C (A). Cells were then assayed using the fluorescencent staining compound Alamar Blue. (B) U2OS cells were treated with BAMLET for 24 h at 37°C. The values are the means of three experiments with the error bar indicating SEM. $^{*}p < 0.05$, $^{**}p < 0.001$, *** $p < 0.001$ were calculated using GraphPad.

3.2.3. TEM of BAMLET Treated U2OS Suggests that OA Accumulates Within the Cell

Having shown that BAMLET kills tumour cells we wanted to see if we could determine if the FA molecules were gaining access into the cells. USOS cells were chosen as their larger size allows for better imaging. These cells were exposed to 0.05 mg/ml (determined from LC_{50} values in Table 3.2) of BAMLET and left to incubate at 37°C for 24 h, after which time samples were spun down and prepared for TEM as described in section 2.23. At the time of examination the majority of cells had shown signs of cell death when visualized under a light microscope (Figure 3.6 B-F). The presence of large FA droplets can be seen within the cell (white arrows (Figure 3.6 B,D,E)). The FA droplets have also formed into larger lipid aggregates in the cell which present as large vacuoles and are almost 2 μm in diameter (Figure 3.6 red circle). The treated cells display signs of apoptotic cell death as seen from the formation of apoptotic bodies within the cell and in the extracellular milieu (red arrow heads). The results show the presence of large droplets inside the cell which are possibly a result of the accumulation of large volumes of OA due to its transportation inside via BAMLET. Furthermore BAMLET appear to activate an apoptotic cell death mechanism due to the accumulation of apoptotic bodies.

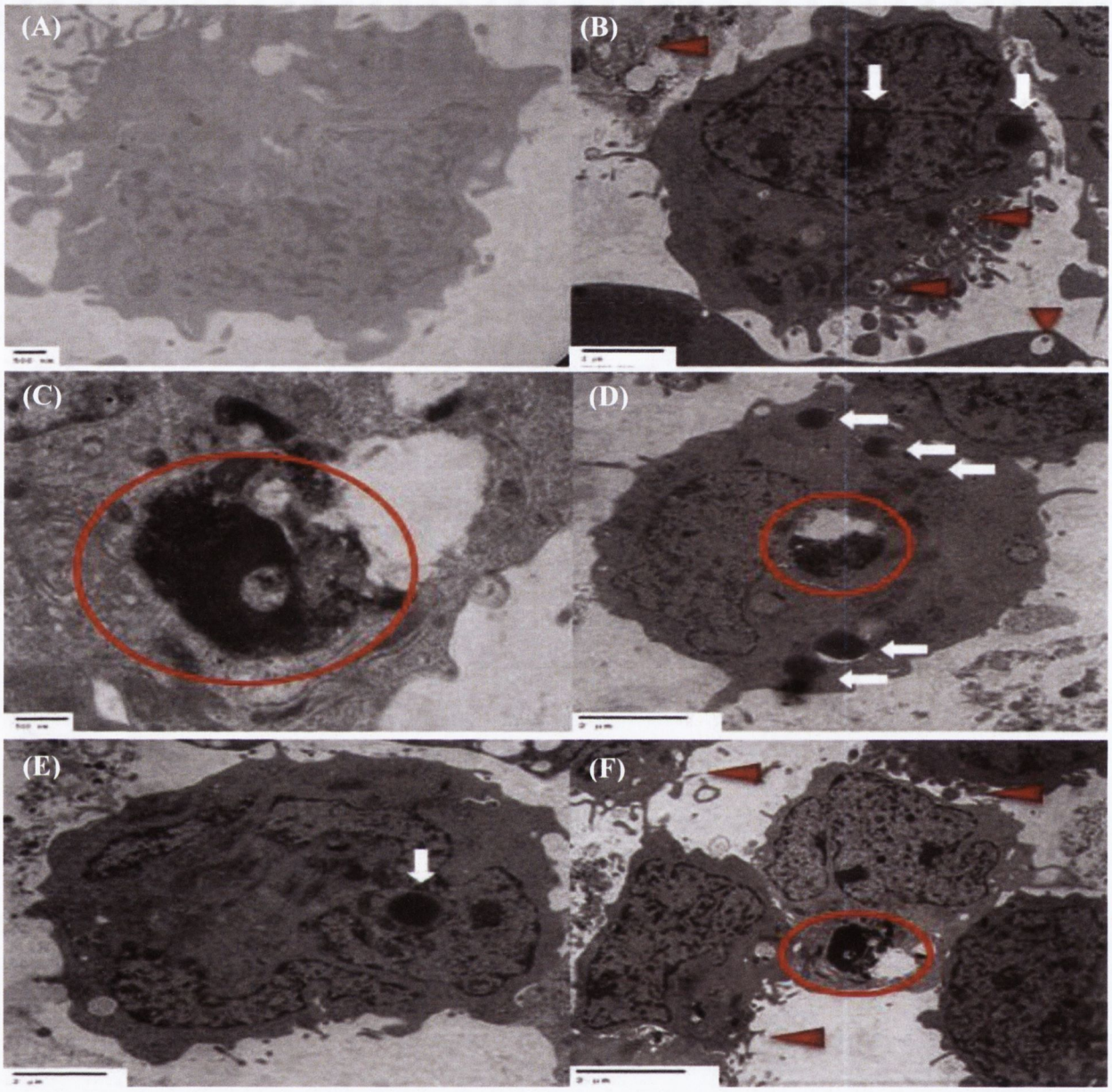

Figure 3.6 TEM of U2OS cells treated with BAMLET.

Cells were treated with 0.05 mg/ml BAMLET. Non-treated U2OS cells (X3000) (A). U2OS cells treated with BAMLET at X2500 magnification show intracellular fat droplets (white arrow) and apoptotic bodies (red arrow) (B). U2OS cell at X6000 displaying large FA droplet aggregation (red circle) (C). X2000 U2OS cell showing numerous FA droplets inside cell (white arrow). Also displaying large FA deposit (red circle) (D). U2OS cell at X2000 displaying large FA droplet inside the nucleus (white arrow) (E). U2OS cells with apoptotic bodies (red arrows) and accumulation of FA (red circle) (F). Representative of two separate experiments.

3.2.4. The AMb-OA Complex Significantly Reduces Viability in Cancer Cells when Compared to Differentiated Cells in vitro.

The tumouricidal properties of HAMLET/BAMLET have been tested by previous groups (Pettersson-Kastberg *et al.*, 2009b, Mossberg *et al.*, 2010c, Hallgren *et al.*, 2008, Brinkmann *et al.*, 2011b, Brinkmann *et al.*, 2011a). The discovery of non-α-LA proteins capable of forming tumouricidal complexes (Wilhelm *et al.*, 2009, Vukojević *et al.*, 2010) led us to ask the question of whether other P-FA complexes could be formed. Similarily to our results, AMb was recently shown to possess tumouricidal capabilities when complexed with OA (Nakamura *et al.*, 2013). Its ability to form into a MG state makes AMb an ideal candidate as a P-FA coupled complex and this MG protein formed a complex with OA using IEC (Figure 3.7). When used to treat cells, $PC12^{undiff}$ cells showed significantly reduced viability after 24 h treatment with AMb in complex with OA, when compared to that observed in $PC12^{diff}$ cells treated in an identical way (Figure 3.8(A)). $PC12^{undiff}$ cells show a significant reduction in cell number at each concentration point when compared to the differentiated cells until approximately 0% viability is observed in both cell lines at 4.8×10^{-5} M (0.82 mg/ml). LC_{50} values for both cell lines also display stark differences. $PC12^{undiff}$ cells have an LC_{50} value of 9.2×10^{-7} M (0.016 mg/ml), which is considerable lower than the LC_{50} value of 7.9×10^{-6} M (0.134 mg/ml) observed in $PC12^{diff}$ cells. U2OS cells were also tested in identical conditions and concentrations to that used for the PC12 cells. U2OS cells were also susceptible to the toxicity produced by AMb-OA, yielding an LC_{50} value of 3.4×10^{-6} M (0.058 mg/ml) (Figure 3.8 (B)). These results demonstrate that AMb can be generated into a cytotoxic complex with OA.

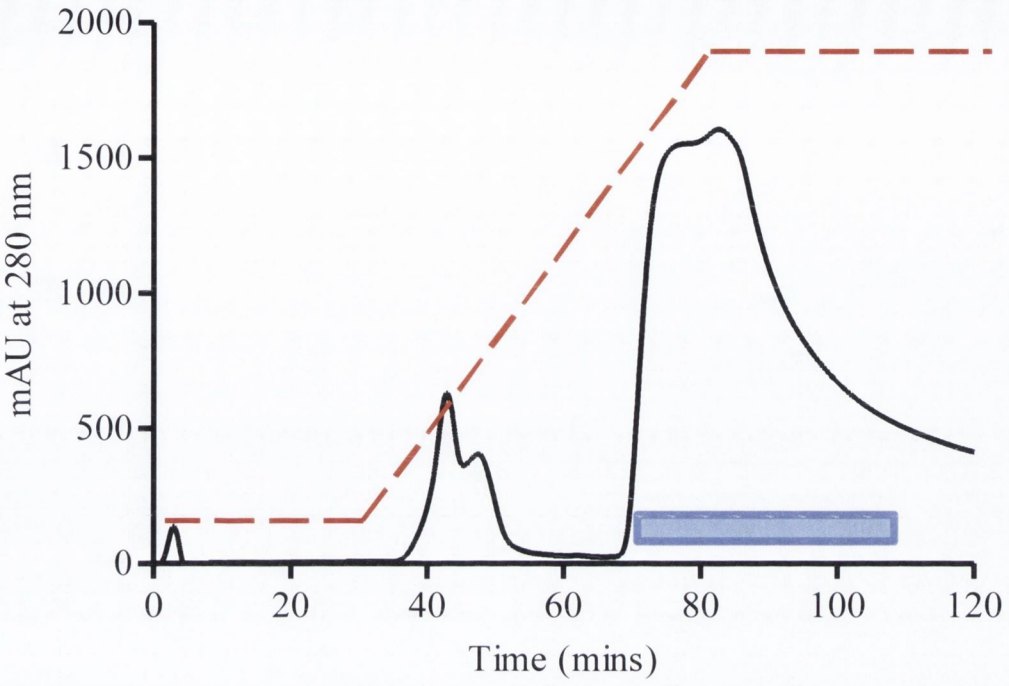

Figure 3.7 The preparation of AMb-OA by IEC on an OA-conditioned exchange column.

AMb native protein was applied to a DEAE-FF 5 ml column conditioned with OA, and the P-FA complex was eluted with a gradient of 1 M NaCl (dashed red line). The solid blue bar indicates the fraction from the column that was collected for further studies.

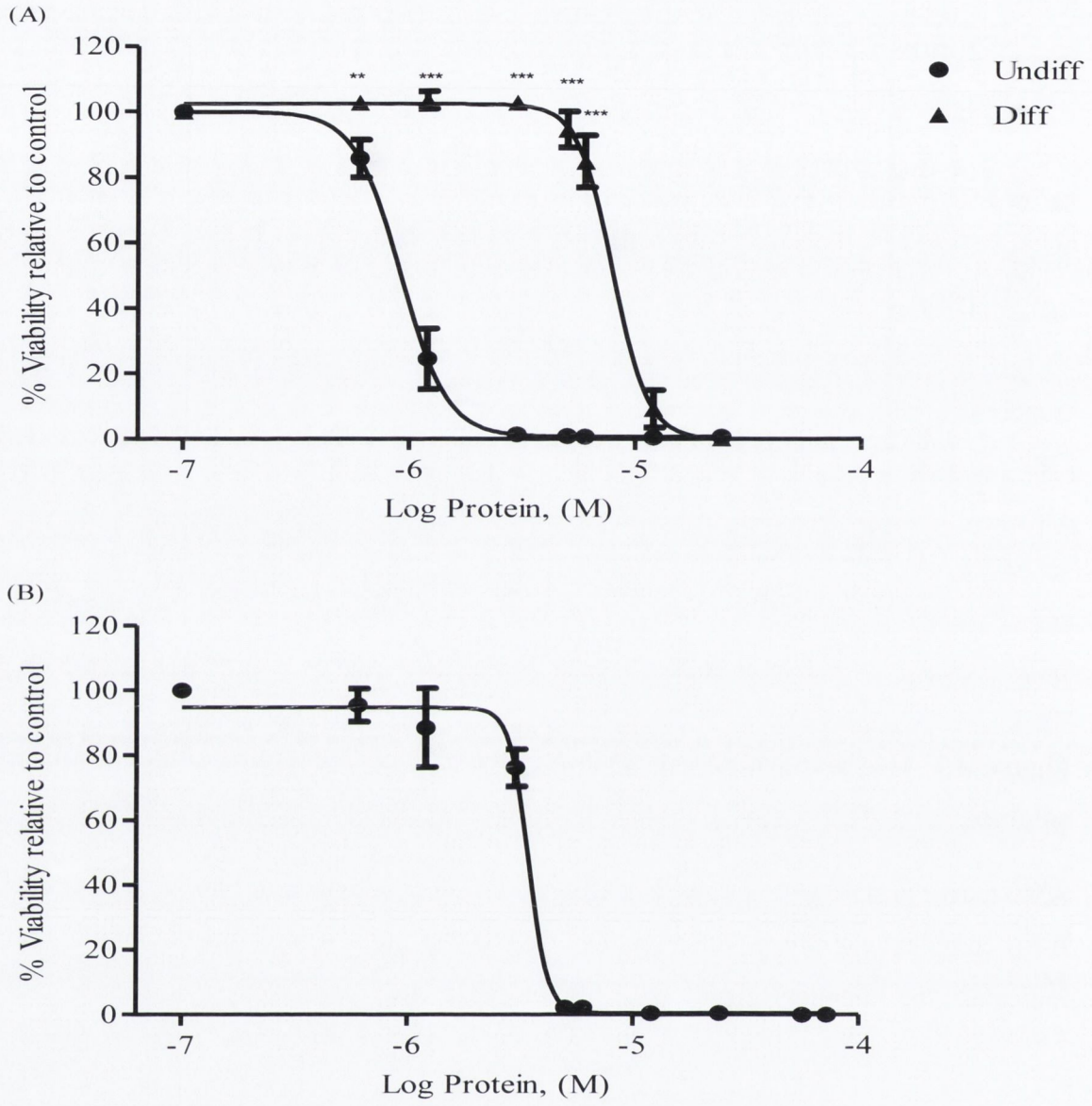

Figure 3.8 Dosage–response viability curve for AMb-OA tested on PC12 and U2OS cells using an Alamar Blue assay

(A) PC12 cell lines treated with AMb-OA (log scale) were exposed to varying concentrations of AMb-OA and incubated for 24 h at 37 °C. (B) U2OS cells were treated with AMb-OA for 24 h at 37°C. The values are the means of three experiments with the error bar indicating SEM. $^{*}p < 0.05$, $^{**}p < 0.001$, *** $p < 0.001$were calculated using GraphPad.

3.2.5. The β-LG-OA Complex Significantly Reduces Viability in Cancer Cells When Compared to Differentiated Cells in vitro.

β-LG has previously been shown to form tumour specific cytotoxic complexes via IEC. β-LG bound to OA (Permyakov *et al.*, 2012) and SO (Lišková *et al.*, 2011) formed a tumouricidal complex similar to that of HAMLET. Using similar methods, we prepared an OA bound β-LG complex (Figure 3.9) and tested them on the PC12 differentiation model and cancerous U2OS cells. β-LG-OA exhibited selective cytotoxicity as demonstrated by analyzing the results with Alamar Blue (Figure 3.10 (A)). LC_{50} values for both $PC12^{undiff}$ cells and U2OS are identical after analysis, yielding results of $1.6x10^{-6}$ M (0.03 mg/ml). In contrast, $PC12^{diff}$ cells exhibit an increased level of resistance towards β-LA-OA as is evident form LC_{50} values obtained from cytotoxicity assays which are $2x10^{-5}$ M (0.37 mg/ml) (Figure 3.10 (B)). From these results we can conclude that β-LG can be engineered into a P-FA complex when bound to OA using IEC and when bound in this state is highly toxic towards PC12 and U2OS cells. When examined using the PC12 differentiation model, β-LG-OA show decreased toxicity against differentiated cells suggesting that it is more cytotoxically selective towards tumour cells.

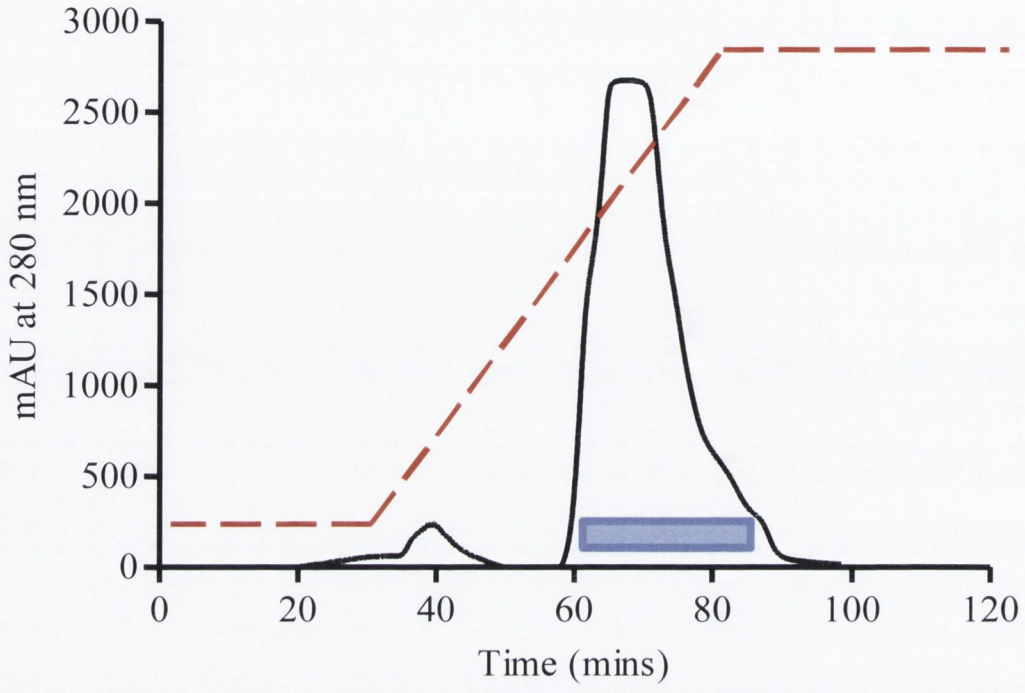

Figure 3.9 The preparation of β-LG-OA by IEC on an OA-conditioned exchange column.

β-LG in its native proteinaceous form was applied to a DEAE-FF 5 ml column conditioned with OA, and the P-FA complex was eluted with a gradient of 1 M NaCl (dashed red line). The solid blue bar indicates the fraction from the column that was collected for further studies.

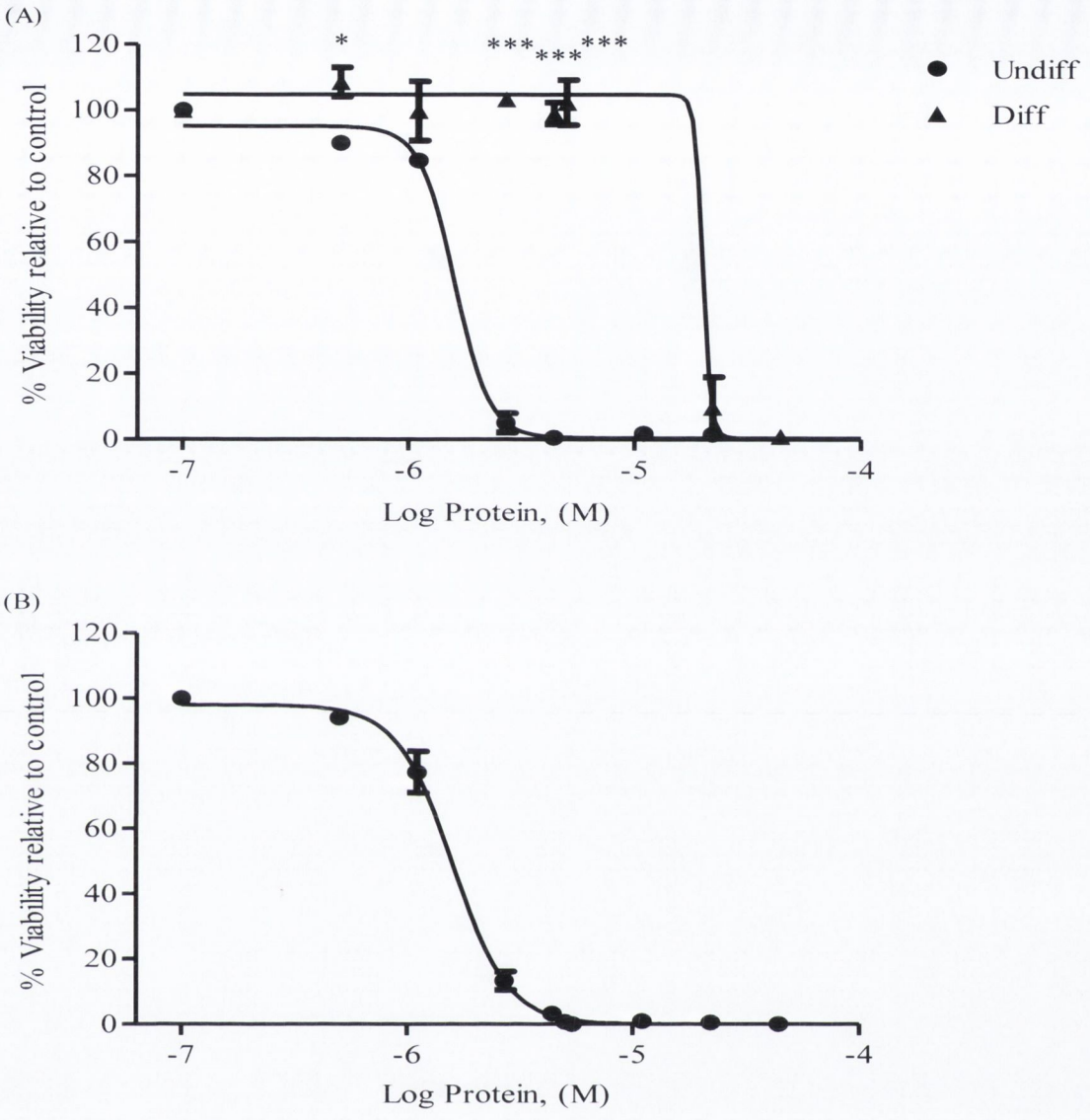

Figure 3.10 Dosage–response viability curve for β-LG-OA tested on PC12 and U2OS cells

(A) PC12 cell lines were treated with β-LG-OA (log scale) and incubated for 24 h at 37 °C. Cells were then assayed using the fluorescencent staining compound Alamar Blue. (B) U2OS cells were treated with β-LG-OA for 24 h at 37°C. The values are the means of three experiments with the error bar indicating SEM. $^{*}p < 0.05$, $^{**}p < 0.001$, *** $p < 0.001$ were calculated using GraphPad.

3.2.6. The Cyto-c-OA Complex Significantly Reduces Viability in Cancer Cells When Compared to Differentiated Cells in vitro.

We wanted to engineer a novel P-FA complex using Cyto-*c*, which was the original MG in terms of discovery (Ohgushi and Wada, 1983a), which behaved similarly to HAMLET/BAMLET. $PC12^{undiff/diff}$ and U2OS cells were incubated with this novel P-FA complex for 24 h after which time the cell viability was calculated using Alamar Blue. Using IEC we generated a tumouricidal Cyto-*c*-OA complex which was highly toxic to cells and displays similar selective efficacy towards $PC12^{diff}$ cells (Figure 3.12(A)) as is seen with other MG protein-FA complexes that were tested. After culturing cells for 24 h with increasing increments of Cyto-*c*-OA this complex displayed toxicity against the tumour cell lines tested and was also quite toxic towards the $PC12^{diff}$ cells. $PC12^{undiff}$ cells gave an LC_{50} value of $1x10^{-6}$ M (0.012 mg/ml) while $PC12^{diff}$ cells gave an LC_{50} value of $1.7x10^{-5}$ M (0.21 mg/ml) (Figure 3.12 (A)). U2OS cells treated under identical circumstances yielded a slightly higher LC_{50} value of $3x10^{-5}$ M (0.04 mg/ml) than observed in $PC12^{undiff}$ cells (Figure 3.12 (B)). These results suggest that the native innocuous MG protein Cyto-*c* can be engineered into a highly toxic, highly selective tumouricidal molecule when bound to OA.

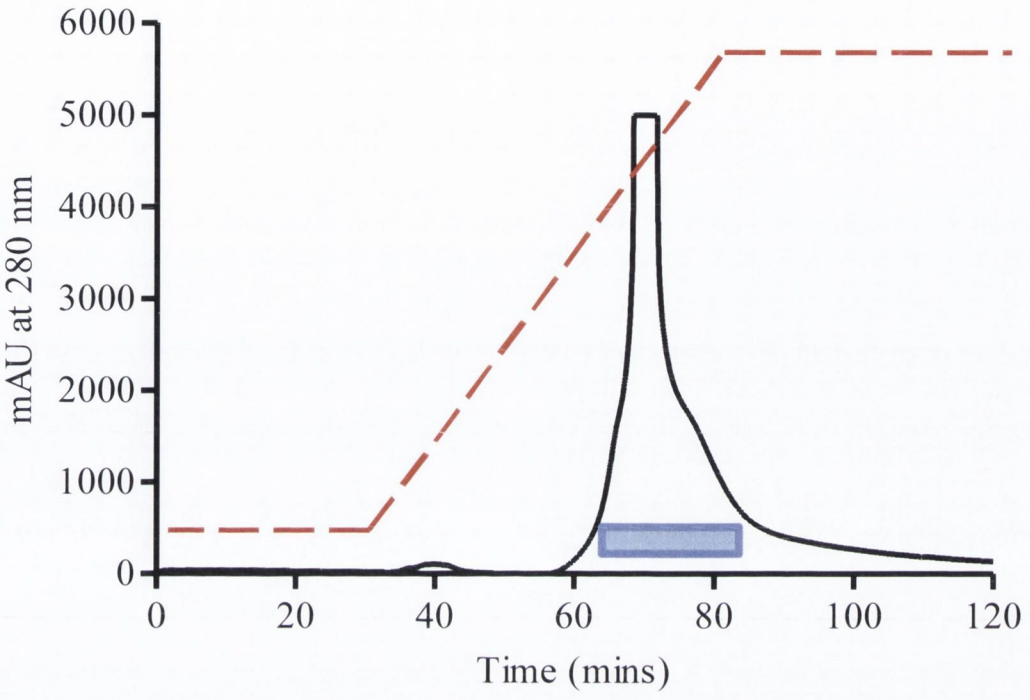

Figure 3.11 The preparation of Cyto-*c*-OA by IEC on an OA-conditioned exchange column.

Native Cyto-*c* protein was applied to a DEAE-FF 5 ml column conditioned with OA, and the P-FA complex was eluted with a gradient of 1 M NaCl (dashed red line). The solid blue bar indicates the fraction from the column that was collected for further studies.

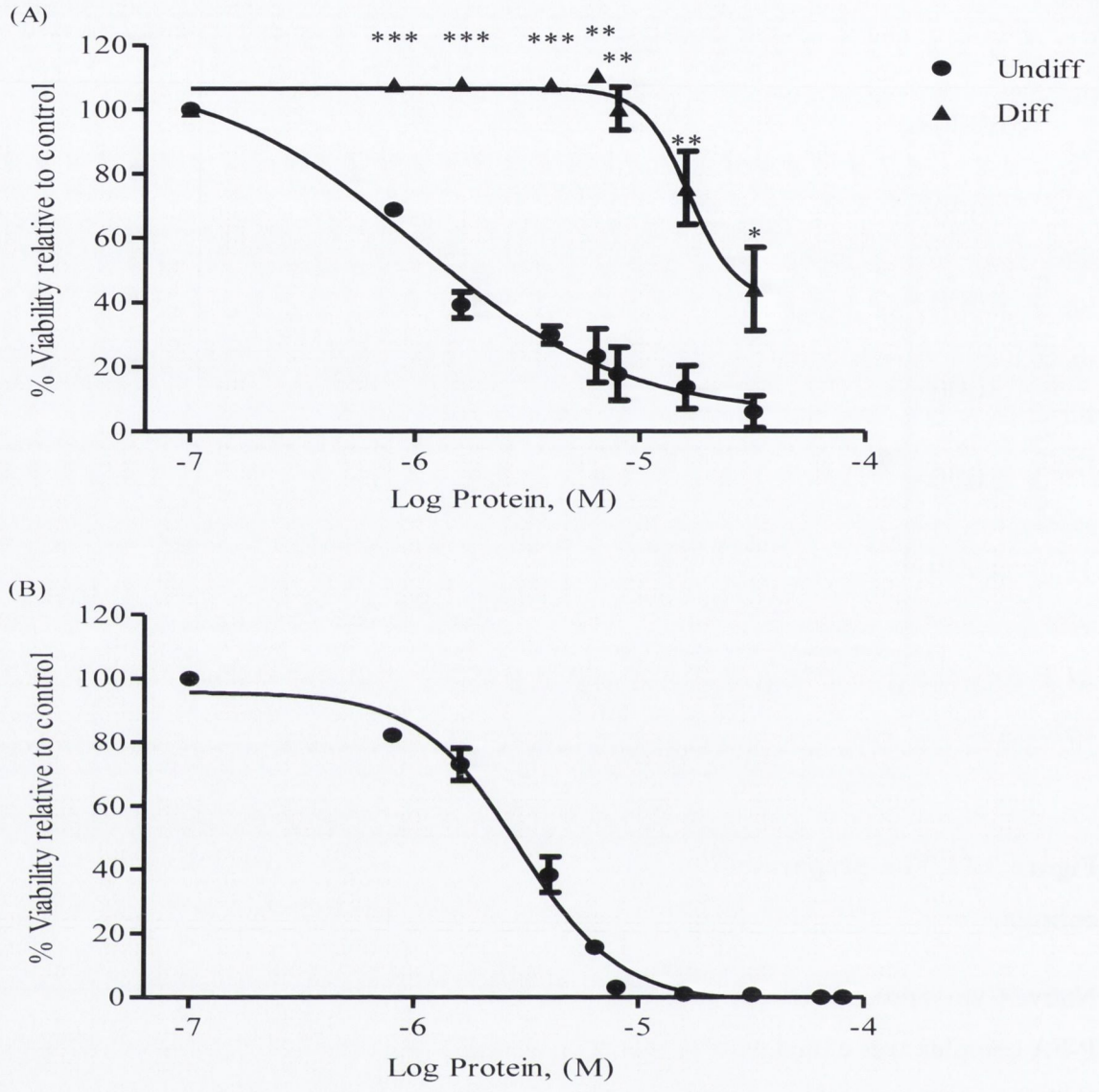

Figure 3.12 Dosage–response viability curve for Cyto-*c*-OA tested on PC12 and U2OS cells using Alamar Blue assay

PC12 cell lines were treated with Cyto-*c*-OA (log scale) and incubated for 24 h at 37 °C (A). Cells were then assayed using the fluorescencent staining compound Alamar Blue. (B) U2OS cells were treated with Cyto-*c*-OA for 24 h at 37°C. The values are the means of three experiments with the error bar indicating SEM. $^{*}p < 0.05$, $^{**}p < 0.001$, *** $p < 0.001$ were calculated using GraphPad.

3.2.7. The Mb-OA Complex Significantly Reduces Viability in Cancer Cells When Compared to Differentiated Cells in vitro

Having used MG proteins we have been able to generate P-FA complexes which display selective toxicity against tumour cells when analyzed using the PC12 differenitaion model of cell differentiation. Nearly all previously studied P-FA complexes have involved the use of MG proteins (Wilhelm *et al.*, 2009, Pettersson *et al.*, 2006, Nakamura *et al.*, 2013, Håkansson *et al.*, 1995, Brinkmann *et al.*, 2011b) suggesting that the MG state of the protein may be integral. In order to address this theory we used Mb which is the non-apo form of AMb. Mb-OA was prepared in identical manner as was applied to the formation of BAMLET, and yielded a similar peak at high salt (Figure 3.13) which was collected and dialysed before *in vitro* experiments were conducted. PC12 and U2OS cells were treated with Mb-OA and analysed using Alamar Blue. Cells treated with Mb-OA highlighted the selective nature of these P-FA complexes towards cancer cells. $PC12^{diff}$ cells showed elevated levels of resistance against Mb-OA. $PC12^{undiff}$ cells yielded an LC_{50} value of 2.1×10^{-7} M (0.003 mg/ml), whereas $PC12^{diff}$ cells gave an LC_{50} value of 4.3×10^{-6} M (0.07 mg/ml) (Figure 3.14 (A)). U2OS treated in identical conditions and concentrations gave an LC_{50} value of 6.1×10^{-7} M (0.01 mg/ml) (Figure 3.14 (B)). We have shown for the first time that Mb can be engineered into a selectively tumouricidal agent. When coupled to OA, Mb displayed a remarkably similar efficacy to that observed in other P-FA. Furthermore we have demonstrated that non-MG proteins can be used to generate cytotoxic P-FA complexes.

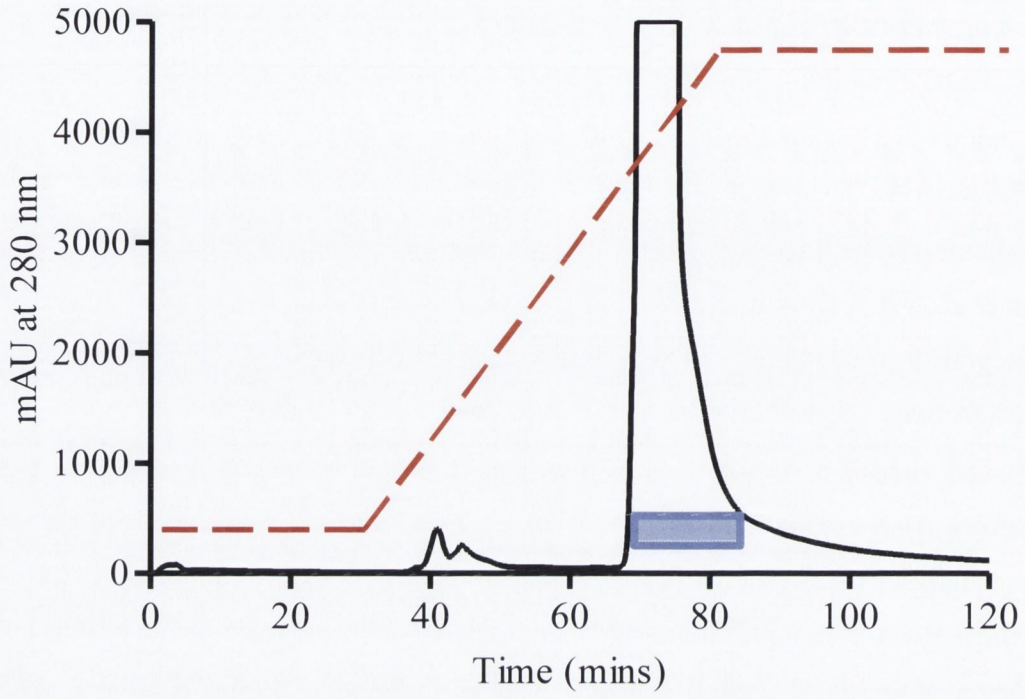

Figure 3.13 The preparation of Mb-OA by IEC on an OA-conditioned exchange column.

Mb native protein was applied to a DEAE-FF 5 ml column conditioned with OA, and the P-FA complex was eluted with a gradient of 1 M NaCl (dashed red line). The solid blue bar indicates the fraction from the column that was collected for further studies.

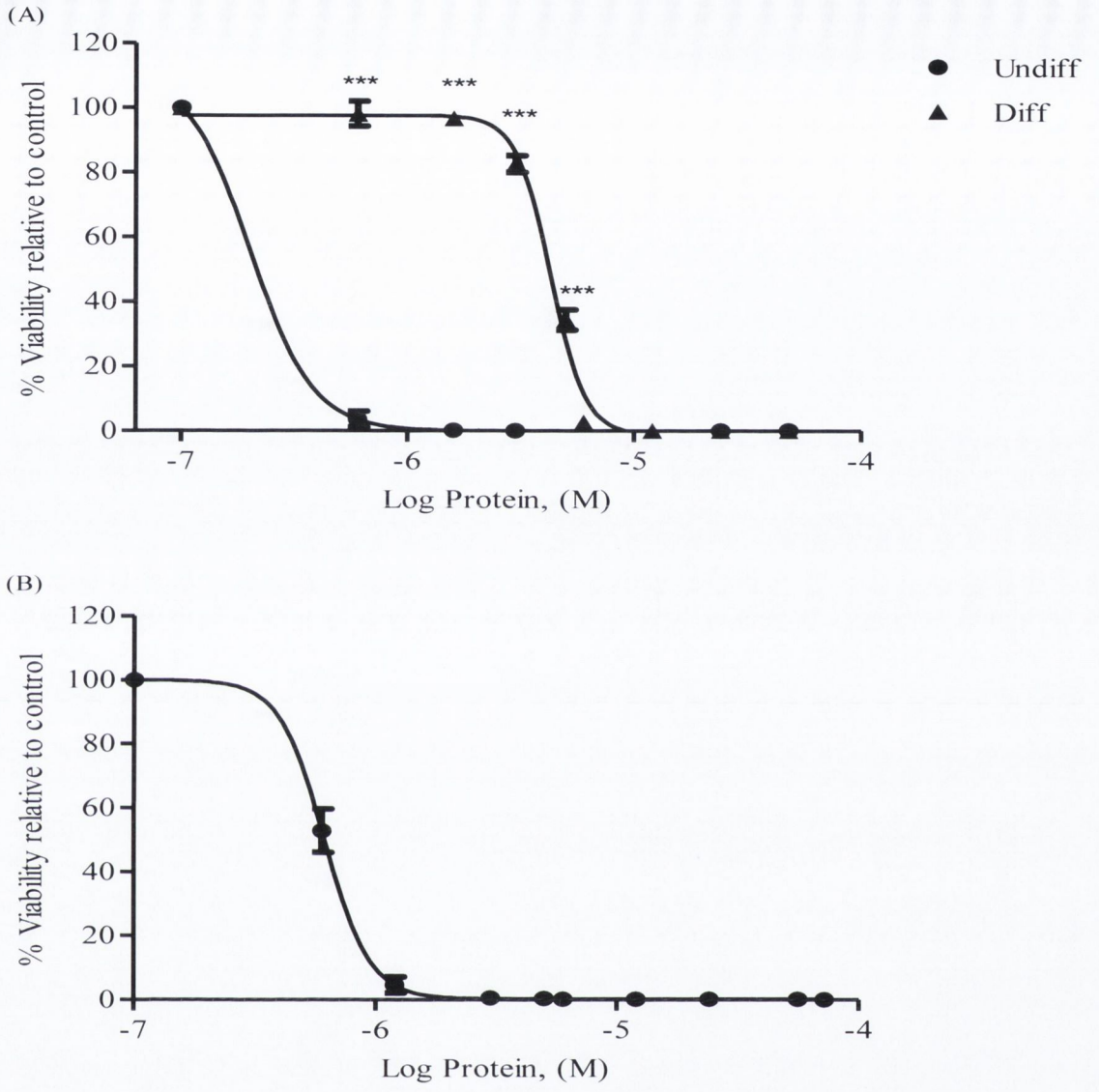

Figure 3.14 Dosage–response viability curve for Mb-OA tested on PC12 and U2OS cells using Alamar Blue assay.

PC12 cell lines were treated with Mb-OA (log scale) and incubated for 24 h at 37 °C. Cells were then assayed using the fluorescencent staining compound Alamar Blue. (B) U2OS cells were treated with Mb-OA for 24 h at 37°C. The values are the means of three experiments with the error bar indicating SEM. $^{*}p < 0.05$, $^{**}p < 0.001$, *** $p < 0.001$ were calculated using GraphPad.

3.2.8. The Ub-OA Complex Significantly Reduces Viability in Cancer Cells When Compared to Differentiated Cells in vitro

Ub is another globular protein which we wanted to examine to see if it could form a similar P-FA complex. Ub-OA complex was formed readily using IEC (Figure 3.15) and when tested Ub-OA complexes displayed selective tumouricidal capabilities towards $PC12^{undiff}$ and U2OS cells *in vitro* and appeared to be less effective against the differentiated phenotype of PC12 cells (Figure 3.16 (A)). $PC12^{diff}$ cells showed significant resistance towards Ub-OA treatment when compared to $PC12^{undiff}$ cells. $PC12^{undiff}$ cells gave an LC_{50} result of 2.5×10^{-5} M (0.21 mg/ml) whilst PC12 cells displaying differentiated phenotype returned LC_{50} values of 9×10^{-5} M (0.77 mg/ml). U2OS gave the lowest LC_{50} values of 2×10^{-5} M (0.17 mg/ml) (Figure 3.16 (B)). Similarly to our Mb-OA experiments, the results presented here show that Ub can be engineered to make a complex with OA using IEC, and that this complex is cytotoxic against tumour cells.

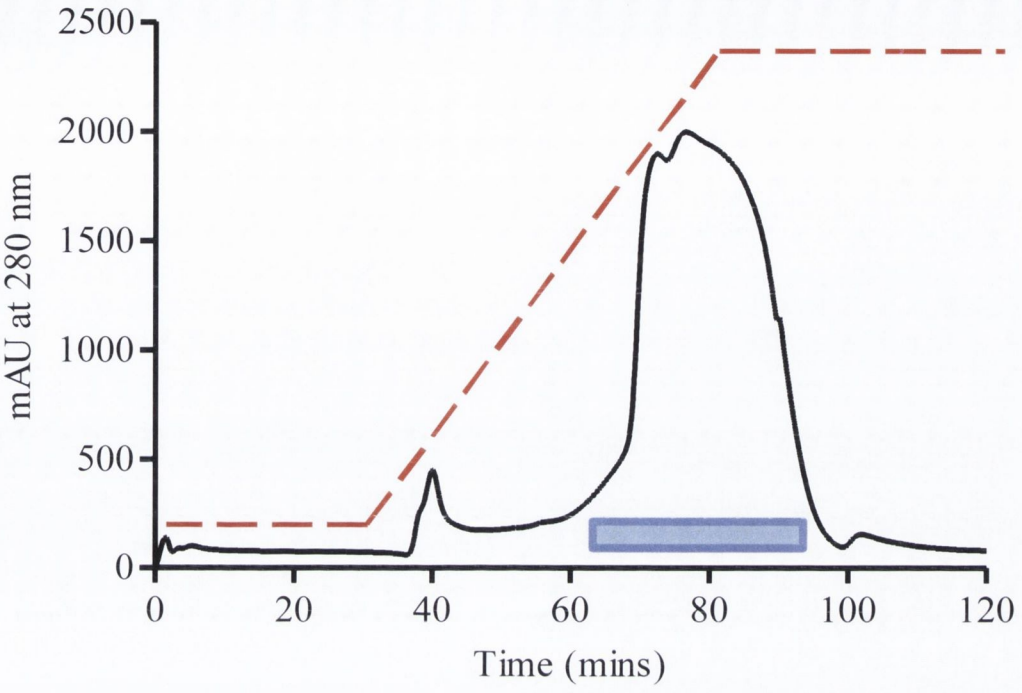

Figure 3.15 The preparation of Ub-OA by IEC on an OA-conditioned exchange column.

The native form of Ub was applied to a DEAE-FF 5 ml column conditioned with OA, and the P-FA complex was eluted with a gradient of 1 M NaCl (dashed red line). The solid blue bar indicates the fraction from the column that was collected for further studies.

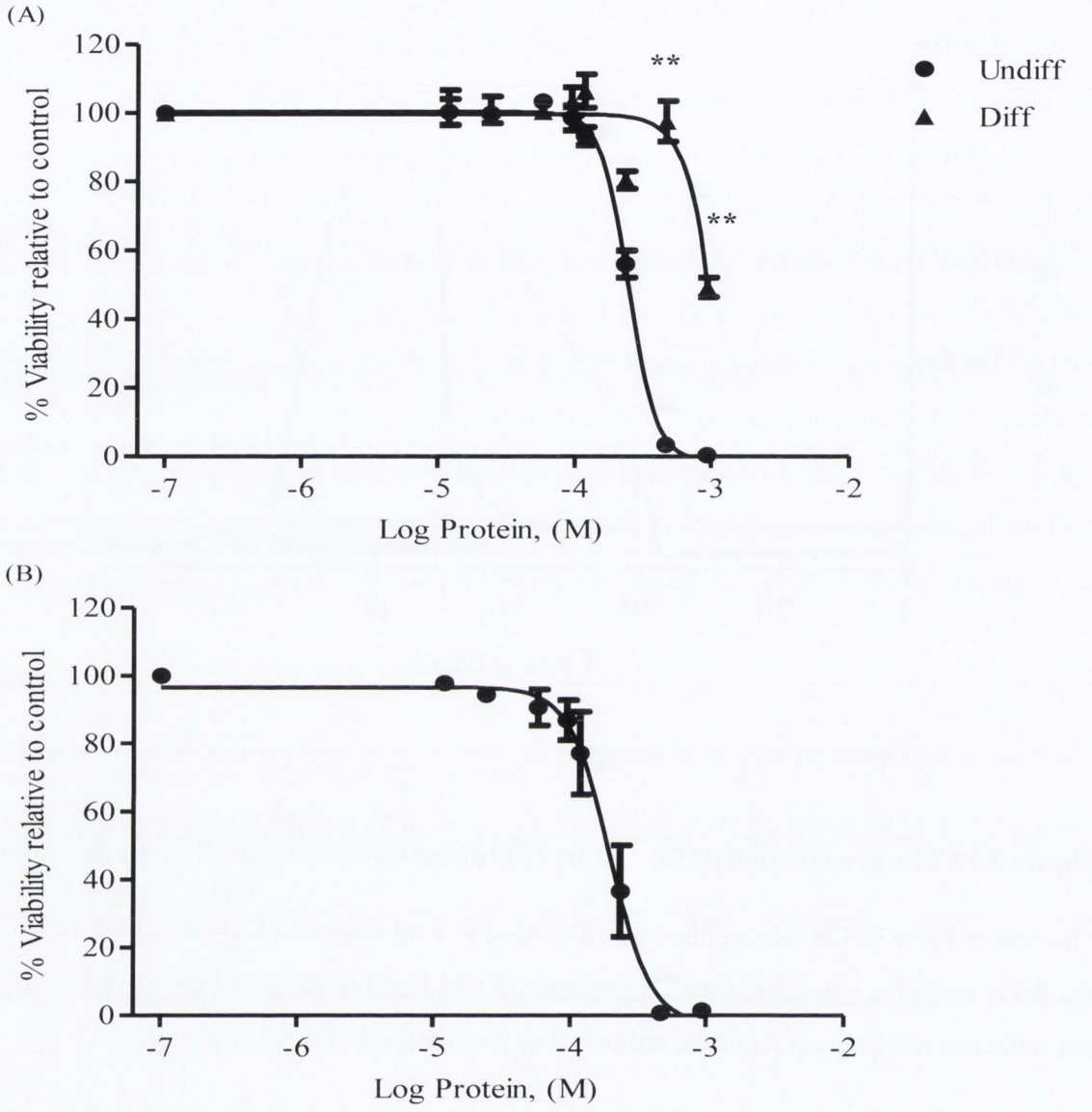

Figure 3.16 Dosage–response viability curve for Ub-OA tested on PC12 and U2OS cells.

PC12 cell lines were treated with Ub-OA (log scale) and incubated for 24 h at 37 °C (A). Cells were then assayed using the fluorescencent staining compound Alamar Blue. (B) U2OS cells were treated with Ub-OA for 24 h at 37°C. The values are the means of three experiments with the error bar indicating SEM. $^{*}p < 0.05$, $^{**}p < 0.001$, *** $p < 0.001$ were calculated using GraphPad.

3.2.9. Non-OA Complexes are Not Cytotoxic Towards Cells

Using non-LA proteins our group has generated cytotoxic tumouricidal complexes bound to OA. To ensure that the toxic element seen in these complexes is not a result of the protein used, we tested the native proteins using our three cell lines tested previously. Cells were incubated with 0.1 mg/ml of the native proteins in the absence of OA as per Section 2.4 to determine whether the protein alone had any cytotoxicity towards tumour cells when not in complex. OA was not added to the proteins at any point. All cells treated showed no notable decrease in cell viability at this concentration (Figure 3.17). This result indicates that the protein component of these P-FA complexes is not toxic to the cells and is not resulting in cell death.

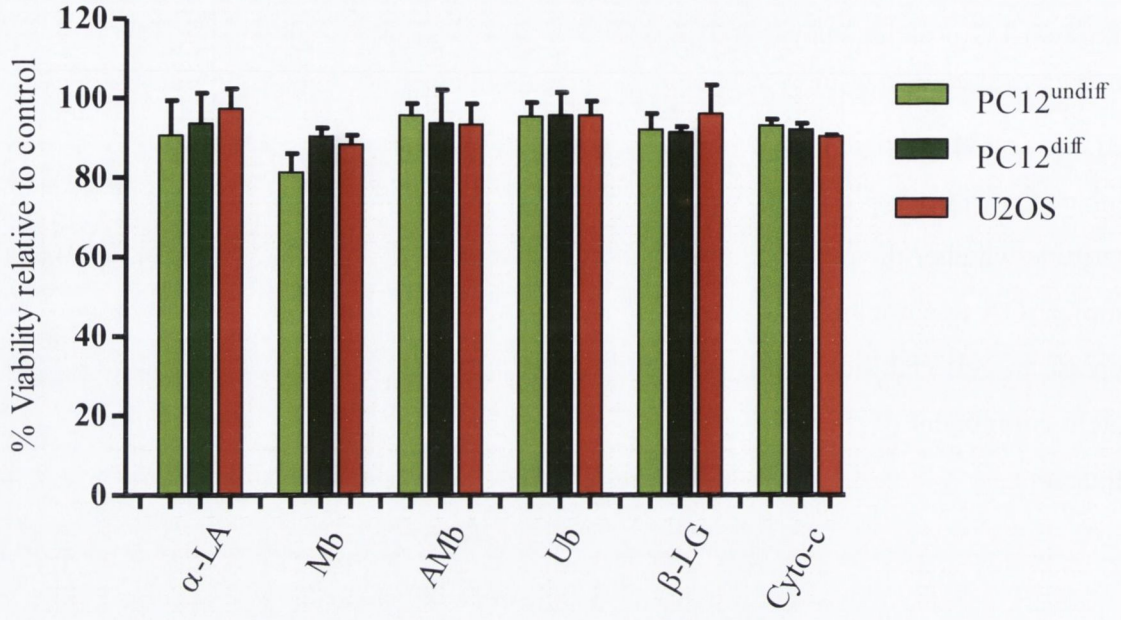

Figure 3.17 Cell lines treated with 0.1 mg/ml of native protein

Cell lines were treated with 0.1 mg/ml of native protein and left to incubate for 24 h at 37°C. $PC12^{undiff}$ (light green bars), $PC12^{diff}$ (dark green bars), and U2OS (red bars) cells treated showed no dramatic decrease in cell viability over 24 h. The values are the means of three experiments with the error bar indicating SEM.

Table 3.2 LC_{50} values (in mg/ml and molarity) for P-FA samples on cell lines.

The values are the means of three experiments using log (inhibitor) vs. response curve with non linear regression calculated on GraphPad.

P-FA	U2OS mg/ml (μM)	$PC12^{undiff}$ mg/ml (μM)	$PC12^{diff}$ mg/ml (μM)
HAMLET	0.048 (3.4)	0.064 (4.5)	0.45 (32)
BAMLET	0.038 (2.7)	0.056 (3.9)	0.84 (59)
AMb-OA	0.058 (3.4)	0.016 (0.9)	0.134 (7.9)
β-LG-OA	0.03 (1.6)	0.03 (1.6)	0.37 (20)
Cyto-*c*-OA	0.04 (30)	0.012 (1.0)	0.21 (17)
Mb-OA	0.01 (0.61)	0.003 (0.2)	0.07 (4.3)
Ub-OA	0.17 (20)	0.21 (25)	0.77 (90)

3.2.10. Biotinylated P-FA Complexes are Taken up in Larger Qualities into Tumour Cells

We have demonstrated that P-FA complexes display selective cytotoxicity towards tumour cells while causing less harm to healthy cells. The exact mechanisms responsible for HAMLET tumour cell selectivity are still unclear although the overexpression of c-Myc, and the glycolytic state of the cells (Storm *et al.*, 2011), in addition to HAMLETs ability to activate ion channel fluxes (Storm *et al.*, 2013) have all been shown to be important. Alexa-HAMLET has been shown to be taken up in larger quantities into tumour cells when compared to differentiated cells however this was performed with two unrelated cell lines (Mossberg *et al.*, 2010c). We sought to identify whether P-FA complexes are more readily absorbed into the tumour cell when compared to the same cell displaying a differentiated phenotype. P-FA complexes were biotinylated and then applied to cells. Alexa Fluor® 647 streptavidin was used to stain the cells. This molecule which is attached to a fluorescent probe binds to biotin and allows for detection within the cell. The concentrations chosen are seen in Table 3.3 and were calculated using the LC_{50} values of $PC12^{undiff}$ cells treated with each protein. The concentrations used were the same for both cell lines as we wanted to observe whether the difference in cell viability was related to the level of P-FA within the cells. PBS with biotin was added to cells as a control. This sample was stained for to eliminate biotin background (Figure 3.18). Using the same concentrations for both cell lines we have shown that biotinylated P-FA complexes are internalized into the $PC12^{undiff}$ cells (Figure 3.19) at a far greater rate than seen in $PC12^{diff}$ cells (Figure 3.20). These results suggest that at equal protein concentrations, cells displaying a tumour phenotype absorb greater quantities of these P-FA complexes which may contribute their increased cytotoxicity.

Table 3.3 List of concentrations used for biotinylation

P-FA	$PC12^{undiff}$ + $PC12^{diff}$ mg/ml (μM)
BAMLET	0.05 (3.5)
AMb-OA	0.01 (0.6)
β-LG-OA	0.03 (1.6)
Cyto-*c*-OA	0.01 (0.8)
Mb-OA	0.003 (0.2)
Ub-OA	0.2 (25)

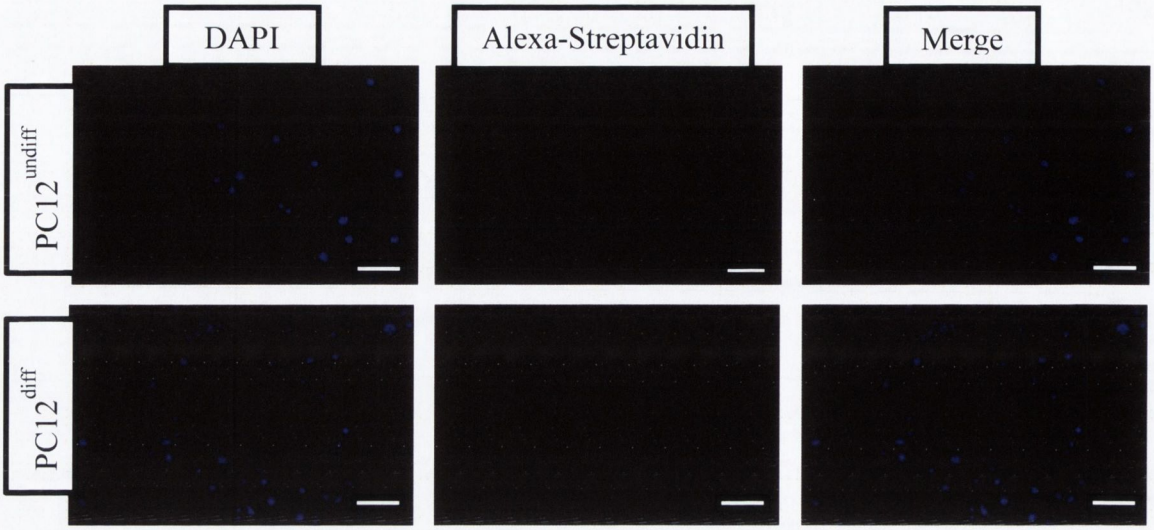

Figure 3.18 PC12$^{undiff/diff}$ cells without biotinylated P-FA complexes

Cells were visualised in the presence of PBS and biotin to act as a control for background biotin. Samples were processed in the same way as with biotinylated P-FA complexes. These results are representative of two separate experiments. Scale bars: 40 μM.

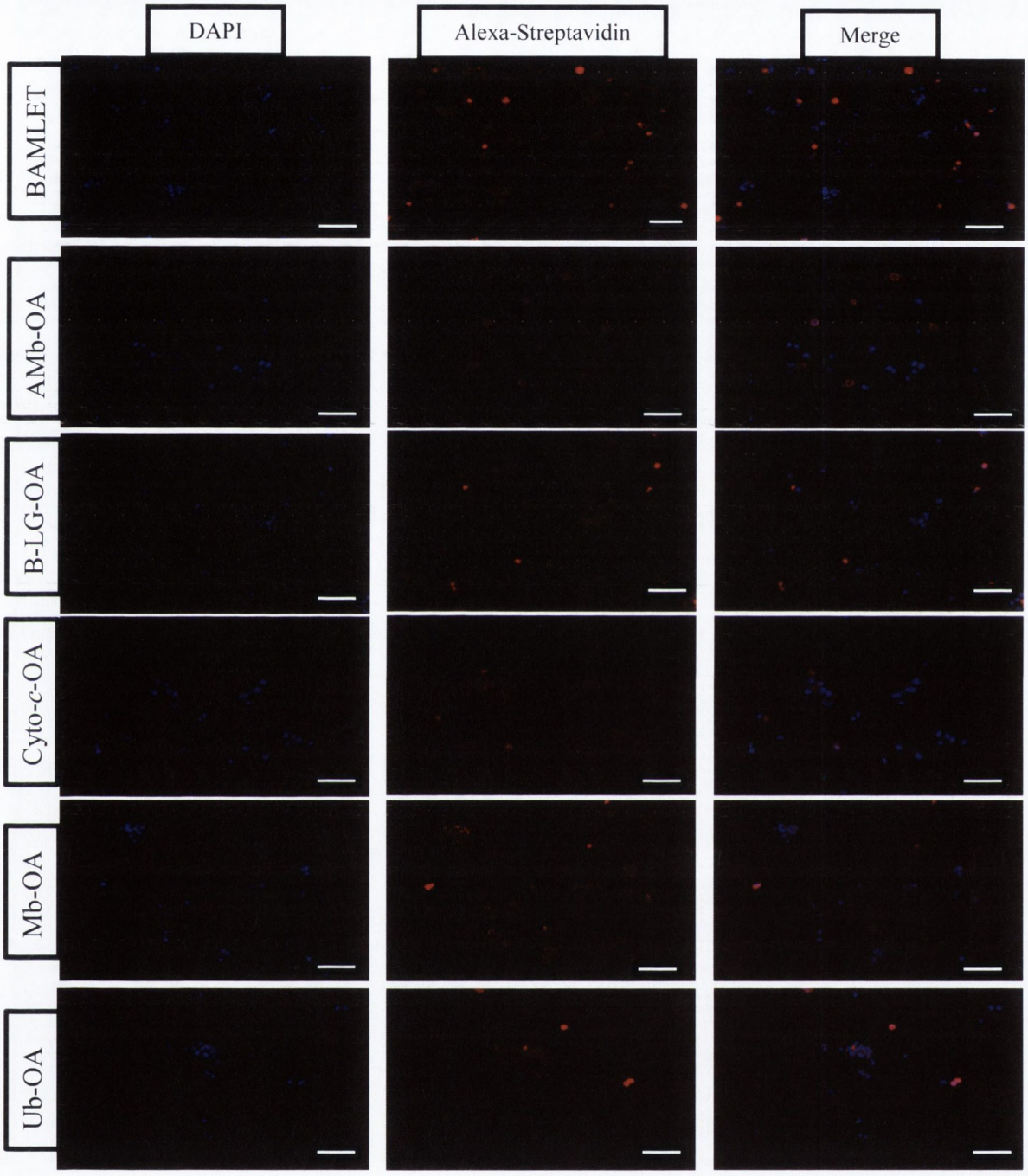

Figure 3.19 Uptake of biotinylated P-FA complexes in PC12^{undiff} cells

Cells were incubated with biotinylated P-FA complexes. Alexa Fluor® 647 streptavidin was used to probe for biotinylated complexes using immunofluorescence. Results are representative of two separate experiments. Scale bars: 40 μM.

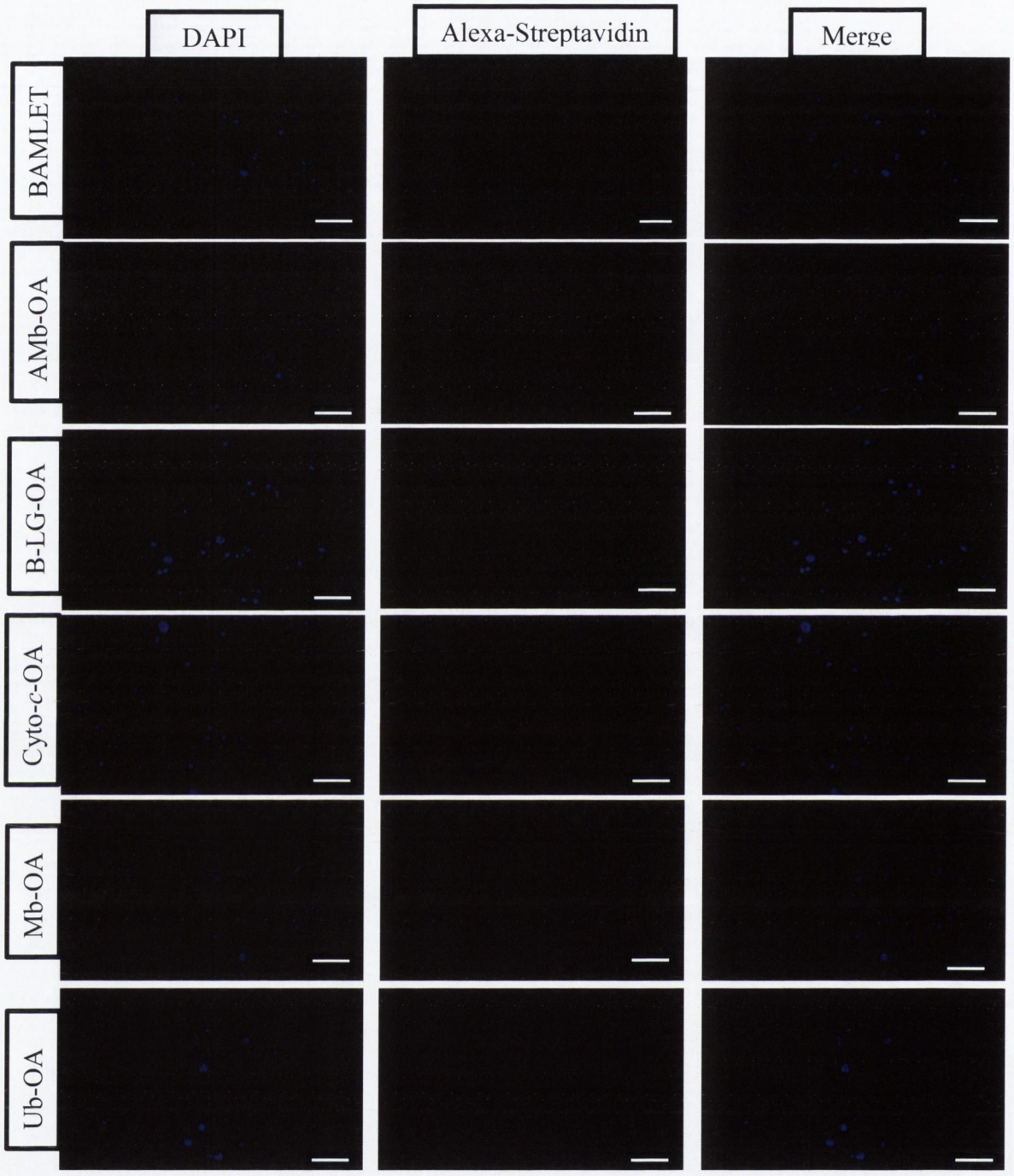

Figure 3.20 Uptake of biotinylated of P-FA complexes in PC12^{diff} cells.

Cells were incubated with biotinylated P-FA complexes. Alexa Fluor® 647 streptavidin was used to probe for biotinylated complexes using immunofluorescence. Results are representative of two separate experiments. Scale bars: 40 μM.

3.2.11. P-FA Complexes do not Display Signs of Aggregation

The monomeric or oligomeric conformation of HAMLET is an area of debate with some experiments supporting the presence of the monomeric state (Mossberg *et al.*, 2010b, Pettersson-Kastberg *et al.*, 2009b) while others contest that it is in an oligomeric form (Spolaore *et al.*, 2010b, Nakamura *et al.*, 2013). The manipulation of the proteins natural environment can trigger a cascade of events that can ultimately lead to protein aggregation (Krebs *et al.*, 2000). One concern that was raised was whether manipulation of the native proteins using the IEC column and the formation of an unnatural OA complex would trigger the normally monomeric proteins to develop into oligomers or fibrils. Another issue with the formation of oligomers is that the toxicity observed in cells incubated with P-FA complexes may be linked to the oligomeric protein rather than the complex itself, as oligomers can be cytotoxic towards all cell types (Dahlgren *et al.*, 2002, Kim *et al.*, 2003, Oddo *et al.*, 2006, Reixach *et al.*, 2004). A further concern with the formation of oligomeric proteins is that they will develop into amyloid fibrils. In the case of ELOA, the OA in the ELOA complex restricted the formation of amyloid fibrils (Wilhelm *et al.*, 2009) however all P-FA complexes may not behave in this way. In order to establish whether the cytotoxity displayed by these novel tumouricidal complexes is a generic function which appears to be related to the P-FA conformation of these molecules, or whether it is attributed to the fact that they were actually in an oligomeric or fibrillar state, the P-FA complexes (Table 3.1) were subjected to ThT, CR spectroscopic, and CR birefringence assays. For all complexes tested they exhibited no signs of aggregation suggesting that these assemblies are in the monomeric form.

3.2.12. ThT Fluorescence of P-FA Complexes

ThT is a key method of determining aggregation in proteins (Biancalana and Koide, 2010). The increase in ThT fluorescence for P-FA complexes (Table 3.1) was measured using a spectrofluorometer with parameters of excitation 440 nm and emission 482 nm. Readings recorded at 482 nm were recorded and averaged over three experiments. All P-FA complexes displayed an increase in absorbance when measured against ThT without any protein present (grey bars), however this is not surprising as ThT binds to hydrophobic pockets in globular proteins normally (Biancalana and Koide, 2010). As a comparison, oligomers isolated from HEWL (see section 2.10) showed a dramatic increase in absorbance when compared to ThT only and other P-FA complexes. As our tests *in vitro* continue for a duration up to 24 h, The P-FA complexes were left to incubated at 37°C for 24 h before being read again to ensure that no fibrillization was occurring over the period which the cells were being treated. No dramatic increase was observed in any of the P-FA or the oligomer control samples examined suggesting that little aggregation was occurring during the period of incubation (Figure 3.21). The results demonstrate that little aggregation has occurred after the formation of these P-FA complexes and that prolonged incubation does not cause an increase in ThT binding.

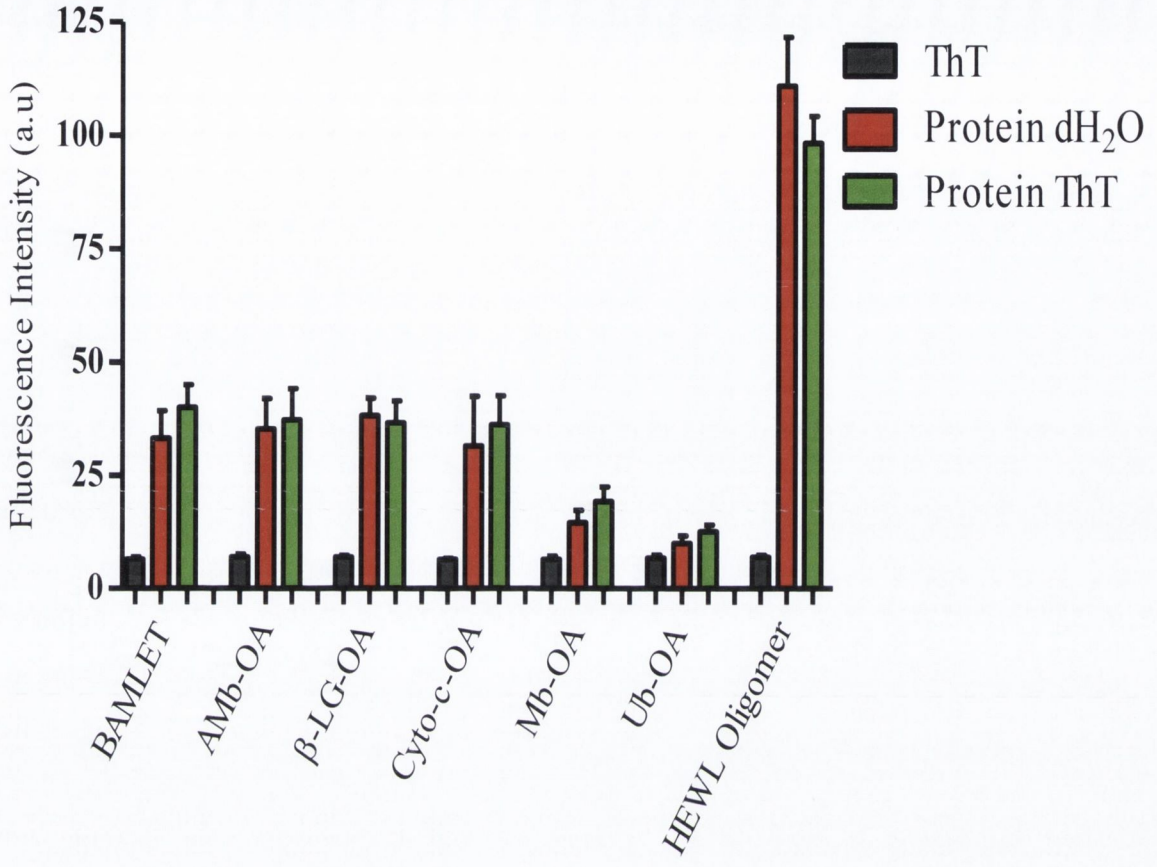

Figure 3.21 ThT fluorescence of P-FA complexes

P-FA complexes (0.5 mM) were treated with ThT and the fluorescence was read using a spectrofluorometer. P-FA complexes and oligomers were made fresh in dH2O (red bars) or left to incubate for 24 h at 37°C (green bars) and added to ThT buffer before analysing at emission 482nm. HEWL oligomer (0.5 mM) was used as a positive control. ThT without protein (grey bars) was used as a comparison for each sample. Results are representational of three experiments.

3.2.13. CR Spectroscopic and Birefringence Assays Using P-FA complexes Display no Signs of Aggregation

The use of ThT is not a fault proof method for determining aggregation and often other methods are required. CR staining is a highly sensitive and reproducible assay capable of determining if aggregates are present in a sample most notably in the amorphous form (Nilsson, 2004). For CR spectroscopy 1 mM P-FA complexes were measured against a control of 1 mM HEWL oligomers and fibrils. After incubation with CR buffer samples were analysed using UV-Vis in a spectral range of 400 nm to 600 nm. A shift in red absorbance from a peak maximum of 490 nm indicates the presence of aggregated protein (Nilsson, 2004). For birefringence the 1 mM P-FA complexes were visualised using 90°cross polarisers. These were then allowed to air dry on top of glass microscopic slides and stained as per section 2.13. From the spectroscopic assay HEWL oligomers show a shift in the red absorbance from a peak maximum of 490 nm for CR alone to 505 nm when in solution with CR. Additionally HEWL fibrils also display a shift in λmax signifying the manifestation of protein aggregates. Conversely, all P-FA complexes show no peak maxima differences from 490 nm suggesting that little aggregation has occurred (Figure 3.22). For birefringence all samples analysed showed absolutely no signs of birefringence after visualisation with a microscope capable of 90° cross polarization. The results demonstrate that no amorphous aggregation has occurred with these P-FA complexes as both assays and ThT above failed to show that oligomers or fibrils were present (Figure 3.23). This suggests that these P-FA complexes are not amorphous aggregates.

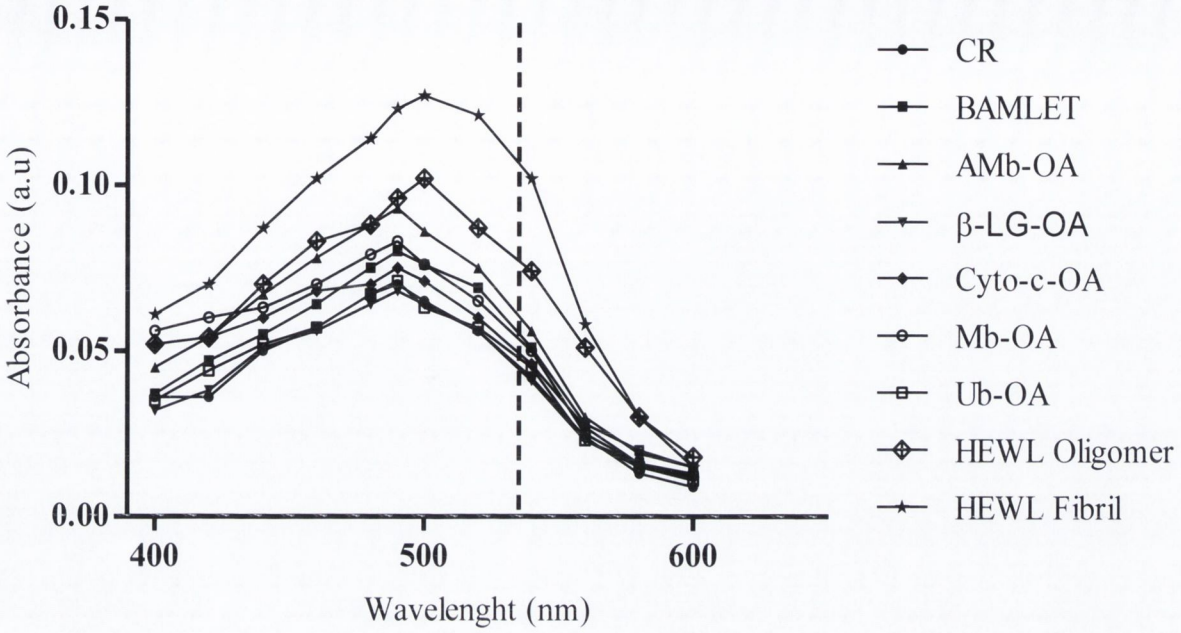

Figure 3.22 CR binding to P-FA complexes

P-FA (1 mM) complexes were allowed to bind to CR in phosphate buffer and analysed using UV-Vis in the absorbance range of 400 nm to 600 nm. As a positive aggregation control, 21 day old HEWL oligomers and fibrils (1 mM) were using in parallel with the these complexes and measured identically. Any significant difference in signal at 540 nm (black dotted line) is considered to be associated with the presence of amyloid-like fibrils. This figure is representative of three experiments.

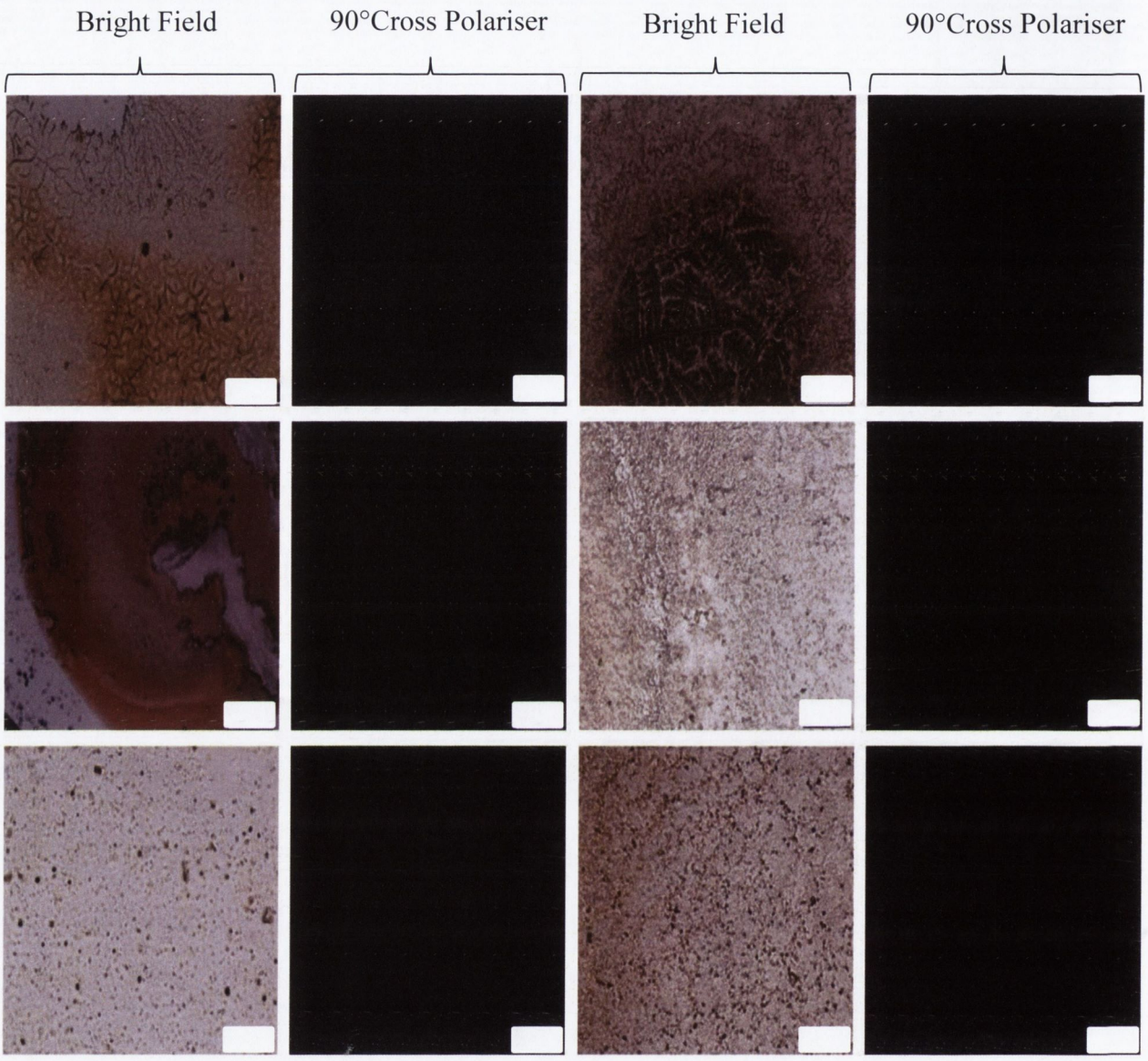

Figure 3.23 CR displays no birefringence upon mixing with P-FA complexes

CR birefringence was used to detect the presence of amyloid fibrils within the P-FA complexes. BAMLET (A and B), AMb-OA (C and D), β-LG-OA (E and F), Cyto-*c*-OA (G and H), Mb-OA (I and J), and Ub-OA (K and L) all display no birefringence when visualised using a 90°cross polarized light microscope. Both light microscopic view and cross polarized can be seen. This result is representative of three separate experiments. Scale bars: 20 μM

Table 3.4 P-FA concentrations used for flow cytometry and immunofluorescence mg/ml and (μM)

P-FA Complex	$PC12^{undiff}$ mg/ml (μM)	$PC12^{diff}$ mg/ml (μM)
BAMLET	0.03 (2.1)	0.5 (35)
AMb-OA	0.01 (0.6)	0.1 (6)
β-LG-OA	0.01 (0.6)	0.2 (11)
Cyto-*c*-OA	0.01 (0.8)	0.1 (7.7)
Mb-OA	0.01 (0.6)	0.05 (2.9)
Ub-OA	0.1 (12.5)	0.4 (47)

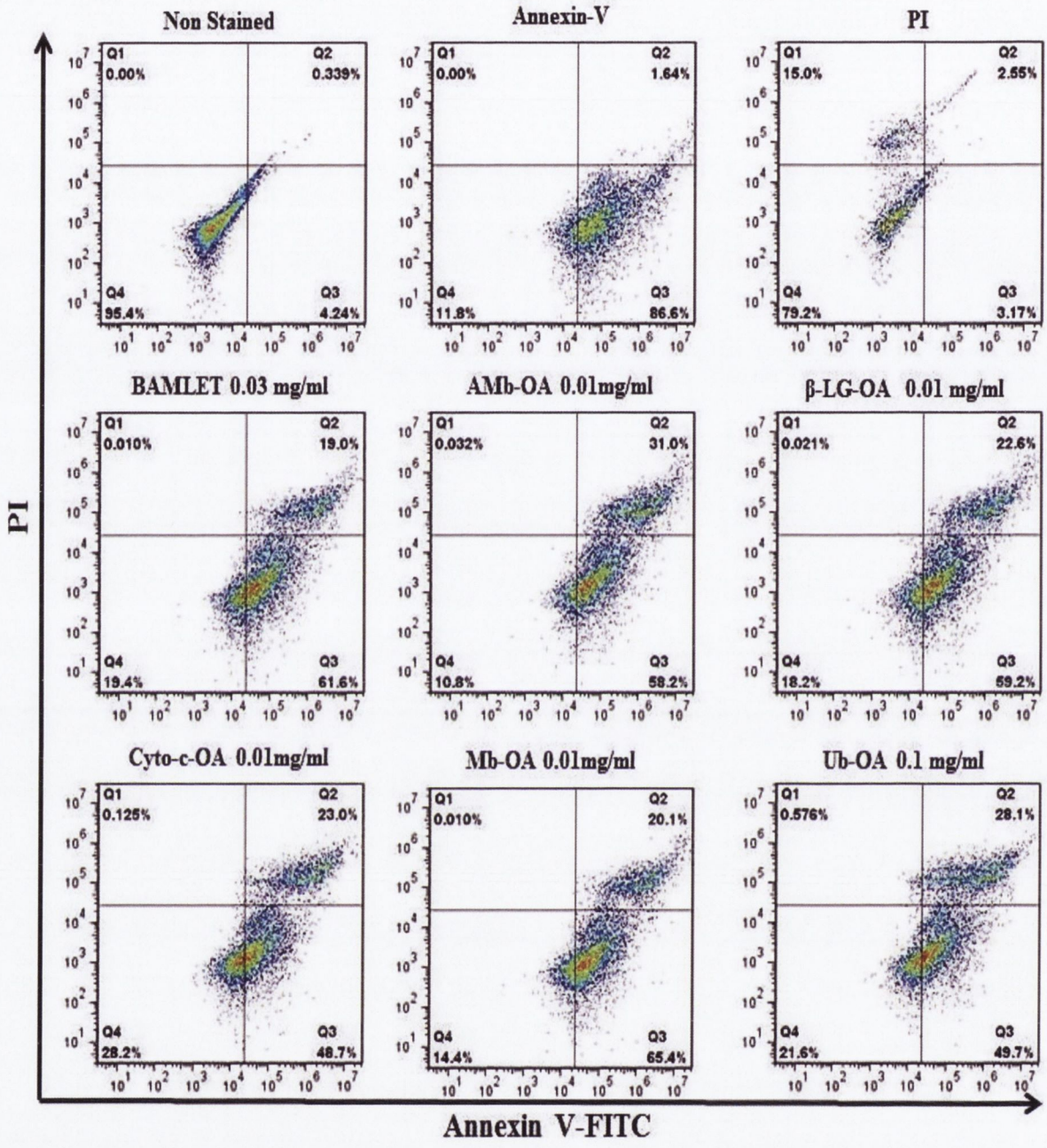

Figure 3.24 PC12^{undiff} cells treated with P-FA complexes induce apoptosis

PC12^{undiff} cells were treated with P-FA complexes and left to incubate for 24 h at 37°C. Untreated cells with no staining, Annexin V only, PI only, and double stained were used for compensation. Non apoptotic dead cells are Annexin V (-)/PI (+) (Q1); late apoptotic cells or necrotic cells exhibit Annexin V (+)/PI (+) (Q2); early apoptotic cells exhibit Annexin V (+)/PI (-) (Q3); viable cells exhibit Annexin V (-)/PI (-) (Q4). This data is representitive of three separate experiments.

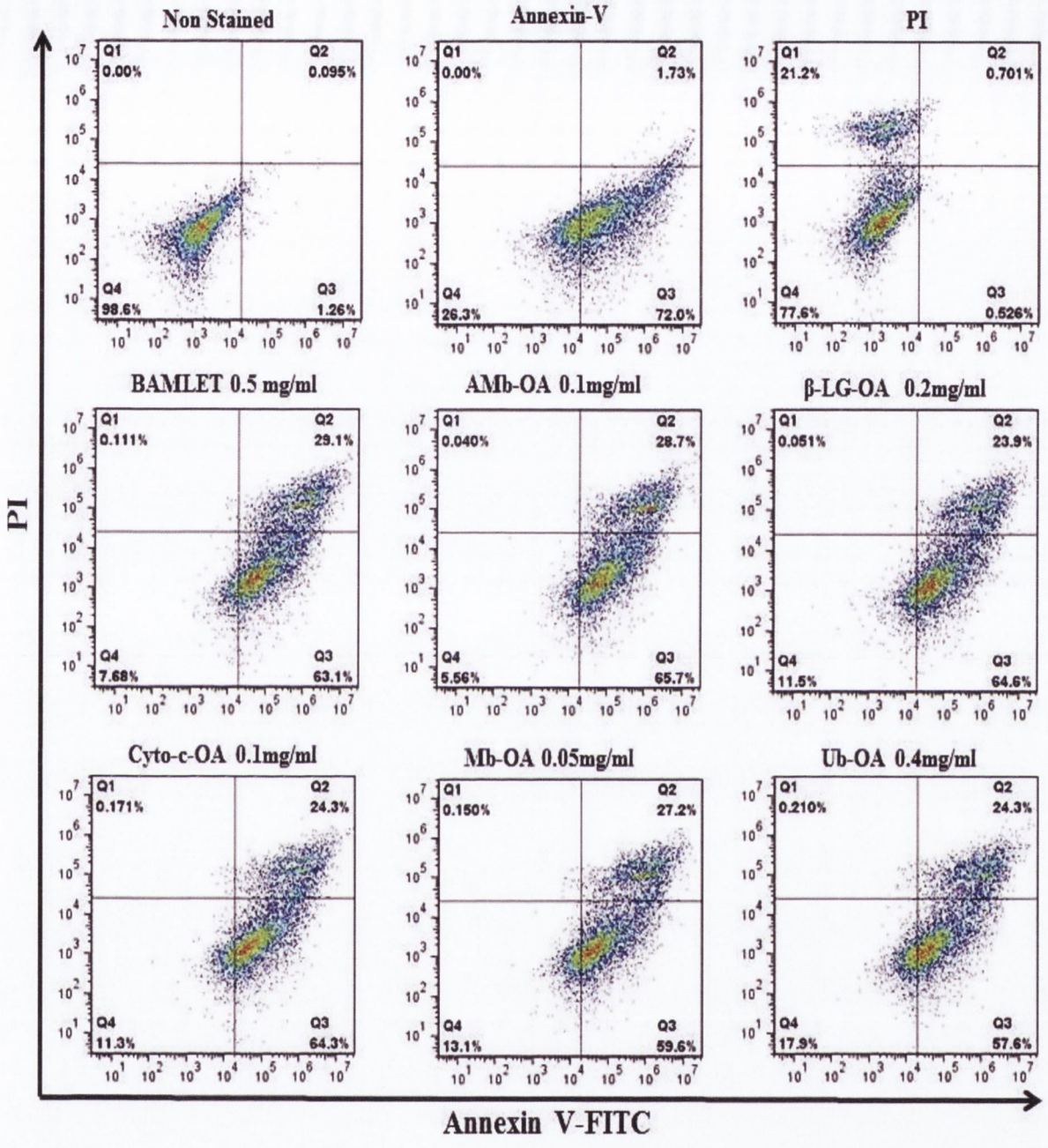

Figure 3.25 PC12^{diff} cells treated with P-FA complexes induce apoptosis

The cells were treated with P-FA complexes and left to incubate for 24 h at 37°C. Untreated cells with no staining, Annexin V only, PI only and double stained were used for compensation. Non apoptotic dead cells are Annexin V (-)/PI (+) (Q1); late apoptotic cells or necrotic cells exhibit Annexin V (+)/PI (+) (Q2); early apoptotic cells exhibit Annexin V (+)/PI (-) (Q3); viable cells exhibit Annexin V (-)/PI (-) (Q4). This data is representative of three separate experiments.

3.2.16. PARP Cleavage of PC12$^{undiff/diff}$ Cells Suggests a Role for Apoptosis in Response to P-FA Complexes

Although Annexin V/PI staining using flow cytometry is a useful technique it is not a definitive mechanism to determine cell death pathways as the membrane of necrotic cells can become labeled as well (Elmore, 2007). In light of this we used a PARP cleavage assay to further analyse the cell death pathway activated by P-FA complexes. In response to apoptotic cell death molecules, the full length PARP protein (116kDa) becomes cleaved to the shorter 89 kDa molecule (Chaitanya *et al.*, 2010). PC12$^{undiff/diff}$ cells were treated with 20 μg P-FA at differing concentrations to ensure adequate cell death had occurred. After cell death had occurred samples were prepared for Western blot analysis. PARP cleavage was observed in all lanes except for the untreated lane which contained cells but no P-FA complex and showed just native PARP protein uncleaved (Figure 3.26). β-actin was also probed for as a loading control. The results from this experiment show that in response to treatment with P-FA complexes, PC12^{undiff} cells experience apoptotic cell death and cleave the full length PARP molecule. Interestingly we could not get a cleaved band for PC12^{diff} cells to display the cleaved band.

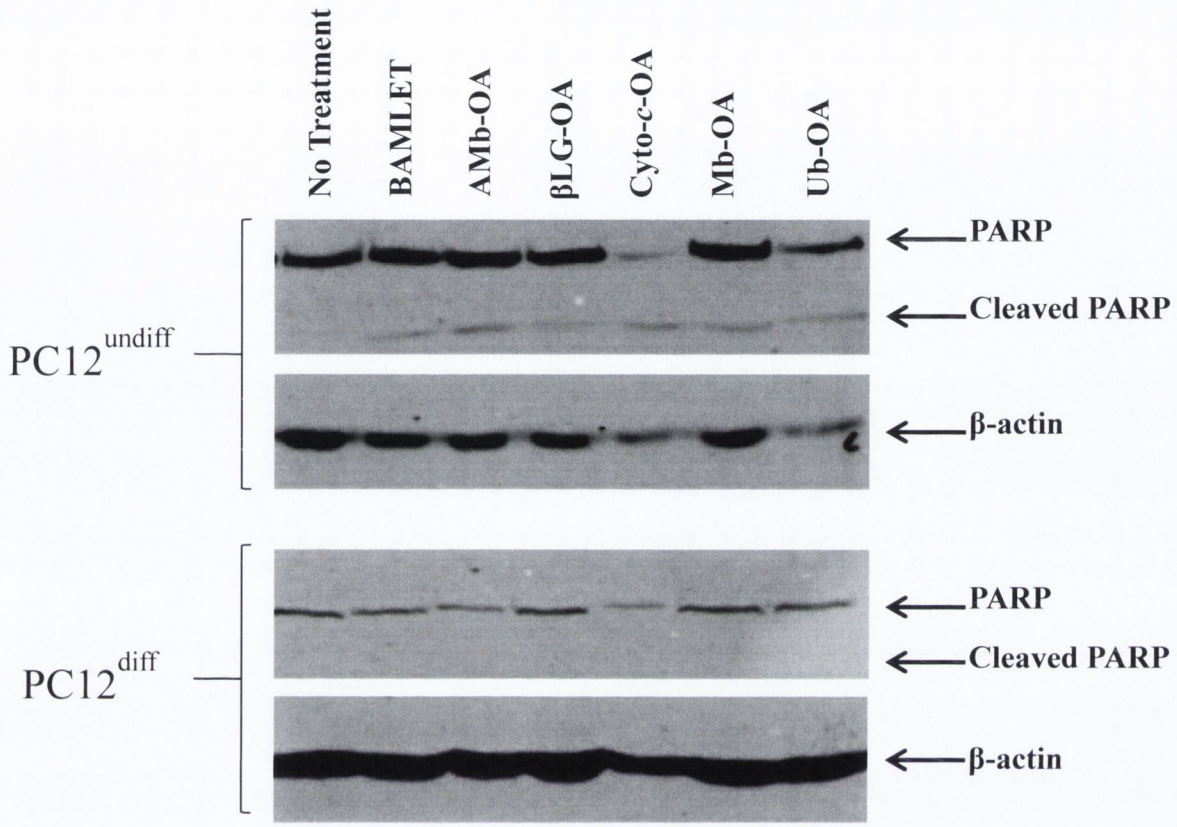

Figure 3.26 Western blot analysis of PARP cleavage in PC12$^{undiff/diff}$ cells

Cell lysates were collected from PC12$^{undiff/diff}$ cells which were incubated with BAMLET (0.02mg/ml), AMb-OA (0.01mg/ml), β-LG-OA (0.02mg/ml), Cyto-*c*-OA (0.01mg/ml), Mb-OA (0.01mg/ml), and Ub-OA (0.1mg/ml). For PC12^{diff} cells were incubated with BAMLET (0.08mg/ml), AMb-OA (0.05mg/ml), β-LG-OA (0.05mg/ml), Cyto-*c*-OA (0.05mg/ml), Mb-OA (0.05mg/ml), and Ub-OA (0.2mg/ml). All samples were incubated for a period of 24 h and then probed for the pro-apoptotic antibody anti-PARP. Cells without any treatment were used as a control. Shown are the full-length PARP (116 kDa) and the larger fragment (89 kDa) of apoptotically cleaved products, as well as β-actin used as a loading control. Results are representative of two separate experiments.

3.2.17. Apoptotic/Necrotic/Healthy Cell Detection Kit Shows that PC12 Cells Trigger Apoptosis

As a final method to confer that apoptotic cell death was occurring in response to treatment with P-FA complexes $PC12^{undiff/diff}$ cells were visualised using immunofluorescence. Cells were treated as per section 2.16 and visualised. This kit allows us to decipher between cells that are going through apoptosis (Annexin V-FITC), necrosis or non apoptiotic (PI), and those which are still in a healthy state (no staining except the nucleus stain DAPI). Cells were treated with the required P-FA complex for 24 h at concentrations used in Table 3.4. All cell groups show marked uptake of the apoptotic dye Annexin V, while cells which are deemed healthy stain for DAPI only. We can see that apoptotic cell death is detected in each group. For $PC12^{undiff}$ cells there was evident Annexin V staining in conjunction with lower levels of PI (Figure 3.29). $PC12^{diff}$ cells show similar levels of Annexin V and PI uptake as was seen in the tumour derivative (Figure. 3.30). The cells in each group show a small uptake of PI however this was negligible in comparison to Annexin V-FITC and was equal to what was observed in the controls. These experiments were carried out in conjunction with controls of cells treated with 10 µl PBS and stained with individual dyes for cell death (Annexin V/PI) to exclude background detection (Figure 3.27 and 3.28). All cells were stained with DAPI in order to visualise the cell. These results demonstrate that $PC12^{undiff/diff}$ cells treated with each P-FA complex are experiencing apoptotic cell death.

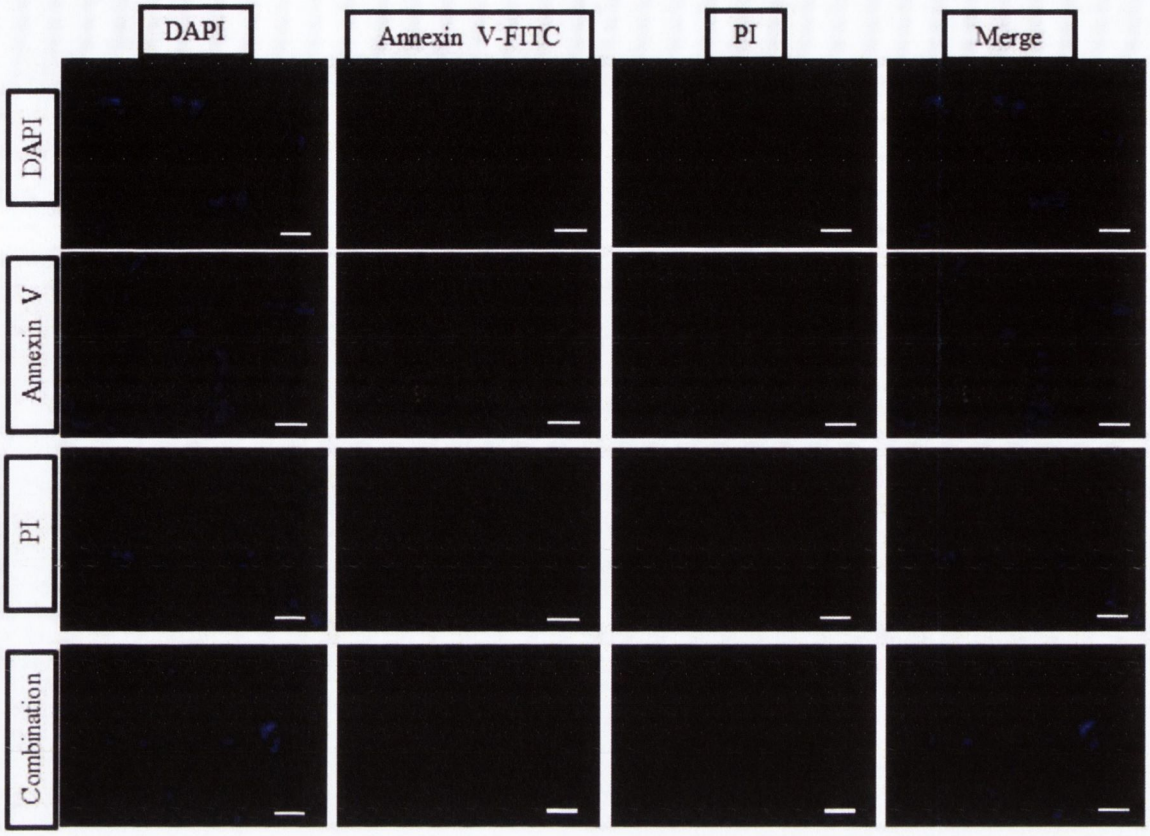

Figure 3.27 Immunofluorescence of PC12^{undiff} cells with single dyes and a combination of dyes in the absence of P-FA complexes

As a control for background staining PC12^{undiff} cells were incubated with 10 µl PBS and left for 24 h at 37°C. All cells were stained with DAPI for visualisation. The cells were then stained with individual cell death dyes (Annexin V and PI) and in combination (DAPI, Annexin V and PI). Results are representative of two separate results. Scale bar: 40 µM

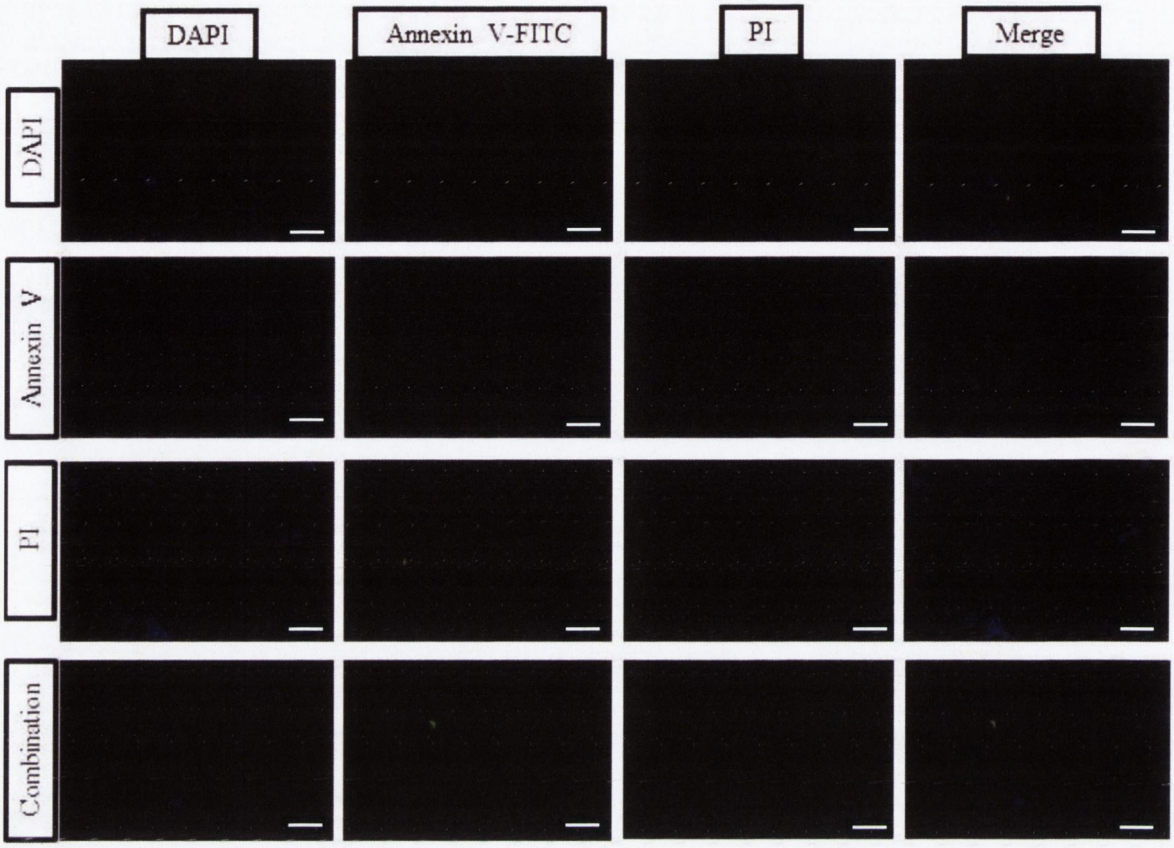

Figure 3.28 Immunofluorescence of PC12^{diff} cells with single dyes and a combination of dyes in the absence of P-FA complexes

As a control for background staining PC12^{diff} cells were incubated with 10 µl PBS and left for 24 h at 37°C. All cells were stained with DAPI for visualisation. The cells were then stained with individual cell death dyes (Annexin V and PI) and in combination (DAPI, Annexin V and PI). Results are representative of two separate results. Scale bar: 40 µM

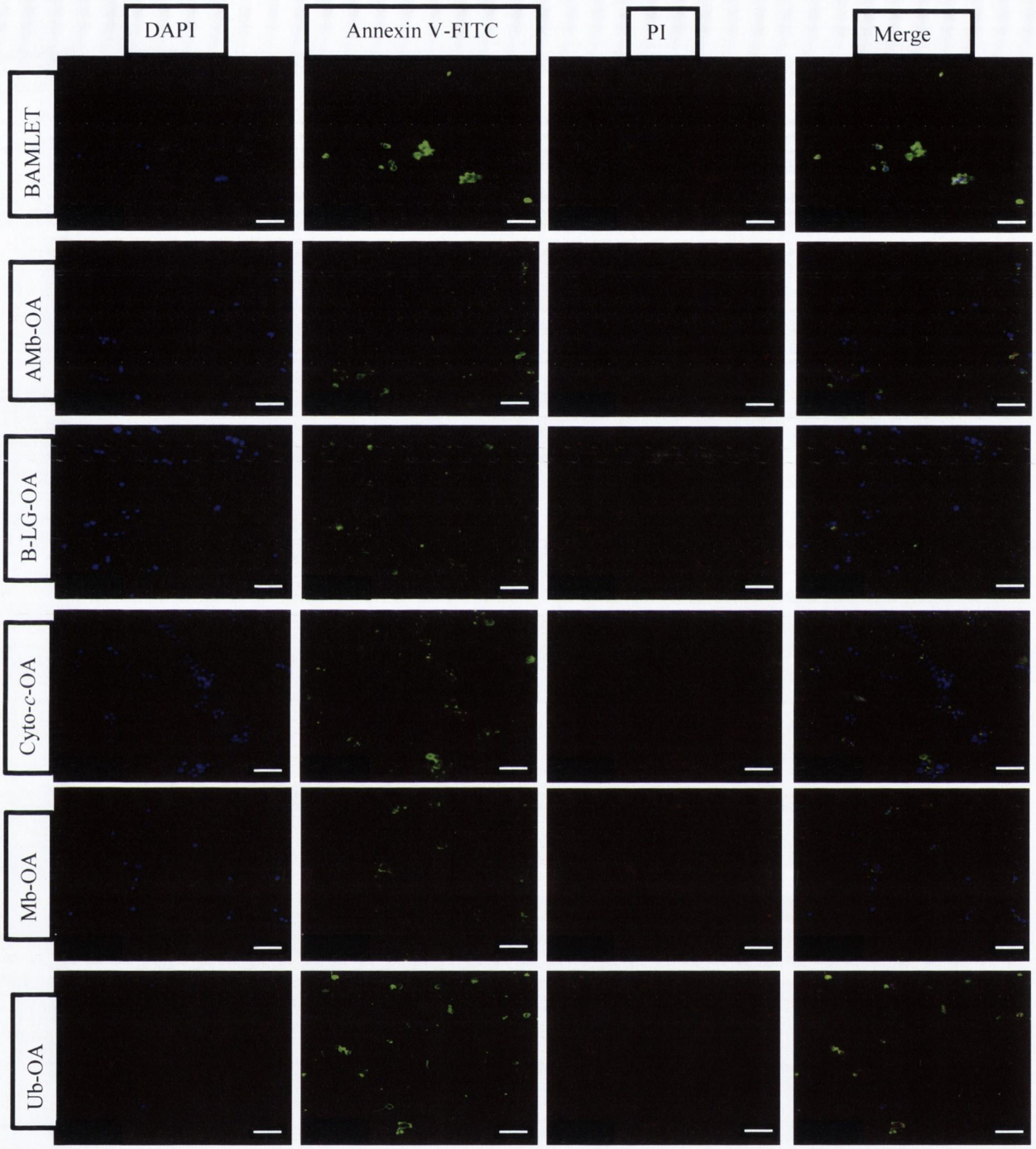

Figure 3.29 Immunofluorescence showing cell death in PC12^{undiff} cells

Cells were treated with protein concentrations contained in Table 4-4 and left for 24 h at 37°C. The cells were then fixed and mounted on slides for visualisation with an immunofluorescence microscope. These results are a representation of two separate experiments. Scale bar: 40 μM.

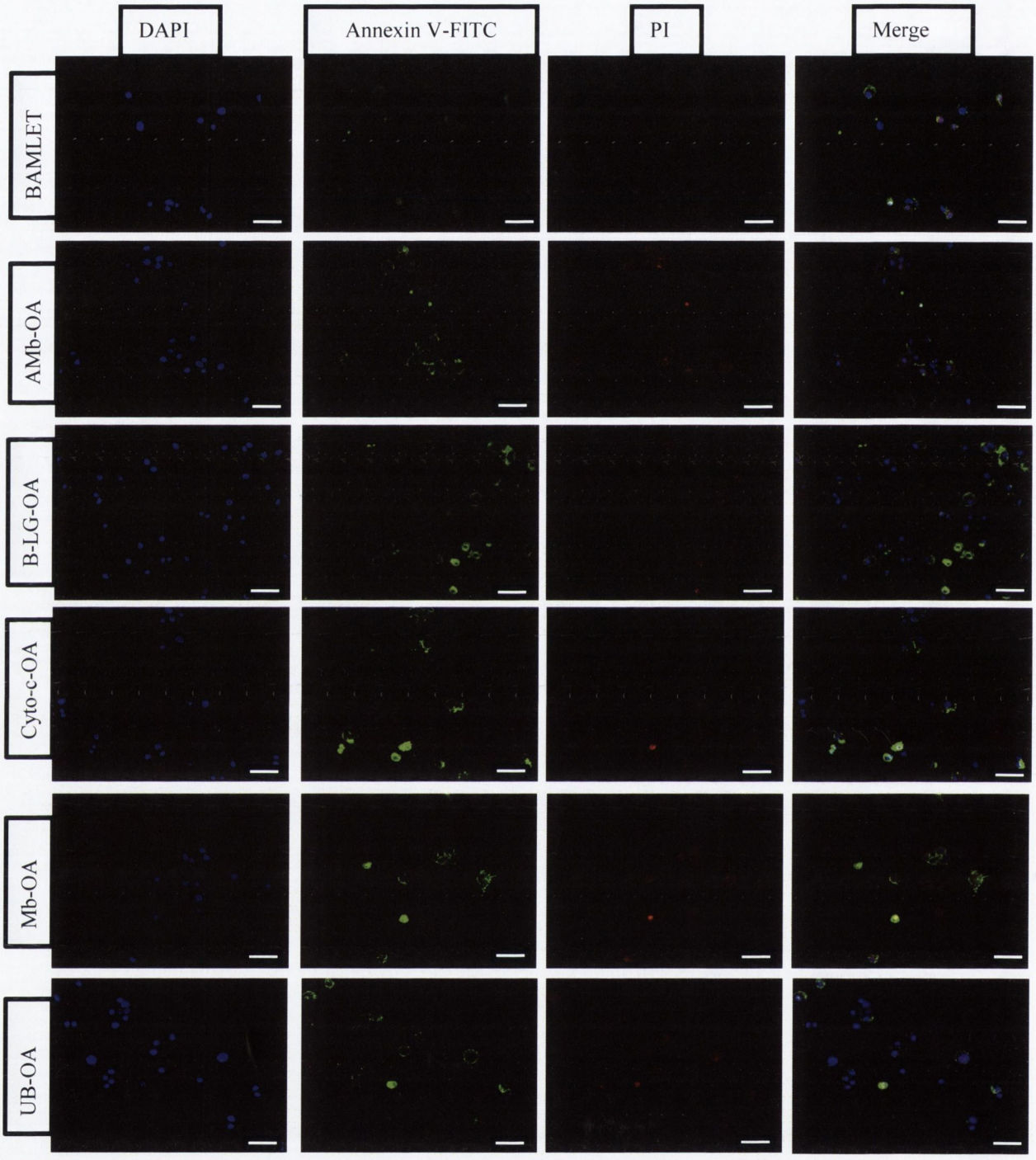

Figure 3.30 Immunofluorescence showing cell death in PC12^{diff} cells

Cells were treated with protein concentrations contained in Table 4-4 and left for 24 h at 37°C. The cells were then fixed and mounted on slides for visualisation with an immunofluorescence microscope. These results are a representation of two separate experiments. Scale bar: 30 μM.

3.3. Discussion

This study presents evidence novel proteins, engineered into complex with OA, can display cytotoxicity towards tumour cells *in vitro*. In addition to this all P-FA complexes tested showed a significant difference in terms of sensitivity towards differentiated cells. This is the first time that these P-FA complexes have been tested using a PC12 differentiation model which provides a useful model for determining differences in drugs targeting tumour and healthy cells *in vitro*. Complexes comprised of Mb, Cyto-*c*, and Ub comprise a group of completely novel compounds which have never been engineered before. Furthermore these complexes displayed a generic ability to activate apoptosis in cells highlighting the conserved mechanism of toxicity utilized by P-FA complexes.

3.3.1. P-FA Complexes Generated from Novel Proteins Display Tumouricidal Cytotoxicity

HAMLET and BAMLET are well studied P-FA complexes *in vitro* and *in vivo* (Rammer *et al.*, 2010, Tolin *et al.*, 2010, Hoque *et al.*, 2013, Mossberg *et al.*, 2010a, Puthia *et al.*, 2013). Our results show for the first time that HAMLET and BAMLET display effectively identical cytotoxicity towards $PC12^{undiff}$ cells when compared to $PC12^{diff}$ cells. Interestingly BAMLET was less toxic against the differentiated phenotype when compared to HAMLET. The cytotoxicity displayed by HAMLET/BAMLET towards these tumor cells is also mirrored in U2OS cancer cells. The significance of this result is that it shows that the PC12 differentiation model which acts like a tumor-versus-healthy cell model is a reliable and useful model for assessing drug selectivity towards tumour cells, and therefore would be useful in determining the cytotoxic capabilities of our other P-FA complexes when measured against these already tested assemblies.

Using a mixture of previously tested and completely novel proteins, we have generated unique P-FA complexes which display cytotoxity towards cells. Using IEC and columns pre-conditioned with OA, we were able to formulate and isolate these complexes. Although bovine α-LA, β-LG and more recently AMb have been engineered into complex with OA, Mb, Ub, and Cyto-*c* have never been tested prior to this experiment and represent a new addition to the growing body of tumouricidal P-FA complexes. All P-FA complexes which were developed displayed similar efficacy against tumor cells and were less toxic against differentiated healthy cells.

We demonstrate for the first time that Mb can be engineered into a tumouricidal complex with OA, which displays selective killing against tumour cells. Interestingly Mb-OA was the most injurious of all compounds tested. A similar effect was observed by using AMb-OA complexes, which although not as potent to cancer cells as its heme rich counterpart, still displayed a high level of selectivity against healthy cells. Both Mb-OA and AMb-OA were highly toxic towards $PC12^{undiff}$ cells and U2OS cells *in vitro*. In complex with FA, both β-LG and Cyto-*c* displayed similar tumouricidal ability towards $PC12^{undiff}$ cells and U2OS cells. $PC12^{diff}$ cells treated with both these complexes also exhibited an increased level of resistance compared with $PC12^{undiff}$ cells as β-LG-OA are approximately 10-fold less sensitive and almost 20-fold in the case of Cyto-*c*. Ub-OA also displayed tumouricidal selectivity. In comparison to other cytotoxic assemblies tested Ub-OA displayed the lowest level of cytotoxicity towards tumor cells from all P-FA complexes tested.

Interestingly we find that Mb-OA is more potent than the heme free AMb-OA. AMb is more easily formed into the MG state than Mb (Jennings and Wright, 1993) and therefore it would be expected that the cytotoxic effects would be higher with this complex as it would be freer to take on more OA. Our results suggest that the heme present in Mb may potentiate the cytotoxic capability of this complex. Free heme has been shown to be toxic to cells *in vitro* (Tsiftsoglou *et al.*, 2006, Taketani, 2005) and has even been show to induce apoptosis (Gonzalez-Michaca *et al.*, 2004) in cells. Furthermore Mb alone has been shown to inhibit proliferation of cultured human proximal tubular cells by inducing DNA damage and blocking DNA/protein synthesis (Iwata and Zager, 1996). It should be noted that Mb did not cause a dramatic decrease in cell viability when used in the native form to treat cells. However, in this state heme would not be free in solution as it would be securely located inside the protein. It is possible that while in complex, the heme constituent of Mb may become partially freed and may potentiate the tumouricidal effects displayed by the complex itself. Future studies will be needed to fully assess the role of free heme on PC12 cells in both phenotypes and to determine whether heme is more unstable when Mb is in complex with OA.

It has been suggested that to become a functional P-FA, the complex must be in a MG state (Fast *et al.*, 2005, Polverino De Laureto *et al.*, 2002). Permyakov *et al.*, demonstrated that the globular β-LG could form a cytotoxic complex with OA and our work further supports

this argument (Permyakov *et al.*, 2012). We have shown that in addition to β-LG globular proteins such as Mb and Ub can all be used to generate tumouricidal OA complexes which are highly toxic. These results compliment earlier work done in our group which has shown that electrostatic interactions between the protein and OA are the main stabilizing factors in these complexes (Xie *et al.*, 2013). Of the P-FA's tested here HAMLET/BAMLET (Brinkmann *et al.*, 2011a, Håkansson *et al.*, 1995), AMb-OA (Nakamura *et al.*, 2013), and β-LG-OA (Lišková *et al.*, 2011, Permyakov *et al.*, 2012) has been shown recently to display HAMLET-like properties. This work supports these previous results and further strengthens the idea that P-FA complexes engineered with OA can be used to kill tumour cells. The use of Mb, UB, and Cyto-*c* represents a completely novel discovery.

One of the key aims of this project was to see if any of our novel P-FA complexes showed similar promise as a potential therapy based drug. Chemotherapeutic drugs primarily work by inhibiting cell proliferation through the inhibition of DNA or RNA synthesis. One of the main problems with conventional chemotherapeutic drugs is that they lack robust specificity towards tumor cells. In order to be a successful anticancer drug, it is imperative to kill tumor cells in a highly efficient manner (Abdullah *et al.*, 2009).

From a therapeutic standpoint, Mb displayed the highest level of toxicity against all cell lines. Mb therefore presents an interesting option as a therapeutic agent yet its ability to kill tumor cells at such low concentrations is marred by the fact that it also destroys healthy cells at similarly low concentrations. As a drug, Mb displays the key component of what is wanted from most chemotherapeutics, tumor cell destruction at low concentrations yet its potency towards healthy cells also makes it a risky option.

Ub-OA was significantly less toxic to tumour cells compared to other complexes tested, and although was not as harmful to differentiated cells as others, this feature makes it a weaker chemotherapeutic drug candidate. It is important to note that this decrease in efficacy may be due to the relatively small size of the Ub molecule. It has been shown that increasing the level of OA in complex can increase its cytotoxicity (Brinkmann *et al.*, 2011a). Ub-OA ratios have been examined in our group, and a single Ub molecule was shown to bind to 2.26 OA molecules (Xie *et al*, unpublished data). We propose that due to its small molecular weight,

Ub cannot bind the same amount of OA that is seen in other complexes, the consequence of which diminishes the cytotoxic action of the complex.

BAMLET is cytotoxic to tumor cells at low concentrations yet displays low levels of toxicity to healthy cells even at high concentrations. The complex is relatively inexpensive to produce, far more accessible than its human equivalent, and repeatedly developed using IEC with remarkable reproducibility. Consequently BAMLET has a substantial amount of promise as a potential therapeutic drug.

These results suggest that the protein moiety of the complex does not have an effect on its ability to induce cell death or selectively target tumour cells. Several unrelated proteins all show similar patterns of cell death in tumour cells, and all were significantly less toxic towards healthy cells. The proteins chosen were unrelated in both structure and function yet all were engineered into tumouricidal drugs. All native proteins tested showed little cytotoxity towards the cell lines and TEM examined cells treated with BAMLET showed large levels of OA residing within the cell. It is now clear that the protein component of these complexes acts a 'mule' in that it transports the normally insoluble OA molecule across the cell membrane and releases the true toxic component of the complex into the cell.

3.3.2. Examination of P-FA Complexes Reveals that they are not fully Aggregated

We analysed our P-FA complexes using a combination of CR spectrometry and birefringence, as well ThT. As a positive control HEWL fibrils and oligomers were used in conjunction with our P-FA complexes. The manipulation of the native state of any protein can theoretically lead to formation of an aggregated protein state (Krebs *et al.*, 2000). The formation of these P-FA complexes involves the addition of OA molecules to the protein and therefore yields a structure that is distinctly unique and different from the native conformation. In the aggregated state normally innocuous molecules can gain the ability to become cytotoxic towards cells, as seen from our own work in Chapter 5 and several other experimental examples (Malisauskas *et al.*, 2005, Sakono and Zako, 2010, Walsh and Selkoe, 2007, Xu *et al.*, 2007). For this reason it is important to ascertain whether P-FA complexes are in an oligomeric state. If these drugs are to be used to treat patients with cancer, using a substance that is itself harmful would be a potential health risk to people.

All P-FA samples analysed showed no significant increase in ThT when compared to the control oligomer sample suggesting that these P-FA complexes have not become fully oligomeric. In conjunction to this, CR birefringent analysis showed no birefringence for any of the P-FA samples suggesting that there was no fibril growth present and that our P-FA complexes had not aggregated at this point. When examined using CR spectroscopy, there was no shift in the maximum absorbance towards the red spectrum further suggesting that no amyloid fibril aggregation had occurred. These results support earlier experiments showing that HAMLET remained in its monomeric form (Mossberg *et al.*, 2010b) and suggests that these P-FA complexes do not take on an oligomeric conformation.

The debate over whether these complexes are monomeric or oligomeric is still unclear as P-FA complexes have been shown to form oligomers as was seen with ELOA (Wilhelm *et al.*, 2009) which has also been shown to exist as an oligomer without OA (Malisauskas *et al.*, 2005). Additionally, HAMLET (Nakamura *et al.*, 2013) and BAMLET (Spolaore *et al.*, 2010b) were also shown to exist in the oligomeric state which is in contrast to our results. For HAMLET and BAMLET we do not see this with our proteins suggesting that each protein may behave in its own distinct way. BAMLET oligomers were isolated after direct mixing of the protein and OA and this may be a reason we observe this difference. HAMLET oligomers were detected using pulse field gradient NMR which is a more sensitive method for detecting protein aggregation and so future work examining these P-FA complexes using this method should be carried out. In addition, AFM provides a useful method for the detection of oligomers (Wilhelm *et al.*, 2009) and recently oligomer specific antibodies have been engineered that recognise generic features on all oligomers (Brännström *et al.*, 2014). Although these results suggest that the P-FA complexes have not formed fully developed amorphous aggregates, it does not discount that aggregation has occurred and further examination using the methods mentioned above would be needed to accurately define the final aggregated state of the complexes.

3.3.3. P-FA Complexes Activate an Apoptotic Cell Death Response

Our results also demonstrate that P-FA complexes kill cells through apoptosis, and all samples tested showed a general pattern of cell death. To investigate the cellular death mechanisms employed by all our P-FA complexes we utilized a combination of Western blot analysis for PARP cleavage, immunofluorescence and flow cytometry.

All P-FA complexes examined using flow cytometry showed a large amount of staining for Annexin V-FITC which is indicative of apoptosis. Interestingly the pattern of cell death was very similar in each sample suggesting that the mechanism employed by these complexes to kill cells is conserved. Similarly immunofluorescence staining also demonstrated that cells incubated with our P-FA complexes died through apoptosis. All P-FA complexes showed a dramatic increase in the levels of Annexin V which had bound to phosphatidylserine (PS) on the outer membrane of the cell. In both experiments cells show low levels of PI detection indicating that there is non-apoptotic/necrotic cell death occurring. What we may observing here is in the absence of phagocytosis, apoptotic bodies may lose their integrity and proceed to secondary necrosis or late apoptosis (Elmore, 2007). From our results we hypothesize that the cells are in fact dying through an apoptotic mediated pathway and the necrotic staining we see is secondary event, occurring after the cell has been destroyed.

Using Western blot analysis $PC12^{undiff}$ cells exhibited cleaved PARP after treatment with P-FA complex tested while the untreated cells showed only the native band. The cleavage of PARP occurs at 89 kDa, a reduction from the normal native protein which is 116 kDa in size and is specifically cleaved by caspases so that it is no longer active, preventing DNA repair and promoting apoptotic processes (Boulares *et al.*, 1999). The cleavage of PARP indicates that these complexes have activated apoptosis in response to treatment. It should be noted that I could not get a cleaved PARP band with $PC12^{diff}$, and we were only able to get the uncleaved native protein. The experiment was repeated numerous times and with varying concentrations of loaded protein, P-FA complex treatments, and % gels, yet only the uncleaved PARP were observed. Expression levels of PARP differ in each cell and it may be that the conversion to a differentiated phenotype in this instance has resulted in lower levels of native PARP within the cell. These results are in agreement with previous work carried out examining HAMLET/BAMLET's effects on cells. These complexes have previously been shown to induce apoptosis cell death in tumour cells (Hallgren *et al.*, 2008, Håkansson *et al.*, 1995, Hakansson *et al.*, 2011, Hallgren *et al.*, 2006, Hoque *et al.*, 2013) and our work compliments these experiments.

All P-FA complexes induced apoptosis in both differentiated and undifferentiated cells suggesting that the method of cell death is similar in both. From our biotinylation experiments we can see that P-FA complexes enter tumour cells in greater quantities and it may be this

factor that determines the selectivity seen. HAMLET has been shown to be taken up less into differentiated cells (Mossberg *et al.*, 2010c) however this is the first time this internalization has been recorded using the PC12 differentiation model. We show that all P-FA complexes are absorbed in greater quantities in $PC12^{undiff}$ cells. In combination with our TEM results where we observed OA molecules inside the cell, and together with our cytotoxicity data, these results suggest that the sheer volume of the P-FA complex that is internalized and therefore the amount of OA that is brought into the cell could have a direct effect on cell susceptibility.

The results above suggest that the protein component of P-FA tumouricidal complexes is not integral to the cytotoxicity displayed and instead the OA molecules are the true cytotoxic entity. Six structurally and functionally different proteins were engineered into tumouricidal FA complexes capable of displaying selective killing against cancer cells. The proteins chosen were of globular and MG conformations and therefore compliment other studies (Permyakov *et al.*, 2012, Xie *et al.*, 2013) which suggest MG proteins are not necessary to form complexes. The PC12 differentiation model also provided a useful assay to determine drug selectivity and toxicity against a single cell displaying different phenotypes and was particularly useful for these P-FA complexes. All complexes display similar selectivity against tumour cells and also identical methods of inducing apoptotic cell death. These P-FA complexes represent a new class of tumouricidal drugs which selectively target tumour cells for destruction and are significantly less toxic towards healthy cells.

4. The Mechanistic and Immunological Effects of BAMLET using an *in vivo* Murine Melanoma Model

4.1. Introduction

The development and production of highly specific and non-toxic cancer therapeutics is one of the most important and elusive challenges facing modern medicine today. Currently, the most common forms of treatment for patients suffering from cancer are surgery, radiation, or chemotherapy, but even now the use of these therapies has reached a plateau in certain instances (Zahorowska *et al.*, 2009). In recent years there has been an emergence of a new class of cancer therapeutic in the shape of a family of P-FA complexes (Pettersson-Kastberg *et al.*, 2009a).

As mentioned previously HAMLET, a partially unfolded complex consisting of human α-LA and OA, shows remarkable specificity towards tumour cells both *in vitro* (Pettersson-Kastberg *et al.*, 2009b) and *in vivo* (Gustafsson *et al.*, 2004). To date HAMLET has been shown to be toxic to numerous malignant cell lines *in vitro* while also displaying relatively less toxicity towards healthy differentiated cells (Min *et al.*, 2012). Not only does HAMLET exhibit this tumouricidal ability but it is also capable of inducing cell death through a myriad of different pathways. HAMLET was shown to trigger apoptotic changes in tumour cells (Håkansson *et al.*, 1995) and this apoptosis cell death was independent of caspases, Bcl-2, or p53 status of the cell (Hallgren *et al.*, 2006).

As important as *in vitro* studies are as preliminary tests for potential therapeutics, the key link in the drug development chain is the production of a compound that can translate into an *in vivo* model. To this end HAMLET has been used in a number of *in vivo* experiments in both human and animal models, all of which have yielded positive results (Fischer *et al.*, 2004, Gustafsson *et al.*, 2004, Mossberg *et al.*, 2007, Puthia *et al.*, 2013, Mossberg *et al.*, 2010a).

Patients with bladder cancer were treated with solutions of HAMLET and showed significant cell shedding when compared to control treated patients (Mossberg *et al.*, 2007). HAMLET was also shown to delay the onset of tumours using a mouse MB49 bladder carcinoma model (Mossberg *et al.*, 2010a). The effect of HAMLET on human skin papillomas was also investigated in a placebo controlled double blind study of these skin cancers treated with HAMLET. Topical application of HAMLET or saline was used daily for two weeks.

HAMLET treated samples showed a dramatic decrease in the size of the papilloma which wasn't observed in the control treatment (Gustafsson *et al.*, 2004). HAMLET was also used to treat brain glioblastoma xenografts that were transplanted into mice. Analysis with MRI scans confirmed that tumour size had significantly decreased in mice treated with HAMLET, and the xenografted mice treated with HAMLET had survival prolonged by an average of 17 days compared to those treated with just α-LA or NaCl (Fischer *et al.*, 2004).

To date, the administration of HAMLET in *in vivo* experiments has been through either topical application as seen in the skin papilloma trial (Gustafsson *et al.*, 2004), intravesically as seen in bladder cancer studies (Mossberg *et al.*, 2007), through intratumoral administration (Fischer *et al.*, 2004) or pre-orally as was administered in the recent investigation into colon cancer (Puthia *et al.*, 2013). The use of HAMLET or any P-FA complex through an i.p injection route has never been examined, possibly due to the fact that the weak binding affinity which the complex has for OA may become broken due to particles and molecules in the blood stream such as albumin, a FA binding protein (Perez *et al.*, 1989).

The ability to administer these complexes directly into the peritoneal cavity may enhance their therapeutic potential as local administration of drugs are more invasive, the treatable cancers are limited, and the i.p route would be more preferable to treat intra-abdominal malignancies (Chaudhary *et al.*, 2010). However there are several challenges with using i.p injections such as premature clearance of small molecular weight drugs from the peritoneal cavity, poor drug penetration into the target tissues, and lack of target specificity (Chaudhary *et al.*, 2010). Identifying whether these P-FA complexes could be supplied via the peritoneal cavity could prove beneficial in determining the potential of these proteins as realistic drug candidates.

For cancer, the standard treatment approaches of radiation, chemotherapy, and surgery have reached a plateau in certain tumours and have become less effective in others. In recent years there has been a shift from broad-spectrum cytotoxic therapy toward targeted treatments which manipulate molecular machinery and specifically destroy targeted cancer cells (Zahorowska *et al.*, 2009). The advantage of using such treatments over the more conventional therapies is that they reduce harm done to normal healthy cells and tissues. Thus

the challenge for researchers is to design compounds that differentiate between tumour and non-tumour (Siegel-Lakhai *et al.*, 2005).

The first and perhaps best example of targeted therapy for cancer is the Bcr-Abl tyrosine kinase inhibitor, imatinib (Gleevec), which is used primarily for the treatment of chronic myelogenic leukemia and became available in 1996 (Devita and Chu, 2008). This molecule works by targeting the *bcr–abl* gene, which encodes a protein with pronounced tyrosine-kinase activity and induces apoptosis by inhibiting protein phosphorylation. This was the first example of a drug targeting a specific molecular marker in a tumour cell and ushered in the era of targeted therapy (Capdeville *et al.*, 2002). The development of Gleevec and the subsequent production of similarly acting drugs has resulted in a dramatic decline in mortality rates related to cancer worldwide (Devita and Chu, 2008).

The use of combinations of tumouricidal drugs or the combination of anti-tumour drugs with radiation, chemotherapy, and surgery have proven to be very successful (Al-Lazikani *et al.*, 2012). In recent years, TLR agonists have emerged as a new form of cancer therapy (Takeda and Akira, 2005). TLRs act as prototype pattern-recognition receptors (PRRs) and recognize distinctive pathogen-associated molecular patterns (PAMPs), which are found on the surface of microorganisms and include such structures as viral/bacterial nucleic acids and lipopolysaccharide (LPS). They can also selectively bind to danger-associated molecular patterns (DAMPs) from damaged tissue (O'Neill *et al.*, 2013).

The binding of these molecular targets to TLRs activates a myriad of downstream events which results in the production of cytokines and chemokines which can have a deleterious effect on foreign organisms (Takeda and Akira, 2005). TLRs can also bind to and stimulate DCs, which in turn promotes T-cell clonal expansion through the upregulation of co-stimulatory molecules which leads to the maturation of effector T-cells (Reis E Sousa, 2004). In this way TLRs not only promote an innate inflammatory response in the host but are also capable of eliciting an adaptive immune response (Dunne *et al.*, 2011).

Using agonists to stimulate TLRs has focused mostly around agonists which bind to TLR 7/8. Imiquimod is an FDA approved TLR7 (and to a lesser extent TLR8) agonist that is currently used as an anti-tumour agent in several cancers (Schon and Schon, 2007). Resiquimod (R848) is an imidazoquinoline molecule which behaves similarly to imiquimod,

in that it also acts as a TLR7/8 agonist. R848 has been shown to suppress regulatory T (Treg) cell function and can also stimulate the induction of innate cytokines such as IL-12 and TNF-α (Peng *et al.*, 2005, Dunne *et al.*, 2011). This chapter will describe the use of BAMLET, a tumouricidal P-FA complex in combination with the TLR7/8 agonist R848.

Metastatic melanoma is a highly aggressive form of cancer that arises from specialised pigmented skin cells known as melanocytes. Under normal physiological conditions, the key role of these cells is to protect the skin from the damaging effects caused by UV radiation (Finn *et al.*, 2012). Melanoma is the most dangerous form of skin cancer worldwide. According to the American Cancer Society (ACS) there were approximately 76,690 new cases of melanoma in the United States last year, with an estimated 9,480 deaths attributed (Siegel *et al.*, 2013). Like all cancers, there are numerous risk factors associated with the development and progression of this disease. The most prevalent and strongest risk factors include a previous melanoma, the presence of benign or atypical nevi (moles or beauty marks), and a familial history of the disorder. External and environmental factors also contribute to the genesis of melanoma such as exposure to UV rays, sensitivity to sunlight, and immunosuppression all playing key roles in affected individuals (Miller and Mihm, 2006).

The histological changes that accompany the transformation of melanocytes into malignant melanoma cells can be classified using the Clark model of melanoma progression (Clark *et al.*, 1984). The Clark model is divided into six different stages of progression categorized as follows: 1) the formation of a benign nevus from the proliferation of structurally normal melanocytes; 2) the pre-existing benign nevus displays aberrant differentiation and growth; 3) in addition to a melanocytic nevus with aberrant growth, melanocytic dysplasia is also observed; 4) the radial growth phase of the tumour whereby cells proliferate intraepidermally and in some cases can present as radial lesions; 5) the primary melanoma begins to progress vertically invading the dermis and fat, and at this point these cells can induce tumour nodules when implanted in nude mice; and 6) the final step in the process of establishing a successful metastatic melanoma sees a tumour that can spread to other organs (Clark *et al.*, 1984, Miller and Mihm, 2006).

In recent years there has been a significant increase in our scientific understanding relating to the development of skin cancers as a direct or indirect consequence of exposure to the damaging UV radiation emitted from the sun. Sun exposure is the leading environmental cause of skin cancer and can be particularly damaging to light skinned or red headed people (Miller and Mihm, 2006). Under normal conditions the skins main defense against sun exposure is to produce melanin. Melanin is a brown-black pigment produced by melanocytes which is then transferred to kertinocytes in the skin via dendritic projections. The main role of this pigment is to absorb UV photons and reactive oxygen species (ROS) thereby preventing nuclei injury which can occur from prolonged exposure. Inability to perform this function can result in DNA damage, genetic alterations such as mutations and increased production of cellular growth factors (Gilchrest *et al.*, 1999).

In addition to environmental factors, genetic inconsistencies can also result in the development and progression of melanoma. Eukaryotic cell proliferation is a highly conserved and tightly governed process. Similar to the production line in a manufacturing plant, the cell must pass through several checkpoints in order to allow it to successfully divide and pass on its genetic information. As a consequence, mistakes in this process can lead to cancer (Massague, 2004). At the G1-S checkpoint commitment to cell division and DNA replication are controlled. The p16-cyclin D-CDK4/6-retinoblastoma protein (RB1) pathway (CDK4 pathway) is one of the key regulators which govern the transcriptional process. Alterations to this pathway are either directly or indirectly involved in 90% of melanoma cases (Walker *et al.*, 1998, Sheppard and Mcarthur, 2013).

Another deregulated pathway that is involved in the onset of melanoma is the RAS-RAF-MEK-ERK signaling pathway, which is involved in regulating cell fate in response to various stimuli. Mutations to the N-RAS and BRAF genes (which are activated and controlled by this pathway) are involved in 80-90% of all melanomas suggesting that mutations to this signaling pathway are an essential event in initiation of melanoma (Glud and Gniadecki, 2013).

Melanoma is a notoriously difficult cancer to treat. Until recently patients diagnosed with malignant melanoma had a very poor prognosis and treatments were often difficult to tolerate. In the past decade there has been an explosion of progress in the understanding of

this disease which has allowed new therapies to be developed which have significantly increased the likelihood of survival post diagnosis (Mullard, 2011). However, despite this the treatment and prognosis of patients with metastatic melanoma remains relatively poor and so there is an urgent need to find and develop new therapies which can alleviate and potentially cure patients (Boyle, 2011).

Surgery and radiation therapy have a role in the treatment of the metastatic form of the disease however they generally have a poor success rate. Similarly chemotherapy does not offer a much greater survival rate for patients with melanoma. Collectively these three different therapies only offer response rates of 5-20% (Bhatia *et al.*, 2009). There are a small number of drugs in use that have been approved by the FDA (United States Food and Drug Administration) for the treatment of melanoma. Decarbazine is a chemotherapeutic alkylating agent and is the drug of choice if treating melanoma with combined chemotherapy. Ipilimumab and vemurafenib were introduced to the market in 2011 and have been successful in treating some melanomas however, they do carry many unwanted side effects (Velho, 2012). Despite the emergence of these new medications, and the optimization and improvement of some older ones, the standard of care has not shifted dramatically enough in the past 20 years and as such the search for new medications must continue.

The immune system plays an important role in tumour surveillance and destruction. However once established, tumour related factors may modulate the immune response to favour tumour growth. Thus in recent years there has been growing interest in identifying immune-modulatory compounds that enhance tumor rejection while also inhibiting tumour-induced immune suppression that favors tumor growth. $CD4^+$ T-cells play a crucial role in adaptive immunity in response to pathogens. The various populations are specifically driven in response to targeted foreign bodies and the entire process is tightly regulated with finite precision (Surh and Sprent, 2008).

Innate immunity is the front line of defense and will initiate a direct attack against pathogens in an identical way each time a challenge is encountered. The adaptive immune system changes in response to repeated attack, and becomes more efficient and finely tuned after repeated exposure (Dempsey *et al.*, 2003). The two main players in adaptive immunity are the Th1 and Th2 cells which activate very different pathways. Th1 responses are typically

cell mediated forms of immunity whereby macrophages and cytotoxic T-cells become activated in response to stimuli. Th2 mediated immunity is sometimes referred to as humoral immunity and involves the production of antibodies by B cells. Both responses have an inhibitory effect on the other and so both are rarely activated simultaneously (Delves and Roitt, 2000, Dempsey *et al.*, 2003).

T cells play an important role in tumor rejection. Upon activation T cells initially develop into non-polarised Th0 precursor cells which are the prototype from which Th1 and Th2 cells are thought to derive. The differentiation of these cells into the functional subsets is dependent on polarizing cytokines produced by innate cells. These Th0 cells can produce a wide range of cytokines which can drive the expansion of a particular T-cell population. The secretion of IL-12 and IL-18 (from DCs) promotes Th1 cells differentiation, which then in turn secrete IL-2, IFN-g and lymphotoxin (LT). IL-2 is a key factor in the proliferation of Treg cells which are involved in controlling the severity of an immune response. (Maggi *et al.*, 2005). Mice which are deficient in either IL-2 or the IL-2R α or β chains have fewer Treg cells and suffer from severe lymphoproliferative autoimmune syndromes, thus demonstrating the importance of IL-2 in Treg cell function (Liston and Rudensky, 2007). The expression of Treg cells in intratumoural regions is often correlated with a poor prognosis due to their ability to restrict a sufficient immune response (Dranoff, 2005).

In the presence of IL-4 (produced by B cells or lymphoid DCs) T cells differentiate into Th2 that produce IL-4, IL-5 and IL-10. The initial polarising event which drives the differentiation of Th0 into these various populations is itself self-perpetuating as Th1 cytokines enhance further Th1 responses and down regulate Th2 cytokines, and vice versa (Amsen *et al.*, 2009). In addition to these more common subsets, Th0 cells can also propagate into Th17 cells under the guidance of TGF-β and IL-6/21, and this population is characterised by their production of the IL-17 family of cytokines (Zou and Restifo, 2010).

Here we demonstrate for the first time that BAMLET significantly delays the onset of tumour development in mice inoculated with B16 melanomas. Furthermore we show for the first time that BAMLET administered through the i.p route is capable of selectively targeting tumour cells for destruction and hence delaying the progression of tumour development in mice. The administration of BAMLET in combination with the TLR 7/8 agonist R848

dramatically decreases tumour volume and increases long term survival in the same murine model. BAMLET may also stimulate a potential humoral immune response in $CD4^+$ T cells due to its upregulation of IL-10 and downregulation of IL-2.

4.2. Results

4.2.1. BAMLET Kills Mouse Melanoma B16 Cells in vitro

In order to determine if BAMLET possesses tumouricidal activity we treated tumour cells with the P-FA *in vitro.* Concentrations used for this experiment can be found in Table 4.1. Cells were treated for 4 h, 18 h, and 24 h time points. After the allotted time, cell viability was assessed using Alamar Blue as described in section 2.5. B16 cells which were treated with BAMLET show a dose dependent decrease in cell viability. These cells also show a decrease in viability over time, with longer incubation periods resulting in increased cell death (Figure 4.1). These results demonstrate that *in vitro* treatment with the P-FA complex BAMLET decreases cell viability in B16 tumour cells in a dose and time dependent manner.

Table 4.1 Concentrations of BAMLET used for treatment of B16 cells *in vitro*. Values given in mg/ml and (μM)

P-FA	mg/ml (μM)	mg/ml (μM)	mg/ml (μM)	mg/ml (μM)	mg/ml (μM)
BAMLET	0.05 (3.5)	0.1 (7)	0.2 (14.1)	0.4 (28.2)	0.8 (56.3)

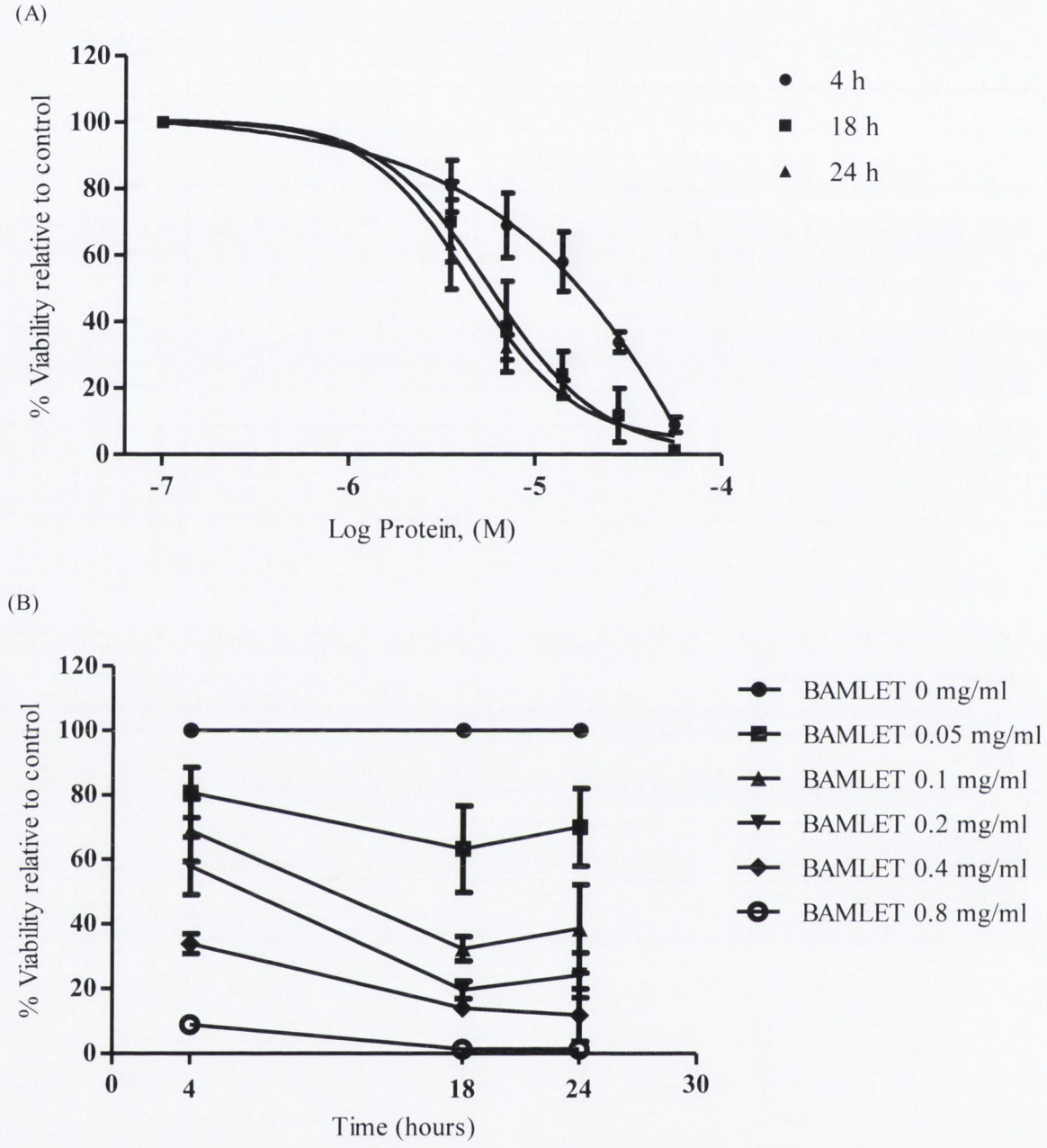

Figure 4.1 B16 cells treated with BAMLET in heat inactivated FCS

B16 cells were treated with media containing heat inactivated FCS for 4 h, 18 h, and 24h (A). After each time point, cell viability was assessed using Alamar Blue and results given as a % of the control. (B) A graph of concentration inhibition of cell viability over 24 h, relative to the control. The values are the means of three experiments with the error bar indicating SEM. $^{*}p < 0.05$, $^{**}p < 0.001$, *** $p < 0.001$ were calculated using GraphPad.

4.2.2. FCS inhibits BAMLETs ability to destroy B16 cells in vitro

We hypothesized that the addition of non-heat inactivated FCS (just termed FCS) in culture would diminish the cytotoxic effects on the P-FA complex. In the absence of serum the killing of B16 tumour cells by BAMLET was both dose and time dependent. Albumin, a main protein component of FCS, has a strong affinity for FAs and can act as a competitor for FA binding (Curry *et al.*, 1999). Heating FCS denatures albumin irreversibly making it inactive (Murayama and Tomida, 2004). In order to investigate if BAMLET efficacy is compromised due to the presence of the highly competitive FA binding protein albumin B16 tumour cells were treated with BAMLET and serum containing media. DMEM media containing 10% FCS was used to treat cells. Cells were treated using P-FA concentrations found in Table 4.1 and cell viability was assessed after 4, 18, and 24 h time points using Alamar Blue as per section 2.5. BAMLET killed tumour cells even in the presence of FCS and did so in a dose and time dependent manner as seen in Figurer 4.2. After 24 h, LC_{50} values for BAMLET in the presence (9 μM) and in the absence of FCS (4.5 μM) show that the efficacy of BAMLET is hindered by the addition of FCS yet still cytotoxic (Table 4.2). This decrease in cytotoxicity suggests that the presence of FCS negatively attenuates the efficacy of BAMLET. However, although reduced, the cytotoxicity is not abrogated and BAMLET is still highly toxic despite the FA binding ability of albumin.

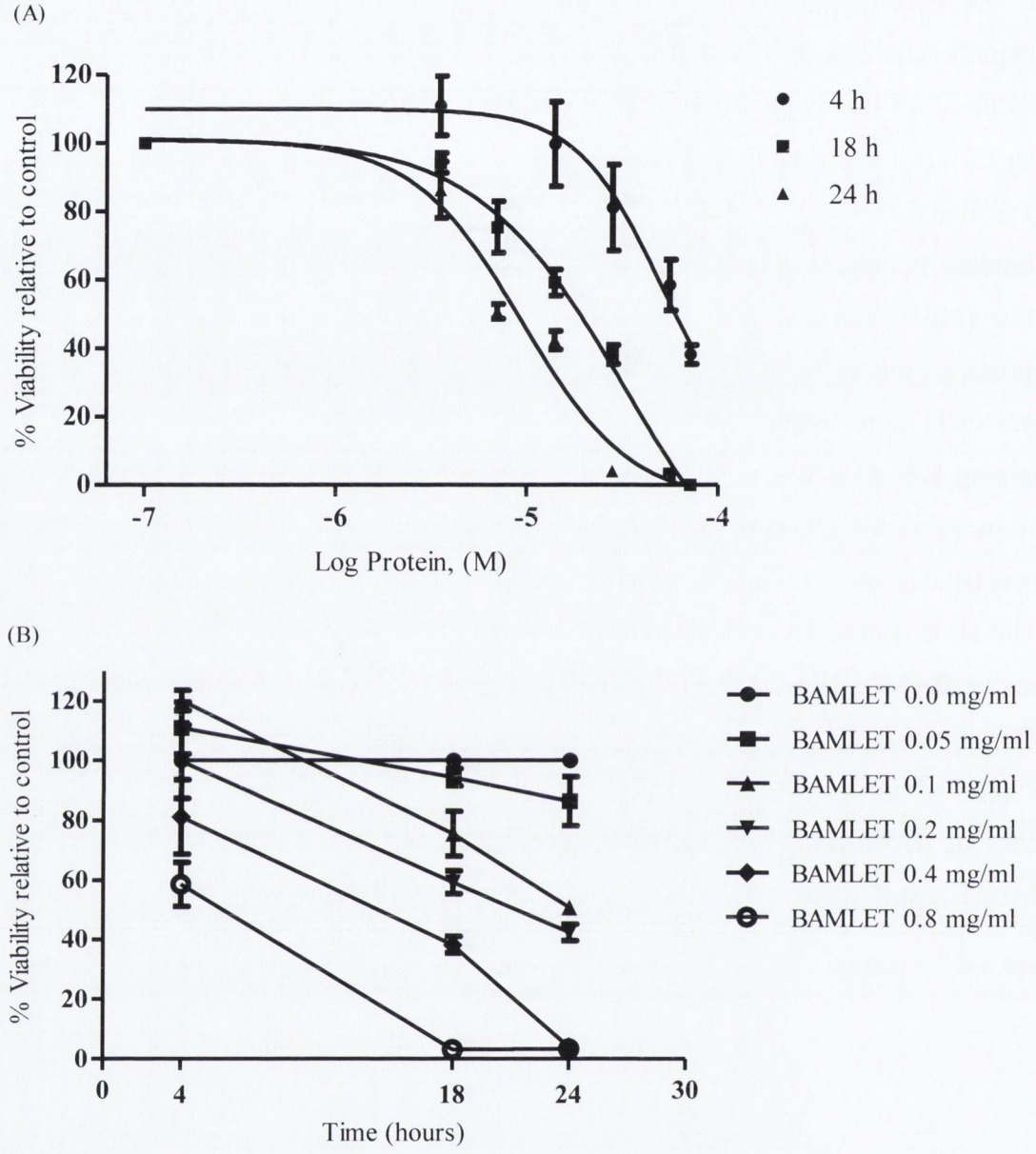

Figure 4.2 B16 cells treated with BAMLET in the presence of FCS

(A) B16 cells were treated with media containing 10% FCS for 4h, 18 h, and 24h. After each time point, cell viability was assessed using Alamar Blue and results given as a % of the control. (B) A graph of concentration inhibition of cell viability over 24 h, relative to the control. The values are the means of three experiments with the error bar indicating SEM. $^{*}p < 0.05$, $^{**}p < 0.001$, *** $p < 0.001$ were calculated using GraphPad.

Table 4.2 LC_{50} values for B16 cells treated with BAMLET in media with (+) or without (-) heat inactivated FCS.

LC_{50} values are means ± SD of three independent experiments carried out by triplicate.

	4 h mg/ml (μM)	18 h mg/ml (μM)	24 h mg/ml (μM)
FCS -	0.57 (40)	0.08 (5.7 ± 6.6)	0.06 (4.5 ± 3.2)
FCS +	0.82 (57)	0.47 (33.3 ± 26)	0.13(9 ± 4)

4.2.3. BAMLET Induces an Apoptotic Cell Death Pathway in B16 Cells in vitro

Having shown that BAMLET resulted in the reduced viability of B16 cells *in vitro*, I sought to determine whether apoptosis or necrosis was being induced in these cells. Two methods were used to determine the mode of cell death.

Firstly cells were treated with BAMLET at increasing concentrations and left for 24 h before being analysed using flow cytometry. To stain for apoptotic cell death FITC-labelled Annexin V was used. General non-apoptotic cell death was stained for using PI. Cells which stain for PI only are found in Q1. Q2 contains cells which stain for both PI and Annexin V. Apoptotic cells stained only with Annexin V are found in Q3, while live cells are displayed in Q4. Cells were gated using the non-stained B16 cells.

Secondly, B16 cells were treated with BAMLET at a concentration of 0.08 mg/ml and left for 24 h. After this time the cells were trypsinised, washed, fixed and then mounted onto glass slides before being stained with immunofluorescent dyes. The stains used were DAPI (blue), PI (red), and Annexin V-FITC (green). As mentioned previously, this kit allows for the separation of healthy and dead cells depending on its propensity to bind to specific dyes. This experiment was carried out in conjunction with controls of cells untreated and stained with individual dyes to exclude background detection.

These results indicate that BAMLET induces apoptotic cell death in B16 cells. Flow cytometry revealed that cells dual stained with Annexin V-FITC/PI showed increased staining for Annexin V. Increasing concentrations of BAMLET resulted in an increase in general cell death and also an increase in apoptotic cell death (Figure 4.3). Cells also stained heavily for both Annexin V and PI. With immunofluorescence B16 cells showed an increase in Annexin V binding after 24h treatment. There is a slight increase in PI staining (Figure 4.4). The results demonstrate that BAMLET kills B16 cells through an apoptotic cell death pathway.

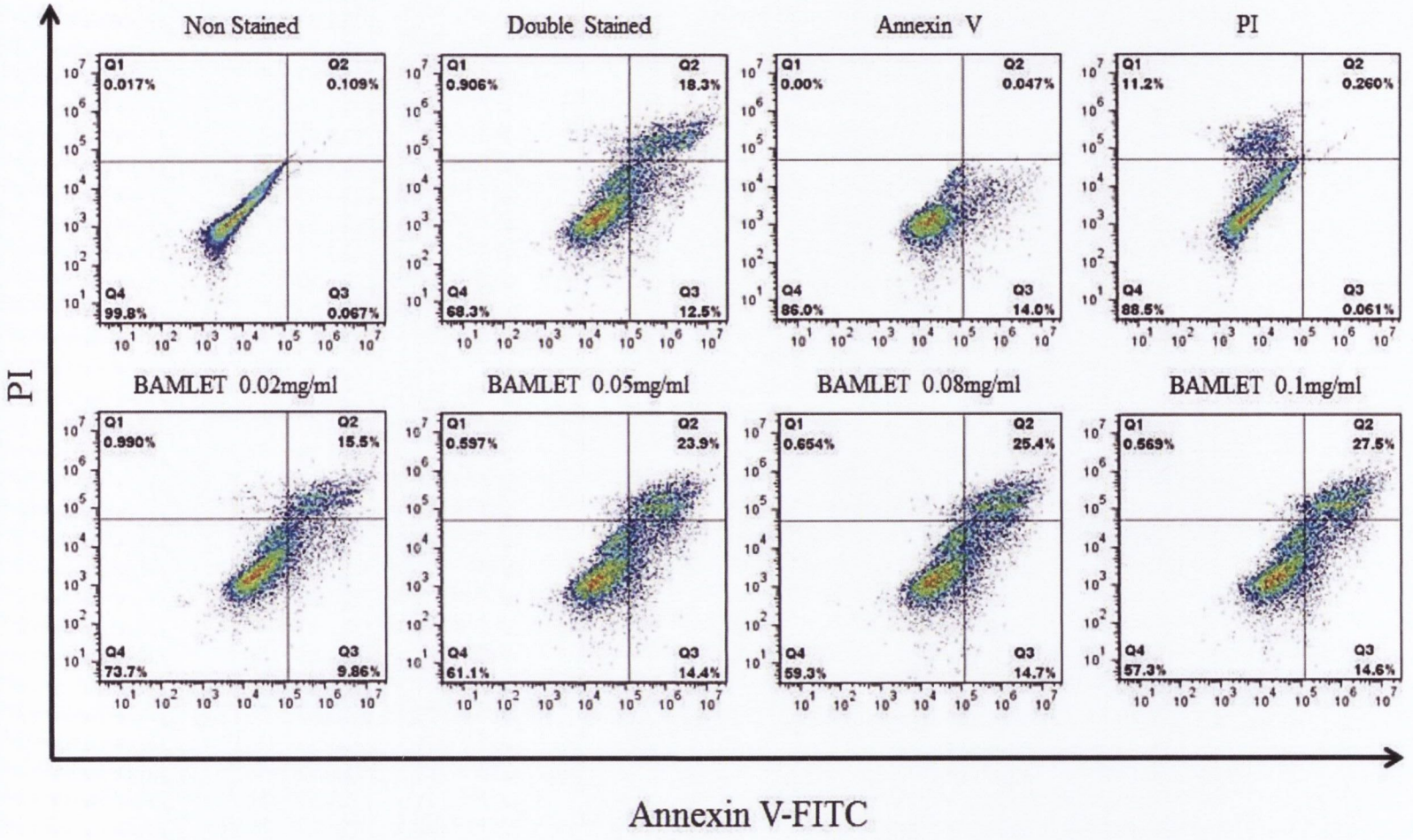

Figure 4.3 B16 cells treated with BAMLET activate an apoptotic cell death pathway

B16 cells were treated with increasing concentrations of BAMLET and analysed flow cytometry. Annexin V-FITC and PI were used to dual stain the samples before reading. Samples were gated using compensatory untreated controls using no staining, double staining, Annexin V-FITC only, and PI only. Plots are representative of three separate experiments.

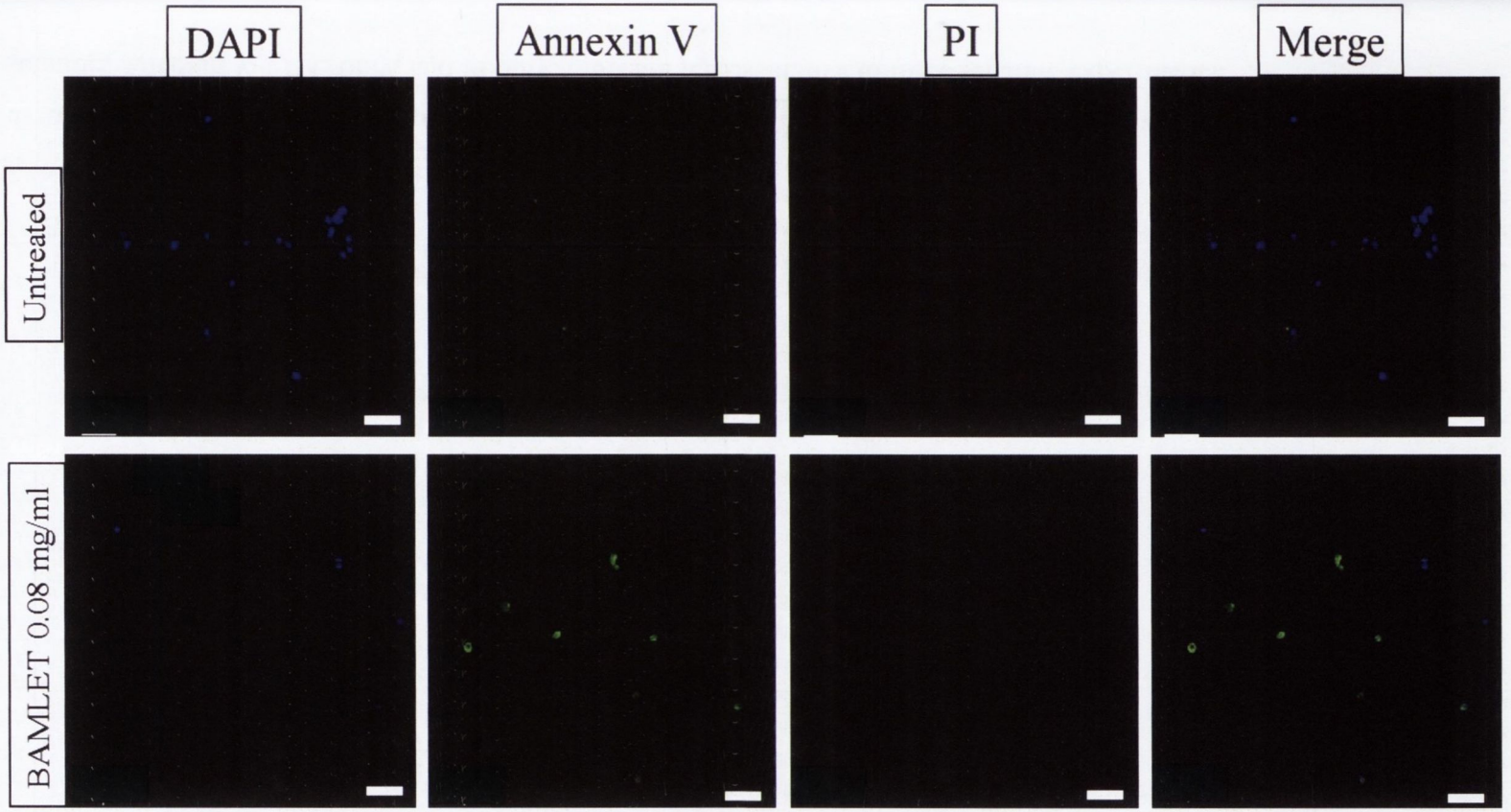

Figure 4.4 Immunofluorescence images of B16 cells stained with apoptotic/necrotic/healthy cells detection kit

B16 cells were treated BAMLET 0.08 mg/ml and left to incubate for 24 h before being stained. The cells were then fixed and mounted on slides for visualisation with an immunofluorescence microscope. BAMLET treated B16 cells show increased Annexin V staining when compared to control. These results are a representation of two separate experiments. Scale bar: 30 μM.

4.2.4. BAMLET Prolonged Survival in a Mouse B16 Melanoma Model and Administration Route of BAMLET did not affect its Efficacy

Having established that the presence of FCS does not inactivate the P-FA complex on B16 cells, we then sought to see whether BAMLET would have a similar effect *in vivo*, using a murine model presenting with a B16 induced melanoma. In addition to this we wanted to establish if the route of injection had any bearing on the overall efficacy of the drug. Injection through i.p is a method of administering many drugs and antibiotics to patients with internal difficulties (Lukas *et al.*, 1971). This mode of injection has numerous advantages over SC administration, as in the example of insulin, i.p injections are more rapidly and evenly absorbed into the system as the pass directly into the portal vein system (Quellhorst, 2002).

To induce tumours female C57/BL mice were inoculated with 2 x 10^6 B16 cells and grouped according to what treatment they would receive (Figure 5.5). Mice (n= 6/group) were injected i.p or SC with 100µl of 0.7 mM or 1.5 mM of BAMLET in PBS. PBS only was used as a control. After day 3 the first injection of BAMLET was administered and then followed routinely as described in section 2.20. No adverse effects were observed in any of the treated groups. With both injection routes, and both concentrations, treatment of mice with BAMLET reduced tumour growth compared to mice administered with PBS (Figure 4.6 A).

The results contained in Table 4.3 show that after the initial measurement of the tumour, PBS treated groups were given as an average of 62.8 mm^3. In comparison to that, all BAMLET treated groups showed no increase in tumour growth at this point. After a midpoint interval of 21 days, tumour size had grown to an average of 496.4 mm^3 in the PBS group, while the largest volume recorded by the treated group was 147.5 mm^3 as seen in the BAMLET 1.5 mM i.p injection group. By the termination stage, the average tumour volume for the control group was recorded at 1291.2 mm^3. In contrast the treated groups were substantially less, with the largest average tumour volume resulting in the 1.5 mM SC group. Throughout, the 0.7 mM SC group recorded the lowest values at each time point, yielding only an average 211.2 mm^3 after the final measurement.

In addition to this we anaylsed the survival of mice for up to 60 days post tumour inoculation (Figure 4.6 B). All BAMLET treated groups showed considerably higher levels of survival than the PBS treated control. These results demonstrate that BAMLET reduces tumour cell

volume in B16 murine melanomas *in vivo* and the route of administration yielded no discernible difference in efficacy. Furthermore it suggests that BAMLET can provide long term protection against tumours *in vivo* as treated mice showed a dramatic increase in survival and reduction in tumour volume compared to the control group for up to 60 days post inoculation.

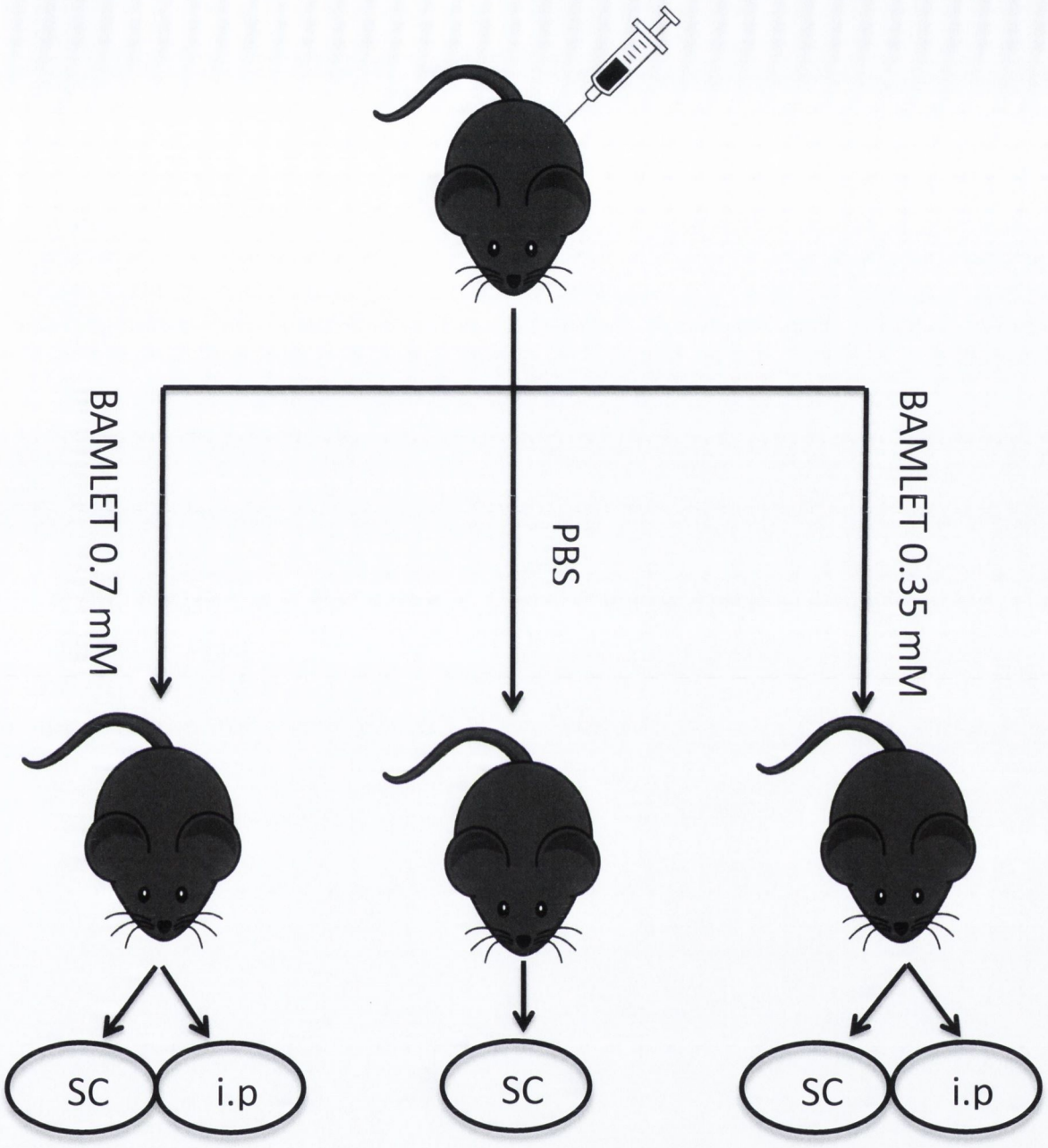

Figure 4.5 Schematic representation of how C57/BL mice were grouped for treatment.

Mice inoculated with B16 tumours were treated with 100 µl of PBS, BAMLET 0.35 mM, or BAMLET 0.7 mM. The BAMLET treated groups were further divided into those that received SC injection of the P-FA complex and those that received BAMLET through the i.p route. PBS treated control mice were administered through SC only. Groups contained 6 mice each.

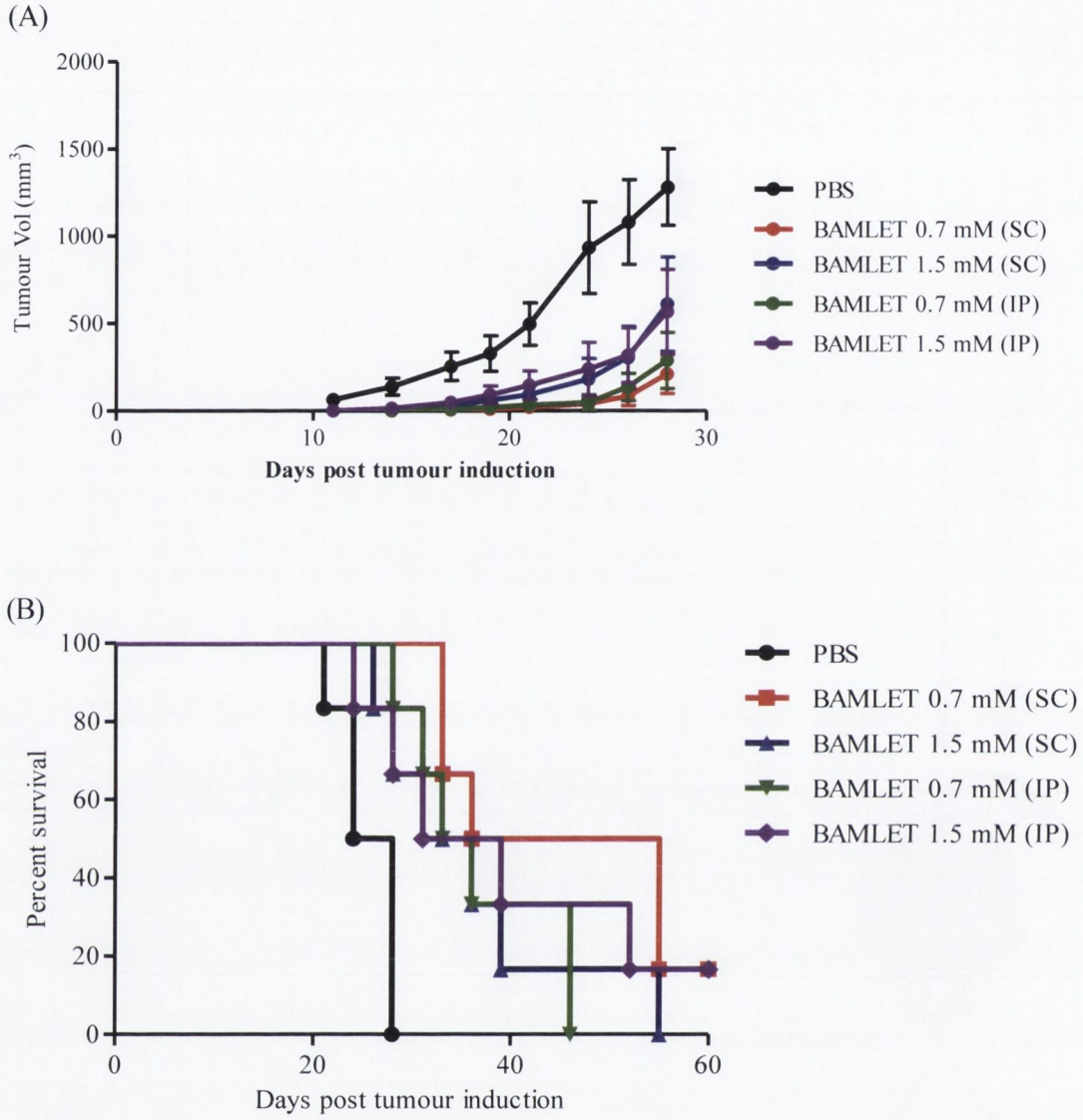

Figure 4.6 Mice treated with BAMLET via SC and i.p show a decreased average tumour volume (mm3) and increased survival compared to control.

(A) Mice were treated with BAMLET (0.7 mM and 1.5 mM) either SC or via i.p administration on days 3, 7, 10, and 14 post tumour induction. Tumour volume was recorded after day 11 post induction and continued for a number of days up until 28 days post induction. (B) Survival plot for mice treated with BAMLET 0.7 mM and 1.5 mM SC or i.p for 60 days. Results are the average of 6 mice per group. Survival statistics were calculated using the Kaplan-Meier method. Work was carried out with the assistance of Dr. Neil Marshall.

Table 4.3 Average tumour volume for mice at 11, 21, 28 days post inoculation.

Tumour volume (mm^3) was measured for BAMLET and PBS group.

Days post tumour induction	PBS	BAMLET 0.7 mM SC	BAMLET 1.5 mM SC	BAMLET 0.7 mM i.p	BAMLET 1.5 mM i.p
11	62.8	0	0	0	0
21	496.4	20.4	93.4	34.4	147.5
28	1291	211.2	504.1	289.9	489.6

4.2.6. BAMLET in Combination with the TLR 7/8 Agonist R848 Decreases Murine Melanoma Volume and Prolongs Survival after a Tumour Re-challenge

Having established that BAMLET works in reducing the tumour volume in a melanoma model in female C57/BL mice we wanted to investigate whether we could improve the efficacy of the drug by using it in combination with another anti-tumour compound. Furthermore we wanted to establish whether treatment with these drugs would reduce tumour growth after the surviving mice were re-challenged with the same tumour. The TLR 7/8 agoinst R848, which has shown promise in privous *in vivo* investigations (Peng *et al.*, 2005, Dunne *et al.*, 2011) was used in combination with BAMLET to investigate this hypothesis. Mice were inoculated with the tumour cells and left for three days before the first tumour measurment was taken. Tumour size was measured as per section 2.20 and tumour size was calcualted in mm^3.

Mice were divided into 5 groups (n=7/group), PBS only, BAMLET 0.35 mM only, BAMLET 0.7 mM only, R848 only, and BAMLET 0.7 mM with R848. Compared to the control group, BAMLET (0.35 mM/0.7 mM) and R848 alone reduced the average tumour volume (Figure 4.7 (A)) and also prolonged the average life span of mice treated (Figure 4.7 (B)). BAMLET in combination showed the largest decrease in average tumour volume when compared to the control.

After 33 days the surviving mice (BAMLET 0.35 mM (n= 2), BAMLET 0.7 mM (n=1), R848 (n=2), and the combination group (n= 4)) were re-challenged with tumour cells and tumour volume was measured until day 57. Mice in the pre-treated groups showed a decrease in tumour development compared to the control mice (Figure 4.8). A single mouse from both the BAMLET 0.35 mM only group and from the combinational group showed no sign of tumour development throughout.

These results show that BAMLET alone and in combination with the TLR 7/8 agonist R848 reduces tumour volume in a murine mouse melanoma model and that the combination of these drugs yields greater efficacy than was observed when the drugs were used individually suggesting that the combining of R848 and BAMLET may improve their abilities to kill tumour cells. There is also a level of long term protection confered by these drugs as mice

re-challenged showed delayed tumour growth compared to control mice. No adverse affects were recorded througout.

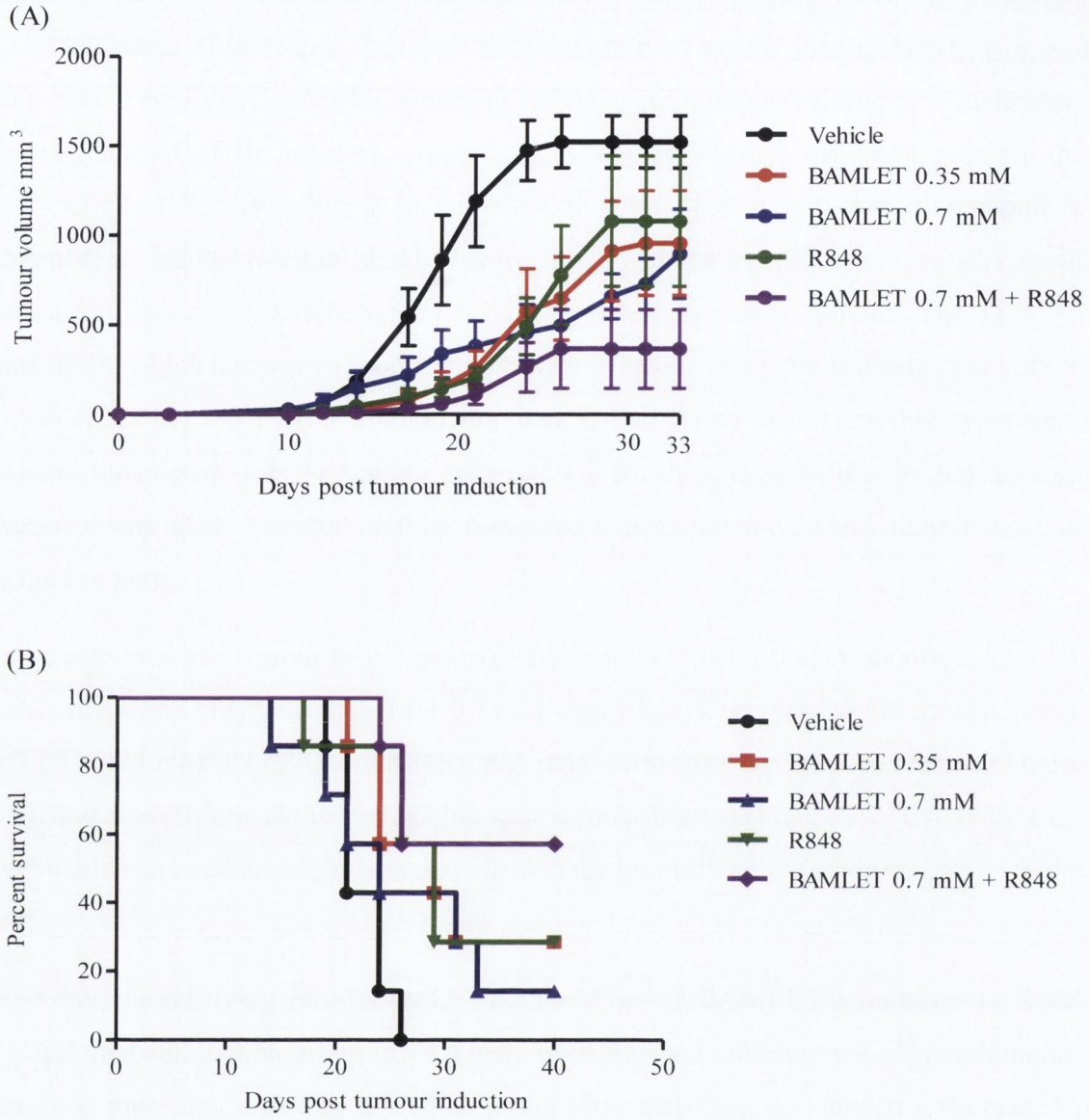

Figure 4.7 Mice treated with the combination of BAMLET 0.7 mM and R848 show the greatest reduction in tumour size and increase in survival.

Groups of mice (n=7) were treated with BAMLET (0.35 mM/0.7 mM), R848 only, and BAMLET 0.7 mM and R848 in combination. Mice treated with PBS only were used as a positive tumour control (A). The survival plot of mice treated with BAMLET and R848 individually and in combination compared to the PBS vehicle control (B). Survival statistics were calculated using the Kaplan-Meier method. *In vivo* experiment was carried out with Lydia Dyck.

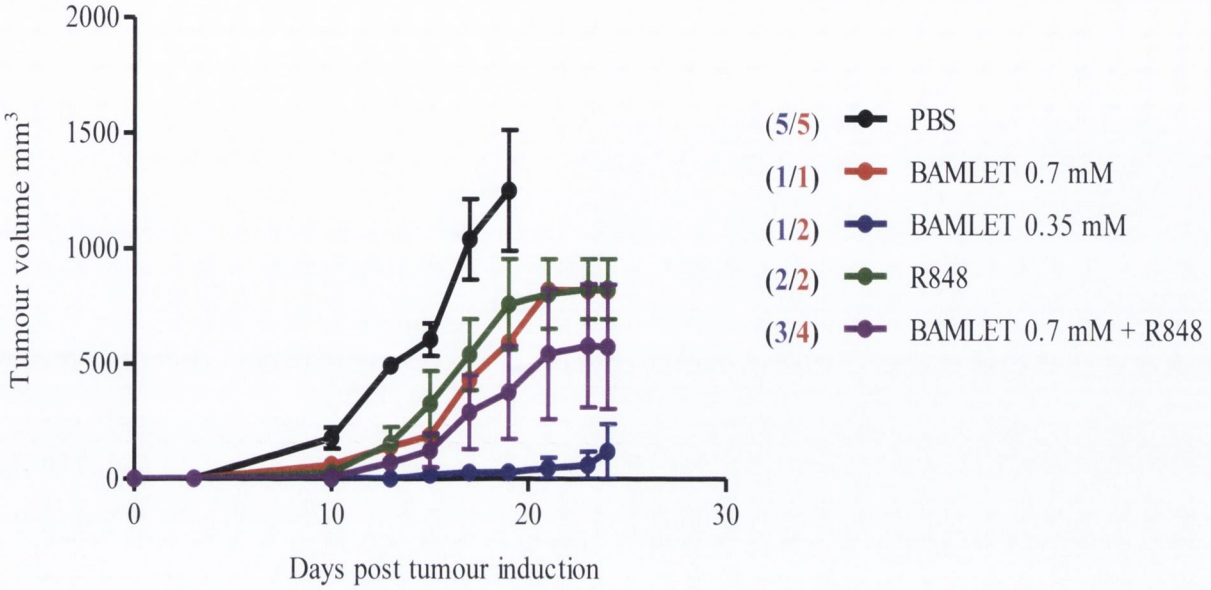

Figure 4.8 Mice re-challenged with B16 tumours show delayed growth in treated groups.

Mice that were previously treated with BAMLET (0.35 mM/ 0.7 mM), R848, and a combination group (BAMLET 0.7 mM + R8484) and had survived without developing any tumours were re-challenged after day 40 with a new installation of tumour cells. Tumour volume was monitored and recorded above. Control mice were treated with PBS (n=5). The number of mice per group is given in (**red**) in brackets, while the number to not survive the re-challenge is denoted in (**blue**) in the brackets.

4.2.7. Effect of BAMLET on CD4$^+$T cell Differentiation

Convalescent mice treated with BAMLET show decreased tumour growth after a re-challenge with additional tumour cells (Figure 4.8). This result suggests mice may become more immune to tumour cells after treatment and that potentially, immunological memory may be involved. In order to determine the effect of BAMLET on cells of the adaptive immune system that are responsible for immunological memory we designed experiments to study the effect BAMLET had on the cytokine production from different populations of CD4$^+$ T cells.

Splenic CD4$^+$ T cells were activated with anti-CD3 and anti-CD28 or left unstimulated. Activated cells were differentiated using cytokines into Th0, Th1 or Th17 cells as per section 2.26.3. Having satisfactorily differentiated the CD4$^+$ T cells populations into Th0, Th1, and Th17 cells, these populations were treated with PBS (control), 0.01 mg/ml BAMLET, or 0.05 mg/ml BAMLET. After 3 days of treatment, the supernatants of the cells were removed and the concentrations of IL-2, IL-10, IL-17, TNF-α, and IFN-γ were determined by ELISA. The results of each CD4$^+$ T cell subset treated with BAMLET were compared to non-treated controls to provide an idea of cytokine production in each cell population.

4.2.7.1. IL-2 secretion in response to treatment with BAMLET.

IL-2 stimulates proliferation and the maturation of effector T-cells and is upregulated in response to infection (Veiopoulou *et al.*, 2004). Having observed that BAMLET reduced tumour cell growth *in vivo* we sought to identify if IL-2 may possess a role in stimulating an immunological response from T cells. In all T cell subsets IL-2 secretion was completely inhibited when compared to the non-treated sample (Figure 5.9). Th0, Th1, and Th17 cells without BAMLET treatment yielded high levels of IL-2 compared to 0.01 mg/ml and 0.05 mg/ml of BAMLET treated samples which displayed a complete reduction in IL-2 secretion (Table 4.4) These results show that BAMLET shuts off the production of IL-2 by $CD4^{+}$T cells

Table 4.4 Average (given in pg/ml) of IL-2 secretion levels in $CD4^{+}$ T cells.

Polarised Th0, Th1, and Th17 cells were treated with 0 mg/ml, 0.01 mg/ml, or 0.05 mg/ml of BAMLET. NA represents measurements that were lower than 0 pg/ml and therefore below the detection level. Data is the average of two separate experiments.

CD4+ T cell Population	Control	BAMLET 0.01 mg/ml	BAMLET 0.05 mg/ml
Th0	2454 pg/ml	NA	NA
Th1	977 pg/ml	NA	NA
Th17	1221 pg/ml	NA	NA

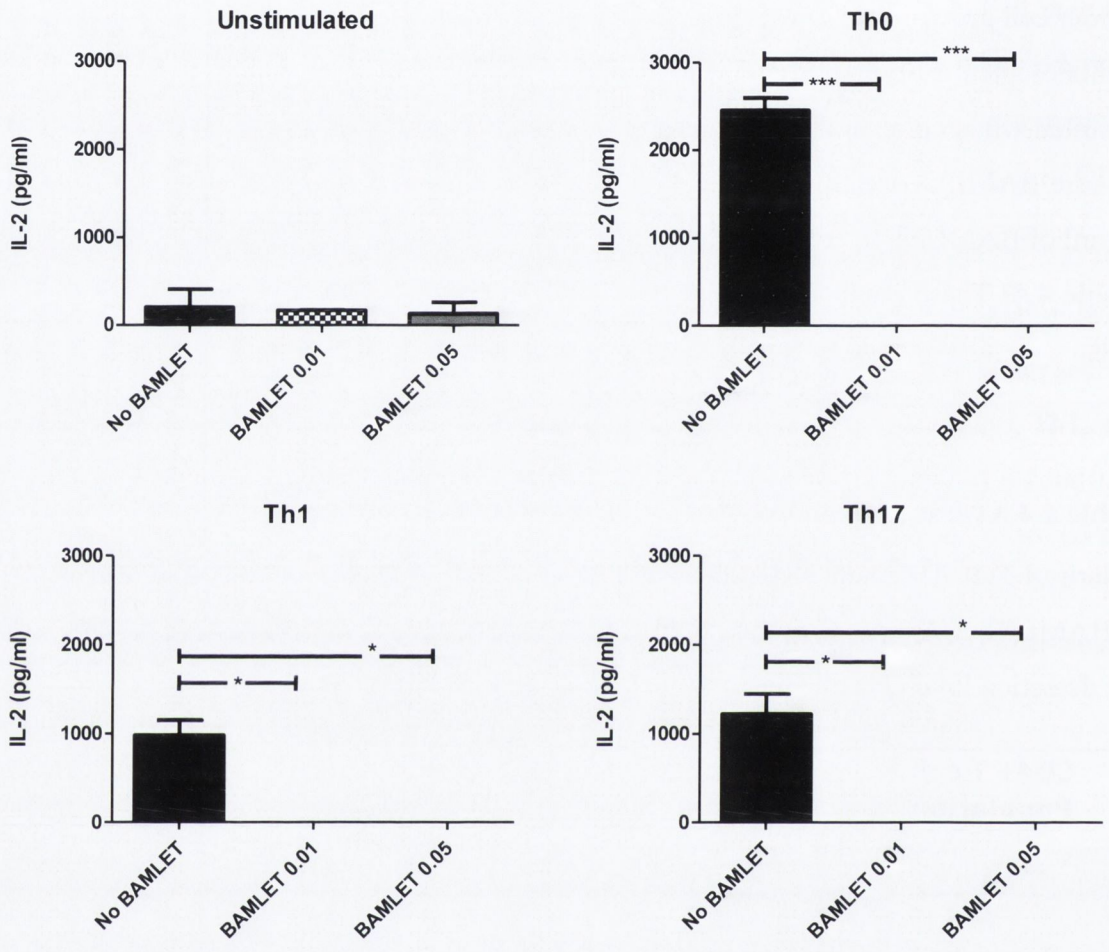

Figure 4.9 . BAMLET blocks IL-2 production in $CD4^+$ T cells

Th0, Th1, and Th17 cells all show a significant decrease in the secretion of IL-2, when compared to the no BAMLET treatment cells. Statistical analysis was performed using a 1-way ANOVA, $^{*}p < 0.05$, $^{**}p < 0.001$, *** $p < 0.001$. Error bars represent S.D. of mean. Data are representative of 2 independent experiments.

4.2.7.2. IL-10 secretion is significantly increased in Th1 cells treated with BAMLET

IL-10 levels were increased in all cell lines treated when compared to those treated without BAMLET (Figure 4.10). In Th1 $CD4^+$ T cells levels of IL-10 were significantly increased compared to the untreated cells indicating that the addition of both 0.01 mg/ml and 0.05 mg/ml of BAMLET caused Th1 cells to upregulate their production of IL-10. The average values for each subset treated with or without BAMLET demonstrate the increase in IL-10 in each group compared to the non-treated control (Table 4.5).

Table 4.5 Average (given in pg/ml) of IL-10 secretion levels in $CD4^+$ T cells

Using specific polarising agents to differentiate anti-CD3 and anti-CD28 stimulated cells, the levels of IL-10 were measured after treated with 0 mg/ml, 0.01 mg/ml, or 0.05 mg/ml of BAMLET. Data is the average of two separate experiments.

$CD4^+$ T cell Population	Control	BAMLET 0.01 mg/ml	BAMLET 0.05 mg/ml
Th0	4214 pg/ml	6600 pg/ml	5682 pg/ml
Th1	2622 pg/ml	5161 pg/ml	5222 pg/ml
Th17	4411 pg/ml	6400 pg/ml	5528 pg/ml

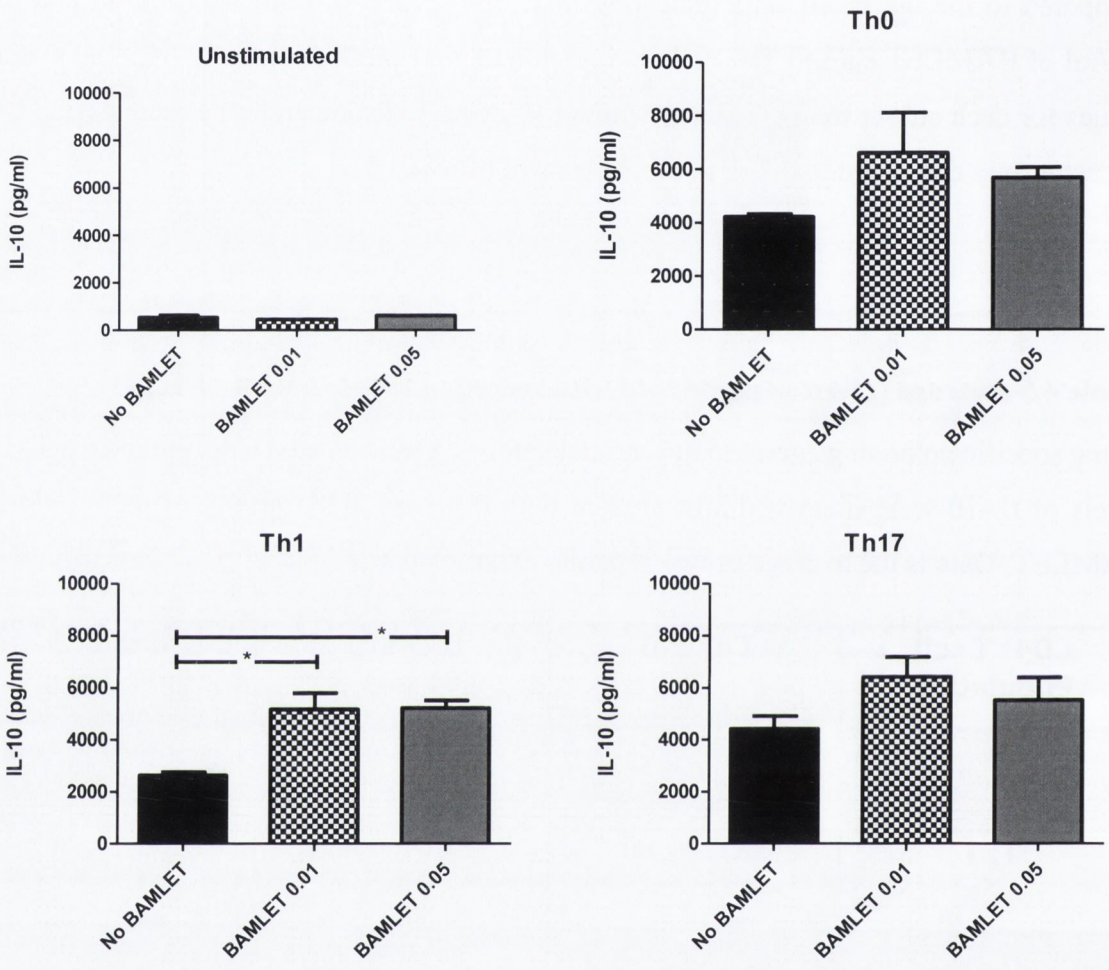

Figure 4.10 BAMLET increases IL-10 production in Th1 cells

When compared to the non-treated cells, BAMLET induced a significant increase in IL-10 in Th1 cells only. Slight increases were measurable in both Th0 and Th17 cells also. Statistical analysis was performed using a 1-way ANOVA, $^{*}p < 0.05$, $^{**}p < 0.001$, *** $p < 0.001$. Error bars represent S.D. of mean. Data are representative of 2 independent experiments.

4.2.7.3. IL-17 is increased in Th17 cells when treated with BAMLET

Similarly to IL-10, IL-17 is upregulated in all $CD4^+$ T cells treated with BAMLET. Interestingly, the largest and most significant increase was observed in Th17 cells treated with the P-FA complex (Figure 4.11). Although the other populations of $CD4^+$ T cells do produce IL-17 under normal circumstances the primary producer of this cytokine is the Th17 cells (Jin and Dong, 2013) and so the increase in production is most important with this cell line. There is also a dose dependent increase seen with all cell lines treated (Table 4.6) showing that BAMLET alters the levels of IL-17 cytokine secretion based on the concentration of BAMLET present.

Table 4.6 Average (given in pg/ml) of IL-17 secretion levels in $CD4^+$ T cells

Cytokine levels from $CD4^+$ T cells treated with no BAMLET and 0.01 mg/ml, or 0.05 mg/ml of BAMLET were measured with ELISA. Data is the average of two separate experiments.

$CD4^+$ T cell Population	Control	BAMLET 0.01 mg/ml	BAMLET 0.05 mg/ml
Th0	494 pg/ml	989 pg/ml	1072 pg/ml
Th1	344 pg/ml	461 pg/ml	578 pg/ml
Th17	1846 pg/ml	2517 pg/ml	2682 pg/ml

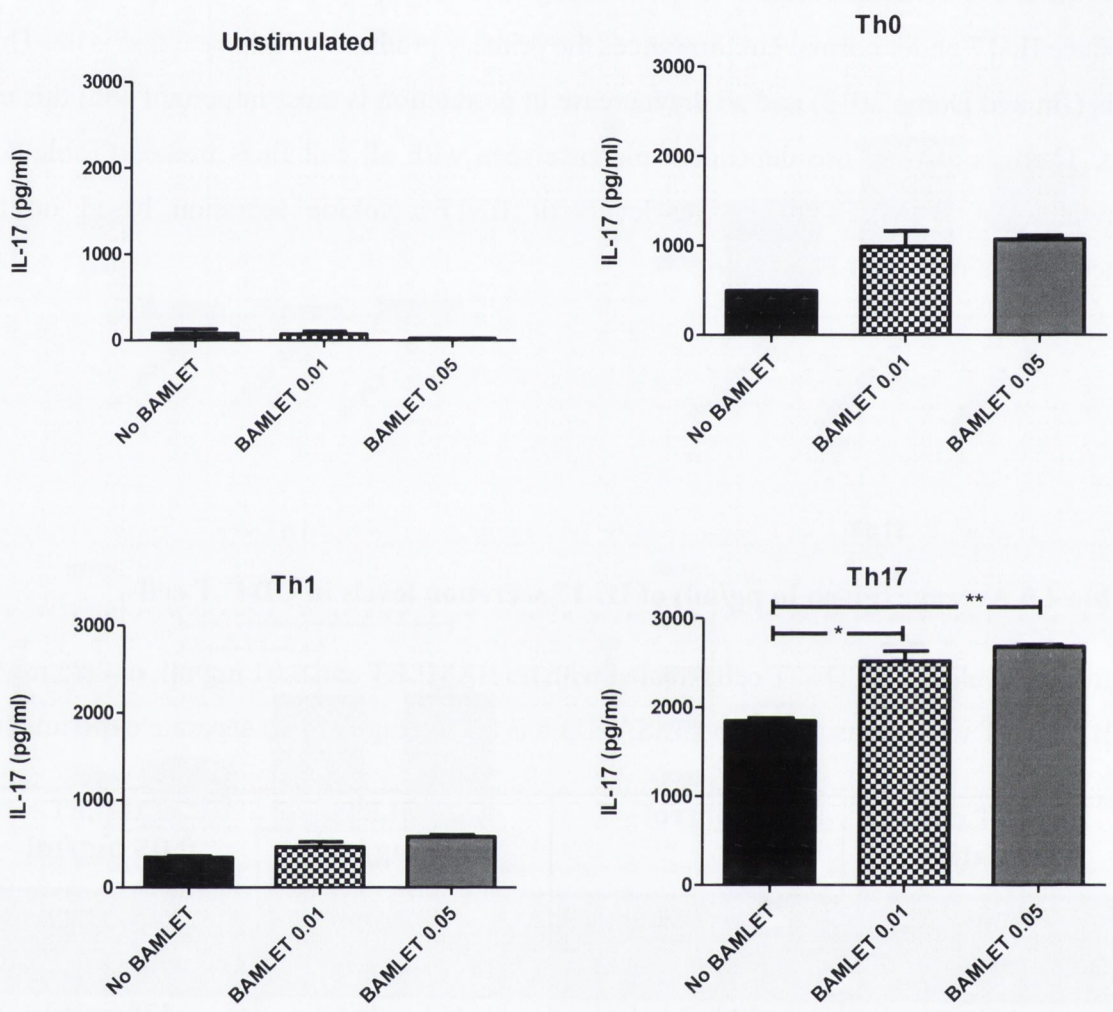

Figure 4.11 BAMLET caused an increase IL-17 in Th17 cells

BAMLET induced a significant increase in IL-17 in Th17 cells only. Slight increases were measurable in both Th0 and Th17 cells also. Statistical analysis was performed using a 1-way ANOVA, $^{*}p < 0.05$, $^{**}p < 0.001$, *** $p < 0.001$. Error bars represent S.D. of mean. Data are representative of 2 independent experiments.

4.2.7.4. BAMLET increased TNF-α secretion in Th0 cells only while having no effect on the other CD4$^+$ T cell populations.

BAMLET had no effect on the production of TNF-α in Th1 or Th17 CD4$^+$ T cells. There was no discernible difference in the cytokine levels when compared to the control group for each cell population, where cells were treated with no BAMLET (Figure 4.12). There was a significant increase in TNF-α levels for Th0 cells treated with BAMLET (Table 4.7) which followed a dose dependent pattern with 0.05 mg/ml of BAMLET almost doubling the levels of TNF-α in these cells when compared the non-BAMLET treatments. Although TNF-α is primarily secreted by Th1 cells and BAMLET seems to have little impact on its secretion in this cell population here, it is interesting to note that there is a dose dependent increase in Th0 cells when treated with BAMLET.

Table 4.7 Average (given in pg/ml) of TNF-α secretion levels in CD4$^+$ T cells

TNF-α levels from polarised anti-CD3 and anti-CD28 stimulated CD4+ T cells treated with 0 mg/ml, 0.01 mg/ml, or 0.05 mg/ml of BAMLET were measured using ELISA. Data is the average of two separate experiments.

CD4$^+$ T cell Population	No BAMLET	BAMLET 0.01 mg/ml	BAMLET 0.05 mg/ml
Th0	475 pg/ml	690 pg/ml	812 pg/ml
Th1	814 pg/ml	778 pg/ml	708 pg/ml
Th17	819 pg/ml	875 pg/ml	544 pg/ml

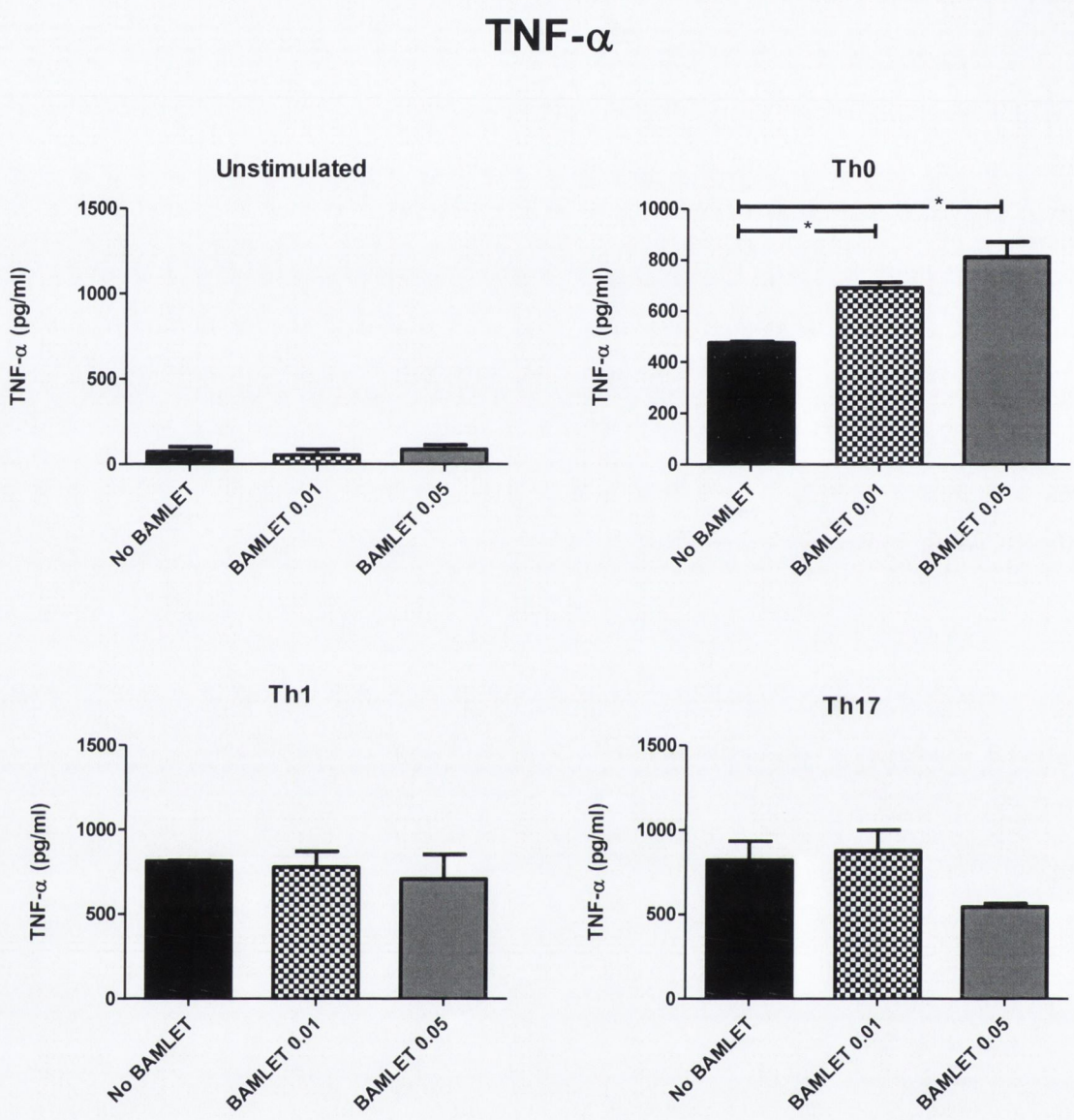

Figure 4.12 BAMLET increases the secretion of TNF-α in Th0 cells.

Th1 and Th17 levels of TNF-α did not show any significant alterations from the non-treated cells when measured with ELISA. BAMLET increased TNF-α levels in Th0 cells. Statistical analysis was performed using a 1-way ANOVA, $^{*}p < 0.05$, $^{**}p < 0.001$, *** $p < 0.001$. Error bars represent S.D. of mean. Data are representative of 2 independent experiments.

4.2.7.5. Treatment with BAMLET causes a reduction in IFN-γ secretion in Th0 and Th17 cells but not in Th1 CD4+ T Cells

IFN-γ secretion is reduced in both Th0 and Th17 subsets of $CD4^+$ T cells yet has no effect on Th1 cells. Using Table 4.8 we can see that Th0 cells showed a significant decrease in IFN-γ levels when compared to the controls, over 50 % decrease for both 0.01 mg/ml and 0.05 mg/ml of BAMLET. Th17 cells treated with the same concentrations displayed a dose dependent decrease in IFN-γ values when compared to the control of no BAMLET treatment. Interestingly there was no decrease in the Th1 subset of cells (Figure 4.13).

Table 4.8 Average (given in ng/ml) of IFN-γ secretion levels in $CD4^+$ T cells

Th0, Th1, and Th17 cells treated with 0 mg/ml, 0.01 mg/ml, or 0.05 mg/ml of BAMLET. Data is the average of two separate experiments.

$CD4^+$ T cell Population	No BAMLET	BAMLET 0.01 mg/ml	BAMLET 0.05 mg/ml
Th0	92 ng/ml	32 ng/ml	38 ng/ml
Th1	104 ng/ml	109 ng/ml	103 ng/ml
Th17	97 ng/ml	63 ng/ml	38 ng/ml

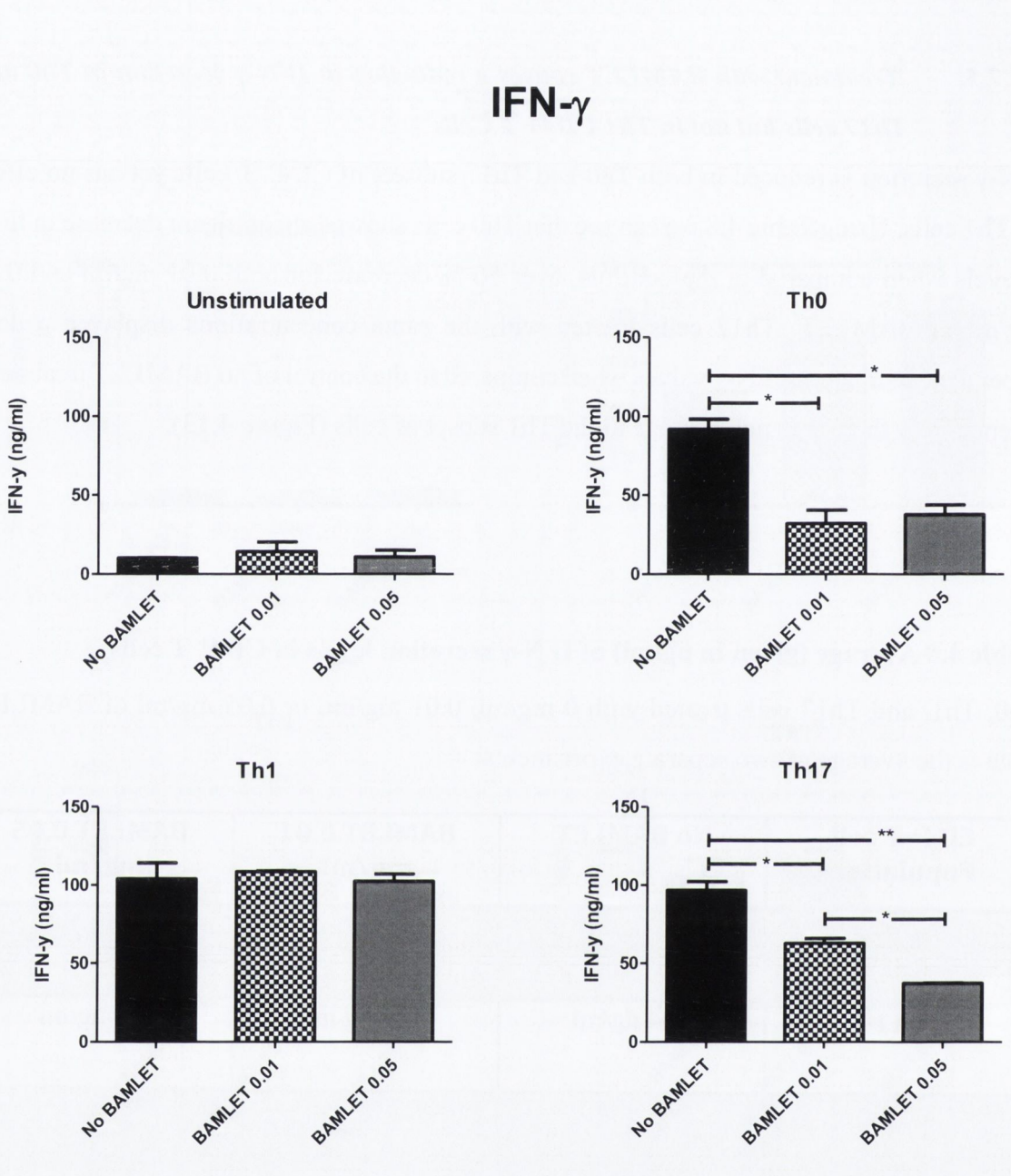

Figure 4.13 BAMLET reduces IFN-γ levels in both Th0 and Th17

ELISA results for cells treated with BAMLET show that IFN-γ levels were significantly decreased in both Th0 cells and Th17 cells. No detectable change in IFN-γ levels were recorded in Th1 cells. Statistical analysis was performed using a 1-way ANOVA, $^{*}p < 0.05$, $^{**}p < 0.001$, *** $p < 0.001$. Error bars represent S.D. of mean. Data are representative of 2 independent experiments.

4.3. Discussion

BAMLET kills B16 tumour cells *in vitro* and also reduced tumour growth in a murine melanoma model. Convalescent mice re-challenged with B16 cells also displayed delayed tumour development suggesting a possible role for immunological protection. Cytokine levels for $CD4^+$T cells were measured after treatment with BAMLET and suggest that a humoral immunological response may be employed in response to this P-FA complex. This study is the first time that a P-FA complex has been tested using a B16 tumour model *in vivo*. Furthermore, this is the first instance where BAMLETs effects on $CD4^+$ T cell cytokine production have been measured.

4.3.1. BAMLET Elicits an Apoptotic Cell Death Pathway in B16 Cells

These results demonstrated that BAMLET killed B16 cells *in vitro* and the level of cell death was time and dose dependant. In light of recent experiments this is not the first time that BAMLET has been tested on B16 cells *in vitro*, and the results attained in our lab showed a similar pattern of death and LC_{50} values (Brinkmann *et al.*, 2013), highlighting the reproducibility of BAMLET and its efficacy against B16 tumour cells. Interestingly BAMLET induced apoptotic cell death in B16 cells *in vitro* which is in agreement with other work examining the cell death properties of BAMLET (Hoque *et al.*, 2013, Rammer *et al.*, 2010). B16 cells treated with BAMLET show a propensity to bind Annexin V when examined using flow cytometry. Cells displayed increased Annexin V staining when compared to the control, and also showed a high percentage of double staining for Annexin V and PI.

These results suggest that after treatment with BAMLET, cells proceed through an apoptotic cell death pathway. This result is also in agreement with previous studies involving other P-FA complexes such as HAMLET (Håkansson *et al.*, 1995, Hakansson *et al.*, 2011, Hallgren *et al.*, 2008, Hallgren *et al.*, 2006). Interestingly cells stain in two populations, single stained and double stained. Although the single staining for Annexin V is suggestive of classic apoptosis, the double staining is more complicated. We hypothese that as the cells die through apoptosis, they eventually become necrotic resulting in the PI staining in addition to Annexin V. This phenomenon is known as secondary necrosis or late apoptosis and occurs when scavenger cells are not around to remove apoptotic bodies. Under normal circumstances when a cell dies through apoptosis it disintegrates into smaller compacted apoptotic bodies

which are targeted for destruction by scavenger cells in the body. In an *in vitro* situation such as this, these scavenger cells are absent and so the apoptotic process proceeds to an autolytic necrotic outcome (Silva, 2010).

In addition, in the absence of scavenger cells, B16 cells treated with BAMLET eventually succumb to secondary necrosis proceeded by apoptosis. Our findings from the live/dead assay further support this claim as they show B16 cells binding to high levels of Annexin V on the surface of the cell and there is also evidence of PI staining once again suggesting that apoptosis was the primary method of cell death followed by secondary necrosis. Future work that can be carried out to clarify this point more would be to reproduce this study using earlier time points as it may be possible to observe the general transition from early to late apoptosis.

4.3.2. BAMLET Induces B16 Cell Death in vitro in the Presence of FCS

We found that incubation of BAMLET and cells in media containing 10% non-heat inactivated FCS did negatively attenuate the efficacy of the drug but did not stop the P-FA complex from inducing high levels of cell death. The culture of cells with P-FA complexes is generally preformed in heat inactive FCS, were the heating of serum results in irreversibly denatured albumin which is inactive (Murayama and Tomida, 2004). A novel feature of my work was to assess whether the presence of non-heat inactivated FCS in the culture media would modify the efficacy of the drug *in vitro*.

Treated cells in serum containing media show a decrease in LC_{50} values at each time point when compared to cells treated in serum free. This suggests that the efficacy of BAMLET is hindered by the addition of FCS, however BAMLET was still capable of killing tumour cells showing that although attenuated, the cytotoxic nature of the P-FA complex is not completed abrogated. This result is an interesting find as it shows that despite the presence of the FA binding protein albumin, BAMLET retains its P-FA conformation. The addition of FCS can alter the performance of many different drugs and can be a stumbling block to many *in vivo* trials in particular if a drug has the potential to interact with albumin. Albumin, the main protein component of FCS, binds to FA, and has been shown in numerous studies to strongly bind in several locations to various FA molecules (Curry *et al.*, 1999, Bhattacharya *et al.*, 2000, Simard *et al.*, 2005, Simard *et al.*, 2006). P-FA complexes are comprised of a protein bound to FA molecules and the electrostatic interactions between the positively-charged

basic groups on α-LA and the negatively-charged carboxylate groups on OA molecules play an essential role in holding the complex together. The binding itself is relatively weak and so the complex remains in a very tentative state throughout (Xie *et al.*, 2013). A main goal of this project was to assess the functionality of BAMLET *in vivo*, and this result suggests that BAMLET will remain folded even when in the presence of albumin. Future work will need to be carried out to determine the structure of BAMLET in the presence of albumin to determine whether the conformation has been compromised.

4.3.3. BAMLET Efficacy in vivo is not Dependent on Route of Administration

This study is the first to demonstrate that BAMLET reduces tumour progression in a murine mouse model and the injection route did not affect the efficacy of the drug. Administration of BAMLET through i.p injection showed similar cytotoxicity to that observed in SC. Furthermore BAMLET treated mice show dramatic increases in survival when compared to the control group over a period of 60 days post tumour inoculation demonstrating the long term protection provided by the complex. These results demonstrate for the first time that BAMLET can be administered through the peritoneal cavity and that systemic treatment works as well as local treatment. As we have demonstrated with our FCS experiments, albumin does not inactivate the P-FA complex and subsequently administration through the peritoneal cavity does not result in BAMLET loss of function.

The method of administering drugs and antibiotics to patients with internal difficulties is often carried out i.p (Lukas *et al.*, 1971). Injections through the i.p route have numerous advantages over SC administration, in the example of insulin, i.p injections are more rapidly and evenly absorbed into the system as the pass directly into the portal vein system (Quellhorst, 2002). It is interesting to note that similarly to SC, higher concentrations of BAMLET appeared to reduce the efficacy of the protein complex *in vivo* and is something that we have yet to elucidate. One possible reason for this may be due to the fact that at a concentration over 0.7mM, BAMLET may have reached its maximum potency, and anything over a certain threshold may not increase the efficacy of the drug. Another possible reason is that at higher concentrations, the protein may become less soluble and even aggregate as higher protein concentrations are invariably linked with increased propensity for proteins to aggregate (Golovanov *et al.*, 2004). Increasing BAMLET concentrations could induce protein aggregation and result in a loss of efficacy for the tumoricidal complex.

Unlike HAMLET, its bovine counterpart has only been used once prior to this in an *in vivo* setting (Xiao *et al.*, 2013) and this is the first *in vivo* study to show that BAMLET or any P-FA complex can diminish the growth of high risk melanoma in a murine skin cancer model. Administration of BAMLET through i.p displayed similar efficacy to that shown with local administration. This novel discovery, and in conjunction with our *in vitro* studies, suggests that BAMLET is not affected by albumin in the blood stream and is capable of locating tumour cells within the body.

This novel result has never been shown before and in conjunction with previous studies which have shown that P-FA complexes reduce tumour growth in various tumour models (Xiao *et al.*, 2013, Mossberg *et al.*, 2007, Mossberg *et al.*, 2010a, Puthia *et al.*, 2013), further strengthens the case for P-FA complexes as a new class of cancer therapeutics. That BAMLET maintains its structural and functional integrity in the presence FCS suggests that it may be a good drug candidate that need not be administered locally.

4.3.4. BAMLET Reduces Tumour Growth in Combination with R848

In addition to BAMLET, the TLR 7/8 agonist R848 reduced tumour growth in a B16 murine model and when in combination with BAMLET their efficacy was increased compared to these drugs individually. Mice were treated via SC injections of BAMLET and R848, and a group treated with a combination of BAMLET/R848. BAMLET and R848 also conferred a long term level of resistance against the tumour cells, as surviving mice from the initial trial that were re-challenged showed a continued reduction in tumour progression when compared to control mice.

In accordance with our previous experiment BAMLET reduced tumour growth when used on its own. Additionally R848, which has also been shown to reduce tumour growth (Stier *et al.*, 2013), also delayed tumour progression when used as an individual treatment. The most dramatic result was seen in the combination group of BAMLET/R848. Mice treated in this group showed a substantial decrease in tumour burden over the course of the trial. The average end stage tumour volume was considerably lower than that observed in the other treated and vehicle group. This group also contained four mice which showed no signs of tumour growth at all over the course of the trial. These results suggest that BAMLET is a

viable candidate for the treatment of murine melanomas and has potential as a future cancer therapeutic.

R848 has previously displayed anti-tumour properties against melanoma cells *in vitro* (Chaperot *et al.*, 2006) and this compound has never been used to treat B16 mice melanomas *in vivo*. In light of these novel results, we suggest that R848 has a potential role as a future melanoma drug. Perhaps the most significant find is that mice treated with the combination of R848 and BAMLET show the largest reduction in tumour size out of all groups when compared to the control. Considering the aggressiveness and speed at which melanoma grow in a murine model, this result is promising and significant. We wanted to discover whether the mixing of these two drugs could potentiate the efficacy of the compounds or whether the combination of R848 and BAMLET would have a negative effect on mouse survival.

There are many risks involved when combining drugs to treat diseases such as reduced efficacy due to drug competition and a higher likelihood of side effects (Terrault, 2009). Mixing these two drugs resulted in no side effects for the mice. Furthermore BAMLET and R848 in combination showed no signs of competitive inhibition and the drug efficacy did not seem to be abrogated in any way, in fact the combining of these two drugs and the increased efficacy seen suggests that these drugs may act synergistically and may increase the cytotoxicity and selectivity of each other.

Several mice displayed no tumour growth after the initial treatment and some even maintained this immunity after the re-challenge suggesting that this drug has an important and measurable inhibitory effect on skin cancer growth and can not only delay the onset of metastatic growth but can completely abolish growth in certain situations. Firstly the delayed onset of tumour development in these re-challenged mice suggests that BAMLET and R848 may trigger an adaptive immune response that confers some level of resistance against this tumour. Work will need to be carried out to examine this hypothesis in more detail, in particular, whether BAMLET or R848 prime the immune system to recognize antigens on the tumour cell surface.

R848 acts by recognizing PAMPs on the surface of pathogens and these PAMPs on the surface of B16 tumour cells may be more readily targeted for destruction due to the previous treatment with the compound. Similarly, BAMLET may have pre-altered the immune system

to target tumour cells. DCs are the main antigen presenting cell in the body and constantly survey the surrounding milieu for antigens on the surface of foreign bodies. Once activated DCs activate the MHC complex which stimulates B cell activation, and also secretes numerous cytokines including IL-12 which triggers the activation and maturation of T-cells (Merad *et al.*, 2013).

We hypothese that BAMLET in addition to directly destroying the tumour due to its cytotoxic nature, may also be interacting with DCs and thus primes the immune system to recognize and target B16 melanoma antigens, which may be a reason for the delayed onset of tumour growth seen in the re-challenge. Further work needs to be carried out to examine whether BAMLET interacts with DCs directly. An important feature of this experiment will be to determine whether BAMLET contains lipopolysaccharides (LPS) which can also stimulate DC activation (Granucci *et al.*, 1999).

Currently our group in collaboration with Lydia Dyck from Professor Kingston Mills laboratory is probing this important question. We will examine BAMLET-DC interactions using a DC line which contains defective TLR4, which is involved in LPS activated maturation of DCs (Ashtekar *et al.*, 2008). This experiment should determine whether DCs can become activated in the absence of LPS. An observation that has to be made when discussing these findings is that the population size used for the re-challenge was considerably smaller than what was used in the initial trial, and too low to gather any concrete conclusions from. This re-challenge was meant only as a very preliminary examination into the possibility that BAMLET may have a lasting effect *in vivo* and further studies using larger sample sizes will be needed to get statistically robust data.

4.3.5. BAMLET may Activate a Humoral Immune Response

$CD4^+$ T cells which were treated with BAMLET show altered cytokine production in relation to those treated with PBS. Anti-CD3 and anti-CD28 stimulated $CD4^+$ T cells were polarised to yield three different populations (Th0, Th1, and Th17) and displayed attenuated cytokine levels after treatment with BAMLET.

Incubation of all T-cell populations with BAMLET completely diminished IL-2 secretion when compared to untreated controls. IL-2 is an important molecule for inducing the proliferation of T-cells and was originally believed to be the key regulator of T-cell

maturation however this theory was challenged in the early 1990's after it was revealed that mice with IL-2 deficient genes displayed normal thymocyte and peripheral T-cell subset composition (Schorle *et al.*, 1991). Therefore the fact that BAMLET downregulates the production of IL-2 does not necessarily mean that it has a negative effect on T-cell production.

IL-2 is however a key factor in the proliferation of Treg cells, the presence of which correlate with a poor prognosis in cancer patients due to their ability to inhibit a sufficient immune response (Dranoff, 2005). A decrease in IL-2 production could be resulting in a decrease in Treg production. This response could be beneficial as a reduction in Treg cells would allow the immune system more freedom to directly attack the melanoma. IL-2 is an important factor in stimulating a Th1 mediated response and can be negatively inhibited by various cytokines, in particular IL-10 (Taga and Tosato, 1992). The complete abrogation of IL-2 in response to BAMLET, and the upregulation of IL-10 suggest that a Th2 response may be activated in place of a Th1. The complete abrogation of IL-2 in response to BAMLET, and the upregulation of IL-10 suggest that a Th2 response may be activated in place of a Th1 response.

In response to treatment with BAMLET, IL-10 levels were increased in all $CD4^+$ T cell populations examined but significantly in the Th1 subset. IL-10 is a pleiotropic cytokine that is involved directly with the innate and adaptive immune system. Overexpression of IL-10 acts as a double edged sword. It inhibits the production of Th1 cytokines such as IFN-γ and IL-2 (Lalani *et al.*, 1997). Despite this there are numerous positives to the overproduction of IL-10.

IL-10 promotes the survival of normal B-cells and is also a potent growth and differentiation factor for activated human B lymphocytes (Levy and Brouet, 1994, Rousset *et al.*, 1992). IL-10 also has a direct effect on T-cells in that it has been shown to inactivate T-cell responses and induce T-cell anergy mainly through the downregulation of IL-2 and thus favours a humoral driven response (Groux *et al.*, 1996, Itoh *et al.*, 1994). IL-10 may have a role in the early stages of DC maturation and promotes antigen uptake by DCs in response to pathogens (Morel *et al.*, 1997).

Importantly, IL-10 promotes the activation of NK cells. NK cells provide an integral link between the adaptive and innate immune system as they are involved early on in the destruction of pathogens including cancer cells, and can provide DCs with adequate amounts of relevant antigens which in turn would stimulate the maturation of DCs and activation of an adaptive immune response (Ochsenbein, 2002, Kelly *et al.*, 2002).

The increase in IL-10, in particular through Th1 cells which are a primary producer of the cytokine (Saraiva *et al.*, 2009) suggest that this cytokine may be functioning in a dual role. IL-10 has been shown to decrease the production of the pro-T-cell producer IL-2 (Itoh *et al.*, 1994), which was evident from our results. This inhibition of IL-2 may promote a shift in immune response towards a state of T-cell anergy where Th1 cell activity is depleted in order to facilitate a more prominent Th2 or humoral immune response which would select for the production of B-cells and NK cells. This shift in immune status could be why we see an improved response to the tumour when mice were re-challenged. We suggest that the immediate antitumouricidal function of BAMLET coupled with a potential induction of NK cells through IL-10 could be a reason as to why tumour growth is delayed when mice are originally inoculated with B16 melanoma.

The delayed, and in some cases completely abrogated growth seen when mice are re-challenged with tumour cells, in combination with the apparent downregulation of IL-2 and increase in IL-10 might suggest that the immune response elicited by BAMLET is one which favours a humoral mechanism, in that Th1 cell production is restricted in order to facilitate a Th2 antigen derived response. Conversely, IL-10 expression has been linked with the progression of tumours (Mocellin *et al.*, 2005). Increased IL-10 has been shown to play an important role in the progression of non-small cell lung cancer through its ability to suppress the immune system. Also cutaneous basal and squamous cell carcinomas have been shown to elevate IL-10 levels which may provide a mechanism for evading the local T cell-mediated immune response (Kim *et al.*, 1995).

We found that BAMLET increased IL-17 production significantly in Th17 T-cells and does so in a dose dependent manner. Th17 cells are the primary producer of IL-17 cytokines and they are by far the most abundant cytokine produced by this particular cell subset (Chen and O'shea, 2008). Th17 cells play a dynamic role in inflammation and tumour immunity. There

are conflicting reports as to the true role of Th17 cells in tumour immunity and the reaction of the cancer in response to the cell appears to be dependent on the particular type of malignancy. In a murine pancreatic model, induction of Th17 in the tumor microenvironment led to delayed tumour growth and improved survival which suggests that Th17 cells may produce an antitumor effect (Gnerlich *et al.*, 2010). Conversely, a murine lung cancer model where the oncogene K-ras was restricted suggested Th17 cell-mediated inflammation played a key role in lung tumourogenesis (Chang *et al.*, 2014).

We found that BAMLET decreased the tumour burden in mice with B16 melanomas and also upregulated the production of IL-17. This work supports earlier work examining the role of Th17 cells in the same murine model, in which it was shown that a Th17 phenotype and the production of IL-17 cytokines was found to reduce the tumour volume *in vivo* (Muranski et al., 2008). Our work also corroborates another study suggesting a role for IL-17 induced lymphocytes in the regression of human metastatic melanoma (Martiniuk *et al.*, 2010). It has been suggested that Th17 cells form and function are uniquely sensitive to a host of factors in the context of tumours and that external factors such as the type of cancer tissue could affect these responses (Zou and Restifo, 2010).

The presence of Th17 cells in the tumour microenvironment has been linked with the production of cytotoxic $CD8^+$ T and NK cells and a downregulation of Treg cells (Kryczek *et al.*, 2009, Martin-Orozco *et al.*, 2009). We hypothesise that the upregulation of IL-17 causes an increase in the antitumour functions of Th17 cells causing a reduction in the tumour burden as was seen in the *in vivo* trial. In agreement with other studies examining the role of Th17 cells and melanoma (Martiniuk *et al.*, 2010, Muranski *et al.*, 2008) we see a dramatic decrease in tumour volume and also an increase in IL-17 production.

We suggest that the antitumour functions attributed to increased IL-17 in this instance could be an increase in NK cells and $CD8^+$ Killer T-cells which as mentioned act as a mechanism by which Th17 cells destroy tumours. Further experiments will be needed to examine if these particular immune cells are upregulated in response to BAMLET treatment.

TNF-α is upregulated in naïve Th0 cells in a dose dependent manner when treated with BAMLET, however there is no shift in Th1 or Th17 cells. TNF-α is an endotoxin-induced glycoprotein that is capable of inducing necrosis in various tumours (Carswell *et al.*, 1975).

Although this was originally thought to be its sole function, TNF-α has been shown to have a multifaceted role in the body and is involved in inflammation, autoimmune, neurological, and cardiovascular diseases (Aggarwal *et al.*, 2012). Production of TNF-α by Th0 cells can have a direct toxic effect on malignant cells, as many murine tumour models have shown tumour cell death in response to treatment with TNF-α (Hori *et al.*, 1987a, Hori *et al.*, 1987b, Brouckaert *et al.*, 1986) and there has even been success treating mouse melanoma models *in vivo* (Talmadge *et al.*, 1988).

Alternatively, TNF-α has also been shown to have a positive effect on tumour progression with regards to melanoma. It has been suggested that TNF-α increases melanoma cell attachment to extracellular matrix (ECM) substrates and promotes migration and invasion (Zhu *et al.*, 2002, Bald *et al.*, 2014). Due to the reduction in tumour volume which we observed when treating mice with BAMLET, we hypothesise that TNF-α is being utilised for a destructive purpose rather than promoting malignant migration. One further possibility is that the increase seen in Th0 TNF-α levels is driving the production of Th22 cell differentiation *in vivo*. Th0 cells are a naïve set of $CD4^+$ T cells capable of differentiating into various T-cell subsets (Romagnani, 1999).

A recently discovered subset of T-cells, known as Th22 cells have been shown to have an important role in skin homeostasis and pathology (Trifari *et al.*, 2009). Interestingly, the promotion of this particular cell type from its original naïve $CD4^+$ T-cell is driven by TNF-α (Ye *et al.*, 2012). The production of TNF-α by these Th0 cells could be potentially driving the expansion of Th22 cells, which would be interesting given its role in tissue regeneration and wound healing, factors that are associated with the development of malignant melanomas. Although the role of Th22 cells in melanoma is as yet unclear it is an exciting possibility that BAMLET may contribute to the production of a further Th22 subset that has a specific role in tissue regeneration. A possible experiment that will need to be carried out in order to confirm this will be to anaylse, using FACS, whether there are Th22 cells present in the spleens of BAMLET treated mice.

IFN-γ is the quintessential Th1 cytokine and is responsible for orchestrating an immune response against intracellular microorganisms (Amsen *et al.*, 2009). In our study we found that IFN-γ was reduced in both the Th0 and Th17 subsets of $CD4^+$ T-cells but most

significantly there was no change in IFN-γ levels in Th1 cells. In Th1 mediated responses we would expect to see a definitive upregulation of IFN-γ which in turn has a plethora of effects throughout the body. IFN-γ production induces direct antimicrobial and antitumor mechanisms through macrophage stimulation, enhances the cell activity of NK cells, inhibits B-cell proliferation through inhibition of LPS, downregulates a Th2 response through suppression of IL-4, and orchestrates leukocyte trafficking (Schroder *et al.*, 2004, Young and Hardy, 1995). In Th1 cells there was no change in IFN-γ levels indicating that BAMLET is not stimulating a Th1 mediated response. Furthermore, Th0 cells show a decrease in IFN-γ production when treated with BAMLET when compared to the control. In the event of a Th1 mediated response, Th0 levels of IFN-γ would be expected to be increased to drive the production of Th1 cell expansion. The downregulation of these cytokines in Th0 cells suggests that the response mediated by BAMLET in this instance is not this type of immune response.

From our results we can conclude that BAMLET reduces tumour volume in a murine melanoma model and prolongs survival when compared to a control group treated with PBS. In addition to this, the injection route chosen did not affect the efficacy of the drug. This is the first time BAMLET or any of these new P-FA complexes have been administered via an i.p injection. Surprisingly the high affinity for FAs displayed by albumin did not seem to disrupt the complex reaching or interacting with the tumour. The TLR 7/8 agonist R848 was also shown to reduce tumour burden and increase survival in the same mouse model. Furthermore, the combination of BAMLET with this molecule increased the survival of mice and also dramatically reduced tumour volume when compared to the vehicle and the single treatments. Immunologically, treatment with BAMLET does not appear to initiate a Th1 cell response and our results suggest that a humoral immune response may be stimulated instead.

5. Isolation and Characterisation of Amyloid Oligomers, Sonicated Fibrils, and Mature Fibrils Prepared from an Innocuous Protein

5.1. Introduction

Protein folding in eukaryotes is a highly organized and regulated system which depends on numerous specialised compartments and molecules to ensure that the process runs efficiently (Hetz, 2012). There are specific molecules in place to facilitate the folding process which include the HSP-60 and HSP-70 molecules (Mayer and Bukau, 2005), and the lesser used HSP-90 and HSP-100 chaperones (Saibil, 2008). The ER also plays a major role in synthesizing and correctly folding proteins (Lin *et al.*, 2008) and can result in the activation of the UPR which tags and removes aberrant protein molecules that have folded incorrectly (Hetz, 2012).

Although not as predominant as the UPR or proteasomes, some extracellular and intracellular macromolecules including proteins are degraded within lysosomes. These proteins are taken up through endocytosis and the degradative lysosomal enzymes digest their contents (Dunn, 1994). Despite the numerous mechanisms employed by the cell to prevent aberrant conformations, abnormally folded proteins can still arise, and are generally termed misfolded. The process of protein folding becomes more intricate and elaborate as protein size and complexity increases and is therefore more likely to lead to dysfunctional proteins (Dobson, 2001).

The phenomenon of protein misfolding has been heavily linked with numerous neurological and systemic diseases (Soto, 2003). Collectively these disorders are often referred to as PCDs (Calamini *et al.*, 2012) and include a battery of inheritable diseases, such as AD and PD (Chiti and Dobson, 2006, Dobson, 2001). AD is the most studied PCD and is characterised by progressive memory loss as well as the impairment of various other cognitive functions (Alistair and Steve, 2009). The global burden of AD is immense with 36 million cases worldwide, which is estimated to triple by 2050. Additionally, the global financial costs of this disease are equally staggering, having cost $604 million to treat in 2010 (Wimo *et al.*, 2013). The onset and progression of AD are multifactorial and still somewhat unclear. Copathogenic interactions between multiple factors result in the impairment of neuronal functionality and ultimately lead to death. Studies into a rarer form of early onset AD known as Familial AD have shown that pathogenic mutations to the presenilin 1 (*PSEN1*), presenilin

2 (*PSEN2*) and amyloid precursor protein (*APP*) genes are the key genetic players which lead to the progression of the disease (Cavallucci *et al.*, 2012). Mutations to these genes lead to the accumulation of Aβ protein which is the primary protein aggregated in AD and the main constituent of senile plaques which are found on the brain (Chiti and Dobson, 2006).

The identification of a pathogenic role for Aβ in AD has led to the construction of the Aβ hypothesis of AD progression. Aβ is a 4 kDa peptide sequence of amino acids 39-43 located on the part of APP that spans the transmembrane domain. APP is cleaved by numerous enzymes to eventually yield the APP intracellular domain, which contains Aβ (predominately $A\beta_{1\text{-}40}$ and $A\beta_{1\text{-}42}$). Numerous studies have identified that the hydrophobic sequence, $A\beta_{1\text{-}42}$, is the true culprit in the pathogenesis of AD *in vivo* (Rowan *et al.*, 2003). Under normal conditions Aβ plays a fundamental role in the development and function of both the central and peripheral nervous system; specifically synapse formation plasticity and behavior (Aydin *et al.*, 2012).

As mentioned previously, mutations to three genes (*APP, PSEN1, PSEN2*) are the main causative event involved in the production of the aberrant $A\beta_{1\text{-}42}$ protein, which displays decreased stability when compared to the native protein (Cavallucci *et al.*, 2012). A substantial body of work has been carried out using various animal models to demonstrate the importance of this protein to the development and symptoms displayed in patients with AD. Transgenic mice designed to overexpress the human mutant forms of APP have been shown to display amyloid plaque deposition, cognitive defectiveness, and synaptic marker disruption (Chen *et al.*, 2000, Reilly *et al.*, 2003, Elder *et al.*, 2010).

A group of approximately 25 unrelated proteins have been shown to be involved in the formation of a number of clinically distinct conditions (Stefani, 2010). The main pathogenic entities of these diseases appear to be the soluble oligomer species and the insoluble fibrils (Pepys, 2006). The formation of oligomers precedes the formation of monomers but precedes the formation of the end stage mature fibrils (Figure 5.1) (Glabe, 2006). As mentioned previously there is considerable debate regarding the true toxic amyloid species. Originally fibrils were thought to be the sole pathological agent in patients suffering from PCDs and when these fibrils were tested on cells *in vitro* (Novitskaya *et al.*, 2006), and in animals *in vivo* (Kohno *et al.*, 1997, Shimada *et al.*, 1989) they elicited a cytotoxic response, further

strengthening the consensus that fibrils were the main culprit in the amyloid story. However, a large body of recent data suggests that the more soluble oligomers are the true cytotoxic components (Budka, 2003, Haass and Selkoe, 2007, Klein *et al.*, 2001a, Sakono and Zako, 2010, Vieira *et al.*, 2007). Despite the shift in opinion in recent years, the true injurious component(s) involved in PCDs has yet to be determined and even though much has been learnt in the past three decades relating to the physiology and pathophysiology of these disorders, much remains to be unearthed before we can fully understand how to treat these classes of diseases.

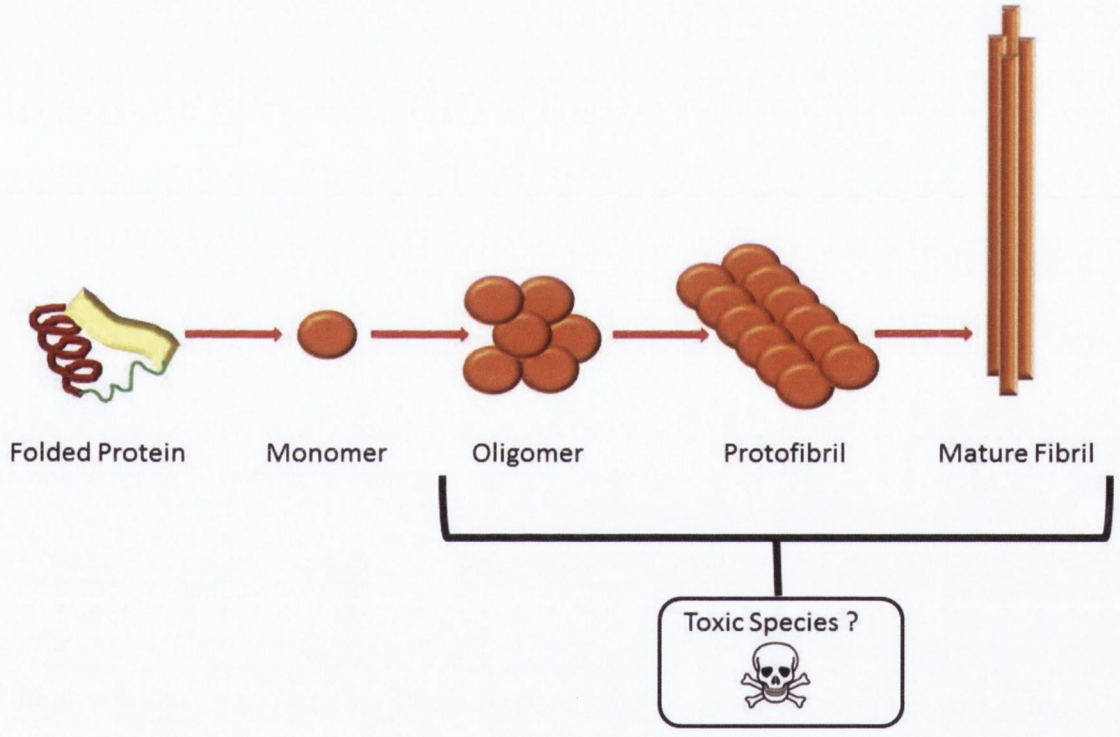

Figure 5.1 The process of amyloid formation.

Various factors can result in the unfolding of the native α-helix rich soluble cellular protein into the aggregated protein. Native protein forms monomers which can continue down the aggregation pathway to form oligomers, protofibrils, and eventually amyloid fibril aggregates. All stages are thought to possess differing levels of toxicity. Adapted from Huang *et al.*, 2013.

Adequate isolation and characterisation of amyloid aggregates is key to the understanding their mechanistic and structural properties. Numerous techniques are available for generating amyloid fibrils and oligomers and can vary greatly depending on the protein. HEWL fibrils were the first non-disease related fibril to be generated and suggested that given the right conditions any protein could be engineered into an aggregated state (Krebs *et al.*, 2000). Since this discovery HEWL has been used as a model for the development and study of aggregate properties by numerous groups (Gharibyan *et al.*, 2007, Arnaudov and De Vries, 2005, Mossuto *et al.*, 2010, Vieira *et al.*, 2007, Xu *et al.*, 2007) and all groups generate HEWL fractions in various ways. Once they have been generated, the isolation and characterisation of amyloid aggregates can be a difficult process. There are numerous techniques used which involve either staining the protein molecule with detectable dyes, or directly visualising the assemblies via microscopy (Nilsson, 2004). In general, only one of these techniques would be considered sufficient for the identification of amyloid fibrils; however, they are prone to generating false negative results (Cooper, 1969). Due to this it is sometimes advisable to use a combination of different identification techniques to eliminate the possibility of error.

There are numerous methods used to determine the presence and kinetics of fibril formation, notably the CR and ThT assays. However, these techniques are sometimes only reliably sensitive to amyloid fibrils and can be problematic when used to distinguish the presence of smaller oligomers or protofibrils (Murphy, 2007, Williams *et al.*, 2005). The inability of these assays to pick up signals for the presence of aggregated samples can lead to erroneous interpretation of the data, often being put down to the fact that the protein is remaining monomeric during a lag time when in reality, these proteinaceous particles can form rapidly during a suppositional lag time, leading to the formation of fully formed fibrils (Murphy, 2007, Poirier *et al.*, 2002). The use of numerous procedures is therefore required to definitively determine whether one is dealing with amyloid oligomers or fibrils, in particular, if one wishes to utilise these protein samples for various experiments.

As mentioned previously, a broad range of human diseases are a result of a proteins failure to correctly adopt and maintain its native conformational state. These protein misfolding-related diseases follow a general and well established cascade of progression, from soluble functional states towards highly insoluble amyloid fibrillar aggregates. One of the most

common subsets of these disorders is those comprising neurodegenerative diseases which result from the formation and deposition of organized amyloid plaques located at various locations across the brain (Chiti and Dobson, 2006). One of the most common forms of these neuron damaging illnesses is AD which has been discussed previously.

The neurological abnormalities displayed by patients with AD are not contained to this disease alone, but are more commonly grouped under the umbrella of dementia, of which AD is the most prevalent type (about 50% of total cases) (Burns and Iliffe, 2009). Dementia also encompasses other disorders such as Frontotemporal lobar degeneration, Dementia with Lewy bodies, and PD. All of these disorders carry with them one common feature, deposition of aggregated protein on the brain leading to the damage or death of nerve cells. Cognitive malfunction is a symptom of this neuronal damage, with inability to preform motor activities, problems with abstract thinking, and most commonly a decline in memory all a result (Thies and Bleiler, 2013).

Several areas of the brain are involved in memory/learning. The hippocampus has been shown to play a pivotal role in the formation of declarative memory and spatial learning. In addition to this, it is also involved in recognition memory and working memory. It is not surprising therefore that damage to this particular area of the brain can result in difficulties with memory (Scoville and Milner, 1957), spatial positioning and awareness (Morris *et al.*, 1982), and learning (Schenk and Morris, 1985). Early stages of AD pathophysiology are characterised by deficiencies in memory specifically related to the medial temporal lobe and the hippocampus (Rowan *et al.*, 2004). Consequently, most patients with early AD and general cognitive impairment display deficits in hippocampus dependent memory suggesting that damage to this particular region of the brain is responsible for memory and cognitive deterioration.

One of the main factors in memory and learning displayed by the hippocampus is the phenomenon of LTP. In the hippocampus, LTP is a long lasting synaptic enhancement which allows synapses to improve their strength and neurotransmitting capabilities for a greater period of time then would normally be allowed (Malenka and Nicoll, 1999). LTP increases glutamate production which subsequently depolarizes the receiving synapse and allows for greater signal transport through neuronal cells. The process itself is also input specific and

will only be stimulated in active neuron cells and restricted to active synapses within these cells (Bliss and Collingridge, 1993). Persistent change in neuronal circuits, or synaptic plasticity, is widely thought to be required for learning and memory. The change in synaptic plasticity along with the specificity of its actions suggest that LTP is integral to the formation of memory (Lynch, 2004).

Having separated specific HEWL fractions through our method of ultracentrifugation and ultrafiltration we characterised these fractions to determine whether successful isolation of oligomers, and fibrils had been achieved. Once we had isolated specific aggregate species we examined their cytotoxic properties in a neuronal tumour versus healthy cell model and examined their effects on rat LTP *in vivo*. Our results demonstrate that HEWL oligomers and fibrils are cytotoxic towards $PC12^{undiff/diff}$ cells and activate apoptotic and secondary necrotic cell death respectively. This study also demonstrates for the first time that HEWL oligomers inhibit LTP in rats suggesting that oligomers share a common property in attenuating memory and learning in patients with dementia.

5.2. Results

5.2.1. HEWL Aggregation was Examined using ThT and ANS

The incubation of HEWL in pH2 buffer at 65°C has been shown to convert the native protein into a fibrillar form (Krebs *et al.*, 2000). ThT is a common technique used to examine the aggregation of proteins and exhibits fluorescence upon binding to β-sheet-rich deposits (Levine, 1999). Furthermore ANS interacts with hydrophobic binding sites within proteins and can reveal information about the aggregated state of the molecule (Hawe *et al.*, 2008). We have incubated 1 mM pH 2 HEWL at 65°C and 37°C for 21 days and measured ThT fluorescence daily (Section 2.11). After 21 days the sample was separated as per Section 2.10, and the resulting aggregates (0.5mM) were probed with ANS and measured against ANS only. The binding of ANS to exposed surfaces leads to an enhanced fluorescent emission and a blue shift of the spectra maximum. Lysozyme at 65°C showed a gradual increase in ThT emission over 21 days. HEWL at 37°C did not show any increase in absorbance when measured against ThT alone (Figure. 5.2). When compared to ANS bound control (emission maximum ~500 nm), oligomers display a shift in wavelength (emission maximum, ~487 nm). Sonicated fibrils showed increased intensity and blue shift of the ANS fluorescence (emission maximum, ~480 nm) Isolated mature fibrils show the largest blue shift in spectra (emission maximum, ~470 nm) (Figure. 5.3).

These results suggest that a combination of increased heat and an acidic environment are crucial for the formation of HEWL fibrils. HEWL in pH 2 buffer at 37°C displayed no increase in absorbance suggesting that no aggregation had occurred over 21 days. Conversely at 65°C HEWL showed increased levels of absorbance when incubated with ThT indicating that in these conditions HEWL becomes more aggregated. Additionally, separated fractions display a step wise decrease in ANS emission from fibrils to oligomers indicating that the more fibrillar HEWL is the more the structure has altered and become more hydrophobic.

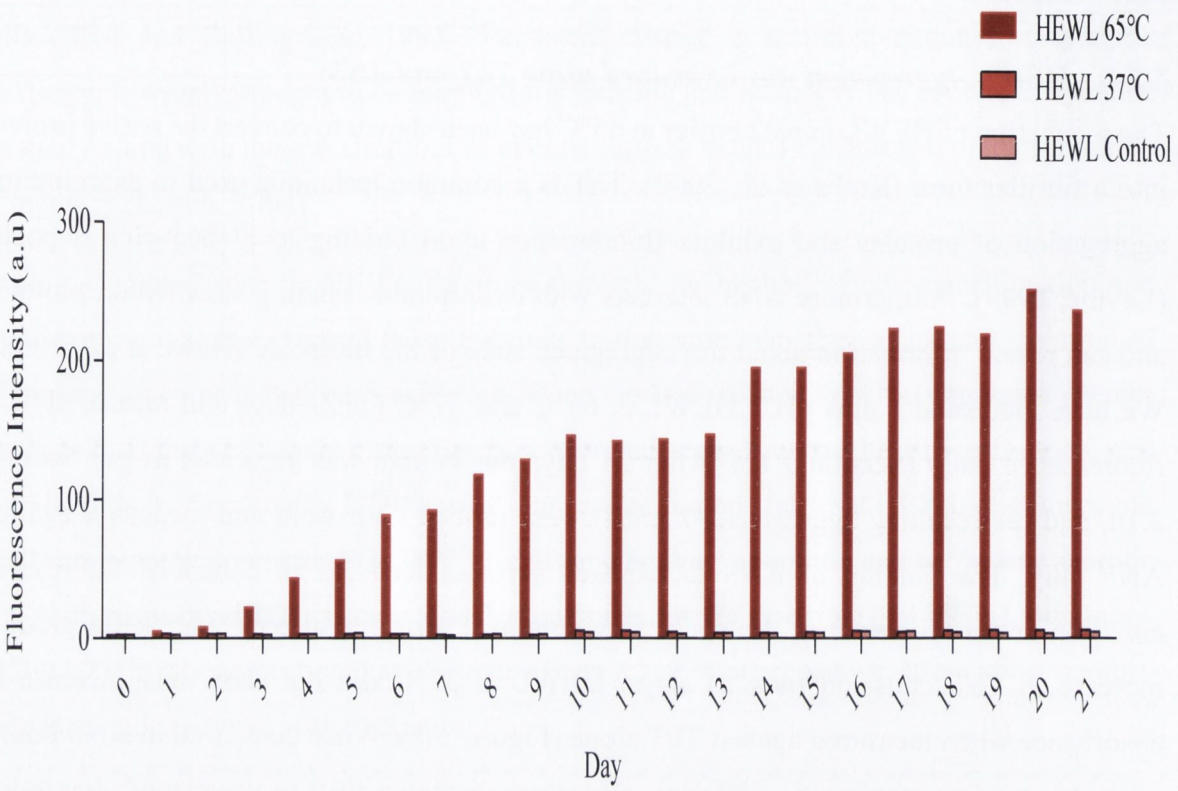

Figure 5.2 Fluorescence emission spectra of ThT in the presence HEWL protein

Fluorescence intensity of 1 mM lysozyme incubated at 65°C (dark red), 37°C (red), and no incubation (light red) was measured by excitation at 440 nm daily for 21 days. All samples were adjusted by subtracting spectra of ThT only. These results are representative of three separate experiments.

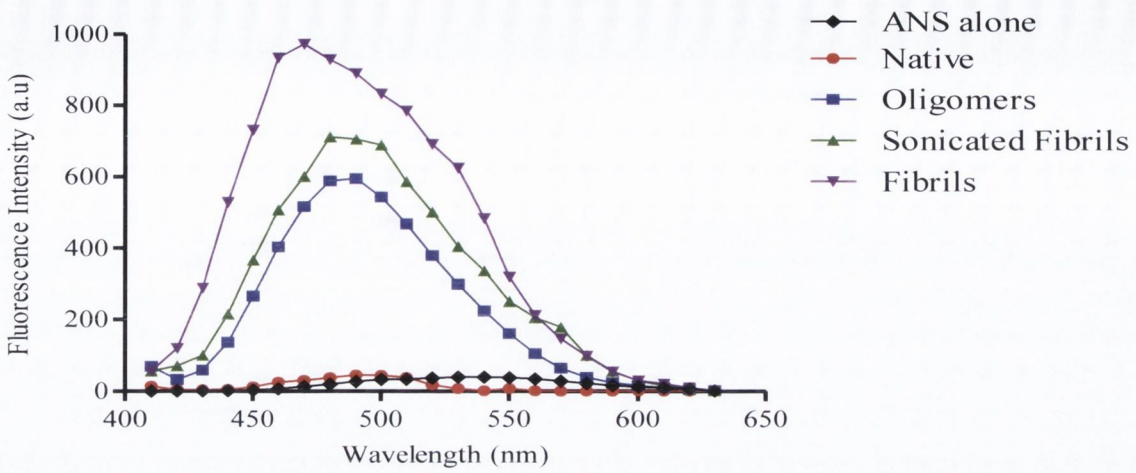

Figure 5.3 Interaction of HEWL oligomers and mature fibrils with the hydrophobic dye ANS.

The fluorescence spectra of ANS bound fibrils (purple), sonicated fibrils (green), oligomers (blue), and control protein (red) are shown. Free ANS in solution is also shown (black). These results are representative of two separate experiments.

5.2.2. CR Binds Amyloid Fibrils

From our ThT experiment we have established that pH 2 HEWL at 65°C conditions becomes highly aggregated. Once in this state we can separate individual fractions and examine their properties using a battery of techniques. For CR birefringence, 1 mM of HEWL untreated, oligomeric, sonicated, and mature fibrils were stained with CR and then visualised using polarised light microscopy for the detection of apple green colouration (Puchtler *et al.*, 1962). The presence of lysozyme aggregates was also detected using a CR spectrophotometric assay. HEWL (1 mM) samples were incubated and measured as per section 2.12. The binding of CR to fibrillar β-sheet results in a red shift in the absorbance spectrum when measured using a spectrophotometer. For birefringence, HEWL fibrils displayed apple green birefringence when visualised using 90°cross polarizers (Figure 5.4 G and H). Control HEWL (Figure 5.4 A and B), oligomers (Figure 5.4 C and D), and sonicated fibrils (Figure 5.4 E and F) show no evidence of birefringence upon exposure to polarised light). Figure 5.5 shows mature fibrils at increased magnifications (X40). The spectroscopic assay results show that monomers (495 nm), oligomers (500 nm), sonicated fibrils (505nm), and mature fibrils (505 nm) all show a shift in the peak maximum from CR alone (490 nm) in the red absorbance direction (Figure 5.6). These results suggest that the mature amyloid fibril fraction isolated from HEWL displays hallmark signs for the presence of amyloid fibrils. Oligomers show no birefringence, but do show a shift in the spectroscopic assay suggesting that although not fibrillar, these samples are aggregated.

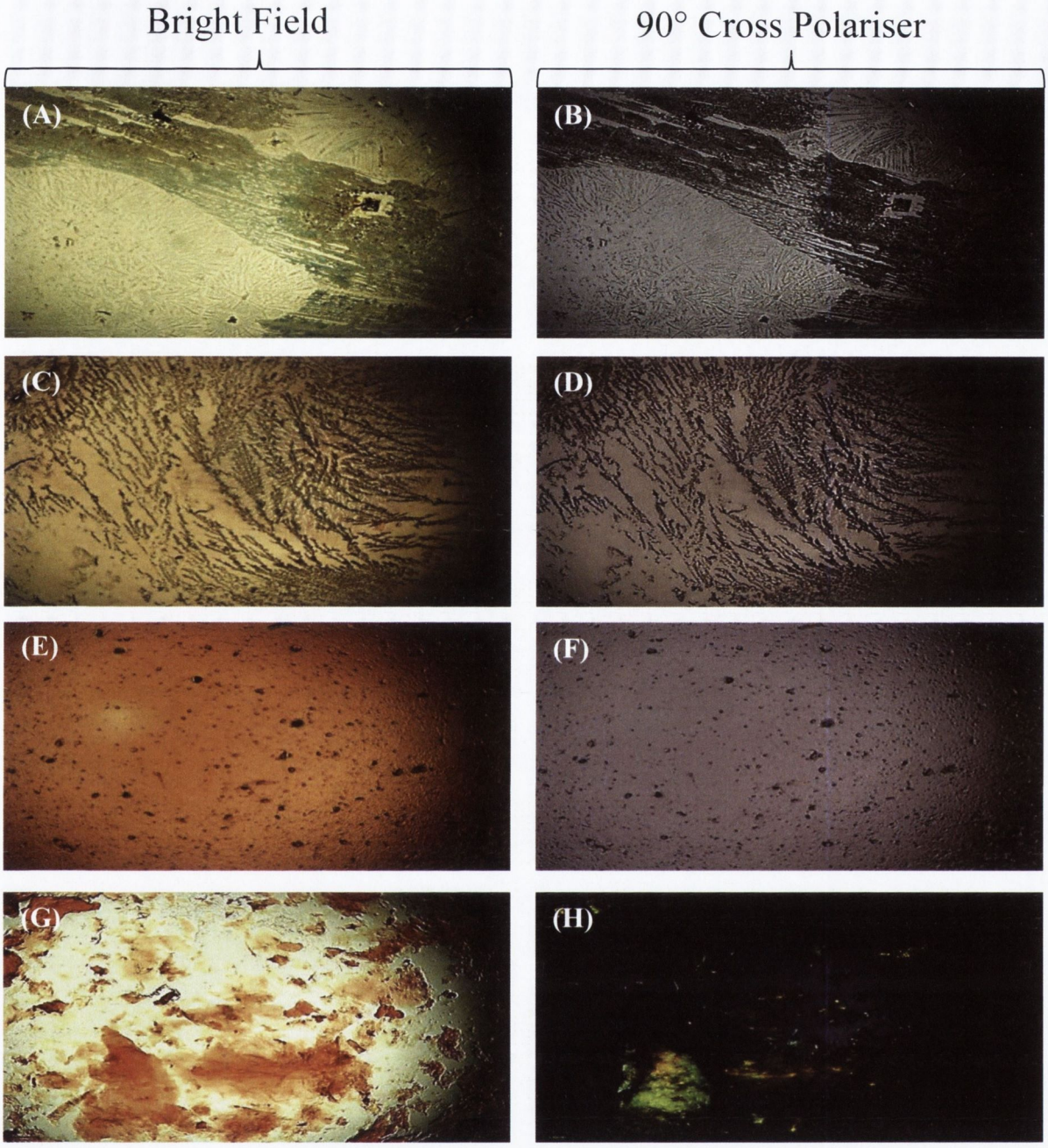

Figure 5.4 CR binds mature amyloid fibrils in vitro

CR birefringence assay of HEWL containing ultracentrifuged/ultrafiltrated fractions. (A-B) Non heated control HEWL, (C-D) prefibrillar, (E-F) sonicated fibrils, and (G-H) mature fibril samples were analysed without cross polarisers (left) and with cross polarisation (right) at 90°. Optical microscopy images were observed using a Nikon Eclipse E400 POL microscope at magnification X10. These results are representative of three separate experiments.

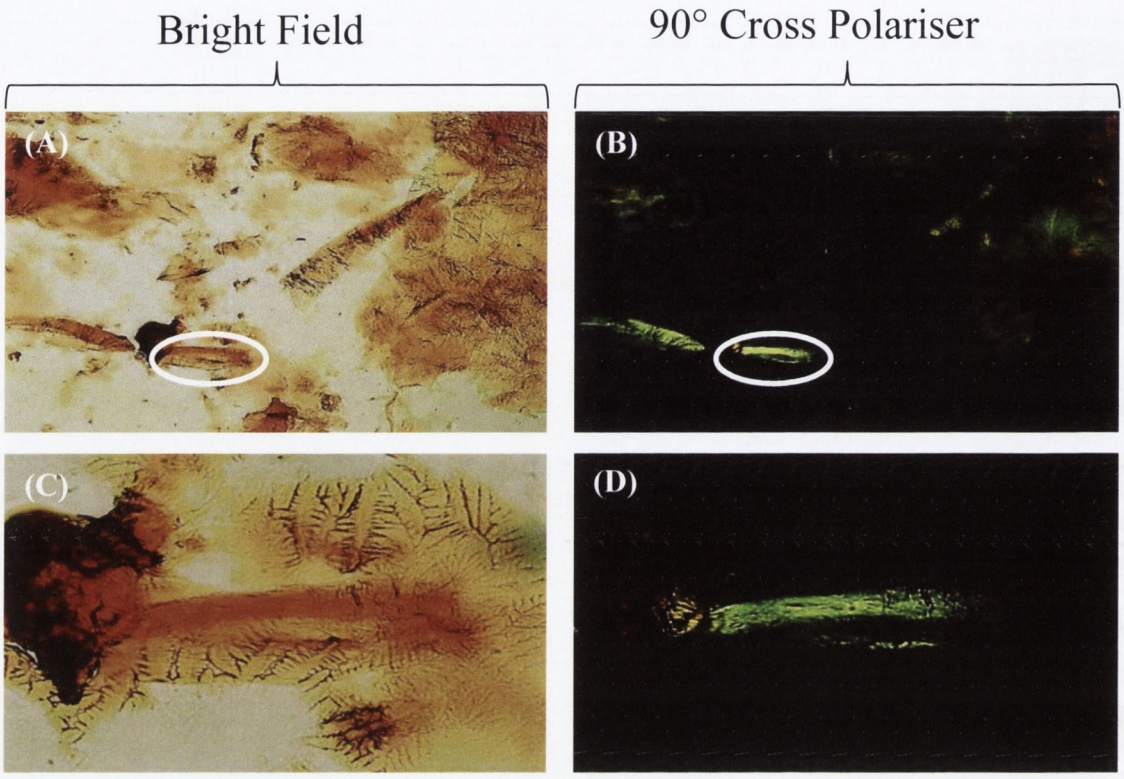

Figure 5.5 CR amyloid binding to amyloid fibril

Fibrillar deposits at X20 in the bright field and with 90°cross polarisers (A and B) displaying apple green birefringence. Large aggregate present (white circle) was visualised at higher magnification X40 (C-D).

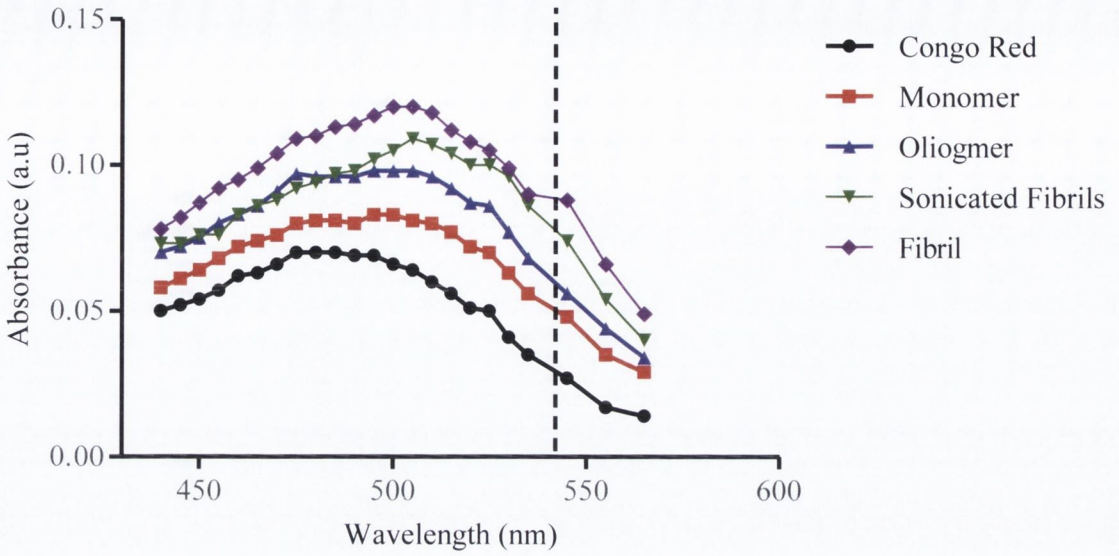

Figure 5.6 CR absorbance spectra of lysozyme separated fractions.

HEWL aggregated fractions were analysed using UV-Vis in the absorbance range of 425 nm to 600 nm. Any significant difference in signal at 540 nm (black dotted line) is considered to be associated with the presence of amyloid-like fibrils. This figure is representative of a single experiment.

5.2.3. AFM Imaging of Amyloid Aggregates

Having established that our separated fractions bind to specific dyes such as ThT and CR, we wanted to use microscopy to visualise the separated HEWL fractions to ensure that the isolation of aggregates had been achieved. In order to obtain high resolution images of isolated HEWL species AFM was used which allows for visualization on the nanometer scale. HEWL fractions were isolated after 21 days and immediately subjected to spin coating to disperse samples evenly on cleaved mica sheets as per section 2.17. Native HEWL displays no signs of aggregation while oligomers appear as small spherically dots on mica (Figure. 5.7 A and B). Sonicated fibrils appear larger in size than oligomers and are similarly round in shape (Figure. 5.7 C) which is as a result the sonicated procedure breaking down of the natural fibrillar structure through ultrasonic waves (Chatani *et al.*, 2009). The mature fibrillar sample displays long twisted fibrils which are far larger in size (over 1μm) (Figure. 5.7 D). The AFM projection of mature fibrils, along with corresponding z-height line sections on the body and twist of the periodic structure are shown (Figure 5.8 A-C). The alpha z-height line section was measured at 3.26 ± 0.65 nm while the beta z-height line section at the crossover was 4.23 ± 0.46 nm, showing that helical twists in the mature fibril are present. These results are evidence that fractions isolated through size-based fractionation using ultracentrifugation/ultrafiltration yield individual aggregate fractions which are characteristically different.

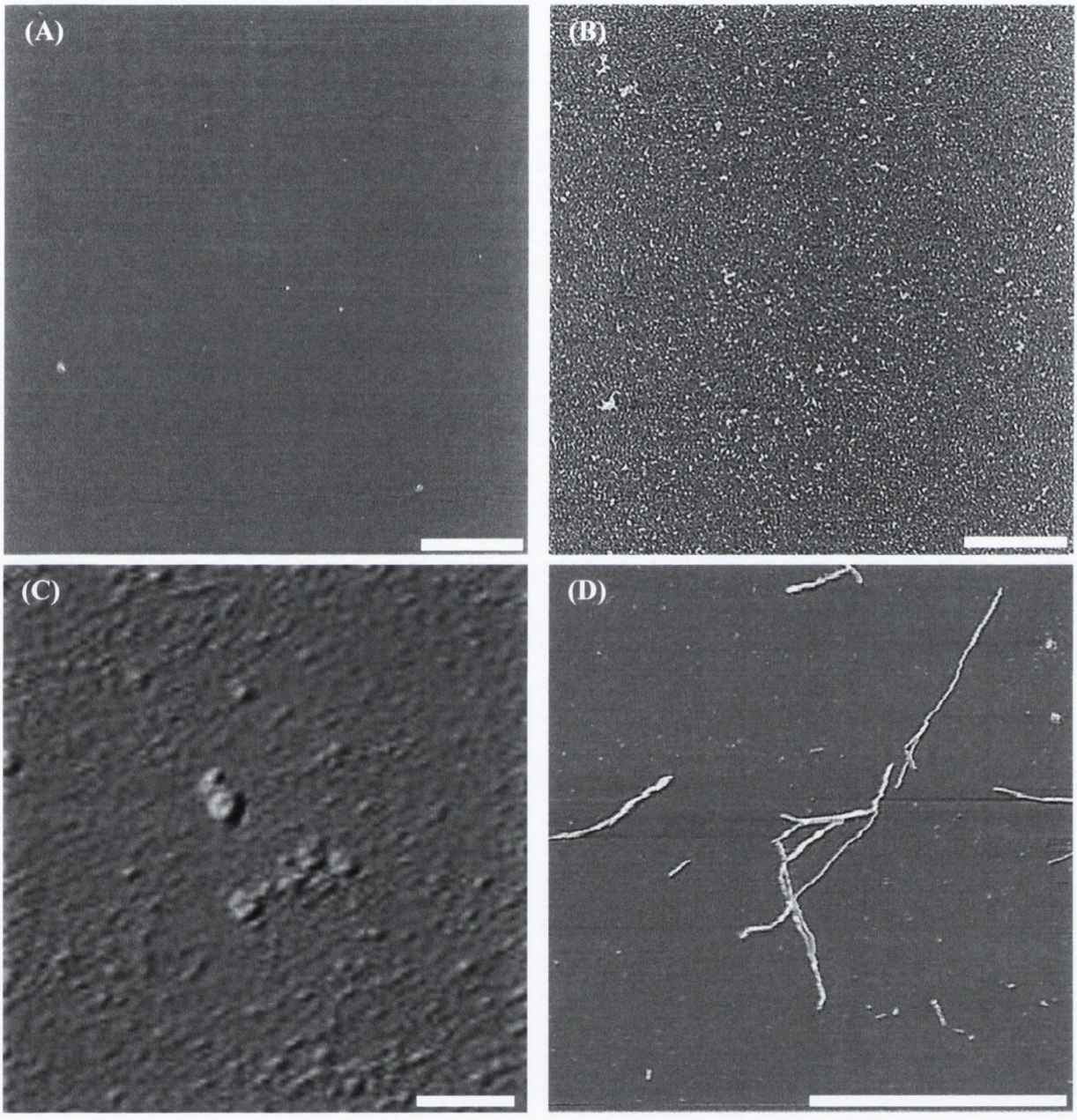

Figure 5.7 AFM of amyloid fibrils at different stages of aggregation

HEWL was visualised using AFM to confirm that separation had been achieved. Native HEWL (A), oligomers (B), sonicated fibrils (C), and mature fibrils (D) were spin coated onto mica discs prior to microscopy. This result is representative of three separate experiments. Scale bar; 1000 nm. Carried out with the assistance of Dr. Eoin McCarthy.

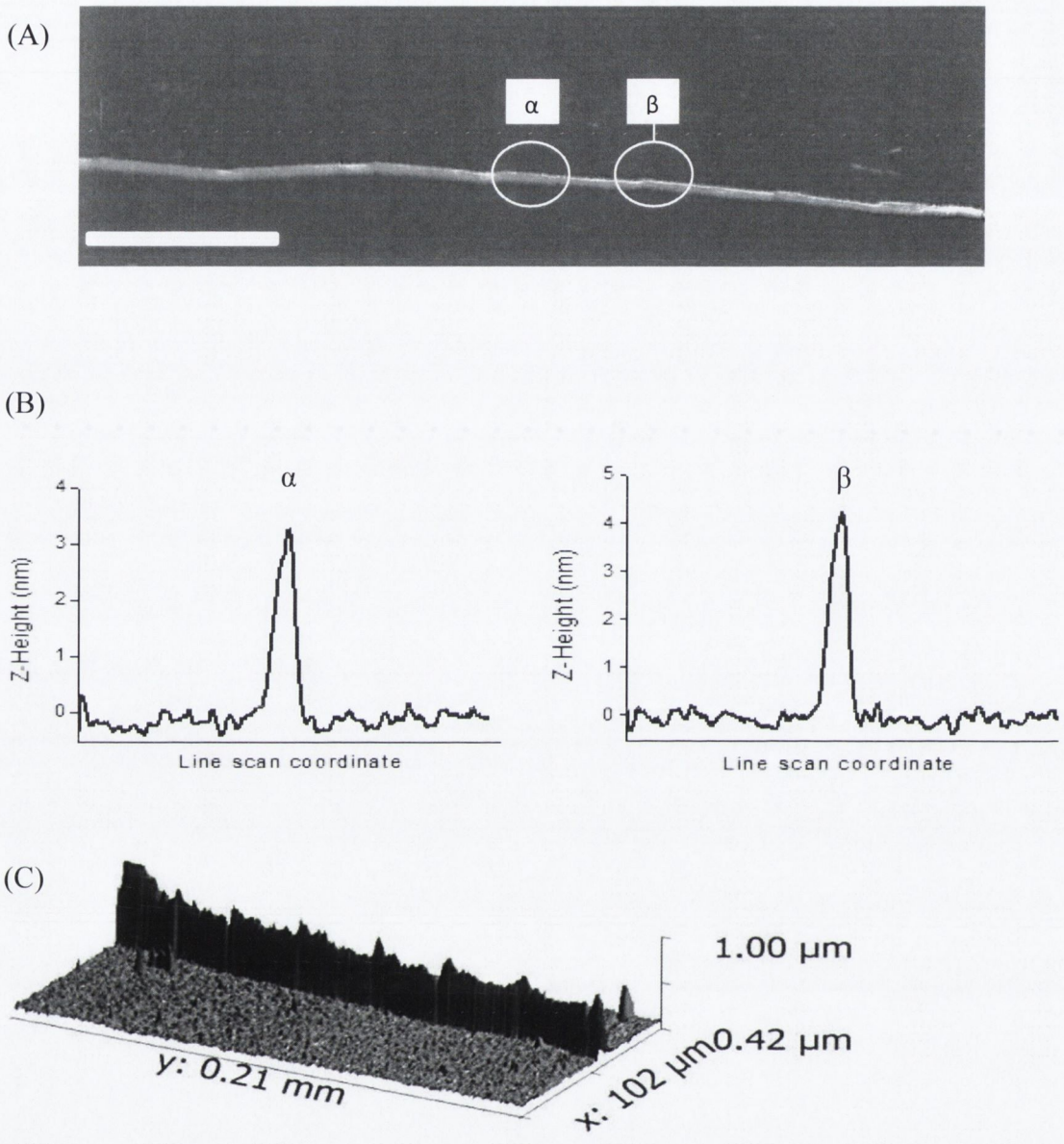

Figure 5.8 AFM imaging, z-height, and 3-dimensional representation of lysozyme fibril.

Mature amyloid fibrils displaying ribbon structure at increased magnification was captured using a 1 µm scan range (A). z-height line sections on areas of the fibril that are in between the twist of the periodic structure (α) and through the twist itself (β) (B). The ribbon structure visualized using the 3-D structural representation (C). Scale bar; 200 nm. Carried out with the assistance of Dr. Eoin McCarthy.

5.2.4. *TEM of Hen Egg White Lysozyme at Different States of Aggregation*

Following the detection and subsequent identification of amyloid fibrils via the use of CR, ThT, and AFM, the process of TEM can often be used as a final conformational test to determine the presence of true fibrils (Nilsson, 2004). TEM is a very powerful and useful tool for studying amyloid fibrils as it can provide evidence of the presence and structure of internalized fibrillar structures such as early aggregates, protofibrils, mature fibrils, and amorphous aggregates (Boniol *et al.*, 2012). As described in section 2.23. Isolated HEWL samples from day 21 were deposited onto carbon coated grids and stained with 2% uranyl acetate prior to visualisation. Due to the high concentration of the isolated protein samples, a 1 in 1,000 dilution was made (1 μM final concentration) prior to loading sample onto the carbon grids. Control HEWL (Figure 5.9 A) and oligomers (Figure 5.9 B) show no signs of aggregation when observed with TEM. Mature amyloid fibrils show extensive fibrillar growth with large amounts of long unbranched fibrillar structures present (Figure 5.9 D). Interestingly sonicated fibrils resemble fibrils, however they are much smaller in length (Figure 5.9 C). These results demonstrate that the separation and isolation method used by our group is a very effective procedure to separate individual aggregated fractions. Mature amyloid fibrils appear as an intertwined net of fibrillar structures while sonicated fibrils are still fibrillar in shape but much smaller in length.

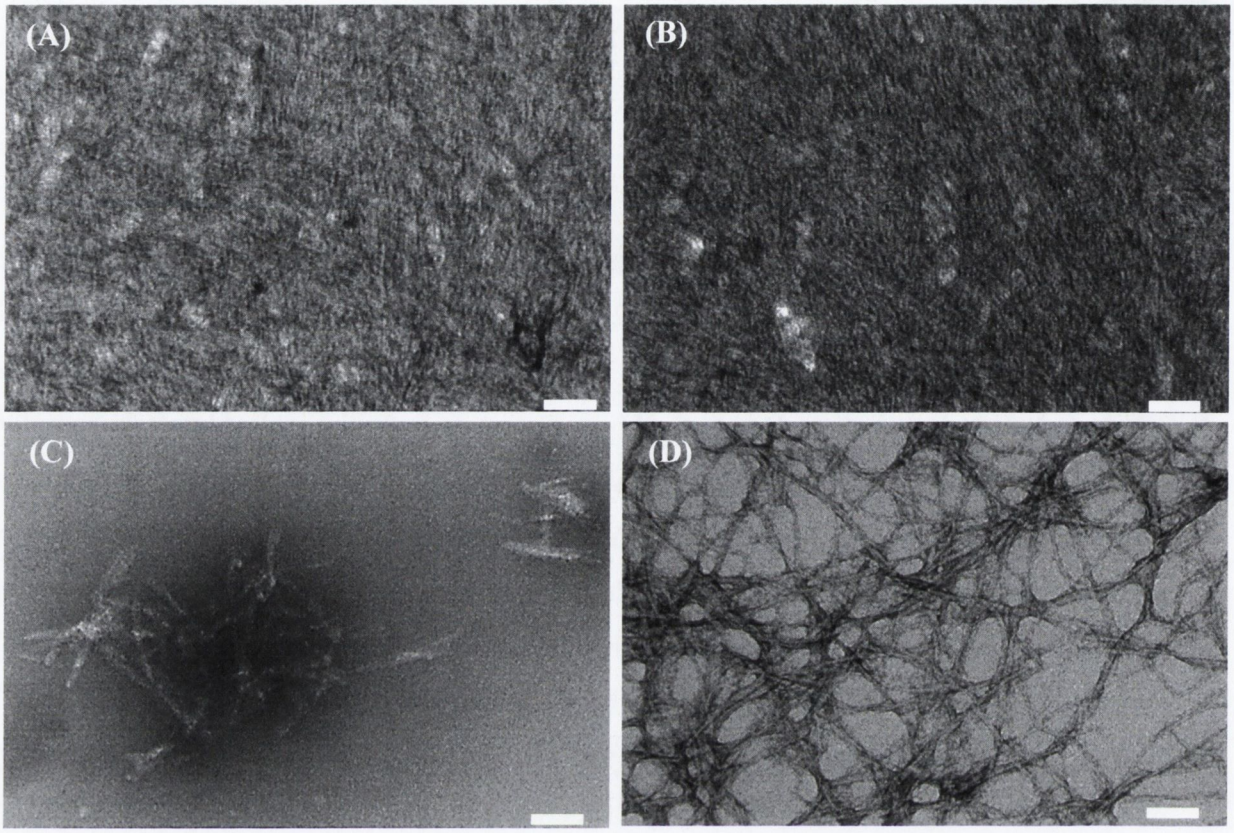

Figure 5.9 TEM of different stages of HEWL aggregation

The different stages of aggregation were examined using TEM. Native HEWL (A) and oligomers after day 21 (B) display no distinguishably aggregation. Sonicated samples (C) and mature fibrils (D) show the presence of smaller fibrillar structures. Fine fibrillar structure can be seen in the day 21 mature fibril sample. Scale bars: 100 nm.

5.2.5. Separated HEWL Aggregates are Cytotoxic to PC12$^{undiff/diff}$ Cells

Having established that the separation techniques used to isolate individual oligomers, sonicated fibrils, and mature fibrils in this experiment were successful we sought to probe the cytotoxic properties of these species. Isolated lysozyme species were added to both cell lines at concentrations in the range of 20 μM to 300 μM (Table 2.3 and Table 2.4) and incubated at 37°C for 24 h. The percentage cell death was calculated using Alamar Blue viability assay as per section 2.5. All samples tested were cytotoxic towards PC12 cells of undifferentiated and differentiated phenotypes. This allowed for the investigation of whether a differentiated phenotype conferred a level of cytotoxic resistance against HEWL fractions. In both cell types oligomers were the most toxic and resulted in the highest level of cell death. The most non-toxic fraction in both cells was the mature HEWL fibrils. Sonicated fibrils displayed higher levels of toxicity than mature fibrils but were not as injurious as oligomers (Fig 5.10 A and B). In accordance with Table 5.1 PC12^{diff} cells incubated with oligomers yield LC_{50} values of 44μM and are almost twice as toxic as sonicated fibrils which have an LC_{50} value of ~ 78 μM. Fibrils are even less toxic than these samples with an LC_{50} value of ~ 92 μM. The LC_{50} value for PC12^{undiff} cells treated with oligomers (~ 28 μM) shows that these cells are more susceptible to toxic oligomeric fragments, when compared against PC12^{diff} cells. LC_{50} values for mature amyloid fibrils (~ 94 μM) and sonicated fibrils (~ 68 μM) are similar to those observed in differentiated cells, and show no discernible difference in susceptibility. Cells treated with monomers showed no signs of cell death. The results demonstrate that the aggregated HEWL fractions generated in this experiment were cytotoxic towards both tumour and healthy neuronal cells. In addition, oligomers showed the highest level of toxicity in both cell lines, and were particularly harmful towards the PC12^{undiff} cells suggesting that the tumour morphology of this cell type makes it more susceptible to injury.

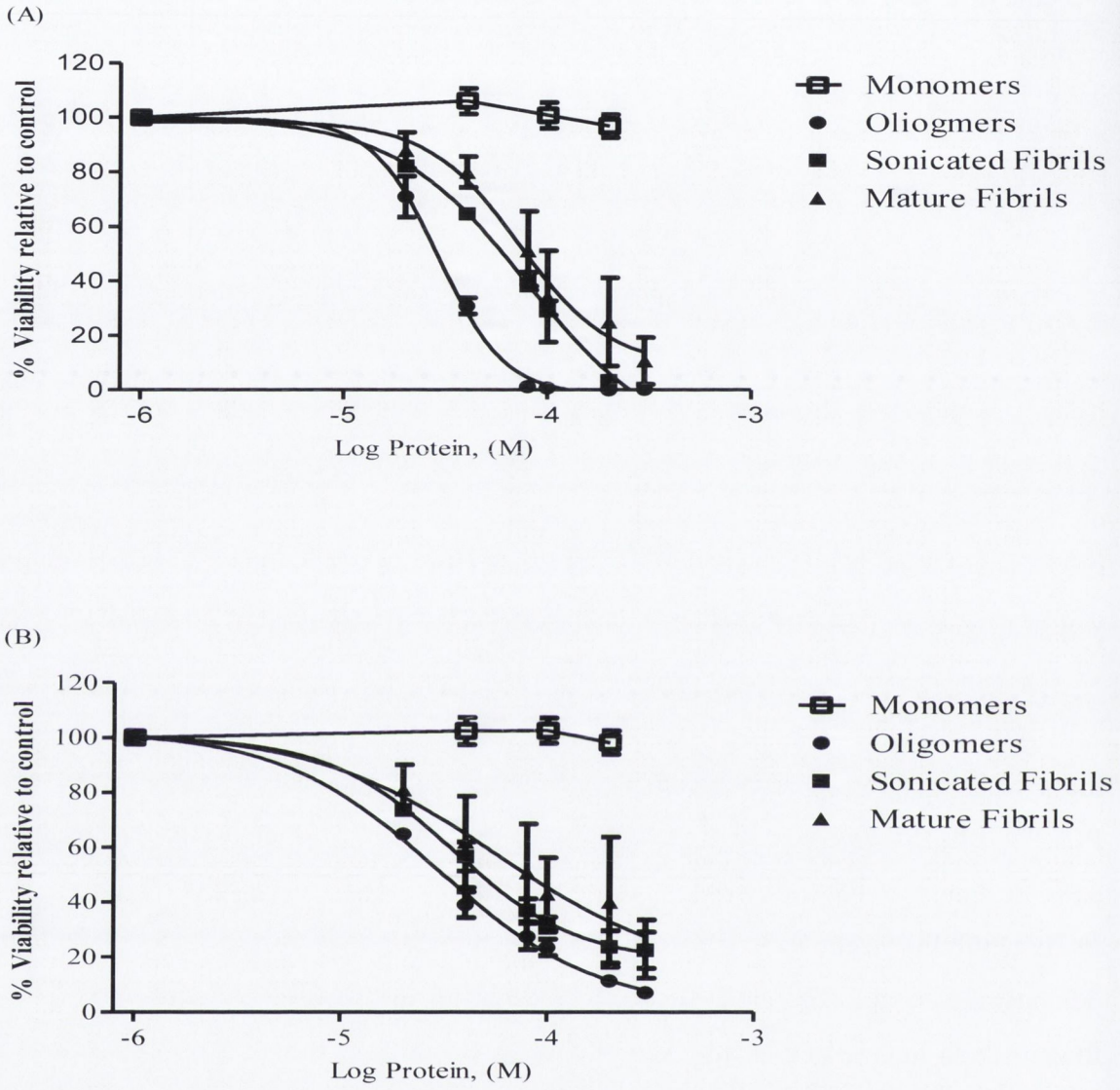

Figure 5.10 Viability results for PC12 cell lines treated with HEWL fractions

Undifferentiated (A) and differentiated (B) PC12 cells were exposed to varying concentrations of prefibrillar, and fibrillar aggregates. Percentage cell viability compared to non-treated control is displayed on the *y*-axis, HEWL concentrations are shown on the *x*-axis. The values (displayed in log) are the means of three experiments with the error bar indicating SEM and were calculated using GraphPad.

5.2.6. Oligomers and Fibrils are Cytotoxic to the Human Osteosarcoma Cell Line U2OS.

In addition to PC12 cells of undifferentiated and differentiated phenotypes, the human osteosarcoma cell line U2OS was also subjected to HEWL oligomers and fibrils to determine if the injurious nature of these species was retained to PC12 alone. Using an identical protocol to that used with PC12 cells, U2OS were treated with increasing concentrations of HEWL samples in the range of 20 μM to 300 μM (Table 2.3) and incubated at 37°C for 24 h. The percentage cell death was calculated using Alamar Blue viability assay. All fractions generated displayed nearly identical viability curves when used to treat U2OS cells, with no discernible difference noticeable. LC_{50} values for oligomers (23 μM), sonicated fibrils (24 μM) and mature amyloid fibrils (24 μM) were all remarkable similar suggesting that all fractions are cytotoxic towards U2OS cells (Table 5.1). Interestingly the level of fibrillar cytotoxity was higher than that observed with PC12 $^{undiff/diff}$ cells suggesting that U2OS are susceptible to all forms of HEWL aggregates.

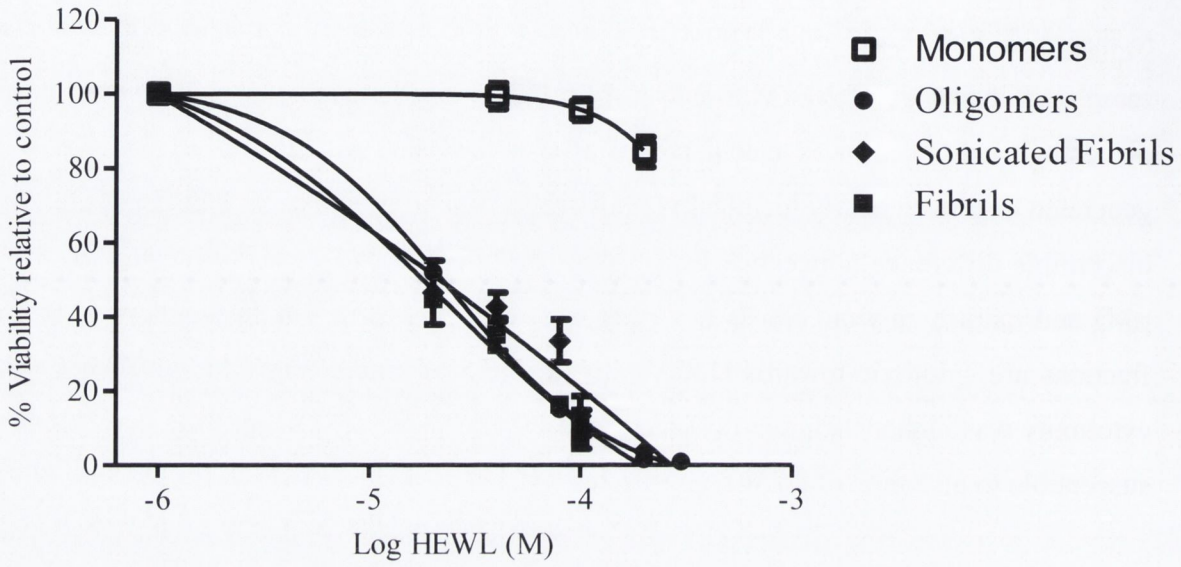

Figure 5.11 U2OS cells treated with HEWL separated fractions

U2OS cells were treated with ultracentrifuged/ultrafiltrated fractions of amyloid fibrils and pre-fibrillar aggregates and incubated for 24 h at 37°C. Cell viability was determined using the Alamar Blue assay. The values (given in log) are the means of three experiments with the error bar indicating SEM and were calculated using GraphPad.

Table 5.1 LC_{50} values (μM) of amyloid oligomers, fibrils, and sonicated fibrils on PC $12^{undiff/diff}$ cells.

LC_{50} values are means ± SD of three independent experiments carried out.

Cell Line	Oligomers (LC_{50} μM)	Sonicated Fibrils (LC_{50} μM)	Fibrils (LC_{50} μM)
$PC12^{undiff}$	28 ± 0.5	68 ± 1.7	94 ± 5.5
$PC12^{diff}$	44 ± 1.1	78 ± 17.2	92 ± 10.2
U2OS	23 ± 0.5	24	24 ± 1.8

5.2.7. HEWL Oligomers, Sonicated Fibrils, and Mature Fibrils Induce Cellular Death via Secondary Necrotic and Apoptotic Pathways

Having established that HEWL pH2 incubated at 65°C for 21 days can be separated into individual and characteristically different species, and that these species cause cell death in $PC12^{undiff/diff}$ cells, we sought to identify the mechanism of cell death induced by these protein aggregates. In doing so we hoped to determine whether HEWL oligomers, sonicated fibrils, and fibrils activated separate cell death mechanisms in tumour and healthy cells. To distinguish between apoptotic and necrotic/non apoptotic cell death, treated cells were stained for Annexin V-FITC (apoptosis) and PI (necrosis/non-apoptotic cell death). Both $PC12^{undiff}$ and $PC12^{diff}$ cells undergoing death were visualised using flow cytometry as per section 2.15. Cells were incubated with 40 μM of HEWL fractions and left for 24 h. From this experiment it is evident that fibrillar structures and oligomers induce high levels of cell death within $PC12^{undiff}$ and $PC12^{diff}$ cells. In $PC12^{undiff}$ cells (Figure 5.12) oligomers induce a primarily apoptotic cell death pathway (65.2%) when compared against the control (0.5%). Alternatively, mature fibrils show high levels of staining for PI and Annexin V (46.3%) while staining less for apoptosis only (37.4%) indicating secondary necrosis, late apoptosis. $PC12^{diff}$ cells (Figure 5.13) show a similar pattern of cell death. Oligomeric treated cells show a propensity for binding Annexin V-FITC (31%) whilst fibrillar treated $PC12^{diff}$ cells showed increased Annexin V/PI double positive staining (44%) when compared to control. $PC12^{undiff/diff}$ cells were also analysed using sonicated fibrils. $PC12^{undiff}$ cells showed increased staining for Annexin V (58.2%) whilst $PC12^{diff}$ cells showed approximately equal staining for Annexin V and dual Annexin V/PI (10.9% and 19.5% respectively). These results suggest that oligomeric treated cells die through an apoptotic cell death pathway in both cell lines. Fibrils induce a secondary necrotic, late apoptotic death pathway. Sonicated fibrils induce similar amounts of apoptosis and late apoptosis in $PC12^{diff}$ cells, while inducing early apoptosis in the undifferentiated type.

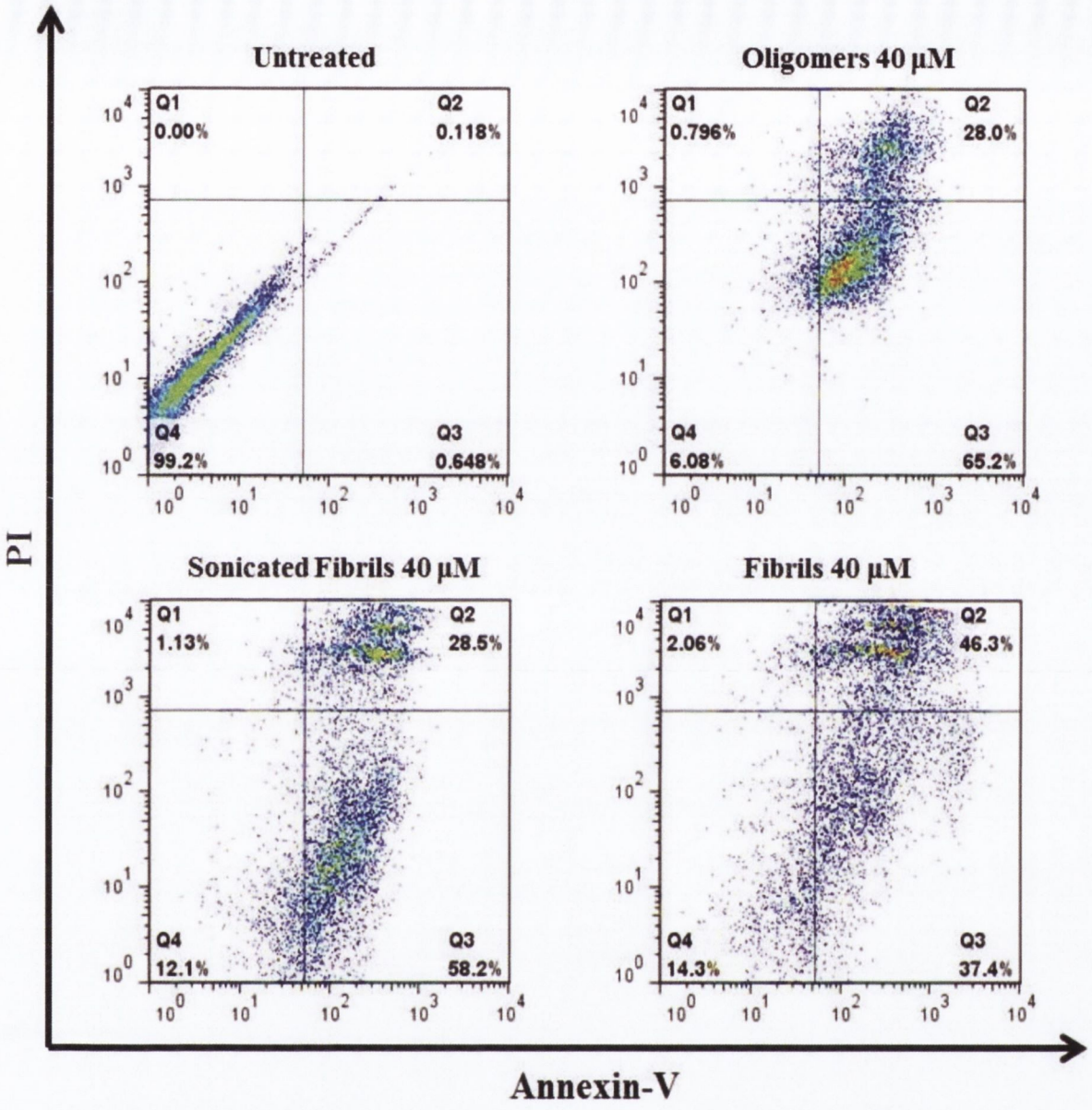

Figure 5.12 Death pathway of PC12^{undiff} cells treated with HEWL aggregates was assessed using Annexin V-FITC/PI and flow cytometry

Cells were treated with HEWL fractions for 24 h and then stained for the presence of both fluorescent markers. X-axis indicates the numbers of Annexin V-FITC-stained cells. Y-axis indicates the numbers of PI-strained cells. Cells were incubated with 40 µM of oligomers, sonicated fibrils, and mature fibrils. All samples were gated according to untreated cells, and compensated using untreated cells stained for both dyes. Data is representative three similar experiments.

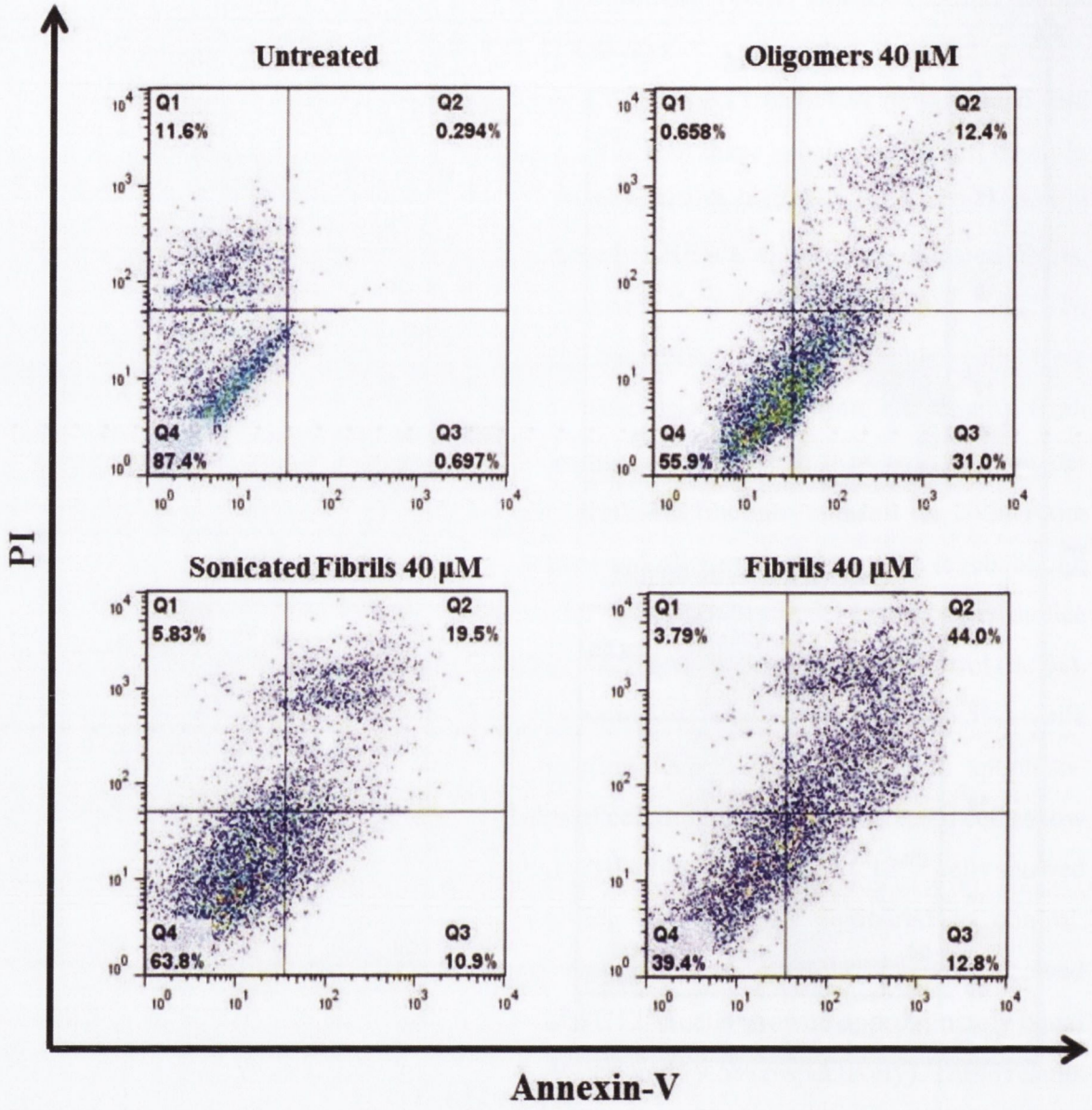

Figure 5.13 Death pathway of PC12^{diff} cells treated with HEWL aggregates was assessed using Annexin V-FITC/PI and flow cytometry

Cells were treated with HEWL fractions for 24 h and then stained for the presence of both fluorescent markers. X-axis indicates the numbers of Annexin V-FITC-stained cells. Y-axis indicates the numbers of PI-strained cells. Cells were incubated with 40 µM of oligomers, sonicated fibrils, and mature fibrils. All samples were gated according to untreated cells, and compensated using untreated cells stained for both dyes. Data is representative three similar experiments.

5.2.8. *PARP Cleavage of PC12$^{undiff/diff}$ Cells Treated with HEWL Fractions Suggests that cells die via an Apoptotic Mechanism*

In addition to flow cytometry which demonstrated that PC12$^{undiff/diff}$ cells may activate an apoptotic cell death mechanism when treated with HEWL aggregates, a further method was used to confirm this result. In response to suicide caspases mentioned previously, PARP produces a specific proteolytic cleavage fragment which can be utilised as a biomarker for cell death (Duriez and Shah, 1997). In order to further determine the mechanism of cellular death in response to treatment with HEWL samples PC12$^{undiff/diff}$ cells were treated with 30 μM of native lysozyme, monomers, oligomers, sonicated fibrils, and mature amyloid fibrils and a Western blot was preformed probing for PARP cleavage on a 12% gel. Samples were loaded at equal protein concentrations (20 μg) as seen from the actin loading control. The uncleaved PARP can be seen at bands of 116 kDa on the gel while the cleaved sample can be observed at 89 kDa. In both cell lines native HEWL and the monomeric fraction showed no apoptotic death. Sonicated fibrils and mature fibrils elicited a slight apoptotic response although oligomers appeared to induce the highest level of apoptotic cell death (Figure 5.14 A). These results suggest that the treatment PC12$^{undiff/diff}$ cells with HEWL isolated oligomers, sonicated fibrils and mature results in the cleavage of the apoptotic marker protein PARP, indicating that apoptosis has been activated in response to these proteinaceous fractions which is in agreement with our flow cytometry data.

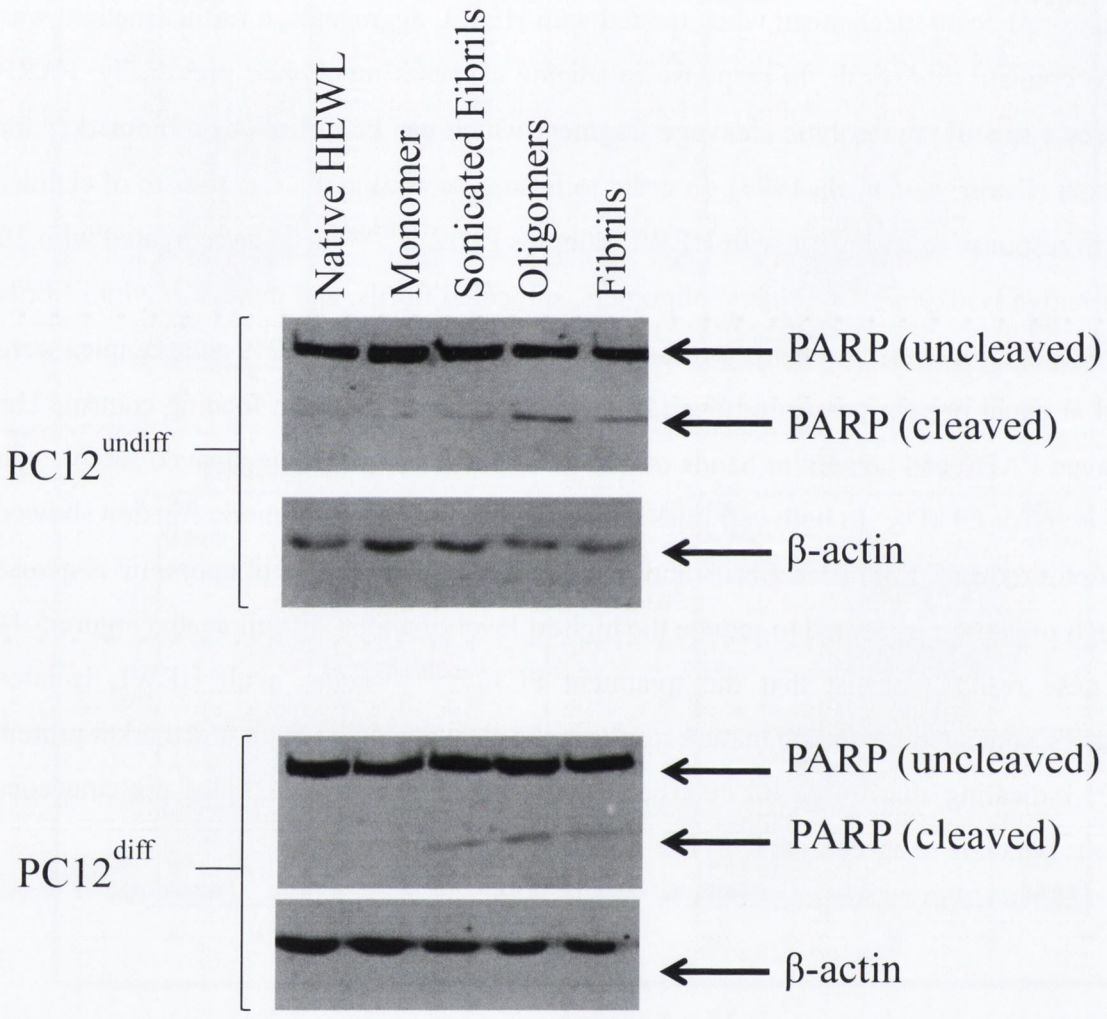

Figure 5.14 Western blot analysis of PARP cleavage in PC12$^{undiff/diff}$ cells

PC12$^{undiff/diff}$ cells were treated with different lysozyme species and analysed for apoptotic death via the identification of cleaved PARP. Cells were treated with 30 μM of separate HEWL fractions and left for 24 h to achieve sufficient cell death. Shown are the full-length PARP (116 kDa) and the smaller fragment (89 kDa) of apoptotically cleaved products, as well as β-actin used as a loading control. Data are representative of two similar experiments.

5.2.9. TEM Imaging of U2OS Cells Treated With HEWL Oligomers and Fibrils

Cell death in U2OS cells was analysed using TEM. TEM is a versatile tool in biology for imaging cellular structures on the nanoscale. We used TEM for the imaging of fibrillar and oligomer treated U2OS cells to observe any changes that may have occurred either externally or internally within the cell. U2OS cells provide a useful cell line for analysing cell death with TEM as their large size allows for more detailed images. Samples were prepared as outlined in section 2.23. Both oligomeric and fibrillar species were isolated fresh immediately prior to treatment. Both samples exhibited signs of apoptotic death such as membrane blebbing, apoptotic body formation, cytoplasmic vacuolization, and nuclear fragmentation, shown in Figures 5.15 and 5.16. These results suggest that U2OS die through apoptosis when treated with HEWL oligomers and fibrils.

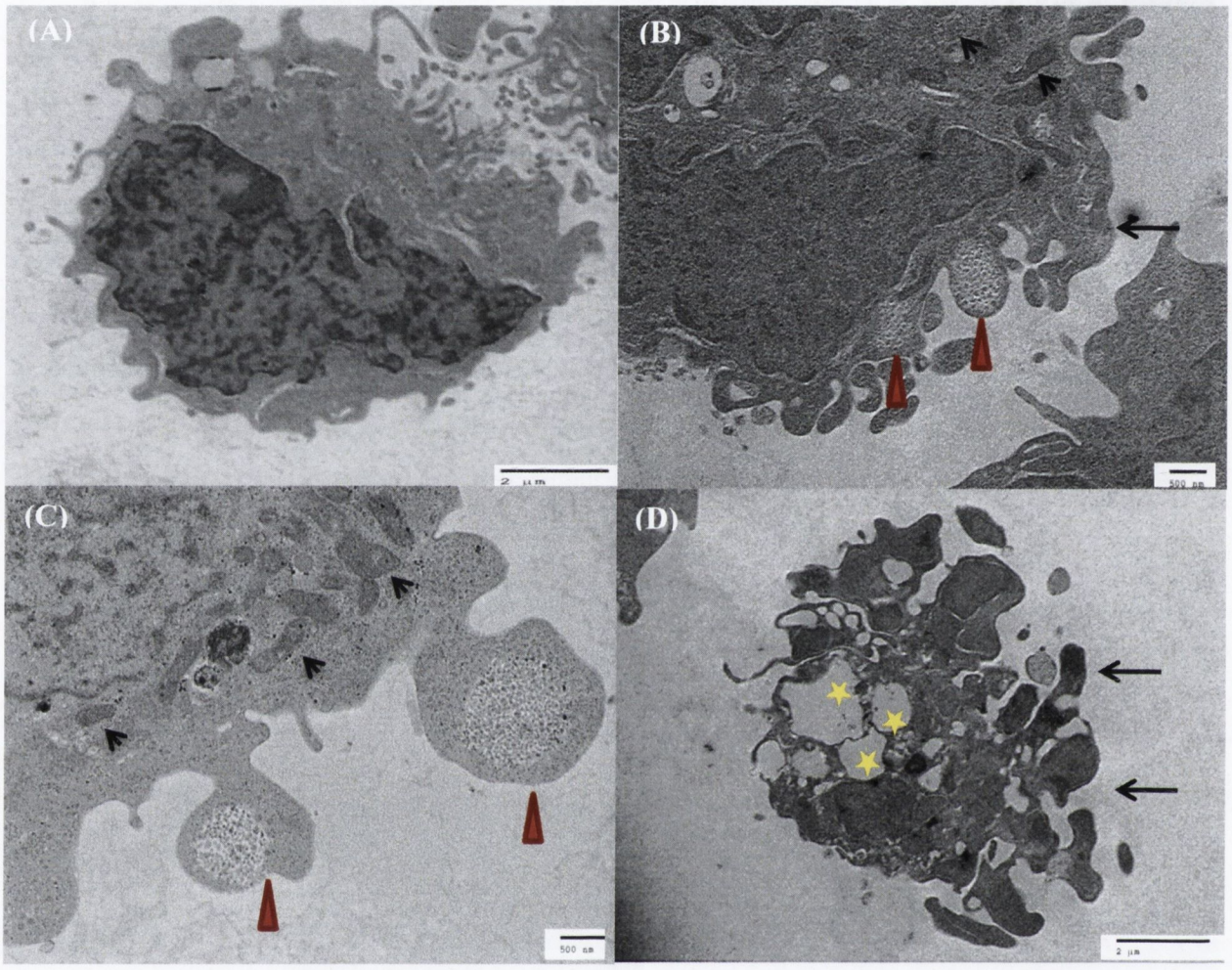

Figure 5.15 TEM of U2OS cells treated with oligomers

Cells were treated with 30 μM oligomer fractions. Non-treated U2OS cells (X1500) (A). Membrane blebbing (red arrow heads) can be identified in U2OS cells magnified X5000 (B and C). Also visible are intact mitochondria indicated by black arrow heads (B and C). U2OS cell at X1500 can be seen displaying cell fragmentation, extracellular apoptotic bodies (black arrows), cytosolic vacuolization (yellow stars) (D). Data is representative of 2 separate experiments.

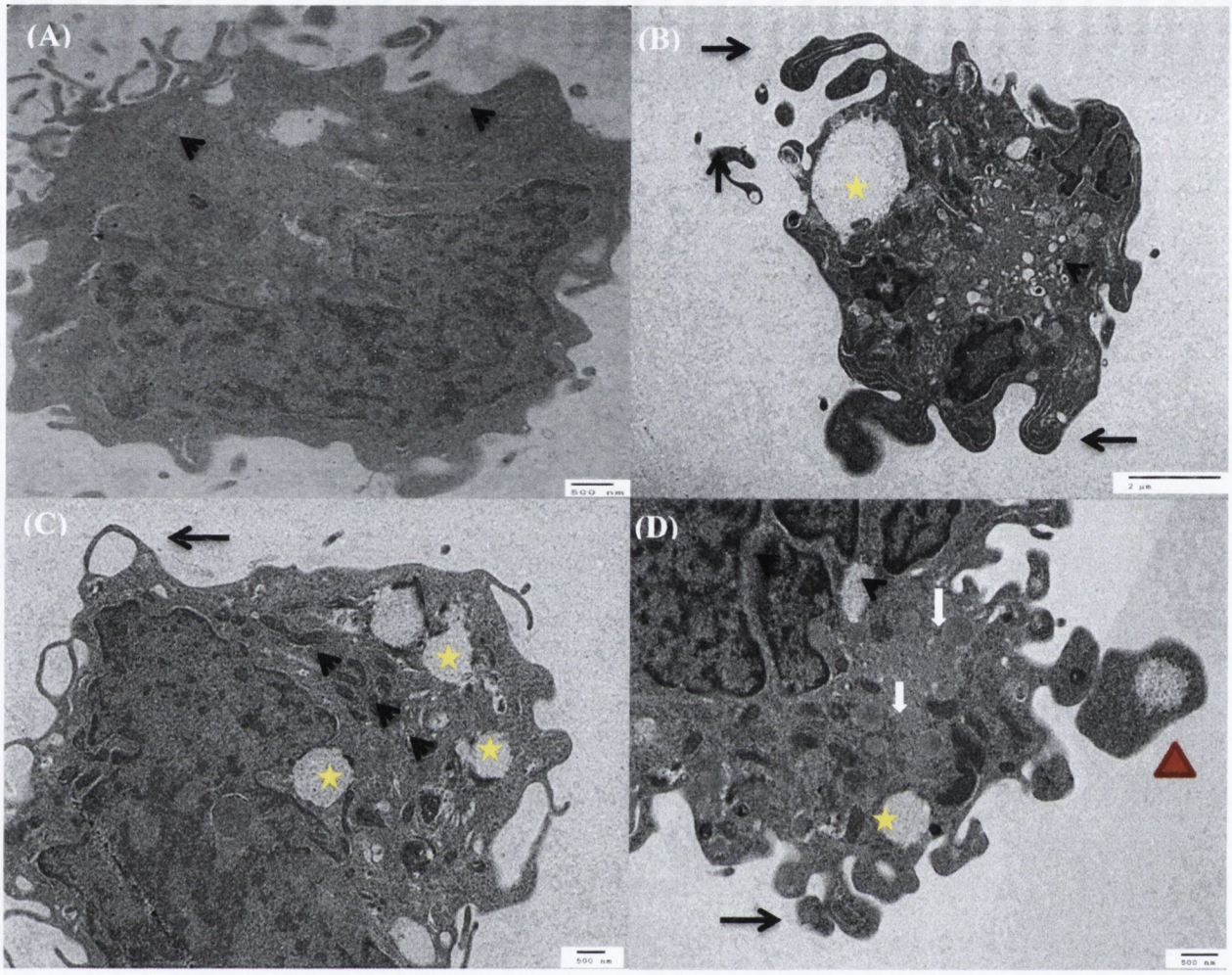

Figure 5.16 TEM of U2OS cells treated with mature fibrils

Cells were treated with 30 μM HEWL fibrils. Non-treated U2OS cells with regular nucleus and mitochondria (black arrow heads) (X1500) (A).U2OS cell at X1500 displaying apoptotic morphology, extracellular apoptotic bodies (black arrows), mitochondria (black arrow head), and cytosolic vacuolization (yellow star) (B). Intact mitochondria (black arrow head), and extracellular apoptotic body (black arrow), and cytosolic vacuolization (yellow star) at X2500 (C). U2OS at X3000 displaying membrane blebbing (red arrow head), internal (white arrow) and external (black arrow) apoptotic bodies, as well as intact mitochondria (black arrow head) (D). Data is representative of 2 separate experiments

5.2.10. HEWL Oligomers but not Sonicated or Mature Fibrillar Fragments Inhibit Hippocampal LTP in vivo

Having examined the structure and aggregated state of the separated HEWL fractions and tested their cytotoxic mechanisms *in vitro*, we sought to examine their mechanistic properties *in vivo*. *In vitro* HEWL oligomers, sonicated fibrils, and mature fibrils have been tested on the neuronal cell line PC12. From this we saw that these fractions from normally innocuous HEWL were cytotoxic. We translated what we have discovered *in vitro* this neuronal cell line to an *in vivo* neuronal cell model. Using our isolated protein aggregates, we examined their ability to inhibit LTP, a leading model for the examination of memory and learning, in rats. The mature fibrils were sonicated and centrifuged in order to isolate out pure amyloid sonicated fibrils as mature fibrils could not diffuse across the hippocampal parenchyma from the injection site. HEWL oligomers and sonicated fibrils were applied to the rat hippocampus and a high frequency stimulus was set to imitate an action potential as described in section 2.19. Figure 5.17 shows that in anaesthetized control rats, HFS induced robust and long lasting potentiation (>3 h) of excitatory synaptic transmission in the Cornu Ammonis 1 (CA1) area of the hippocampus after intracerebroventricular (i.c.v) injection of either 15 μl of distilled water (n=3) or 1 mM of non-aggregated HEWL (15 nmol, n=4) (combined group, 151±15%, n=7, $p<0.05$, compared with pre-HFS baseline). In contrast, injection of the same volume of HEWL oligomers (350 μM) completely inhibited LTP at 3 h post HFS (5.25 nmol, 99±6%, n=5, $p>0.05$, compared with baseline, $p<0.05$, compared with control LTP) without affecting baseline synaptic transmission (105±13%, n=3, $p>0.05$, compared with pre-injection recording, data not shown). Interestingly, soluble fibrillar fragments generated by sonication of mature fibrils failed to inhibit LTP even when a much higher dose was injected (1.5 mM in 15 μl, 22.5 nmol, 137±10%, n=4, $p>0.05$. compared with control LTP). Our results show that treatment with HEWL oligomers dramatically inhibited LTP activity when compared to sonicated fibrils. Oligomers generated from a completely innocuous protein can inhibit LTP in rats and suggest that a generic mechanism is employed by all oligomeric species to impair learning in degenerative diseases.

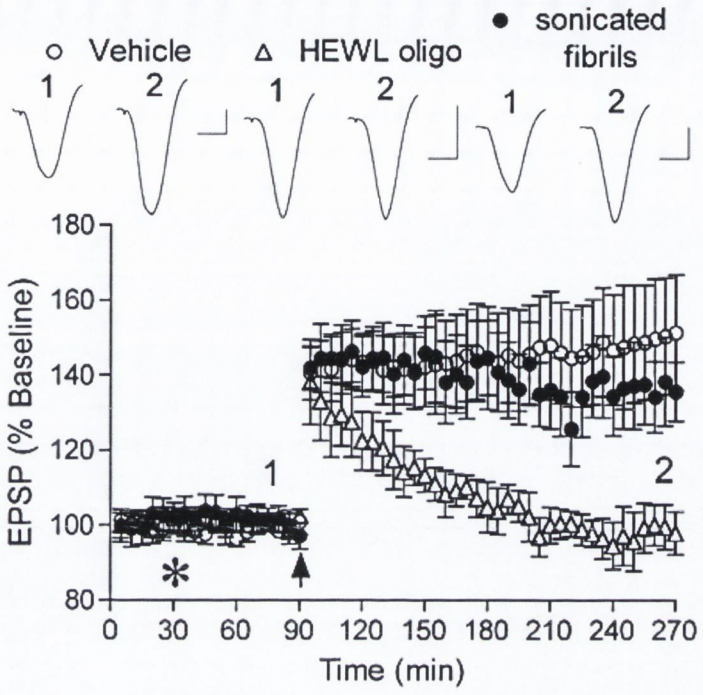

Figure 5.17 HEWL oligomers but not fibrillar fragments inhibit hippocampal LTP *in vivo*

Injection via i.c.v of vehicle (asterisk) or non-aggregated HEWL 1 h before high frequency conditioning stimulation (arrow) did not affect LTP (open circles). In contrast, animals injected with HEWL oligomers were unable to maintain LTP (open triangles). Injection (i.c.v) of sonicated mature fibrils had no effect on LTP (closed circles). HFS was administered at 90 mins (1) after which the LTP response was measured unitl 270 min (2). Insets show representative EPSP traces at the time indicated. Horizontal bar, 10 ms; vertical bar, 1 mV. These results are the means (control n=3/ sonicated fibril n=4/ oligomers n=5) the experiments. Error bars, ± SEM. The LTP examination was carried out by Dr. Igor Klyubin.

5.3. Discussion

The current study demonstrates that HEWL amyloid fibrils, sonicated fibrils, and oligomers, judiciously isolated via ultracentrifugation and ultrafiltration, are highly toxic to cultured PC12 cells of both differentiated and undifferentiated states and that their cell death responses are specific to each. In addition to this U2OS cells are also highly vulnerable to the cytotoxic effects of these amyloid fractions. Prefibrillar soluble aggregates and sonicated/mature fibrils displayed cytotoxicity towards rat PC12 cells, with differentiated cells showing an enhanced level of resistance against oligomers. These fractions also induce differing cell death pathways in $PC12^{undiff/diff}$ cells with oligomers activating an apoptotic response while fibrils generate secondary necrotic death. Interestingly in rats, HEWL oligomers inhibited LTP a leading model for the examination of memory and learning while sonicated fibrils had no effect. This is the first time HEWL has been shown to have any effect on LTP and it is also the first instance that an innocuous protein has been shown to interfere with this event *in vivo*.

5.3.1. Native HEWL can be Engineered into Distinct Amyloid Fractions

The prolonged incubation of native HEWL protein at 65° in pH2 conditions resulted in the formation of oligomers, which preceded the conversion of mature fibrils, consistent with current knowledge on amyloid formation (Gharibyan *et al.*, 2007, Mossuto *et al.*, 2010). When compared with the oligomers, the mature HEWL fibrils isolated in this experiment showed all the hallmark spectroscopic signatures of amyloid fibril development such as increased ThT binding, a shift in CR absorbance, and relatively more pronounced CR birefringence. Fibrils also appear to have more hydrophobic regions in contrast to sonicated fibrils and oligomers when measured using ANS. Fibrils displayed a shift towards the blue spectrum suggesting that the transition from native HEWL protein towards fibrillar aggregate coincides with a change in the protein environment, whereby the protein loses its native 3-D structural packing and increases its exposure of its hydrophobic residues. This work compliments what has been shown in other experiments using ANS and protein aggregates (Finke and Jennings, 2001, Hawe *et al.*, 2008).

Having established that our isolated fractions showed characteristic binding patterns to amyloid specific dyes we next sought to visualize them using the microscopic techniques TEM and AFM. For TEM all fractions separated were distinctly different upon examination after negative staining. Mature amyloid fibrils were characteristically large, linear, and

twisted in shape and size, and composed of a dense matrix of intertwining fibrillar strands. Sonicated fibrils appear much shorter in length and do not form the dense mesh that was seen with the mature sample but still retain a fibrillar structure and shape. The reduction in size but the retention of fibrillar shape that is seen after sonication is in keeping with previous knowledge (Volpicelli-Daley *et al.*, 2014). Oligomer samples did not yield a clear image which could be due to the small size or perhaps the concentration of the oligomer sample was too concentrated which is why it is hard to make out any distinguishable structures.

With AFM, mature fibrils appear to be long single stranded filaments displaying a characteristic left handed 'twist' when visualized using increased magnification. It should be noted that this conformation may also represent proteofibrillar fractions which have formed together and more intensive AFM would be needed to truly distinguish between the two. In contrast, the oligomeric fractions appeared as circular or semi-circular spots which are a characteristic feature (Lee *et al.*, 2011a). In agreement with other studies (Chatani *et al.*, 2009) sonicated samples are less linear in shape and do not display the long characteristic string like shape proving that no further elongation of the aggregate was achieved and that the size-based purification procedure was successful. TEM is a more sensitive method for visualizing smaller objects and the lack of definitive features observed in sonicated fibrils with AFM could be a result of this difference.

These results demonstrate that our modified method for isolating HEWL oligomers and fibrils was successful in separating these fractions. Although the conversion of HEWL into an amyloid fibril sample is not novel (Krebs *et al.*, 2000), the significance of this work was in trying to isolate pure oligomeric, and fibrillar fractions from the resulting mixture. We propose that our method of generating and purifying different amyloid aggregates could be used to purify aggregates from any protein and may prove beneficial for groups looking to examine the mechanisms of particular species.

5.3.2. HEWL Aggregates Induce Cell Death

Our study demonstrates that separated HEWL oligomers, sonicated fibrils, and mature fibrils display toxicity towards both $PC12^{undiff/diff}$ cells *in vitro*. All amyloid fractions tested were cytotoxic to cells, with oligomers resulting in the highest level cell death in both lines. Furthermore, the morphological conformation of the cell appears to influence cell

susceptibility with tumour cells being more sensitive towards HEWL oligomers. This data suggests that although soluble oligomers are damaging to cells, they may not be the only toxic component involved in neurodegenerative disease, and that fibrils, which are increasingly thought to possess little cytotoxic capabilities (Vieira *et al.*, 2007), may in some cases be toxic. This theory is further strengthened as oligomeric and fibrillar fractions were also toxic towards U2OS cells. Oligomers, sonicated fibrils, and mature fibrils all resulted in similar LC_{50} values suggesting that the aggregated state of the protein had no effect on its ability to induce cell death in this cell line. In addition, sonicated fibrils were more toxic than mature fibrils, but less toxic than oligomers in PC12 cells suggesting, that sonication of fibrils increase their toxicity which in in accordance with previous studies (Xue et al., 2010). Both AFM and TEM demonstrate that sonicated samples are smaller in size than mature fibrils, and yet considerably larger than the oligomer which indicates that there is a direct correlation between the physical size and ability to induce cell death.

There is considerable debate regarding the true pathogenic role of oligomers and mature fibrils in these neurodegenerative diseases. Our work shows that oligomers are toxic towards cells which is universally known (Bucciantini *et al.*, 2002), however we have shown that fibrils possess cytotoxic capabilities which is in contrast to previous experiments claiming these aggregates may not be toxic at all (Giannakopoulos *et al.*, 2003, Reixach *et al.*, 2004, Vieira *et al.*, 2007). For PC12 cells the protective role displayed by cell differentiation was consistent with earlier work examining cell susceptibility towards amyloid injury in differentiated and undifferentiated human neurotypic SH-SY5Y cells (Cecchi et al., 2008). A possible reason for this is that oligomers promote Ca^{2+} dysregulation and membrane disruption which could be a factor as $PC12^{undiff}$ cells have higher levels of intracellular Ca^{2+} (Ondrias et al., 2011), however examinations into these various factors was beyond the scope of this project but could be looked into in the future.

It should be noted that although our fibril samples display toxicity towards U2OS and $PC12^{undiff/diff}$ cells we cannot rule out the possibility that breakage of fibrils is occurring at this point which can contribute to cell death. In forming a fibril, oligomers elongate to form full length protofiliments however breakages often occur, leading to the formation of smaller protofiliments that are similar to oligomers and highly toxic (Kahler *et al.*, 2013). Despite

this, our mechanism of isolation has dramatically reduced the amount of broken protofiliments present, as seen from our AFM and TEM.

5.3.3. HEWL Oligomers, Sonicated Fibrils and Mature Fibrils Induce Cell Death via Apoptotic and Secondary Necrotic Pathways

Using dual staining, we have shown that oligomer treated $PC12^{undiff/diff}$ cells display increased Annexin V staining indicative of apoptosis while cells treated with mature fibrils produce Annexin V/PI double positive staining, suggesting secondary necrotic/late apoptotic death. Sonicated fibrils used to treat $PC12^{undiff}$ cells showed increased apoptotic staining, whereas the $PC12^{diff}$ cells showed relatively equal amounts of staining for both apoptosis and secondary necrosis, suggesting that these cells are entering the later stages of the apoptotic cycle of cell death. Furthermore, PC12 $^{undiff//diff}$ cells exhibited cleaved PARP, an apoptotic indicator, when treated with oligomers, sonicated fibrils, and mature fibrils. Both monomeric and native treated cells show no signs of apoptotic death which is supported by the evidence that neither of these samples are cytotoxic to cells. HEWL oligomers produced the highest level of apoptotic death whilst sonicated fibrils and mature fibrils gave slightly lower levels of cleaved PARP. This data in collaboration with our FACS analysis suggests that cells treated with HEWL oligomers are dying through an apoptotic cell death pathway. This work supports earlier work (Gharibyan *et al.*, 2007) which suggests that lysozyme oligomers induce apoptosis. Interestingly, our fibrillar samples show lower levels of PARP and also higher levels of PI suggesting that they may be experiencing necrotic cell death in addition to apoptosis. TEM of oligomeric and fibrillar treated U2OS cells shows that cells are undergoing apoptotic cell death with several apoptotic markers such as the presence of apoptotic bodies, cytoplasmic vacuolization, and cell membrane blebbing all visible. This further supports the idea that cells treated with these fractions undergo some level of apoptosis.

5.3.4. HEWL Oligomers but not Sonicated Fibrils Inhibit LTP in vivo

We found that HEWL oligomers inhibited hippocampal LTP *in vivo*, a process linked with memory loss and function. The role of oligomers and fibrils in neurodegeneration is a well-studied field. LTP is beneficial for understanding the role of certain aggregated proteins in cognitive dysfunction often associated with diseases such as AD (Klyubin et al., 2011) and PD (Diogenes *et al.*, 2012). This is the first time that HEWL oligomers have been shown to

affect LTP and perhaps more significantly, this is the first time a non-disease related protein has attenuated LTP. Despite the fact that these oligomers are not as potent at inhibiting LTP as, for example, Aβ oligomers (Klyubin et al., 2011), the data provides new insight into the role of protein misfolding in neurodegenerative diseases as well as potential benefits of immunotherapies using conformation selective antibodies. It has previously been shown that insoluble amyloid fibrils formed by Aβ protein did not affect LTP *in vivo* (Klyubin *et al.*, 2012). One reason for the lack of effect is that, due to diffusional restrictions, such large aggregates are not reaching hippocampal parenchyma from the injection site in the ventricle. However we used a sonication approach to produce soluble fragments of mature fibrils while maintaining general fibrillar structure (Chatani *et al.*, 2009). Sonicated fibrils had no effect on LTP and were less toxic than oligomers *in vitro* with neuronal cells and so the observed difference in the abilities of oligomers and mature fibril fragments to inhibit LTP *in vivo* is in accord with this data and probably reflects the different nature of the interaction between neurons and these different HEWL aggregates.

These results suggest that a common mechanism of hippocampal LTP damage and inhibition is employed by oligomers irrespective of their origin. Aβ oligomers, not fibrils, have been shown to inhibit LTP *in vivo* (Walsh *et al.*, 2002). Additionally, synthetic Aβ of differing conformations was shown to also inhibit LTP in rats (Cullen *et al.*, 1997). Aβ is not the only peptide sequence to illicit a LTP inhibitory response as α-synuclein has also been shown to inhibit LTP (Diogenes *et al.*, 2012). These proteins have a well-defined role in cognitive disruption which is why their ability to impair LTP is not all that surprising and fits the modern consensus regarding their pathology. What is striking about our results is that the HEWL protein has no role in memory or in disrupting learning capabilities under normal circumstances yet can impair LTP *in vivo*, suggesting that the oligomeric form of any protein could in theory effect cognitive function. We acknowledge the fact that much higher concentrations of HEWL oligomers were needed to inhibit LTP but as it has no relation to neurodegeneration this result is not surprising.

As the LTP model is the gold standard model for mapping changes in learning and memory it could be suggested that HEWL oligomers prepared from ultracentrifugation/filtration impair cognitive functions in rats. Further work would be needed to establish the long term and physical effects of these in rats and to determine if there are changes to memory using

recognition or spatial tests (Wang *et al.*, 2009). The results from this experiment however shed new light on the role of amyloid oligomers in damaging the hippocampus and disrupting cognitive capabilities in patients with memory and learning difficulties as a result of certain diseases.

The true toxic component involved in the cell/tissue damage symptomatic of neurodegenerative diseases is still a proverbial grey area in the world of amyloid pathology (Stefani, 2010, Lansbury and Lashuel, 2006). Our results demonstrate that fibrils and oligomers prepared from innocuous HEWL and carefully separated through ultracentrifugation and ultrafiltration exhibit toxicity towards neuronal PC12 cells and U2OS cells. In neuronal cells oligomers are more harmful than fibrils and additionally, the differential phenotype provided a level of protection against these oligomers. Furthermore, oligomers illicit an apoptotic cell death response whereas fibrils may use a combination of apoptosis and necrosis. Oligomers inhibit LTP in rats *in vivo* although sonicated fibrils appear to have no effect on the inhibition process. While both oligomers and fibrils have been shown to be damaging *in vitro*, LTP experiments have yet to show that fibrils possess the ability to disrupt LTP signaling *in vivo*, further highlighting the complicated matrix that surrounds the efficacy of these protein species. Knowledge of these subtle differences would be very important when designing anti-fibrillogenesis therapeutics. Our findings confirm that innocuous hen lysozyme can be engineered to produce both cytotoxic soluble prefibrillar aggregates and mature amyloid fibrils, further strengthening the claim that fibrillar conformation, and not the identity of the protein, is key to cellular toxicity and the underlying specific cell death mechanism.

6. General Discussion

This study demonstrates a multifaceted role for proteins which is dependant of their conformation. In one form proteins can form complexes with FA that display cytotoxic selectivity towards tumour cells. However in another arrangement, proteins can induce cell death in both tumour and healthy cells and can inhibit LTP responses *in vivo*.

Protein synthesis and correct protein folding are among the most complex and challenging events the cellular protein factory will encounter (Hetz, 2012). Protein folding and misfolding is tightly governed and is reliant on numerous molecules such as HSP chaperones (Li and Srivastava, 2004), the UPR (Chakrabarti *et al.*, 2011), and degradative lysosomal enzymes which digest proteins taken up via endocytosis (Dunn, 1994). There are over 100,000 different proteins within the body and the folding machinery must deal with assembling each molecule individually and in a very quick time (Calamini *et al.*, 2012). Therefore due to sheer numbers, the actual event of protein misfolding is not uncommon as approximately 30% of all proteins will be degraded (Yewdell, 2005). An important feature of this work was to highlight the fact that although protein misfolding can lead to the development of CPDs which can be extremely debilitating to patients, not all proteins folding carry negative consequences. In this way protein folding can be said to have two sides, one of which is the 'good' or beneficial side while the other is the 'bad' or harmful side.

We have demonstrated that P-FA complexes can target tumour cells for destruction and are significantly less toxic towards differentiated cells. PC12 cells were used as a model for studying differences between tumour and healthy cells. Normally displaying an undifferentiated phenotype, culturing these cells on collagen coated surfaces and with the addition of NGF induces a change to a differentiated phenotype, resulting in cells which present characteristics similar to sympathetic neurons in primary cell culture such as displaying the ability to adhere to surfaces and branching varicose processes (Greene and Tischler, 1976). Not only does PC12 serve as a good model for studying various aspects of neurobiology and neurochemistry, it also provides a reliable assay for studying differences between tumour and healthy cells. By using this model it is possible to analyze the effects of various drugs on a single cell displaying a cancerous and a normal differentiated phenotype. Although P-FA complexes have been tested on different cell lines this study represent the first time that any P-FA complex has been assessed using the PC12 differentiation model. HAMLET showed the characteristic selective killing towards the PC12 tumour cell in this

model and was only toxic to differentiated cells at high concentrations suggesting that this PC12 model was a useful system to show differential selective killing by P-FA complexes.

Compared to HAMLET, the quintessential P-FA complex, all engineered assemblies demonstrated similar efficacy towards tumour cells whilst displaying a reduction in differentiated cell targeting. This result is important for two reasons. Firstly it demonstrates the usefulness of the PC12 model as a means to decipher drug-tumour cell selectivity. PC12 cells have primarily been used in the neuronal field and are a useful model for the study of neurosecretion and neuronal differentiation. To the authors' knowledge this is the first time that the PC12 differentiation model has been used to assess the tumouricidal effects of anti-cancer drugs. The use of the PC12 differentiation model provides an early indicator of whether drugs possess the ability to differentiate between healthy and cancerous cells as shown by our P-FA complexes. Furthermore it provides a robust comparison between a single cell displaying different phenotypes. Many *in vitro* experiments involving HAMLET (Brinkmann *et al.*, 2011a, Håkansson *et al.*, 1995, Hakansson *et al.*, 2011, Permyakov *et al.*, 2012, Pettersson *et al.*, 2006) have been conducted on two unrelated cell lines, one displaying a malignant phenotype, the other a normal cell phenotype. The uniqueness of this model is that it allows us to examine the effects of HAMLET and other P-FA complexes on the same cell, displaying both phenotypes, and therefore reducing concerns over selectivity based on what particular cell type was being used.

The use of conventional chemotherapeutic drugs has proven very successful in the treatment of cancer however a major issue with this class of drugs is that they lack specificity and can result in serious side effects due to their ability to attack normal healthy cells. One of the key goals of cancer therapy is to develop drugs that specifically target tumour cells only (Abdullah *et al.*, 2009). All P-FA complexes displayed toxicity towards tumour cells. It was originally hypothesized that the protein component of HAMLET was the cytotoxic entity, capable of targeting tumour cells for destruction, and the FA component held the complex together and allowed it cross the cell membrane (Pettersson-Kastberg *et al.*, 2009b). In recent years this view has changed and similar to our results, other P-FA complexes have been made from non-LA related proteins, capable of causing apoptosis in cancer cells (Nakamura *et al.*, 2013, Permyakov *et al.*, 2012, Vukojević *et al.*, 2010, Wilhelm *et al.*, 2009).

The discovery of ELOA, a non-milk related protein capable of forming a HAMLET-like complex, drove the research surrounding the mechanistic properties behind HAMLET in a new direction, one which questioned the toxic role of the protein. In addition to our group, Nakamura *et al.*, have developed a functioning AMb-OA complex that killed tumour cells *in vitro* (Nakamura *et al.*, 2013). The complex of β-LG-OA has also been developed and displayed similar efficacy (Lišková *et al.*, 2011, Permyakov *et al.*, 2012).

As mentioned previously there are several alternative methods for the development of P-FA complexes. Similarly there is increasing variation in the cytotoxic capabilities of these drugs as seen in the literature. We use an IEC method similar to that first used for the development of HAMLET. All our P-FA complexes displayed a generic ability to target tumour cells at higher rates than that observed in differentiated cells suggesting that this method of preparation was highly reproducible with regards to engineering the complex. There is a need for groups working with P-FA complexes to utilize a similar method of preparation in order to eliminate any discrepancies observed in the results. We suggest that the IEC method is a highly robust and reproducible method for the production of tumouricidal P-FA complexes.

It has also been shown that increasing the levels of OA within the complex also increases its cytotoxicity (Brinkmann *et al.*, 2011a). As mentioned previously, OA has been shown to have cytotoxic effects against cancer cells *in vitro* (Permyakov et al., 2012, Tolin et al., 2010, Zhu et al., 2005). In conjunction with these other studies, our work suggests that OA is the true cytotoxic component of these P-FA complexes. We, like others, hypothese that as OA is poorly soluble in aqueous solution at neutral pH (Vorum *et al.*, 1992), and the formation of a complex encapsulates the OA molecules and protects it from this undesirable environment. As the protein moiety of these complexes does not seem to be an important factor, we suggest that P-FA complexes act as a delivery system for OA allowing it cross the cell membrane by enhancing its solubility thus facilitating its transport into the cell. As a general observation, all our P-FA complexes are transparent after the addition of PBS, or dH_2O. Due to the presence of FA, we would expect a turbid solution however, the transparency observed suggests that there is no longer free FA in solution and that it has been taken up by the protein.

Our work also shows that the MG conformation of the complex is not an integral feature. It was previously thought that the MG state of the protein granted it flexibility and facilitated

complex formation (Mok *et al.*, 2007, Mossberg *et al.*, 2010b, Svanborg *et al.*, 2003). The discovery that β-LG-OA can form tumouricidal complexes with OA (Permyakov *et al.*, 2012) challenged this hypothesis. We have provided further evidence that proteins do not have to be MG in order to bind to OA. Both Mb and Ub formed tumouricidal complexes with OA, and were formed in an identical way as all other MG-OA complexes. Furthermore our group has previously shown that electrostatic interactions between the positively-charged basic groups on the α-LA protein and the negatively charged carboxylate groups on OA molecules are key to the intermolecular integrity of the α-LA-OA complex. Therefore we draw the conclusion that the proteinaceous component does not provide cytotoxity and rather it is the OA molecules.

The development of P-FA complexes capable of destroying tumour cells is a very interesting idea for future chemotherapeutic drugs. As we have shown the native proteins, even at high concentrations, are relatively harmless to cells *in vitro*, and were extremely toxic when in complex with OA. The selective nature of these complexes for the most part appears to follow a pattern, where the more toxic to the tumour cell, the more toxic to the healthy cell. In addition to the tumouricidal selectivity displayed by these complexes, they also elicited similar cell death mechanisms with apoptotic cell death being stimulated in all cells tested with each P-FA complex. The similarities in cytotoxicity and cell death suggest that P-FA complexes are a unique group of tumouricidal drugs which display a generic pattern of activity. It has been shown that HAMLET exploits conserved features of cancer cells for its activity yet these exact features are still not fully known. Recent studies have shown that HAMLET sensitivity towards tumour cells was directly related to c-Myc expression (Storm *et al.*, 2011), indicating a possible target for this FA complex. As there is a general trend of selectivity towards tumour cells displayed by our P-FA complexes it would be interesting to examine if they had all shared a similar affinity for c-Myc, and whether the expression of this oncogene was a reason that all proteinaceous-OA nanoparticles target tumour cells over healthy ones.

As seen from our results, Mb-OA is the most cytotoxic of our complexes towards tumour cells, and subsequently differentiated cells. Similarly the 'apo' state of this protein was also highly toxic to both cell lines. From a drug perspective the goal of anti-cancer therapeutics is to destroy tumour cells while causing the least amount of harm to healthy cells as possible

and because of this reason we conclude that Mb-OA and AMb-OA are not desirable anti-tumour drug candidates based on our results. Ub-OA was the less harmful towards healthy cells, but was also the least effective against $PC12^{undiff}$ cells. BAMLET was highly toxic towards tumour cells and showed the greatest fold difference in LC_{50} values between tumour and differentiated cells suggesting that BAMLET presents the best option in terms of potential as a future drug target.

Having established that BAMLET provided the greatest potential as a drug candidate we sought to examine its capacity to reduce tumour growth in a melanoma model in mice. Additionally we wanted to assess the possibility of using BAMLET as a combinational drug therapy, an area of cancer therapeutics that has shown great promise due to the increasing incidence of drug resistance (Al-Lazikani *et al.*, 2012). To date only one other study has examined the anti-tumour effects of BAMLET *in vivo*. Xiao *et al.*, demonstrated that intravesical BAMLET therapy caused a reduction in tumour growth/progression in an orthotopic rat bladder tumour model (Xiao *et al.*, 2013). Additionally this is the first time that any P-FA complex has been used to treat B16 murine melanomas.

BAMLET significantly reduced tumour volume in treated mice and continued to reduce tumour progression for a period of up to 60 days post tumour inoculation. Furthermore the route of injection had no effect on the drug's efficacy. The route of administration can have a large effect on how a drug responds and reacts in the body (Lee *et al.*, 2011b). As HAMLET has been shown to be in a relatively unstable conformation (Fast *et al.*, 2005) the addition of FCS, the main component of which is the FA binding protein albumin (Simard *et al.*, 2005), could potentially out compete the protein for the OA molecules, thus rendering the complex inactive. We found that FCS does not significantly reduce BAMLET activity *in vitro*. In light of this we administered BAMLET through two injection routes, SC and i.p. The i.p injection was equally effective at reducing tumour growth in the murine melanoma model suggesting that even when in the presence of albumin within the bloodstream, BAMLET retains its P-FA conformation. This is the first occasion that a P-FA complex has been used through an i.p route of administration and these results are very encouraging as many internal malignancies would be impossible to treat without the use of i.p injections (Lukas *et al.*,

1971) suggesting that P-FA complexes could be used to treat tumours that are not treatable through direct administration.

BAMLET also proved useful as a combinational therapeutic drug in the same mouse model. The use of combination therapy is an emerging field of cancer treatment and has yielded very promising results in a number of trials (Lane, 2006). One concern was the combination of the two drugs would have a negative effect of mouse survival as combining drugs can culminate in decreased efficacy due to competitional issues and can also yield greater side effects (Terrault, 2009). In contrast to this, the combination of BAMLET with the TLR agonist R848 enhanced the efficacy of the treatment and resulted in a larger reduction in tumour burden when compared to the drugs individually. The mice that survived the initial trial were re-challenged with tumour cells again and any long term effects of BAMLET and R848 were observed.

Interestingly BAMLET and R848 treated mice showed a reduction in tumour progression compared to mice in the untreated groups. Although this novel discovery suggests that BAMLET may invoke an immunological response in mice, it should be noted that the sample size used was too small to gain statistical significance. However it does provide preliminary information about the potential immunological effects of mice treated with this P-FA complex. This lasting protection is a new feature displayed by BAMLET and has never been observed before and suggests that mice may have developed a level of immunity against the tumour cells.

This work complements the results generated from the ELISA data, in which isolated $CD4^+$ T cell subsets were incubated with BAMLET and their cytokine levels were measured. Treatment of Th0, Th1, and Th17 cells with BAMLET resulted in the upregulation of IL-17, a cytokine directly involved in the regression of human metastatic melanoma (Martiniuk *et al.*, 2010). Additionally IL-17 can also increase production of cytotoxic $CD8^+$ T cells and NK cells and downregulates the production of Treg cells in response to tumours (Kryczek *et al.*, 2009, Martin-Orozco *et al.*, 2009). TNF-α production is increased in Th0 cells which has been shown to promote the expansion of Th22 cells, a cytokine involved in tissue regeneration and wound healing (Trifari *et al.*, 2009). In addition to our work, IL-6, IL-8, and

TNF-α have been shown to be upregulated in non-immune differentiated cells treated with HAMLET suggesting a possible role for innate immunity (Storm *et al.*,2013) however this aspect of immunity was not examined in this project and should be assessed in future work. Interestingly treatment with BAMLET resulted in the cessation of IL-2 production from each T-cell population. The reduction of IL-2 results in a decrease in Treg (Maggi *et al.*, 2005) cells therefore enables the immune system to better deal with tumour cells. Treg cell production will be examined to determine whether the production of this cytokine is attenuated in response to BAMLET treatment.

Although we did not assess cytokine secretion in cells treated with R848, this molecule has also been shown to induce Treg cell-mediated suppression and so could also have a similar effect on the immune system (Van *et al.*, 2011, Peng *et al.*, 2005). It would also be interesting to probe the effects of R848 on $CD4^+$ T cell populations to see if there are similar effects on cytokine production. Additionally the abrogation of IL-2 coincided with an increase in IL-10 production which has been shown to occur in previous studies (Taga and Tosato, 1992). The IL-10 cytokine is involved with the innate and adaptive immune system and its secretion has been shown to inhibit the production of Th1 cytokines such as IFN-γ and IL-2 (Lalani *et al.*, 1997). Overproduction of IL-10 has also been shown to promote B-cell maturation and survival (Levy and Brouet, 1994, Rousset *et al.*, 1992) and promotes the activation of NK cells (Ochsenbein, 2002, Kelly *et al.*, 2002). Importantly, IL-10 downregulation of IL-2 results in T-cell anergy and therefore favours a humoral driven response (Groux *et al.*, 1996, Itoh *et al.*, 1994). Mice displayed reduced tumour development and in some cases complete absence of tumour growth even after the re-challenge.

The downregulation of IL-2 and increase in IL-10 suggests that the immune response elicited by BAMLET is one which favours a humoral mechanism. We propose that humoral immunity may be a reason mice expressed protective responses to the tumour when mice were re-challenged as mice are primed to recognize and destroy tumour cell PAMPs. This was also observed with mice monitored for 60 days post inoculation. These mice showed reduced levels of tumour growth over a lengthy period of time further supporting the idea that a long term immunological effect is promoted in response to BAMLET treatment. As mentioned previously in terms of cancer treatment (Figure 1.3) the P-FA complex HAMLET

targets numerous hallmarks such as the tumour cells ability to avoid cell death, promote tumour cell proliferation, and manipulate the cells ability to derive energy. We propose that in addition to these factors, the P-FA complex BAMLET may also target those cells which attempt to avoid immunological detection. When re-challenged with tumour cells mice continue to show reduced tumour development. Furthermore BAMLET appears to activate a Th2 driven humoral immune response which may enable the host to remain immunologically primed as was demonstrated from our ELISA data. As a result of this we postulate that P-FA complexes may have an additional mechanism to promote tumour cell destruction and this may represent a new way in which P-FA complexes target the hallmarks of cancer.

The results of these experiments suggest that BAMLET is an effective tumouricidal drug that displays specific tumour cell cytotoxity *in vitro* and can reduce tumour volume in a murine melanoma model *in vivo*. Furthermore the complex remained stable even in the presence of albumin in culture and in the bloodstream suggesting that it could prove effective as a drug for the treatment of cancers which are difficult to access and not treatable by cutaneous or direct application. The similar homology and mechanistic properties, the relative simplicity in acquiring, and the comparatively cheaper cost make BAMLET a potentially better option from a cost productive therapeutic aspect as well as a laboratory based material.

The ability of proteins to attain tumouricidal properties when in a misfolded form and complexed to OA is a new and exciting feature that emphasises a 'good side' to protein misfolding. Conversely, there is also a better known 'bad side' to protein misfolding, that can been seen in numerous PCDs such as AD and PD (Selkoe, 2004). In order to investigate this dysfunctional protein misfolding event and to characterise the aggregates formed we used HEWL, an innocuous protein, which has never displayed any role in degenerative disorders unlike the human version of lysozyme which is involved in the development of hereditary systemic amyloidosis (Pepys *et al.*, 1993).

HEWL was engineered into amyloid fibrils through increasing the temperature and acidity of its environment (Krebs *et al.*, 2000). The solution was separated into two distinct fractions, the prefibrillar soluble oligomers, and less soluble mature amyloid fibrils. Amyloid fibrils were further separated to give sonicated fibrils which are characteristically different from the

full length form (Lee *et al.*, 2011c). The characterisation of the separated fractions is key to determining their mechanistic and structural properties and is something often overlooked by groups. To achieve relatively pure aggregated samples, 21 day old HEWL was separated through size exclusion methods and then characterised using a battery spectroscopic and microscopic techniques to ensure adequate separation was achieved.

Despite recent scientific advancements in a host of protein-related neurodegenerative diseases, the main causative agent of cellular death has yet to be definitively identified. A number of studies support the idea that mature amyloid fibrils are the main pathogenic entities involved in amyloidosis (Mossuto *et al.*, 2010, Yoshiike *et al.*, 2007). Conversely, a number of studies have supported the idea that non-fibrillar soluble oligomers play a direct role in cellular damage and death (Glabe, 2006, Vieira *et al.*, 2007, Sakono and Zako, 2010). With these discoveries the perception of the role for amyloid fibrils has changed and it has been suggested that their true function may be that of an evolutionary protection mechanism employed by the body, and they may just be an end product of a pathogenic event in which the fundamental damage was carried out at an earlier phase by the soluble oligomers (Kirkitadze *et al.*, 2002).

Our results demonstrate that both oligomers and fibrils possess cytotoxic capabilities against differentiated and undifferentiated PC12 neuronal cells and the bone tumour cell line U2OS. As mentioned previously the PC12 differentiation model allows for the examination of drug selectivity against malignant cells and so this model was also useful when examining the cytotoxic properties on HEWL protein species and whether these aggregates were more or less harmful towards tumour or healthy cells. HEWL aggregates were cytotoxic towards both PC12 cell lines however oligomers were more toxic towards the tumour cells. Sonicated and mature fibrils showed no difference in toxicity suggesting that the cancerous morphology of PC12 cells does not make them more susceptible to these aggregates.

Oligomers showed an increase in toxicity towards $PC12^{undiff}$ cells however, this was not seen in U2OS cells treated with the same fractions. In U2OS all samples were equally harmful towards to cell. In the context of neurodegeneration U2OS cells do not provide any additional information, yet as they are susceptible to all fractions they do demonstrate that fibrils possess cytotoxic capabilities. For PC12 cells the protective role displayed by cell differentiation

towards oligomers was consistent with earlier work which examined the effects on cell susceptibility to amyloid injury in both the differentiated and undifferentiated phenotypes of human neurotypic SH-SY5Y cells. Retinoic acid-differentiated cells were considerably more resistant to prefibrillar Aβ1-40, Aβ1-42, and HypF-N oligomers (Cecchi *et al.*, 2008). A possible reason for this, which is also supported by other studies (Olesen *et al.*, 1998), is that phenotypic alterations which are a consequence of differentiation modify aggregate binding to the cell surface. Cholesterol density and the presence of newly expressed receptors in the plasma membrane of differentiated cells have both been shown to be key factors in this process (Cecchi *et al.*, 2008). Another feature which has also been shown to play a role in differing levels of susceptibility is ROS. ROS may mediate Aβ (25-35) toxicity in $PC12^{undiff}$ cells but not in $PC12^{diff}$ cells (Sung *et al.*, 2003). The varying degree of insult caused by amyloid aggregates is not only due to differentiated states. For many years, numerous experiments have shown that a plethora of cell lines of unrelated states and origin convey a wide range of susceptibility towards amyloid injury (Mazziotti and Perlmutter, 1998, Janciauskiene and Ahren, 1998, Bloom *et al.*, 2005).

It is important to note that while oligomers have been shown to universally display inherent toxicity, in contrast, fibrils exhibit more varied results. A large number of completely unrelated proteins which have formed oligomers have all exhibited a common pathological function (Conway *et al.*, 2000, Marzban *et al.*, 2003). It is currently thought that oligomers may share a membrane permeabilization mechanism of pathogenesis, whereby irregular Ca^{2+} homeostasis may result in internal damage to the cell. Elevated intracellular levels of Ca^{2+} can lead to cell death and have also been linked to amyloid toxicity with regards AD. Dysregulation of Ca^{2+} ions as a result of treatment with amyloid oligomers has also been shown to induce membrane disruption and death in cells (Glabe, 2006). In contrast to this, mature fibrils exhibit much greater diversity with regard to pathogenicity and unlike oligomers may employ a number of various mechanisms of cytotoxicity. Fibrils formed from differing proteins and indeed from the same peptides show dramatic differences in terms of conformational variation (Prusiner *et al.*, 1998, Collinge, 2001, Aguzzi and Haass, 2003) and hence this may be responsible for the variations observed in terms of cytotoxic capability.

A recent study conducted by Mossuto *et al.*, demonstrated that different methods of protein aggregation, most notably the production of fibrils with a smaller core, influence cellular

cytotoxicity (Mossuto *et al.*, 2010) In fact, this discrepancy in conformation may be of significant importance with regards to cell cytotoxicity and may explain the inconsistency displayed by numerous experiments examining the cytotoxic ability of fibrils. Examination of HEWL fibrillar core and atomic structure was beyond the scope of this work but could provide addition information which may shed light regarding its toxicity in PC12 cells.

Interestingly, oligomers but not sonicated fibrils generated from HEWL inhibited LTP in rats *in vivo*. This novel find suggests that a protein which has no role in disease or cognitive functioning can negatively attenuate synaptic plasticity. LTP is the gold standard method for the examination of learning and memory (Lynch, 2004) and provides a useful insight into cognitive dysfunction in response to insult (Barry *et al.*, 2011). Proteins associated with neurodegenerative disease such as Aβ oligomers (Klyubin et al., 2011) and α-synuclein (Diogenes *et al.*, 2012) has been shown to affect LTP responses in previous experiments. This work presents the first instance of HEWL oligomers inhibiting LTP, and in addition is the first time LTP has been inhibited by a non-disease related protein. This work suggests that there is a generic mechanism utilized by oligomers to disrupt LTP signaling and this feature could be conserved throughout oligomeric proteins. As oligomers display a universal pathological function (Conway *et al.*, 2000, Marzban *et al.*, 2003) and are structurally similar, as demonstrated by conformation-dependent antibodies which recognizing generic specific oligomeric epitopes, we hypothesize that oligomers share a universal method of promoting cognitive dysfunction.

In this study we have demonstrated that protein misfolding can have a profound effect on cells both *in vitro* and *in vivo*, and this effect can be either negative or positive depending on the protein in question. We have shown that misfolded proteins which obtain FAs to form P-FA complexes can display tumouricidal selectivity in a PC12 neuronal cell model and also reduce tumour volume in mice with cutaneous melanomas. Conversely we have also demonstrated that innocuous protein can be engineered into a non-selective cytotoxic molecule that also inhibits LTP *in vivo*, a fundamental event linked with cognitive dysfunction in patients with Dementia. As such proteins can essentially behave as a double edged sword, displaying anti-tumour properties in one conformation whilst damaging neuronal cells and impairing learning in another. This work highlights the remarkable complexity and versatility of proteins in general, from normal functioning globular proteins

which are essential for life, to the FA complexes which grant proteins a tumouricidal gain of function, and to the aggregated peptides which can lead to the onset of numerous degenerative disorders.

6.1. Future Directions

This research has identified a number of areas for future work some of which are currently ongoing and others which are already been designed as future projects for prospective students.

A number of the P-FA complexes developed are novel findings and present a new potential form of cancer treatment. Paper work is being finalised on a patent on Ub-OA and will be submitted in the near future. We hope to develop further the work carried out here on Ub-OA, and other P-FA complexes, by examining their efficacy in a number of mice models, including the murine melanoma model used here. A 4 year IRCSET PhD project is currently underway which will look to tackle some of these ideas in particular, with Ub-OA.

The promising results shown by the murine melanoma trial will be investigated further. Work is currently been conducted in collaboration with Lydia Dyck from the Mills group examining whether BAMLET activates LPS mediated destruction of cells. Using DCs which have a knockdown for LPS stimulating factor TLR4, BAMLET will be used to see whether cell death still occurs in the absence of LPS. Examining whether this is the sole cause of the cell death seen in response to treatment in the *in vivo* model will prove important for concluding its overall efficacy and potential as a drug treatment option.

7. References

Abdullah, N. M., Rosania, G. R. & Shedden, K. 2009. Selective Targeting of Tumorigenic Cancer Cell Lines by Microtubule Inhibitors. *PloS One,* 4, E4470.

Aggarwal, B. B., Gupta, S. C. & Kim, J. H. 2012. Historical Perspectives on Tumor Necrosis Factor and its Superfamily: 25 Years Later, A Golden Journey. *Blood.* 19;119(3):651-65.

Agger, T. & Bro, C. 2009. Methods for Preparing Cytotoxic Complexes of Emulsifier and Fatty Acid. Google Patents.

Aguzzi, A. & Haass, C. 2003. Games Played by Rogue Proteins in Prion Disorders and Alzheimer's Disease. *Science,* 302, 814-818.

Aits, S., Gustafsson, L., Hallgren, O., Brest, P., Gustafsson, M., Trulsson, M., Mossberg, A. K., Simon, H. U., Mograbi, B. & Svanborg, C. 2009. HAMLET (Human Alpha-Lactalbumin Made Lethal to Tumor Cells) Triggers Autophagic Tumor Cell Death. *Int J Cancer,* 124, 1008-19.

Alberti, S., Halfmann, R., King, O., Kapila, A. & Lindquist, S. 2009. A Systematic Survey Identifies Prions and Illuminates Sequence Features of Prionogenic Proteins. *Cell,* 137, 146-158.

Alistair, B. & Steve, I. 2009. Alzheimer's Disease. *BMJ,* 338.

Al-Lazikani, B., Banerji, U. & Workman, P. 2012. Combinatorial Drug Therapy for Cancer in the Post-Genomic Era. *Nat Biotech,* 30, 679-692.

Amsen, D., Spilianakis, C. G. & Flavell, R. A. 2009. How are Th1 and Th2 Effector Cells Made? *Curr Opin Immunol.,* 21, 153-160.

Amundson, S. A., Myers, T. G. & Fornace, A. J., Jr. 1998. Roles for p53 in Growth Arrest and Apoptosis: Putting on the Brakes After Genotoxic Stress. *Oncogene,* 17, 3287-99.

Andersen, C. B., Yagi, H., Manno, M., Martorana, V., Ban, T., Christiansen, G., Otzen, D. E., Goto, Y. & Rischel, C. 2009. Branching in Amyloid Fibril Growth. *Biophys J,* 96, 1529-36.

Anderson, P. J., Brooks, C. L. & Berliner, L. J. 1997. Functional Identification of Calcium Binding Residues in Bovine Alpha-Lactalbumin. *Biochemistry,* 36**,** 11648-54.

Andrade, L. N., De Lima, T. M., Curi, R. & Castrucci, A. M. 2005. Toxicity of Fatty Acids on Murine and Human Melanoma Cell Lines. *Toxicol In Vitro,* 19**,** 553-60.

Anel, A., Richieri, G. V. & Kleinfeld, A. M. 1993. Membrane Partition of Fatty Acids and Inhibition of T Cell Function. *Biochemistry,* 32**,** 530-536.

Anfinsen, C. B. 1973. Principles that Govern the Folding of Protein Chains. *Science,* 181**,** 223-30.

Apetri, M. M., Maiti, N. C., Zagorski, M. G., Carey, P. R. & Anderson, V. E. 2006. Secondary Structure of α-Synuclein Oligomers: Characterization by Raman and Atomic Force Microscopy. *J Mol Biol,* 355**,** 63-71.

Armstrong, R. A. 2009. The Molecular Biology of Senile Plaques and Neurofibrillary Tangles in Alzheimer's Disease. *Folia Neuropathol,* 47**,** 289-99.

Arnaudov, L. N. & De Vries, R. 2005. Thermally Induced Fibrillar Aggregation of Hen Egg White Lysozyme. *Biophys J,* 88**,** 515-526.

Artwohl, M., Lindenmair, A., Roden, M., Waldhäusl, W.-K., Freudenthaler, A., Klosner, G., Ilhan, A., Luger, A. & Baumgartner-Parzer, S. M. 2009. Fatty Acids Induce Apoptosis in Human Smooth Muscle Cells Depending on Chain Length, Saturation, and Duration of Exposure. *Atherosclerosis,* 202**,** 351-362.

Ashtekar, A. R., Zhang, P., Katz, J., Deivanayagam, C. C. S., Rallabhandi, P., Vogel, S. N. & Michalek, S. M. 2008. TLR4-Mediated Activation of Dendritic Cells by the Heat Shock Protein Dnak from Francisella Tularensis. *J Leukoc Biol,* 84**,** 1434-1446.

Aydin, D., Weyer, S. W. & Muller, U. C. 2012. Functions of the APP Gene Family in the Nervous System: Insights from Mouse Models. *Exp Brain Res.,* 217**,** 423-34.

Backendorf, C., Visser, A. E., De Boer, A. G., Zimmerman, R., Visser, M., Voskamp, P., Zhang, Y.-H. & Noteborn, M. 2008. Apoptin: Therapeutic Potential of an Early Sensor of Carcinogenic Transformation. *Annu Rev Pharmacol Toxicol,* 48, 143-169.

Bald, T., Quast, T., Landsberg, J., Rogava, M., Glodde, N., Lopez-Ramos, D., Kohlmeyer, J., Riesenberg, S., Van Den Boorn-Konijnenberg, D., Homig-Holzel, C., Reuten, R., Schadow, B., Weighardt, H., Wenzel, D., Helfrich, I., Schadendorf, D., Bloch, W., Bianchi, M. E., Lugassy, C., Barnhill, R. L., Koch, M., Fleischmann, B. K., Forster, I., Kastenmuller, W., Kolanus, W., Holzel, M., Gaffal, E. & Tuting, T. 2014. Ultraviolet-Radiation-Induced Inflammation Promotes Angiotropism and Metastasis in Melanoma. *Nature,* 507, 109-113.

Barhoum, S., Booth, V. & Yethiraj, A. 2013. Diffusion NMR Study of Complex Formation in Membrane-Associated Peptides. *Eu. Biophys J,* 42, 405-14.

Barry, A. E., Klyubin, I., Mc Donald, J. M., Mably, A. J., Farrell, M. A., Scott, M., Walsh, D. M. & Rowan, M. J. 2011. Alzheimer's Disease Brain-Derived Amyloid-Beta-Mediated Inhibition of LTP *in vivo* is Prevented by Immunotargeting Cellular Prion Protein. *J Neurosci,* 31, 7259-63.

Barth, S., Glick, D. & Macleod, K. F. 2010. Autophagy: Assays and Artifacts. *J Pathol,* 221, 117-24.

Bateman, D. A. & Wickner, R. B. 2012. [PSI+] Prion Transmission Barriers Protect Saccharomyces Cerevisiae from Infection: Intraspecies 'Species Barriers'. *Genetics,* 190, 569-79.

Begin, M. E., Sircar, S. & Weber, J. M. 1989. Differential Sensitivity of Tumorigenic and Genetically Related Non-Tumorigenic Cells to Cytotoxic Polyunsaturated Fatty Acids. *Anticancer Res,* 9, 1049-52.

Bellamy, C. O. 1997. p53 and Apoptosis. *Br Med Bull,* 53, 522-38.

Berman, H. M., Westbrook, J., Feng, Z., Gilliland, G., Bhat, T. N., Weissig, H., Shindyalov, I. N. & Bourne, P. E. 2000. The Protein Data Bank. *Nucleic Acids Res,* 28, 235-242.

Bhatia, S., Tykodi, S. S. & Thompson, J. A. 2009. Treatment of Metastatic Melanoma: an Overview. *Oncology* , 23, 488-96.

Bhattacharya, A. A., Grüne, T. & Curry, S. 2000. Crystallographic Analysis Reveals Common Modes of Binding of Medium and Long-Chain Fas to Human Serum Albumin. *J Mol Biol,* 303, 721-732.

Biancalana, M. & Koide, S. 2010. Molecular Mechanism of Thioflavin-T Binding to Amyloid Fibrils. *Biochim. Biophys. Acta,* 1804, 1405-12.

Bliss, T. V. & Collingridge, G. L. 1993. A Synaptic Model of Memory: Long-Term Potentiation in the Hippocampus. *Nature,* 361, 31-9.

Bloom, G. S., Ren, K. & Glabe, C. G. 2005. Cultured Cell and Transgenic Mouse Models for Tau Pathology Linked to Beta-Amyloid. *Biochim Biophys Acta,* 1739, 116-24.

Boniol, M., Autier, P., Boyle, P. & Gandini, S. 2012. Cutaneous Melanoma Attributable to Sunbed Use: Systematic Review and Meta-Analysis. *BMJ,* 345.

Borutaite, V. 2010. Mitochondria as Decision-Makers in Cell Death. *Environ Mol Mutagen,* 51, 406-16.

Bouchard, M., Zurdo, J., Nettleton, E. J., Dobson, C. M. & Robinson, C. V. 2000. Formation of Insulin Amyloid Fibrils Followed by FTIR Simultaneously with CD and Electron Microscopy. *Protein Sci,* 9, 1960-7.

Boulares, A. H., Yakovlev, A. G., Ivanova, V., Stoica, B. A., Wang, G., Iyer, S. & Smulson, M. 1999. Role of Poly(ADP-Ribose) Polymerase (PARP) Cleavage in Apoptosis. Caspase 3-Resistant PARP Mutant Increases Rates of Apoptosis in Transfected Cells. *J Biol Chem.,* 274, 22932-40.

Boyle, G. M. 2011. Therapy for Metastatic Melanoma: An Overview and Update. *Expert Rev Anticancer Ther.,* 11, 725-37.

Brännström, K., M. Lindhagen-Persson, M., Gharibyan, A. L., Iakovleva, I., Vestling, M., Sellin, M. E., Brännström, T., Morozova-Roche, L., Forsgren, L. & Olofsson, nders. 2014. "A Generic Method for Design of Oligomer-Specific Antibodies." PLoS ONE 9(3): e90857.

Brest, P., Gustafsson, M., Mossberg, A. K., Gustafsson, L., Duringer, C., Hamiche, A. & Svanborg, C. 2007. Histone Deacetylase Inhibitors Promote the Tumoricidal Effect of HAMLET. *Cancer Res,* 67**,** 11327-34.

Brew, K., Vanaman, T. C. & Hill, R. L. 1968. The Role of Alpha-Lactalbumin and the A Protein in Lactose Synthetase: A Unique Mechanism for the Control of a Biological Reaction. *Proc Natl Acad Sci U S A,* 59**,** 491-7.

Brinkmann, C. R., Heegaard, C. W., Petersen, T. E., Jensenius, J. C. & Thiel, S. 2011a. the Toxicity of Bovine α-Lactalbumin Made Lethal to Tumor Cells is Highly Dependent on Oleic Acid and Induces Killing in Cancer Cell Lines and Noncancer-Derived Primary Cells. *FEBS J,* 278**,** 1955-1967.

Brinkmann, C. R., Thiel, S., Larsen, M. K., Petersen, T. E., Jensenius, J. C. & Heegaard, C. W. 2011b. Preparation and Comparison of Cytotoxic Complexes Formed Between Oleic Acid and Either Bovine Or Human Alpha-Lactalbumin. *J. Dairy Sci.,* 94**,** 2159-70.

Brinkmann, C. R., Thiel, S. & Otzen, D. E. 2013. Protein–Fatty Acid Complexes: Biochemistry, Biophysics and Function. *FEBS J,* 280**,** 1733-1749.

Brouckaert, P. G., Leroux-Roels, G. G., Guisez, Y., Tavernier, J. & Fiers, W. 1986. in Vivo Anti-Tumour Activity of Recombinant Human and Murine TNF, Alone and in Combination with Murine IFN-Gamma, on A Syngeneic Murine Melanoma. *Int J Cancer,* 38**,** 763-9.

Bucciantini, M., Giannoni, E., Chiti, F., Baroni, F., Formigli, L., Zurdo, J., Taddei, N., Ramponi, G., Dobson, C. M. & Stefani, M. 2002. Inherent Toxicity of Aggregates Implies A Common Mechanism for Protein Misfolding Diseases. *Nature,* 416**,** 507-511.

Bucciantini, M., Nosi, D., Forzan, M., Russo, E., Calamai, M., Pieri, L., Formigli, L., Quercioli, F., Soria, S., Pavone, F., Savistchenko, J., Melki, R. & Stefani, M. 2012. Toxic

Effects of Amyloid Fibrils on Cell Membranes: The Importance of Ganglioside GM1. *FASEB J,* 26**,** 818-31.

Budka, H. 2003. Neuropathology of Prion Diseases. *Br Med Bull,* 66**,** 121-30.

Burns, A. & Iliffe, S. 2009. Dementia. *BMJ,* 338.

Bychkova, V. E., Pain, R. H. & Ptitsyn, O. B. 1988. The 'Molten Globule' State is Involved in the Translocation of Proteins Across Membranes? *FEBS Lett,* 238**,** 231-234.

Cabrita, L. D., Dobson, C. M. & Christodoulou, J. 2010. Protein Folding on the Ribosome. *Curr Opin Struct Biol,* 20**,** 33-45.

Calamini, B., Silva, M. C., Madoux, F., Hutt, D. M., Khanna, S., Chalfant, M. A., Saldanha, S. A., Hodder, P., Tait, B. D., Garza, D., Balch, W. E. & Morimoto, R. I. 2012. Small-Molecule Proteostasis Regulators for Protein Conformational Diseases. *Nat. Chem. Biol.,* 8**,** 185-196.

Capdeville, R., Buchdunger, E., Zimmermann, J. & Matter, A. 2002. Glivec (STI571, Imatinib), A Rationally Developed, Targeted Anticancer Drug. *Nat Rev Drug Discov,* 1**,** 493-502.

Carswell, E. A., Old, L. J., Kassel, R. L., Green, S., Fiore, N. & Williamson, B. 1975. An Endotoxin-Induced Serum Factor that Causes Necrosis of Tumors. *Proc Natl Acad Sci U S A,* 72**,** 3666-70.

Cavallucci, V., D'amelio, M. & Cecconi, F. 2012. Abeta Toxicity in Alzheimer's Disease. *Mol. Neurobiol.,* 45**,** 366-78.

Cecchi, C., Pensalfini, A., Liguri, G., Baglioni, S., Fiorillo, C., Guadagna, S., Zampagni, M., Formigli, L., Nosi, D. & Stefani, M. 2008. Differentiation Increases the Resistance of Neuronal Cells to Amyloid Toxicity. *Neurochem. Res.,* 33**,** 2516-2531.

Chaitanya, G. V., Steven, A. J. & Babu, P. P. 2010. PARP-1 Cleavage Fragments: Signatures of Cell-Death Proteases in Neurodegeneration. *Cell Commun Signal,* 8**,** 31.

Chakrabarti, A., Chen, A. W. & Varner, J. D. 2011. A Review of the Mammalian Unfolded Protein Response. *Biotechnol Bioeng,* 108**,** 2777-93.

Chang, S. H., Mirabolfathinejad, S. G., Katta, H., Cumpian, A. M., Gong, L., Caetano, M. S., Moghaddam, S. J. & Dong, C. 2014. T Helper 17 Cells Play A Critical Pathogenic Role in Lung Cancer. *Proc Natl Acad Sci U S A*, 111 (15) 5664-5669.

Chaperot, L., Blum, A., Manches, O., Lui, G., Angel, J., Molens, J.-P. & Plumas, J. 2006. Virus Or TLR Agonists Induce Trail-Mediated Cytotoxic Activity of Plasmacytoid Dendritic Cells. *J Immunol,* 176**,** 248-255.

Chatani, E., Lee, Y.-H., Yagi, H., Yoshimura, Y., Naiki, H. & Goto, Y. 2009. Ultrasonication-Dependent Production and Breakdown Lead to Minimum-Sized Amyloid Fibrils. *Proc Natl Acad Sci U S A,* 106**,** 11119-11124.

Chatterton, D. E. W., Smithers, G., Roupas, P. & Brodkorb, A. 2006. Bioactivity of β-Lactoglobulin and α-Lactalbumin—Technological Implications for Processing. *Int Dairy J,* 16**,** 1229-1240.

Chaudhary, K., Haddadin, S., Nistala, R. & Papageorgio, C. 2010. Intraperitoneal Drug Therapy: An Advantage. *Curr Clin Pharmacol,* 5**,** 82-8.

Chen, G., Chen, K. S., Knox, J., Inglis, J., Bernard, A., Martin, S. J., Justice, A., Mcconlogue, L., Games, D., Freedman, S. B. & Morris, R. G. 2000. A Learning Deficit Related to Age and Beta-Amyloid Plaques in A Mouse Model of Alzheimer's Disease. *Nature,* 408**,** 975-9.

Chen, M. & Wang, J. 2008. Gaucher Disease: Review of the Literature. *Arch Pathol Lab Med,* 132**,** 851-3.

Chen, Z. & O'Shea, J. J. 2008. Th17 Cells: A New Fate for Differentiating Helper T Cells. *Immunol Res.,* 41**,** 87-102.

Chien, P., Weissman, J. S. & Depace, A. H. 2004. Emerging Principles of Conformation-Based Prion Inheritance. *Annu Rev Biochem,* 73**,** 617-56.

Chiti, F. & Dobson, C. M. 2006. Protein Misfolding, Functional Amyloid, and Human Disease. *Annu Rev Biochem.,* 75, 333-366.

Christofferson, D. E. & Yuan, J. 2010. Necroptosis as an Alternative Form of Programmed Cell Death. *Curr Opin Cell Biol,* 22, 263-268.

Clark, W. H., Jr., Elder, D. E., Guerry, D. T., Epstein, M. N., Greene, M. H. & Van Horn, M. 1984. A Study of Tumor Progression: the Precursor Lesions of Superficial Spreading and Nodular Melanoma. *Hum. Pathol.,* 15, 1147-65.

Cohen, T., Frydman-Marom, A., Rechter, M. & Gazit, E. 2006. Inhibition of Amyloid Fibril Formation and Cytotoxicity by Hydroxyindole Derivatives. *Biochemistry,* 45, 4727-4735.

Collinge, J. 2001. Prion Diseases of Humans and Animals: Their Causes and Molecular Basis. *Annu Rev Neurosci,* 24, 519-550.

Colomer, R. & Menendez, J. A. 2006. Mediterranean Diet, Olive Oil and Cancer. *Clin Transl Oncol,* 8, 15-21.

Conway, K. A., Harper, J. D. & Lansbury, P. T., Jr. 2000. Fibrils Formed *in vitro* from Alpha-Synuclein and Two Mutant Forms Linked to Parkinson's Disease Are Typical Amyloid. *Biochemistry,* 39, 2552-63.

Cooper, J. H. 1969. An Evaluation of Current Methods for the Diagnostic Histochemistry of Amyloid. *J. Clin. Pathol.,* 22, 410-3.

Cornelius, A. S., Yerram, N. R., Kratz, D. A. & Spector, A. A. 1991. Cytotoxic Effect of Cis-Parinaric Acid in Cultured Malignant Cells. *Cancer Res,* 51, 6025-30.

Cras, P., Kawai, M., Lowery, D., Gonzalez-Dewhitt, P., Greenberg, B. & Perry, G. 1991. Senile Plaque Neurites in Alzheimer Disease Accumulate Amyloid Precursor Protein. *Proc Natl Acad Sci USA,* 88, 7552-6.

Cullen, W. K., Suh, Y. H., Anwyl, R. & Rowan, M. J. 1997. Block of LTP in Rat Hippocampus in Vivo by Beta-Amyloid Precursor Protein Fragments. *Neuroreport,* 8, 3213-7.

Curry, S., Brick, P. & Franks, N. P. 1999. Fa Binding to Human Serum Albumin: New Insights from Crystallographic Studies. *Biochimica Et Biophysica Acta (BBA) - Molecular and Cell Biology of Lipids,* 1441, 131-140.

Cury-Boaventura, M. F., Pompéia, C. & Curi, R. 2004. Comparative Toxicity of Oleic Acid and Linoleic Acid on Jurkat Cells. *Clin Nutr,* 23, 721-732.

Dabora, J. M. & Marqusee, S. 1994. Equilibrium Unfolding of *Escherichia coli* Ribonuclease H: Characterization of a Partially Folded State. *Protein Sci,* 3, 1401-8.

Dahlgren, K. N., Manelli, A. M., Stine, W. B., Baker, L. K., Krafft, G. A. & Ladu, M. J. 2002. Oligomeric and Fibrillar Species of Amyloid-β Peptides Differentially Affect Neuronal Viability. *J Biol Chem.,* 277, 32046-32053.

De Martel, C. & Franceschi, S. 2009. Infections and Cancer: Established Associations and New Hypotheses. *Crit Rev Oncol Hematol,* 70, 183-94.

Delves, P. J. & Roitt, I. M. 2000. The Immune System. *N Engl J Med,* 343, 37-49.

Dempsey, P. W., Vaidya, S. A. & Cheng, G. 2003. The Art of War: Innate and Adaptive Immune Responses. *Cell Mol Life Sci,* 60, 2604-21.

Devita, V. T. & Chu, E. 2008. A History of Cancer Chemotherapy. *Cancer Res.,* 68, 8643-8653.

Di Agostino, S., Cortese, G., Monti, O., Dell'Orso, S., Sacchi, A., Eisenstein, M., Citro, G., Strano, S. & Blandino, G. 2008. The Disruption of the Protein Complex Mutant p53/p73 Increases Selectively the Response of Tumor Cells to Anticancer Drugs. *Cell Cycle,* 7, 3440-3447.

Dill, K. A., Ozkan, S. B., Weikl, T. R., Chodera, J. D. & Voelz, V. A. 2007. The Protein Folding Problem: When Will it Be Solved? *Curr Opin Struct Biol,* 17, 342-346.

Dinner, A. R., Šali, A., Smith, L. J., Dobson, C. M. & Karplus, M. 2000. Understanding Protein Folding via Free-Energy Surfaces from Theory and Experiment. *Trends Biochem Sci,* 25, 331-339.

Diogenes, M. J., Dias, R. B., Rombo, D. M., Vicente Miranda, H., Maiolino, F., Guerreiro, P., Nasstrom, T., Franquelim, H. G., Oliveira, L. M., Castanho, M. A., Lannfelt, L., Bergstrom, J., Ingelsson, M., Quintas, A., Sebastiao, A. M., Lopes, L. V. & Outeiro, T. F. 2012. Extracellular Alpha-Synuclein Oligomers Modulate Synaptic Transmission and Impair LTP via NMDA-Receptor Activation. *J. Neurosci.,* 32**,** 11750-62.

Dobson, C. M. 2001. The Structural Basis of Protein Folding and its Links with Human Disease. *Philos Trans R Soc Lond B Biol Sci.,* 356**,** 133-145.

Dobson, C. M. 2003. Protein Folding and Misfolding. *Nature,* 426**,** 884-90.

Dobson, C. M. 2004. Experimental Investigation of Protein Folding and Misfolding. *Methods,* 34**,** 4-14.

Doyle, S. L., Lysaght, J. & Reynolds, J. V. 2010. Obesity and Post-Operative Complications in Patients Undergoing Non-Bariatric Surgery. *Obes Rev,* 11**,** 875-86.

Dranoff, G. 2005. the Therapeutic Implications of Intratumoral Regulatory T Cells. *Clin. Cancer Res.,* 11**,** 8226-9.

Dubnovitsky, A., Sandberg, A., Rahman, M. M., Benilova, I., Lendel, C. & Härd, T. 2013. Amyloid-β Protofibrils: Size, Morphology and Synaptotoxicity of an Engineered Mimic. *PloS One,* 8**,** E66101.

Dumont, M. E. & Richards, F. M. 1988. the pH-Dependent Conformational Change of Diphtheria Toxin. *J Biol Chem,* 263**,** 2087-97.

Dunker, A. K., Brown, C. J., Lawson, J. D., Iakoucheva, L. M. & Obradović, Z. 2002. Intrinsic Disorder and Protein Function†. *Biochemistry,* 41**,** 6573-6582.

Dunker, A. K., Lawson, J. D., Brown, C. J., Williams, R. M., Romero, P., Oh, J. S., Oldfield, C. J., Campen, A. M., Ratliff, C. M., Hipps, K. W., Ausio, J., Nissen, M. S., Reeves, R., Kang, C., Kissinger, C. R., Bailey, R. W., Griswold, M. D., Chiu, W., Garner, E. C. & Obradovic, Z. 2001. Intrinsically Disordered Protein. *J Mol Graph Model,* 19**,** 26-59.

Dunker, A. K., Oldfield, C. J., Meng, J., Romero, P., Yang, J. Y., Chen, J. W., Vacic, V., Obradovic, Z. & Uversky, V. N. 2008a. The Unfoldomics Decade: An Update on Intrinsically Disordered Proteins. *BMC Genomics,* 9 Suppl 2, S1.

Dunker, A. K., Silman, I., Uversky, V. N. & Sussman, J. L. 2008b. Function and Structure of Inherently Disordered Proteins. *Curr Opin Struct Biol,* 18, 756-764.

Dunn Jr, W. A. 1994. Autophagy and Related Mechanisms of Lysosome-Mediated Protein Degradation. *Trends Cell Biol.,* 4, 139-143.

Dunne, A., Marshall, N. A. & Mills, K. H. 2011. TLR Based Therapeutics. *Curr. Opin. Pharmacol.,* 11, 404-11.

Duriez, P. J. & Shah, G. M. 1997. Cleavage of Poly(ADP-Ribose) Polymerase: A Sensitive Parameter to Study Cell Death. *Biochem. Cell Biol.,* 75, 337-49.

Düringer, C., Hamiche, A., Gustafsson, L., Kimura, H. & Svanborg, C. 2003. HAMLET Interacts with Histones and Chromatin in Tumor Cell Nuclei. *J Biol Chem,* 278, 42131-42135.

Dymkowska, D., Szczepanowska, J. & Wojtczak, L. 2004. Fatty-Acid–Induced Apoptosis in Ehrlich Ascites Tumor Cells. *Toxicol Mech Methods,* 14, 73-77.

Dyson, H. J. & Wright, P. E. 2004. Unfolded Proteins and Protein Folding Studied by NMR. *Chem. Rev.,* 104, 3607-22.

Dyson, H. J. & Wright, P. E. 2005. Intrinsically Unstructured Proteins and their Functions. *Nat Rev Mol Cell Biol,* 6, 197-208.

Eilers, M. & Schatz, G. 1986. Binding of A Specific Ligand Inhibits Import of A Purified Precursor Protein Into Mitochondria. *Nature,* 322, 228-32.

Eisenberg, D. & Jucker, M. 2012. The Amyloid State of Proteins in Human Diseases. *Cell,* 148, 1188-203.

Elder, G. A., Gama Sosa, M. A. & De Gasperi, R. 2010. Transgenic Mouse Models of Alzheimer's Disease. *Mt. Sinai J. Med.,* 77, 69-81.

Ellis, R. J. & Hartl, F. U. 1999. Principles of Protein Folding in the Cellular Environment. *Curr Opin Struct Biol,* 9, 102-110.

Elmore, S. 2007. Apoptosis: A Review of Programmed Cell Death. *Toxicol. Pathol.,* 35, 495-516.

Eskelinen, E. L. 2005. Maturation of Autophagic Vacuoles in Mammalian Cells. *Autophagy,* 1, 1-10.

Falk, R. H., Comenzo, R. L. & Skinner, M. 1997. The Systemic Amyloidoses. *N Engl J Med,* 337, 898-909.

Fändrich, M., Forge, V., Buder, K., Kittler, M., Dobson, C. M. & Diekmann, S. 2003. Myoglobin Forms Amyloid Fibrils by Association of Unfolded Polypeptide Segments. *Proc Natl Acad Sci U S A,* 100, 15463-15468.

Fast, J., Mossberg, A. K., Svanborg, C. & Linse, S. 2005. Stability of HAMLET--A Kinetically Trapped Alpha-Lactalbumin Oleic Acid Complex. *Protein Sci.,* 14, 329-40.

Feng, Y. Q., Wand, A. J. & Sligar, S. G. 1991. 1H and 15N NMRr Resonance Assignments and Preliminary Structural Characterization of *Escherichia coli* Apocytochrome b562. *Biochemistry,* 30, 7711-7.

Fezoui, Y. & Teplow, D. B. 2002. Kinetic Studies of Amyloid β-Protein Fibril Assembly: Differential Effects of α-Helix Stabilization. *J Biol Chem,* 40, 36948-54

Fink, A. L. 1999. Chaperone-Mediated Protein Folding. *Physiol Rev,* 79, 425-49.

Fink, S. L. & Cookson, B. T. 2005. Apoptosis, Pyroptosis, and Necrosis: Mechanistic Description of Dead and Dying Eukaryotic Cells. *Infect Immun,* 73, 1907-16.

Finke, J. M. & Jennings, P. A. 2001. Early Aggregated States in the Folding of Interleukin-1beta. *J Biol Phys,* 27, 119-31.

Finn, L., Markovic, S. N. & Joseph, R. W. 2012. Therapy for Metastatic Melanoma: The Past, Present, and Future. *BMC Med.,* 10, 23.

Fischer, W., Gustafsson, L., Mossberg, A.-K., Gronli, J., Mork, S., Bjerkvig, R. & Svanborg, C. 2004. Human α-Lactalbumin Made Lethal to Tumor Cells (HAMLET) Kills Human Glioblastoma Cells in Brain Xenografts by an Apoptosis-Like Mechanism and Prolongs Survival. *Cancer Res.,* 64, 2105-2112.

Fontana, A., Spolaore, B. & Polverino De Laureto, P. 2013. The Biological Activities of Protein/Oleic Acid Complexes Reside in the Fatty Acid. *Biochim Biophys Acta,* 1834, 1125-43.

Garman, E. F. 2014. Developments in X-Ray Crystallographic Structure Determination of Biological Macromolecules. *Science,* 343, 1102-1108.

Garry, D. J., Meeson, A., Yan, Z. & Williams, R. S. 2000. Life Without Myoglobin. *Cell. Mol. Life Sci.,* 57, 896-898.

Gast, K., Zirwer, D., Muller-Frohne, M. & Damaschun, G. 1998. Compactness of the Kinetic Molten Globule of Bovine Alpha-Lactalbumin: A Dynamic Light Scattering Study. *Protein Sci,* 7, 2004-11.

Gerl, R. & Vaux, D. L. 2005. Apoptosis in the Development and Treatment of Cancer. *Carcinogenesis,* 26, 263-70.

German, J. B., Dillard, C. J. & Ward, R. E. 2002. Bioactive Components in Milk. *Curr Opin Clin Nutr Metab Care,* 5, 653-8.

Gerothanassis, I. P., Troganis, A., Exarchou, V. & Barbarossou, K. 2002. Nuclear Magnetic Resonance (Nmr) Spectroscopy: Basic Principles and Phenomena, and their Applications to Chemistry, Biology and Medicine. *Chem Educ Res Pract,* 3, 229-252.

Gharibyan, A. L., Zamotin, V., Yanamandra, K., Moskaleva, O. S., Margulis, B. A., Kostanyan, I. A. & Morozova-Roche, L. A. 2007. Lysozyme Amyloid Oligomers and Fibrils Induce Cellular Death via Different Apoptotic/Necrotic Pathways. *J Mol Biol,* 365, 1337-1349.

Giannakopoulos, P., Herrmann, F. R., Bussiere, T., Bouras, C., Kovari, E., Perl, D. P., Morrison, J. H., Gold, G. & Hof, P. R. 2003. Tangle and Neuron Numbers, but not Amyloid Load, Predict Cognitive Status in Alzheimer's Disease. *Neurology,* 60, 1495-500.

Gilchrest, B. A., Eller, M. S., Geller, A. C. & Yaar, M. 1999. The Pathogenesis of Melanoma Induced by Ultraviolet Radiation. *N Engl J Med,* 340, 1341-8.

Glabe, C. G. 2006. Common Mechanisms of Amyloid Oligomer Pathogenesis in Degenerative Disease. *Neurobiol Aging,* 27, 570-5.

Glenner, G. G. & Wong, C. W. 1984. Alzheimer's Disease: Initial Report of the Purification and Characterization of a Novel Cerebrovascular Amyloid Protein. *Biochem Biophys Res Commun,* 120, 885-90.

Glud, M. & Gniadecki, R. 2013. Micrornas in the Pathogenesis of Malignant Melanoma. *J. Eur. Acad. Dermatol. Venereol.,* 27, 142-150.

Gnerlich, J. L., Mitchem, J. B., Weir, J. S., Sankpal, N. V., Kashiwagi, H., Belt, B. A., Porembka, M. R., Herndon, J. M., Eberlein, T. J., Goedegebuure, P. & Linehan, D. C. 2010. Induction of Th17 Cells in the Tumor Microenvironment Improves Survival in a Murine Model of Pancreatic Cancer. *J. Immunol.,* 185, 4063-71.

Golovanov, A. P., Hautbergue, G. M., Wilson, S. A. & Lian, L. Y. 2004. A Simple Method for Improving Protein Solubility and Long-Term Stability. *J Am Chem Soc,* 126, 8933-9.

Gonzalez-Michaca, L., Farrugia, G., Croatt, A. J., Alam, J. & Nath, K. A. 2004. Heme: A Determinant of Life and Death in Renal Tubular Epithelial Cells. *Am J Physiol Renal Physiol,* 286, F370-7.

Gottesman, M. M. 2002. Mechanisms of Cancer Drug Resistance. *Annu Rev Med,* 53, 615-27.

Granucci, F., Ferrero, E., Foti, M., Aggujaro, D., Vettoretto, K. & Ricciardi-Castagnoli, P. 1999. Early Events in Dendritic Cell Maturation Induced by LPS. *Microbes Infect,* 1, 1079-84.

Greene, L. A. & Tischler, A. S. 1976. Establishment of A Noradrenergic Clonal Line of Rat Adrenal Pheochromocytoma Cells which Respond to Nerve Growth Factor. *Proc Natl Acad Sci U S A,* 73, 2424-2428.

Groppo, R. & Richter, J. D. 2009. Translational Control from Head to Tail. *Curr Opin Cell Biol,* 21, 444-451.

Groux, H., Bigler, M., De Vries, J. E. & Roncarolo, M. G. 1996. Interleukin-10 Induces a Long-Term Antigen-Specific Anergic State in Human $CD4^+$ T Cells. *J Exp Med,* 184, 19-29.

Gunasekaran, K. & Nussinov, R. 2007. How Different Are Structurally Flexible and Rigid Binding Sites? Sequence and Structural Features Discriminating Proteins that do and do not Undergo Conformational Change Upon Ligand Binding. *J Mol Biol,* 365, 257-73.

Gunning, P. W., Landreth, G. E., Layer, P., Ignatius, M. & Shooter, E. M. 1981. Nerve Growth Factor-Induced Differentiation of PC12 Cells: Evaluation of Changes in RNA and DNA Metabolism. *J. Neurosci.,* 1, 368-79.

Gustafsson, L., Aits, S., Onnerfjord, P., Trulsson, M., Storm, P. & Svanborg, C. 2009. Changes in Proteasome Structure and Function Caused by HAMLET in Tumor Cells. *PloS One,* 4, E5229.

Gustafsson, L., Hallgren, O., Mossberg, A.-K., Pettersson, J., Fischer, W., Aronsson, A. & Svanborg, C. 2005. HAMLET Kills Tumor Cells by Apoptosis: Structure, Cellular Mechanisms, and Therapy. *J Nutr,* 135, 1299-1303.

Gustafsson, L., Leijonhufvud, I., Aronsson, A., Mossberg, A. K. & Svanborg, C. 2004. Treatment of Skin Papillomas with Topical Alpha-Lactalbumin-Oleic Acid. *N Engl J Med,* 350, 2663-72.

Gustavsson, Å., Engström, U. & Westermark, P. 1991. Normal Transthyretin and Synthetic Transthyretin Fragments from Amyloid-Like Fibrils *in vitro*. *Biochem Biophys Res Commun,* 175, 1159-1164.

Haass, C. & Selkoe, D. J. 2007. Soluble Protein Oligomers in Neurodegeneration: Lessons from the Alzheimer's Amyloid Beta-Peptide. *Nat Rev Mol Cell Biol,* 8, 101-12.

Hakansson, A. P., Roche-Hakansson, H., Mossberg, A.-K. & Svanborg, C. 2011. Apoptosis-Like Death in Bacteria Induced by HAMLET, A Human Milk Lipid-Protein Complex. *PloS One,* 6**,** E17717.

Håkansson, A., Zhivotovsky, B., Orrenius, S., Sabharwal, H. & Svanborg, C. 1995. Apoptosis Induced by a Human Milk Protein. *Proc Natl Acad Sci U S A,* 92**,** 8064-8068.

Hallgren, O., Aits, S., Brest, P., Gustafsson, L., Mossberg, A.-K., Wullt, B. & Svanborg, C. 2008. Apoptosis and Tumor Cell Death in Response to HAMLET (Human A-Lactalbumin Made Lethal to Tumor Cells). *Adv Exp Med Biol*, 606,217-40

Hallgren, O., Gustafsson, L., Irjala, H., Selivanova, G., Orrenius, S. & Svanborg, C. 2006b. HAMLET Triggers Apoptosis but Tumor Cell Death is Independent of Caspases, Bcl-2 and p53. *Apoptosis,* 11**,** 221-33.

Hanahan, D. & Weinberg, R. A. 2000. The Hallmarks of Cancer. *Cell*, 100, 57-70.

Hanahan, D. & Weinberg, R. A. 2011. Hallmarks of Cancer: The Next Generation. *Cell,* 144**,** 646-74.

Harding, M. M., Williams, D. H. & Woolfson, D. N. 1991. Characterization of A Partially Denatured State of A Protein by Two-Dimensional NMR: Reduction of the Hydrophobic Interactions in Ubiquitin. *Biochemistry,* 30**,** 3120-3128.

Hardy, J. A. & Higgins, G. A. 1992. Alzheimer's Disease: The Amyloid Cascade Hypothesis. *Science,* 256**,** 184-5.

Hartl, F. U. 1996. Molecular Chaperones in Cellular Protein Folding. *Nature,* 381**,** 571-580.

Hartwell, L. H. & Weinert, T. A. 1989. Checkpoints: Controls that Ensure the Order of Cell Cycle Events. *Science,* 246**,** 629-34.

Haupt, S., Berger, M., Goldberg, Z. & Haupt, Y. 2003. Apoptosis - the p53 Network. *J Cell Sci,* 116**,** 4077-4085.

Hawe, A., Sutter, M. & Jiskoot, W. 2008. Extrinsic Fluorescent Dyes as Tools for Protein Characterization. *Pharm. Res.,* 25**,** 1487-1499.

Hebert, D. N. & Molinari, M. 2007. In and Out of the ER: Protein Folding, Quality Control, Degradation, and Related Human Diseases. *Physiol Rev,* 87**,** 1377-1408.

Herold, M. & Kirschner, K. 1990. Reversible Dissociation and Unfolding of Aspartate Aminotransferase from *Escherichia coli*: Characterization of a Monomeric Intermediate. *Biochemistry,* 29**,** 1907-13.

Hetz, C. 2012. The Unfolded Protein Response: Controlling Cell Fate Decisions Under ER Stress and Beyond. *Nat Rev Mol Cell Biol,* 13**,** 89-102.

Hilt, W. & Wolf, D. H. 1995. Proteasomes of the Yeast *S. cerevisiae*: Genes, Structure and Functions. *Mol Biol Rep,* 21**,** 3-10.

Hochstrasser, M. 2009. Origin and Function of Ubiquitin-Like Proteins. *Nature,* 458**,** 422-429.

Hoffner, G. & Djian, P. 2014. Monomeric, Oligomeric and Polymeric Proteins in Huntington Disease and Other Diseases of Polyglutamine Expansion. *Brain Sci,* 4**,** 91-122.

Hoque, M., Dave, S., Gupta, P. & Saleemuddin, M. 2013. Oleic Acid may be the Key Contributor in the BAMLET-Induced Erythrocyte Hemolysis and Tumoricidal Action. *PloS One,* 8**,** E68390.

Hori, K., Ehrke, M. J., Mace, K. & Mihich, E. 1987b. Effect of Recombinant Tumor Necrosis Factor on Tumoricidal Activation of Murine Macrophages: Synergism Between Tumor Necrosis Factor and Gamma-Interferon. *Cancer Res.,* 47**,** 5868-74.

Hori, K., Ehrke, M. J., Mace, K., Maccubbin, D., Doyle, M. J., Otsuka, Y. & Mihich, E. 1987a. Effect of Recombinant Human Tumor Necrosis Factor on the Induction of Murine Macrophage Tumoricidal Activity. *Cancer Res.,* 47**,** 2793-8.

Huang, L., Su, X. & Federoff, H. J. 2013. Single-Chain Fragment Variable Passive Immunotherapies for Neurodegenerative Diseases. *Int J Mol Sci,* 14**,** 19109-27.

Huber, H. J., Dussmann, H., Kilbride, S. M., Rehm, M. & Prehn, J. H. 2011. Glucose Metabolism Determines Resistance of Cancer Cells to Bioenergetic Crisis after Cytochrome-*c* Release. *Mol Syst Biol,* 7, 470.

Huberts, D. H. & van der Klei, I. J. 2010. Moonlighting Proteins: an Intriguing Mode of Multitasking. *Biochim Biophys Acta,* 1803, 520-525.

Hughson, F. M. & Baldwin, R. L. 1989. Use of Site-Directed Mutagenesis to Destabilize Native Apomyoglobin Relative to Folding Intermediates. *Biochemistry,* 28, 4415-22.

Ishii, T. & Haga, S. 1984. Immuno-Electron-Microscopic Localization of Complements in Amyloid Fibrils of Senile Plaques. *Acta Neuropathol,* 63, 296-300.

Ishimi, Y., Kojima, M., Yamada, M. & Hanaoka, F. 1987. Binding Mode of Nucleosome-Assembly Protein (AP-I) and Histones. *Eur J Biochem,* 162, 19-24.

Itoh, K., Inoue, T., Ito, K. & Hirohata, S. 1994. The Interplay of Interleukin-10 (IL-10) and Interleukin-2 (IL-2) in Humoral Immune Responses: IL-10 Synergizes with IL-2 to Enhance Responses of Human B Lymphocytes in a Mechanism which is Different from Upregulation of CD25 Expression. *Cell. Immunol.,* 157, 478-488.

Iuchi, S., Hoffner, G., Verbeke, P., Djian, P. & Green, H. 2003. Oligomeric and Polymeric Aggregates Formed by Proteins Containing Expanded Polyglutamine. *Proc Natl Acad Sci U S A,* 100, 2409-14.

Iversen, L. L., Mortishire-Smith, R. J., Pollack, S. J. & Shearman, M. S. 1995. The Toxicity *in vitro* of Beta-Amyloid Protein. *Biochem J,* 311 (Pt 1), 1-16.

Iwata, M. & Zager, R. A. 1996. Myoglobin Inhibits Proliferation of Cultured Human Proximal Tubular (Hk-2) Cells. *Kidney Int,* 50, 796-804.

Janciauskiene, S. & Ahren, B. 1998. Different Sensitivity to the Cytotoxic Action of IAPP Fibrils in Two Insulin-Producing Cell Lines, HIT-T15 and RINm5F Cells. *Biochem Biophys Res Commun,* 251, 888-93.

Jeng, M. F., Englander, S. W., Elove, G. A., Wand, A. J. & Roder, H. 1990. Structural Description of Acid-Denatured Cytochrome *c* by Hydrogen Exchange and 2D NMR. *Biochemistry,* 29**,** 10433-7.

Jennings, P. & Wright, P. 1993. Formation of a Molten Globule Intermediate Early in the Kinetic Folding Pathway of Apomyoglobin. *Science,* 262**,** 892-896.

Joerger, A. C. & Fersht, A. R. 2010. The Tumor Suppressor p53: From Structures to Drug Discovery. *Cold Spring Harb Perspect Bio*, 2, a000919.

Jin, S. & Levine, A. J. 2001. The p53 Functional Circuit. *J Cell Sci,* 114**,** 4139-4140.

Jin, W. & Dong, C. 2013. IL-17 Cytokines in Immunity and Inflammation. *Emerg Microbes Infect,* 2**,** E60.

Kahler, A., Sticht, H. & Horn, A. H. C. 2013. Conformational Stability of Fibrillar Amyloid-Beta Oligomers via Protofilament Pair Formation – A Systematic Computational Study. *PloS One,* 8**,** E70521.

Kamijima, T., Ohmura, A., Sato, T., Akimoto, K., Itabashi, M., Mizuguchi, M., Kamiya, M., Kikukawa, T., Aizawa, T., Takahashi, M., Kawano, K. & Demura, M. 2008. Heat-Treatment Method for Producing Fatty Acid-Bound Alpha-Lactalbumin that Induces Tumor Cell Death. *Biochem Biophys Res Commun,* 376**,** 211-4.

Kant, S., Kumar, A. & Singh, S. M. 2012. Fatty Acid Synthase Inhibitor Orlistat Induces Apoptosis in T Cell Lymphoma: Role of Cell Survival Regulatory Molecules. Biochim Biophys Acta, 1820**,** 1764-1773.

Karran, E., Mercken, M. & Strooper, B. D. 2011. The Amyloid Cascade Hypothesis for Alzheimer's Disease: An Appraisal for the Development of Therapeutics. *Nat Rev Drug Discov,* 10**,** 698-712.

Kastan, M. B. & Bartek, J. 2004. Cell-Cycle Checkpoints and Cancer. *Nature,* 432**,** 316-323.

Katzman, R., Terry, R., Deteresa, R., Brown, T., Davies, P., Fuld, P., Renbing, X. & Peck, A. 1988. Clinical, Pathological, and Neurochemical Changes in Dementia: A Subgroup with Preserved Mental Status and Numerous Neocortical Plaques. *Ann Neurol,* 23, 138-44.

Kaya-Dagistanli, F., Tanriverdi, G., Altinok, A., Ozyazgan, S. & Ozturk, M. 2013. The Effects of Alpha Lipoic Acid on Liver Cells Damages and Apoptosis Induced by Polyunsaturated Fatty Acids. *Food Chem Toxicol,* 53, 84-93.

Kayed, R., Head, E., Thompson, J. L., Mcintire, T. M., Milton, S. C., Cotman, C. W. & Glabe, C. G. 2003. Common Structure of Soluble Amyloid Oligomers Implies Common Mechanism of Pathogenesis. *Science,* 300, 486-489.

Kelly, J. M., Darcy, P. K., Markby, J. L., Godfrey, D. I., Takeda, K., Yagita, H. & Smyth, M. J. 2002. Induction of Tumor-Specific T Cell Memory by NK Cell-Mediated Tumor Rejection. *Nat. Immunol.,* 3, 83-90.

Kendrew, J. C., Bodo, G., Dintzis, H. M., Parrish, R. G., Wyckoff, H. & Phillips, D. C. 1958. A Three-Dimensional Model of the Myoglobin Molecule Obtained by X-Ray Analysis. *Nature,* 181, 662-666.

Kendrew, J. C., Bodo, G., Dintzis, H. M., Parrish, R. G., Wyckoff, H. & Phillips, D. C. 1958. A Three-Dimensional Model of the Myoglobin Molecule Obtained by X-Ray Analysis. *Nature,* 181, 662-666.

Kerscher, O., Felberbaum, R. & Hochstrasser, M. 2006. Modification of Proteins by Ubiquitin and Ubiquitin-Like Proteins. *Annu. Rev. Cell Dev. Biol.,* 22, 159-180.

Khurana, R., Coleman, C., Ionescu-Zanetti, C., Carter, S. A., Krishna, V., Grover, R. K., Roy, R. & Singh, S. 2005. Mechanism of Thioflavin T Binding to Amyloid Fibrils. *J Struct Biol,* 151, 229-38.

Kim, H.-J., Chae, S.-C., Lee, D.-K., Chromy, B., Lee, S. C., Park, Y.-C., Klein, W. L., Krafft, G. A. & Hong, S.-T. 2003. Selective Neuronal Degeneration Induced by Soluble Oligomeric Amyloid Beta Protein. *The FASEB Journal,* 17, 118-120.

Kim, J., Kundu, M., Viollet, B. & Guan, K.-L. 2011. AMPK and mTOR Regulate Autophagy Through Direct Phosphorylation of Ulk1. *Nat Cell Biol,* 13**,** 132-141.

Kim, J., Modlin, R. L., Moy, R. L., Dubinett, S. M., Mchugh, T., Nickoloff, B. J. & Uyemura, K. 1995. Il-10 Production in Cutaneous Basal and Squamous Cell Carcinomas. A Mechanism for Evading the Local T Cell Immune Response. *J Immunol.,* 155**,** 2240-7.

Kimura, Y. 2002. Carp Oil Or Oleic Acid, but Not Linoleic Acid Or Linolenic Acid, Inhibits Tumor Growth and Metastasis in Lewis Lung Carcinoma–Bearing Mice. *J Nutr,* 132**,** 2069-2075.

Kirkitadze, M. D., Bitan, G. & Teplow, D. B. 2002. Paradigm Shifts in Alzheimer's Disease and Other Neurodegenerative Disorders: the Emerging Role of Oligomeric Assemblies. *J Neurosci Res,* 69**,** 567-577.

Kisselev, A. F. & Goldberg, A. L. 2001. Proteasome Inhibitors: From Research Tools to Drug Candidates. *Chem Biol,* 8**,** 739-58.

Klein, W. L., Krafft, G. A. & Finch, C. E. 2001. Targeting Small A[beta] Oligomers: the Solution to an Alzheimer's Disease Conundrum? *Trends Neurosci.,* 24**,** 219-24.

Klunk, W. E., Jacob, R. F. & Mason, R. P. 1999. Quantifying Amyloid β-Peptide (Aβ) Aggregation Using the Congo Red-Aβ (CR–Aβ) Spectrophotometric Assay. *Analytical Biochemistry,* 266**,** 66-76.

Klunk, W. E., Pettegrew, J. W. & Abraham, D. J. 1989. Two Simple Methods for Quantifying Low-Affinity Dye-Substrate Binding. *J Histochem Cytochem,* 37**,** 1293-7.

Klyubin, I., Mably, A., Minogue, A., Hu, N.-W., Farrell, M., Walsh, D. & Rowan, M. 2012. Alzheimer's Disease Human Brain Beta-Amyloid-Containing Extracts Inhibit Hippocampal Long-Term Potentiation in Rats *in vivo*: Relationship Between Soluble and Insoluble Preparations. *Alzheimers Dement,* 8**,** P648.

Klyubin, I., Ondrejcak, T., Hayes, J., Cullen, W. K., Mably, A. J., Walsh, D. M. & Rowan, M. J. 2014. Neurotransmitter Receptor and Time Dependence of the Synaptic Plasticity

Disrupting Actions of Alzheimer's Disease Aβ *in vivo*. *Philos Trans R Soc Lond B Biol Sci,* 369.

Klyubin, I., Wang, Q., Reed, M. N., Irving, E. A., Upton, N., Hofmeister, J., Cleary, J. P., Anwyl, R. & Rowan, M. J. 2011. Protection Against Abeta-Mediated Rapid Disruption of Synaptic Plasticity and Memory by Memantine. *Neurobiol. Aging,* 32**,** 614-23.

Kohler, C., Gogvadze, V., Hakansson, A., Svanborg, C., Orrenius, S. & Zhivotovsky, B. 2001. A Folding Variant of Human Alpha-Lactalbumin Induces Mitochondrial Permeability Transition in Isolated Mitochondria. *Eur J Biochem,* 268**,** 186-91.

Köhler, C., Håkansson, A., Svanborg, C., Orrenius, S. & Zhivotovsky, B. 1999. Protease Activation in Apoptosis Induced by MAL. *Exp Cell Res,* 249**,** 260-268.

Kohno, K., Palha, J., Miyakawa, K., Saraiva, M., Ito, S., Mabuchi, T., Blaner, W., Iijima, H., Tsukahara, S., Episkopou, V., Gottesman, M., Shimada, K., Takahashi, K., Yamamura, K. & Maeda, S. 1997. Analysis of Amyloid Deposition in a Transgenic Mouse Model of Homozygous Familial Amyloidotic Polyneuropathy. *Am. J. Pathol.,* 150**,** 1497-1508.

Kopito, R. R. & Ron, D. 2000. Conformational Disease. *Nat Cell Biol,* 2**,** E207-E209.

Kowall, N. W., Beal, M. F., Busciglio, J., Duffy, L. K. & Yankner, B. A. 1991. An *in vivo* Model for the Neurodegenerative Effects of Beta Amyloid and Protection by Substance P. *Proc Natl Acad Sci U S A,* 88**,** 7247-7251.

Krebs, M. R. H., Wilkins, D. K., Chung, E. W., Pitkeathly, M. C., Chamberlain, A. K., Zurdo, J., Robinson, C. V. & Dobson, C. M. 2000. Formation and Seeding of Amyloid Fibrils from Wild-Type Hen Lysozyme and a Peptide Fragment from the [beta]-Domain. *J. Mol. Biol.,* 300**,** 541-549.

Kryczek, I., Banerjee, M., Cheng, P., Vatan, L., Szeliga, W., Wei, S., Huang, E., Finlayson, E., Simeone, D., Welling, T. H., Chang, A., Coukos, G., Liu, R. & Zou, W. 2009. Phenotype, Distribution, Generation, and Functional and Clinical Relevance of Th17 Cells in the Human Tumor Environments. *Blood,* 114**,** 1141-9.

Krysko, D. V., Vanden Berghe, T., D'herde, K. & Vandenabeele, P. 2008. Apoptosis and Necrosis: Detection, Discrimination and Phagocytosis. *Methods,* 44, 205-221.

Krzewska, J. & Melki, R. 2007. The Yeast Prion Proteins Sup35p and Ure2p. *Protein Misfolding, Aggregation, and Conformational Diseases.* 6, 165-182

Kuwajima, K. 1989. The Molten Globule State as A Clue for Understanding the Folding and Cooperativity of Globular-Protein Structure. *Proteins,* 6, 87-103.

Kuwajima, K. 1996. The Molten Globule State of Alpha-Lactalbumin. *FASEB J,* 10, 102-9.

Lalani, I., Bhol, K. & Ahmed, A. R. 1997. Interleukin-10: Biology, Role in Inflammation and Autoimmunity. *Ann Allergy Asthma Immunol,* 79, 469-484.

Lambert, M. P., Barlow, A. K., Chromy, B. A., Edwards, C., Freed, R., Liosatos, M., Morgan, T. E., Rozovsky, I., Trommer, B., Viola, K. L., Wals, P., Zhang, C., Finch, C. E., Krafft, G. A. & Klein, W. L. 1998. Diffusible, Nonfibrillar Ligands Derived from Abeta1-42 are Potent Central Nervous System Neurotoxins. *Proc Natl Acad Sci U S A,* 95, 6448-53.

Lancet 1983. Eskimo Diets and Diseases. *Lancet,* 321, 1139-1141.

Lane, D. 2006. Designer Combination Therapy for Cancer. *Nat Biotech,* 24, 163-164.

Lansbury, P. T. & Lashuel, H. A. 2006. A Century-Old Debate on Protein Aggregation and Neurodegeneration Enters the Clinic. *Nature,* 443, 774-779.

Lansbury, P. T. 1999. Evolution of Amyloid: What Normal Protein Folding May Tell Us About Fibrillogenesis and Disease. *Proc Natl Acad Sci U S A,* 96, 3342-3344.

Lecker, S. H., Goldberg, A. L. & Mitch, W. E. 2006. Protein Degradation by the Ubiquitin-Proteasome Pathway in Normal and Disease States. *J Am Soc Nephrol,* 17, 1807-19.

Lee, C. & Yu, M. H. 2005. Protein Folding and Diseases. *J Biochem Mol Biol,* 38, 275-80.

Lee, J., Culyba, E. K., Powers, E. T. & Kelly, J. W. 2011a. Amyloid-β Forms Fibrils by Nucleated Conformational Conversion of Oligomers. *Nat. Chem. Biol.,* 7, 602-609.

Lee, S., Glendenning, P. & Inderjeeth, C. A. 2011b. Efficacy, Side Effects and Route of Administration are More Important than Frequency of Dosing of Anti-Osteoporosis Treatments in Determining Patient Adherence: A Critical Review of Published Articles from 1970 to 2009. *Osteoporos Int,* 22**,** 741-53.

Lee, Y. J., Savtchenko, R., Ostapchenko, V. G., Makarava, N. & Baskakov, I. V. 2011c. Molecular Structure of Amyloid Fibrils Controls the Relationship Between Fibrillar Size and Toxicity. *PloS One,* 6**,** E20244.

Lenz, T. L. 2012. Lessening Chemotherapy Side Effects with Lifestyle Medicine. *Am J Lifestyle Med,* 6**,** 219-221.

Levine, H., 3rd 1999. Quantification of Beta-Sheet Amyloid Fibril Structures with Thioflavin T. *Methods Enzymol.,* 309**,** 274-84.

Levy, Y. & Brouet, J. C. 1994. Interleukin-10 Prevents Spontaneous Death of Germinal Center B Cells by Induction of the Bcl-2 Protein. *J Clin Invest,* 93**,** 424-8.

Li, Z. & Srivastava, P. 2004. Heat-Shock Proteins. *Curr Protoc Immunol,* 58:1T:A.1T.1–A.1T.6.

Li, Z., Menoret, A. & Srivastava, P. 2002. Roles of Heat-Shock Proteins in Antigen Presentation and Cross-Presentation. *Curr Opin Immunol,* 14**,** 45-51.

Lima, T. M., Kanunfre, C. C., Pompéia, C., Verlengia, R. & Curi, R. 2002. Ranking the Toxicity of Fatty Acids on Jurkat and Raji Cells by Flow Cytometric Analysis. *Toxicol In Vitro,* 16**,** 741-747.

Lin, J. H., Walter, P. & Yen, T. S. B. 2008. Endoplasmic Reticulum Stress in Disease Pathogenesis. *Annu Rev Pathol,* 3**,** 399-425.

Lin, L., Pinker, R. J., Forde, K., Rose, G. D. & Kallenbach, N. R. 1994. Molten Globular Characteristics of the Native State of Apomyoglobin. *Nat. Struct. Mol. Biol.,* 1**,** 447-452.

Linkermann, A. & Green, D. R. 2014. Necroptosis. *N Eng J Med,* 370**,** 455-465.

Lišková, K., Auty, M. A. E., Chaurin, V., Min, S., Mok, K. H., O'Brien, N., Kelly, A. L. & Brodkorb, A. 2011. Cytotoxic Complexes of Sodium Oleate with β-Lactoglobulin. *Eur J Lipid Sci Technol,* 113, 1207-1218.

Liston, A. & Rudensky, A. Y. 2007. Thymic Development and Peripheral Homeostasis of Regulatory T Cells. *Curr Opin Immunol,* 19, 176-185.

Lobo, N. A., Shimono, Y., Qian, D. & Clarke, M. F. 2007. The Biology of Cancer Stem Cells. *Annu Rev Cell Dev Biol,* 23, 675-99.

Lomas, D. A. & Carrell, R. W. 2002. Serpinopathies and the Conformational Dementias. *Nat Rev Genet,* 3, 759-768.

Lorenzo, A. & Yankner, B. A. 1994. Beta-Amyloid Neurotoxicity Requires Fibril Formation and is Inhibited by Congo Red. *Proc Natl Acad Sci U S A,* 91, 12243-12247.

Lorenzo, A. & Yankner, B. A. 1996. Amyloid Fibril Toxicity in Alzheimer's Disease and Diabetesa. *Ann N Y Acad Sci,* 777, 89-95.

Lu, X., Wintrode, P. L. & Surewicz, W. K. 2007. β-Sheet Core of Human Prion Protein Amyloid Fibrils as Determined by Hydrogen/Deuterium Exchange. *Proc Natl Acad Sci U S A,* 104, 1510-1515.

Lukas, G., Brindle, S. D. & Greengard, P. 1971. The Route of Absorption of Intraperitoneally Administered Compounds. *J Pharmacol Exp Ther,* 178, 562-4.

Luqmani, Y. A. 2005. Mechanisms of Drug Resistance in Cancer Chemotherapy. *Med Princ Pract,* 14 Suppl 1, 35-48.

Lynch, M. A. 2004. Long-Term Potentiation and Memory. *Physiol Rev,* 84, 87-136.

Macrae, F. A. 1993. Fat and Calories in Colon and Breast Cancer: From Animal Studies to Controlled Clinical Trials. *PrevMed,* 22, 750-766.

Madureira, A. R., Pereira, C. I., Gomes, A. M. P., Pintado, M. E. & Xavier Malcata, F. 2007. Bovine Whey Proteins – Overview on their Main Biological Properties. *Food Res Int,* 40, 1197-1211.

Maggi, E., Cosmi, L., Liotta, F., Romagnani, P., Romagnani, S. & Annunziato, F. 2005. Thymic Regulatory T Cells. *Autoimmun Rev,* 4, 579-586.

Maji, S. K., Wang, L., Greenwald, J. & Riek, R. 2009. Structure–Activity Relationship of Amyloid Fibrils. *FEBS Lett,* 583, 2610-2617.

Majumdar, A., Capetillo-Zarate, E., Cruz, D., Gouras, G. K. & Maxfield, F. R. 2011. Degradation of Alzheimer's Amyloid Fibrils by Microglia Requires Delivery of ClC-7 to Lysosomes. *Mol Biol Cell,* 22, 1664-76.

Makin, O. S. & Serpell, L. C. 2005. Structures for Amyloid Fibrils. *FEBS J,* 272, 5950-5961.

Malchiodi-Albedi, F., Paradisi, S., Matteucci, A., Frank, C. & Diociaiuti, M. 2011. Amyloid Oligomer Neurotoxicity, Calcium Dysregulation, and Lipid Rafts. *Int J Alzheimers Dis,* 2011.

Malenka, R. C. & Nicoll, R. A. 1999. Long-Term Potentiation--A Decade of Progress? *Science,* 285, 1870-4.

Malisauskas, M., Ostman, J., Darinskas, A., Zamotin, V., Liutkevicius, E., Lundgren, E. & Morozova-Roche, L. A. 2005. Does the Cytotoxic Effect of Transient Amyloid Oligomers from Common Equine Lysozyme *in vitro* Imply Innate Amyloid Toxicity? *J. Biol. Chem.,* 280, 6269-6275.

Maloy, A. L., Longnecker, D. S. & Greenberg, E. R. 1981. The Relation of Islet Amyloid to the Clinical Type of Diabetes. *Hum Pathol,* 12, 917-22.

Mareel, M. & Leroy, A. 2003. Clinical, Cellular, and Molecular Aspects of Cancer Invasion. *Physiol Rev,* 83, 337-376.

Marks, L. R., Clementi, E. A. & Hakansson, A. P. 2012. The Human Milk Protein-Lipid Complex HAMLET Sensitizes Bacterial Pathogens to Traditional Antimicrobial Agents. *PloS One,* 7, E43514.

Markwick, P. R., Malliavin, T. & Nilges, M. 2008. Structural Biology by NMR: Structure, Dynamics, and Interactions. *PloS Comput. Biol.,* 4, E1000168.

Martin, J., Langer, T., Boteva, R., Schramel, A., Horwich, A. L. & Hartl, F. U. 1991. Chaperonin-Mediated Protein Folding At the Surface of Groel Through A 'Molten Globule'-Like Intermediate. *Nature,* 352, 36-42.

Martiniuk, F., Damian, D. L., Thompson, J. F., Scolyer, R. A., Tchou-Wong, K. M. & Levis, W. R. 2010. Th17 is Involved in the Remarkable Regression of Metastatic Malignant Melanoma to Topical Diphencyprone. *J Drugs Dermatol,* 9, 1368-72.

Martin-Orozco, N., Muranski, P., Chung, Y., Yang, X. O., Yamazaki, T., Lu, S., Hwu, P., Restifo, N. P., Overwijk, W. W. & Dong, C. 2009. T Helper 17 Cells Promote Cytotoxic T Cell Activation in Tumor Immunity. *Immunity,* 31, 787-98.

Martins De Lima, T., Cury-Boaventura, M. F., Giannocco, G., Nunes, M. T. & Curi, R. 2006. Comparative Toxicity of Fatty Acids on A Macrophage Cell Line (J774). *Clin Sci (Lond),* 111, 307-17.

Marzban, L., Park, K. & Verchere, C. B. 2003. Islet Amyloid Polypeptide and Type 2 Diabetes. *Exp Gerontol,* 38, 347-51.

Massague, J. 2004. G1 Cell-Cycle Control and Cancer. *Nature,* 432, 298-306.

Mattson, M. P., Cheng, B., Davis, D., Bryant, K., Lieberburg, I. & Rydel, R. E. 1992. Beta-Amyloid Peptides Destabilize Calcium Homeostasis and Render Human Cortical Neurons Vulnerable to Excitotoxicity. *J Neurosci,* 12, 376-89.

Mayer, M. P. & Bukau, B. 2005. Hsp70 Chaperones: Cellular Functions and Molecular Mechanism. *Cell. Mol. Life Sci.,* 62, 670-84.

Mazziotti, M. & Perlmutter, D. H. 1998. Resistance to the Apoptotic Effect of Aggregated Amyloid-Beta Peptide in Several Different Cell Types Including Neuronal- and Hepatoma-Derived Cell Lines. *Biochem. J.,* 332, 517-524.

Mcconkey, D. J., Zhivotovsky, B. & Orrenius, S. 1996. Apoptosis — Molecular Mechanisms and Biomedical Implications. *Molecular Aspects of Medicine,* 17, 1-110.

Mcintosh, G. H., Regester, G. O., Le Leu, R. K., Royle, P. J. & Smithers, G. W. 1995. Dairy Proteins Protect Against Dimethylhydrazine-Induced Intestinal Cancers in Rats. *J. Nutr.*, 125, 809-16.

Mclean, C. A., Cherny, R. A., Fraser, F. W., Fuller, S. J., Smith, M. J., Beyreuther, K., Bush, A. I. & Masters, C. L. 1999. Soluble Pool of Abeta Amyloid As A Determinant of Severity of Neurodegeneration in Alzheimer's Disease. *Ann Neurol,* 46, 860-6.

Menendez, J. A., Vazquez-Martin, A., Ropero, S., Colomer, R. & Lupu, R. 2006. HER2 (erbB-2)-Targeted Effects of the Omega-3 Polyunsaturated Fatty Acid, Alpha-Linolenic Acid (ALA; 18:3n-3), in Breast Cancer Cells: the "Fat Features" of the "Mediterranean Diet" As an "Anti-HER2 Cocktail". *Clin Transl Oncol,* 8, 812-20.

Menendez, J. A., Vellon, L., Colomer, R. & Lupu, R. 2005. Oleic Acid, the Main Monounsaturated Fatty Acid of Olive Oil, Suppresses HER-2/neu (erbB-2) Expression and Synergistically Enhances the Growth Inhibitory Effects of Trastuzumab (Herceptin) in Breast Cancer Cells with HER-2/neu Oncogene Amplification. *Ann Oncol,* 16, 359-71.

Merad, M., Sathe, P., Helft, J., Miller, J. & Mortha, A. 2013. The Dendritic Cell Lineage: Ontogeny and Function of Dendritic Cells and their Subsets in the Steady State and the Inflamed Setting. *Annu. Rev. Immunol.,* 31, 563-604.

Mercer, N., Ramakrishnan, B., Boeggeman, E. & Qasba, P. K. 2011. Applications of Site-Specific Labeling to Study HAMLET, A Tumoricidal Complex of α-Lactalbumin and Oleic Acid. *PloS One,* 6, E26093.

Merz, P. A., Wisniewski, H. M., Somerville, R. A., Bobin, S. A., Masters, C. L. & Iqbal, K. 1983. Ultrastructural Morphology of Amyloid Fibrils from Neuritic and Amyloid Plaques. *Acta Neuropathol,* 60, 113-24.

Miller, A. J. & Mihm, M. C. 2006. Melanoma. *N Engl J Med,* 355, 51-65.

Miller, D. R. 2006. A Tribute to Sidney Farber – The Father of Modern Chemotherapy. *Br J Haematol,* 134, 20-26.

Min, S., Meehan, J., Sullivan, L. M., Harte, N. P., Xie, Y., Davey, G. P., Svanborg, C., Brodkorb, A. & Mok, K. H. 2012. Alternatively Folded Proteins with Unexpected Beneficial Functions. *Biochem Soc Trans,* 40, 746-51.

Mishra, R., Sorgjerd, K., Nystrom, S., Nordigarden, A., Yu, Y. C. & Hammarstrom, P. 2007. Lysozyme Amyloidogenesis is Accelerated by Specific Nicking and Fragmentation but Decelerated by Intact Protein Binding and Conversion. *J Mol Biol,* 366, 1029-44.

Mizuguchi, M., Arai, M., Ke, Y., Nitta, K. & Kuwajima, K. 1998. Equilibrium and Kinetics of the Folding of Equine Lysozyme Studied by Circular Dichroism Spectroscopy. *J Mol Biol,* 283, 265-77.

Mocellin, S., Marincola, F. M. & Young, H. A. 2005. Interleukin-10 and the Immune Response Against Cancer: A Counterpoint. *J Leukoc Biol,* 78, 1043-1051.

Mok, K. H., Pettersson, J., Orrenius, S. & Svanborg, C. 2007. HAMLET, Protein Folding, and Tumor Cell Death. *Biochem Biophys Res Commun,* 354, 1-7.

Morel, A. S., Quaratino, S., Douek, D. C. & Londei, M. 1997. Split Activity of Interleukin-10 on Antigen Capture and Antigen Presentation by Human Dendritic Cells: Definition of A Maturative Step. *Eur. J. Immunol.,* 27, 26-34.

Morris, K. F. & Johnson, C. S. 1992. Diffusion-Ordered Two-Dimensional Nuclear Magnetic Resonance Spectroscopy. *J. Am. Chem. Soc.,* 114, 3139-3141.

Morris, R. G., Garrud, P., Rawlins, J. N. & O'Keefe, J. 1982. Place Navigation Impaired in Rats with Hippocampal Lesions. *Nature,* 297, 681-3.

Mossberg, A. K., Wullt, B., Gustafsson, L., Mansson, W., Ljunggren, E. & Svanborg, C. 2007. Bladder Cancers Respond to Intravesical Instillation of HAMLET (Human Alpha-Lactalbumin Made Lethal to Tumor Cells). *Int. J. Cancer,* 121, 1352-9.

Mossberg, A.-K., Hou, Y., Svensson, M., Holmqvist, B. & Svanborg, C. 2010a. HAMLET Treatment Delays Bladder Cancer Development. *J Urol,* 183, 1590-1597.

Mossberg, A., Mok, K.H., Morozova-Roche, L. A. & Svanborg, C. 2010b. Structure and Function of Human A-Lactalbumin Made Lethal to Tumor Cells (HAMLET)-Type Complexes. *FEBS J,* 277, 4614-4625.

Mossberg, A.-K., Puchades, M., Halskau, Ø., Baumann, A., Lanekoff, I., Chao, Y., Martinez, A., Svanborg, C. & Karlsson, R. 2010c. HAMLET Interacts with Lipid Membranes and Perturbs their Structure and Integrity. *Plos One,* 5, E9384.

Mossuto, M. F., Dhulesia, A., Devlin, G., Frare, E., Kumita, J. R., De Laureto, P. P., Dumoulin, M., Fontana, A., Dobson, C. M. & Salvatella, X. 2010. The Non-Core Regions of Human Lysozyme Amyloid Fibrils Influence Cytotoxicity. *J Mol Biol,* 402, 783-96.

Mukherjee, S. 2010. The Emperor of All Maladies : A Biography of Cancer, New York, Scribner.

Mullard, A. 2011. Dual Fronts Poised to Transform Melanoma Therapy. *Nat Rev Drug Discov,* 10, 325-6.

Muranski, P., Boni, A., Antony, P. A., Cassard, L., Irvine, K. R., Kaiser, A., Paulos, C. M., Palmer, D. C., Touloukian, C. E., Ptak, K., Gattinoni, L., Wrzesinski, C., Hinrichs, C. S., Kerstann, K. W., Feigenbaum, L., Chan, C. C. & Restifo, N. P. 2008. Tumor-Specific Th17-Polarized Cells Eradicate Large Established Melanoma. *Blood,* 112, 362-73.

Murayama, K. & Tomida, M. 2004. Heat-Induced Secondary Structure and Conformation Change of Bovine Serum Albumin Investigated by Fourier Transform Infrared Spectroscopy. *Biochemistry,* 43, 11526-11532.

Murphy, R. M. 2007. Kinetics of Amyloid Formation and Membrane Interaction with Amyloidogenic Proteins. *Biochim. Biophys. Acta,* 1768, 1923-34.

Nakamura, T., Aizawa, T., Kariya, R., Okada, S., Demura, M., Kawano, K., Makabe, K. & Kuwajima, K. 2013. Molecular Mechanisms of the Cytotoxicity of Human Alpha-Lactalbumin Made Lethal to Tumor Cells (HAMLET) and Other Protein-Oleic Acid Complexes. *J Biol Chem,* 288, 14408-16.

Nath, D. & Shadan, S. 2009. the Ubiquitin System. *Nature,* 458, 421-421..

Nelson, A., Pollard, H. B. & Rojas, E. 1993. Giant Multilevel Cation Channels Formed by Alzheimer Disease Amyloid B-Protein [AβP-(1-40)] in Bilayer Membranes. *Proc Natl Acad Sci U S A,* 90**,** 10573-10577.

Nielsen, S. B., Wilhelm, K., Vad, B., Schleucher, J., Morozova-Roche, L. A. & Otzen, D. 2010. The Interaction of Equine Lysozyme:Oleic Acid Complexes with Lipid Membranes Suggests a Cargo Off-Loading Mechanism. *J Mol Biol,* 398**,** 351-361.

Nikolakopoulou, Z., Shaikh, M. H., Dehlawi, H., Michael-Titus, A. T. & Parkinson, E. K. 2013. The Induction of Apoptosis in Pre-Malignant Keratinocytes by Omega-3 Polyunsaturated Fatty Acids Docosahexaenoic Acid (DHA) and Eicosapentaenoic Acid (EPA) is Inhibited by Albumin. *Toxicol Lett,* 218**,** 150-158.

Nilius, B., Owsianik, G., Voets, T. & Peters, J. A. 2007. Transient Receptor Potential Cation Channels in Disease. *Physiol Rev.* 2007 Jan;87(1):165-217.

Nilsson, M. R. 2004. Techniques to Study Amyloid Fibril Formation *in vitro*. *Methods,* 34**,** 151-160.

Noren, S. R., Williams, T. M., Pabst, D. A., Mclellan, W. A. & Dearolf, J. L. 2001. The Development of Diving in Marine Endotherms: Preparing the Skeletal Muscles of Dolphins, Penguins, and Seals for Activity During Submergence. *J Comp Physiol B,* 171**,** 127-34.

Novitskaya, V., Bocharova, O. V., Bronstein, I. & Baskakov, I. V. 2006. Amyloid Fibrils of Mammalian Prion Protein Are Highly Toxic to Cultured Cells and Primary Neurons. *J Biol Chem,* 281**,** 13828-13836.

Oberdoerster, J. & Rabin, R. A. 1999. NGF-Differentiated and Undifferentiated PC12 Cells Vary in Induction of Apoptosis by Ethanol. *Life Sci.,* 64**,** Pl267-Pl272.

Ochsenbein, A. F. 2002. Principles of Tumor Immunosurveillance and Implications for Immunotherapy. *Cancer Gene Ther.,* 9**,** 1043-55.

Oddo, S., Caccamo, A., Tran, L., Lambert, M. P., Glabe, C. G., Klein, W. L. & Laferla, F. M. 2006. Temporal Profile of Amyloid-B (Aβ) Oligomerization in an *in vivo* Model of Alzheimer Disease. *J Biol Chem,* 281**,** 1599-1604.

Ohgushi, M. & Wada, A. 1983. 'Molten-Globule State': A Compact Form of Globular Proteins with Mobile Side-Chains. *FEBS Lett,* 164**,** 21-4.

Olesen, O. F., Dago, L. & Mikkelsen, J. D. 1998. Amyloid Beta Neurotoxicity in the Cholinergic but not in the Serotonergic Phenotype of RN46A Cells. *Brain Res Mol Brain Res,* 57**,** 266-74.

Ondrias, K., Lencesova, L., Sirova, M., Labudova, M., Pastorekova, S., Kopacek, J. & Krizanova, O. 2011. Apoptosis Induced Clustering of IP(3)R1 in Nuclei of Non-Differentiated PC12 Cells. *J Cell Physiol,* 226**,** 3147-55.

O'neill, L. A. J., Golenbock, D. & Bowie, A. G. 2013. the History of Toll-Like Receptors [Mdash] Redefining Innate Immunity. *Nat Rev Immunol,* 13**,** 453-460.

Onufriev, A., Case, D. A. & Bashford, D. 2003. Structural Details, Pathways, and Energetics of Unfolding Apomyoglobin. *J Mol Biol,* 325**,** 555-67.

Ordway, G. A. & Garry, D. J. 2004. Myoglobin: An Essential Hemoprotein in Striated Muscle. *J Exp Biol,* 207**,** 3441-6.

Ow, Y.-L. P., Green, D. R., Hao, Z. & Mak, T. W. 2008. Cytochrome *c*: Functions Beyond Respiration. *Nat Rev Mol Cell Biol,* 9**,** 532-542.

Palleros, D. R., Reid, K. L., Mccarty, J. S., Walker, G. C. & Fink, A. L. 1992. Dnak, hsp73, and their Molten Globules. Two Different Ways Heat Shock Proteins Respond to Heat. *J Biol Chem,* 267**,** 5279-85.

Pavet, V., Portal, M. M., Moulin, J. C., Herbrecht, R. & Gronemeyer, H. 2011. Towards Novel Paradigms for Cancer Therapy. *Oncogene,* 30**,** 1-20.

Pelengaris, S. & Khan, M. 2003. The Many Faces of c-Myc. *Arch Biochem Biophys,* 416**,** 129-36.

Pellegrini, A., Thomas, U., Bramaz, N., Hunziker, P. & Von Fellenberg, R. 1999. Isolation and Identification of Three Bactericidal Domains in the Bovine Alpha-Lactalbumin Molecule. *Biochim Biophys Acta,* 1426**,** 439-48.

Peng, G., Guo, Z., Kiniwa, Y., Voo, K. S., Peng, W., Fu, T., Wang, D. Y., Li, Y., Wang, H. Y. & Wang, R.-F. 2005. Toll-Like Receptor 8-Mediated Reversal of $CD4^+$ Regulatory T Cell Function. *Science,* 309, 1380-1384.

Pepys, M. B. 2006. Amyloidosis. *Annu. Rev. Med.,* 57, 223-41.

Pepys, M. B., Hawkins, P. N., Booth, D. R., Vigushin, D. M., Tennent, G. A., Soutar, A. K., Totty, N., Nguyen, O., Blake, C. C. F., Terry, C. J., Feest, T. G., Zalin, A. M. & Hsuan, J. J. 1993. Human Lysozyme Gene Mutations Cause Hereditary Systemic Amyloidosis. *Nature,* 362, 553-557.

Perez, M. D., Diaz De Villegas, C., Sanchez, L., Aranda, P., Ena, J. M. & Calvo, M. 1989. Interaction of Fatty Acids with Beta-Lactoglobulin and Albumin from Ruminant Milk. *J Biochem,* 106, 1094-7.

Permyakov, E. A. & Berliner, L. J. 2000. Alpha-Lactalbumin: Structure and Function. *FEBS Lett,* 473, 269-74.

Permyakov, S. E., Knyazeva, E. L., Khasanova, L. M., Fadeev, R. S., Zhadan, A. P., Roche-Hakansson, H., Håkansson, A. P., Akatov, V. S. & Permyakov, E. A. 2012. Oleic Acid is A Key Cytotoxic Component of HAMLET-Like Complexes. *Biol Chem,* 393, 85-92.

Pettersson, J., Mossberg, A.-K. & Svanborg, C. 2006. α-Lactalbumin Species Variation, HAMLET Formation, and Tumor Cell Death. *Biochem Biophys Res Commun,* 345, 260-270.

Pettersson-Kastberg, J., Aits, S., Gustafsson, L., Mossberg, A., Storm, P., Trulsson, M., Persson, F., Mok, K. H. & Svanborg, C. 2009a. Can Misfolded Proteins Be Beneficial? The HAMLET Case. *Ann Med,* 41, 162-76.

Pettersson-Kastberg, J., Mossberg, A. K., Trulsson, M., Yong, Y. J., Min, S., Lim, Y., O'brien, J. E., Svanborg, C. & Mok, K. H. 2009b. Alpha-Lactalbumin, Engineered to Be Nonnative and Inactive, Kills Tumor Cells When in Complex with Oleic Acid: A New Biological Function Resulting from Partial Unfolding. *J Mol Biol,* 394, 994-1010.

Philo, J. S., Rosenfeld, R., Arakawa, T., Wen, J. & Narhi, L. O. 1993. Refolding of Brain-Derived Neurotrophic Factor from Guanidine Hydrochloride: Kinetic Trapping in a Collapsed Form which is Incompetent for Dimerization. *Biochemistry,* 32, 10812-8.

Pickart, C. M. 2001. Mechanisms Underlying Ubiquitination. *Annu Rev Biochem,* 70, 503-33.

Pike, C. J., Walencewicz, A. J., Glabe, C. G. & Cotman, C. W. 1991. *In vitro* Aging of Beta-Amyloid Protein Causes Peptide Aggregation and Neurotoxicity. *Brain Res,* 563, 311-4.

Poirier, M. A., Li, H., Macosko, J., Cai, S., Amzel, M. & Ross, C. A. 2002. Huntingtin Spheroids and Protofibrils as Precursors in Polyglutamine Fibrilization. *J Biol Chem.* 43:41032-7.

Polverino De Laureto, P., Frare, E., Gottardo, R. & Fontana, A. 2002. Molten Globule of Bovine α-Lactalbumin at Neutral pH Induced by Heat, Trifluoroethanol, and Oleic Acid: A Comparative Analysis by Circular Dichroism Spectroscopy and Limited Proteolysis. *Proteins,* 49, 385-397.

Proskuryakov, S. Y., Konoplyannikov, A. G. & Gabai, V. L. 2003. Necrosis: A Specific Form of Programmed Cell Death? *Exp Cell Res,* 283, 1-16.

Prusiner, S. B., Scott, M. R., Dearmond, S. J. & Cohen, F. E. 1998. Prion Protein Biology. *Cell,* 93, 337-348.

Ptitsyn, O. B. 1991. How Does Protein Synthesis Give Rise to the 3D-Structure? *FEBS Lett,* 285, 176-181.

Ptitsyn, O. B. 1995. Structures of Folding Intermediates. *Curr. Opin. Struct. Biol.,* 5, 74-78.

Ptitsyn, O. B., Pain, R. H., Semisotnov, G. V., Zerovnik, E. & Razgulyaev, O. I. 1990. Evidence for a Molten Globule State as a General Intermediate in Protein Folding. *FEBS Lett,* 262, 20-24.

Puchtler, H., Sweat, F. & Levine, M. 1962. On the Binding of Congo Red by Amyloid. *J Histochem Cytochem,* 10, 355-364.

Puthia, M., Storm, P., Nadeem, A., Hsiung, S. & Svanborg, C. 2013. Prevention and Treatment of Colon Cancer by Peroral Administration of HAMLET (Human A-Lactalbumin Made Lethal to Tumour Cells). *Gut*.0,1-12.

Quellhorst, E. 2002. Insulin Therapy During Peritoneal Dialysis: Pros and Cons of Various Forms of Administration. *J Am Soc Nephrol,* 13**,** S92-S96.

Querfurth, H. W. & Laferla, F. M. 2010. Alzheimer's Disease. *N Engl J Med,* 362**,** 329-44.

Rammer, P., Groth-Pedersen, L., Kirkegaard, T., Daugaard, M., Rytter, A., Szyniarowski, P., Høyer-Hansen, M., Povlsen, L. K., Nylandsted, J., Larsen, J. E. & Jäättelä, M. 2010. BAMLET Activates a Lysosomal Cell Death Program in Cancer Cells. *Mol. Cancer Ther.,* 9**,** 24-32.

Redfield, C. 1999. Molten Globules. *Curr Biol,* 9**,** R313.

Redfield, C., Smith, R. A. & Dobson, C. M. 1994. Structural Characterization of a Highly-Ordered 'Molten Globule' At Low pH. *Nat Struct Biol,* 1**,** 23-9.

Regan, L. 2003. Molten Globules Move Into Action. *Proc Natl Acad Sci U S A,* 100**,** 3553-3554.

Reilly, J. F., Games, D., Rydel, R. E., Freedman, S., Schenk, D., Young, W. G., Morrison, J. H. & Bloom, F. E. 2003. Amyloid Deposition in the Hippocampus and Entorhinal Cortex: Quantitative Analysis of a Transgenic Mouse Model. *Proc Natl Acad Sci U S A,* 100**,** 4837-42.

Reis E Sousa, C. 2004. Toll-Like Receptors and Dendritic Cells: For Whom the Bug Tolls. *Semin. Immunol.,* 16**,** 27-34.

Reixach, N., Deechongkit, S., Jiang, X., Kelly, J. W. & Buxbaum, J. N. 2004. Tissue Damage in the Amyloidoses: Transthyretin Monomers and Nonnative Oligomers are the Major Cytotoxic Species in Tissue Culture. *Proc. Natl. Acad. Sci. U. S. A.,* 101**,** 2817-2822.

Richardson, R. S., Noyszewski, E. A., Kendrick, K. F., Leigh, J. S. & Wagner, P. D. 1995. Myoglobin O_2 Desaturation During Exercise. Evidence of Limited O_2 Transport. *J Clin Invest,* 96, 1916-1926.

Rivoltini, L., Canese, P., Huber, V., Iero, M., Pilla, L., Valenti, R., Fais, S., Lozupone, F., Casati, C., Castelli, C. & Parmiani, G. 2005. Escape Strategies and Reasons for Failure in the Interaction Between Tumour Cells and the Immune System: How Can We Tilt the Balance Towards Immune-Mediated Cancer Control? *Expert Opin Biol Ther,* 5, 463-476.

Robson, B. & Pain, R. H. 1976. the Mechanism of Folding of Globular Proteins. Suitability of a Penicillinase from *Staphylococcus aureus* as a Model for Refolding Studies. *Biochem J,* 155, 325-30.

Romagnani, S. 1999. Th1/Th2 Cells. *Inflamm Bowel Dis,* 5, 285-94.

Roos-Mattjus, P. & Sistonen, L. 2004. the Ubiquitin-Proteasome Pathway. *Ann Med,* 36, 285-95.

Rottkamp, C. A., Atwood, C. S., Joseph, J. A., Nunomura, A., Perry, G. & Smith, M. A. 2002. The State Versus Amyloid-Beta: The Trial of the Most Wanted Criminal in Alzheimer Disease. *Peptides,* 23, 1333-41.

Rousset, F., Garcia, E., Defrance, T., Peronne, C., Vezzio, N., Hsu, D. H., Kastelein, R., Moore, K. W. & Banchereau, J. 1992. Interleukin 10 is a Potent Growth and Differentiation Factor for Activated Human B Lymphocytes. *Proc Natl Acad Sci U S A,* 89, 1890-3.

Rowan, M. J., Klyubin, I., Cullen, W. K. & Anwyl, R. 2003. Synaptic Plasticity in Animal Models of Early Alzheimer's Disease. *Philos Trans R Soc Lond B Biol Sci,* 358, 821-8.

Rowan, M. J., Klyubin, I., Wang, Q. & Anwyl, R. 2004. Mechanisms of the Inhibitory Effects of Amyloid Beta-Protein on Synaptic Plasticity. *Exp Gerontol,* 39, 1661-7.

Rowe, C. C., Ellis, K. A., Rimajova, M., Bourgeat, P., Pike, K. E., Jones, G., Fripp, J., Tochon-Danguy, H., Morandeau, L., O'Keefe, G., Price, R., Raniga, P., Robins, P., Acosta, O., Lenzo, N., Szoeke, C., Salvado, O., Head, R., Martins, R., Masters, C. L., Ames, D. &

Villemagne, V. L. 2010. Amyloid Imaging Results from the Australian Imaging, Biomarkers and Lifestyle (AIBL) Study of Aging. *Neurobiol Aging,* 31, 1275-83.

Rudan, I., Boschi-Pinto, C., Biloglav, Z., Mulholland, K. & Campbell, H. 2008. Epidemiology and Etiology of Childhood Pneumonia. *Bull World Health Organ,* 86, 408-16.

Saibil, H. R. 2008. Chaperone Machines in Action. *Curr Opin Struct Biol,* 18, 35-42.

Sakono, M. & Zako, T. 2010. Amyloid Oligomers: Formation and Toxicity of Aβ Oligomers. *FEBS J,* 277, 1348-1358.

Sakudo, A. & Ikuta, K. 2009. Prion Protein Functions and Dysfunction in Prion Diseases. *Curr Med Chem,* 16, 380-9.

Saraiva, M., Christensen, J. R., Veldhoen, M., Murphy, T. L., Murphy, K. M. & O'garra, A. 2009. Interleukin-10 Production by Th1 Cells Requires Interleukin-12-Induced STAT4 Transcription Factor and ERK MAP Kinase Activation by High Antigen Dose. *Immunity,* 31, 209-19.

Sawyers, C. 2004. Targeted Cancer Therapy. *Nature,* 432, 294-297.

Scheim, D. E. 2009. Cytotoxicity of Unsaturated Fatty Acids in Fresh Human Tumor Explants: Concentration Thresholds and Implications for Clinical Efficacy. *Lipids Health Dis,* 8, 54.

Schenk, F. & Morris, R. G. 1985. Dissociation Between Components of Spatial Memory in Rats after Recovery from the Effects of Retrohippocampal Lesions. *Exp Brain Res,* 58, 11-28.

Schon, M. & Schon, M. P. 2007. The Antitumoral Mode of Action of Imiquimod and Other Imidazoquinolines. *Curr Med Chem,* 14, 681-7.

Schorle, H., Holtschke, T., Hunig, T., Schimpl, A. & Horak, I. 1991. Development and Function of T Cells in Mice Rendered Interleukin-2 Deficient by Gene Targeting. *Nature,* 352, 621-624.

Schroder, K., Hertzog, P. J., Ravasi, T. & Hume, D. A. 2004. Interferon-Gamma: An Overview of Signals, Mechanisms and Functions. *J Leukoc Biol,* 75, 163-89.

Schroder, M. & Kaufman, R. J. 2005. The Mammalian Unfolded Protein Response. *Annu Rev Biochem,* 74, 739-89.

Schroder, M. 2008. Endoplasmic Reticulum Stress Responses. *Cell Mol Life Sci,* 65, 862-94.

Schuler, M. & Green, D. R. 2001. Mechanisms of p53-Dependent Apoptosis. *Biochem Soc Trans,* 29, 684-8.

Scott, A. M., Wolchok, J. D. & Old, L. J. 2012. Antibody Therapy of Cancer. *Nat Rev Cancer,* 12, 278-287.

Scoville, W. B. & Milner, B. 1957. Loss of Recent Memory After Bilateral Hippocampal Lesions. *J Neurol Neurosurg Psychiatry,* 20, 11-21.

Selkoe, D. J. 2003. Folding Proteins in Fatal Ways. *Nature,* 426, 900-904.

Selkoe, D. J. 2004. Cell Biology of Protein Misfolding: the Examples of Alzheimer's and Parkinson's Diseases. *Nat Cell Biol,* 6, 1054-1061.

Shadidi, M. & Sioud, M. 2003. Selective Targeting of Cancer Cells Using Synthetic Peptides. *Drug Resist Updat,* 6, 363-371.

Sheppard, K. E. & Mcarthur, G. A. 2013. The Cell-Cycle Regulator CDK4: an Emerging Therapeutic Target in Melanoma. *Clin Cancer Res,* 19, 5320-8.

Shimada, K., Maeda, S., Murakami, T., Nishiguchi, S., Tashiro, F., Yi, S., Wakasugi, S., Takahashi, K. & Yamamura, K. 1989. Transgenic Mouse Model of Familial Amyloidotic Polyneuropathy. *Mol Biol Med,* 6, 333-43.

Shirahama, T. & Cohen, A. S. 1967. High-Resolution Electron Microscopic Analysis of the Amyloid Fibril. *J Cell Biol,* 33, 679-708.

Siegel, R., Naishadham, D. & Jemal, A. 2013. Cancer Statistics, 2013. *CA Cancer J Clin,* 63, 11-30.

Siegel-Lakhai, W. S., Beijnen, J. H. & Schellens, J. H. 2005. Current Knowledge and Future Directions of the Selective Epidermal Growth Factor Receptor Inhibitors Erlotinib (Tarceva) and Gefitinib (Iressa). *Oncologist,* 10**,** 579-89.

Silva, M. T. 2010. Secondary Necrosis: The Natural Outcome of the Complete Apoptotic Program. *FEBS Lett.,* 584**,** 4491-4499.

Simard, J. R., Zunszain, P. A., Ha, C.-E., Yang, J. S., Bhagavan, N. V., Petitpas, I., Curry, S. & Hamilton, J. A. 2005. Locating High-Affinity FA-Binding Sites on Albumin by X-Ray Crystallography and NMR Spectroscopy. *Proc Natl Acad Sci U S A.,* 102**,** 17958-17963.

Simard, J. R., Zunszain, P. A., Hamilton, J. A. & Curry, S. 2006. Location of High and Low Affinity FA Binding Sites on Human Serum Albumin Revealed by NMR Drug-Competition Analysis. *J Mol Biol,* 361**,** 336-351.

Simons, T. B. 1988. Calcium and Neuronal Function. *Neurosurg Rev,* 11**,** 119-129.

Sitia, R. & Braakman, I. 2003. Quality Control in the Endoplasmic Reticulum Protein Factory. *Nature,* 426**,** 891-4.

Soto, C. 2003. Unfolding the Role of Protein Misfolding in Neurodegenerative Diseases. *Nat Rev Neurosci,* 4**,** 49-60.

Sousa, M. M., Cardoso, I., Fernandes, R., Guimaraes, A. & Saraiva, M. J. 2001. Deposition of Transthyretin in Early Stages of Familial Amyloidotic Polyneuropathy: Evidence for Toxicity of Nonfibrillar Aggregates. *Am J Pathol,* 159**,** 1993-2000.

Spolaore, B., Pinato, O., Canton, M., Zambonin, M., Polverino De Laureto, P. & Fontana, A. 2010a. Alpha-Lactalbumin Forms with Oleic Acid A High Molecular Weight Complex Displaying Cytotoxic Activity. *Biochemistry,* 49**,** 8658-67.

Stefani, M. 2004. Protein Misfolding and Aggregation: New Examples in Medicine and Biology of the Dark Side of the Protein World. *Biochim Biophys Acta,* 1739**,** 5-25.

Stefani, M. 2010. Biochemical and Biophysical Features of Both Oligomer/Fibril and Cell Membrane in Amyloid Cytotoxicity. *FEBS J,* 277**,** 4602-4613.

Stier, S., Maletzki, C., Klier, U. & Linnebacher, M. 2013. Combinations of TLR Ligands: A Promising Approach in Cancer Immunotherapy. *Clin Dev Immunol,* 2013**,** 14.

Storey, S. & Wald, G. 2008. Novel Agents in Cystic Fibrosis. *Nat Rev Drug Discov,* 7**,** 555-556.

Storm, P., Aits, S., Puthia, M. K., Urbano, A., Northen, T., Powers, S., Bowen, B., Chao, Y., Reindl, W., Lee, D. Y., Sullivan, N. L., Zhang, J., Trulsson, M., Yang, H., Watson, J. D. & Svanborg, C. 2011. Conserved Features of Cancer Cells Define their Sensitivity to HAMLET-Induced Death; c-Myc and Glycolysis. *Oncogene,* 30**,** 4765-4779.

Storm, P., Kjaer Klausen, T., Trulsson, M., Ho Cs, J., Dosnon, M., Westergren, T., Chao, Y., Rydström, A., Yang, H., Pedersen, S. F. & Svanborg, C. 2013. A Unifying Mechanism for Cancer Cell Death Through Ion Channel Activation by HAMLET. *PloS One,* 8**,** E58578.

Stratton, M. R., Campbell, P. J. & Futreal, P. A. 2009. The Cancer Genome. *Nature,* 458**,** 719-724.

Strayer, D. R., Carter, W. A. & Brodsky, I. 1986. Familial Occurrence of Breast Cancer is Associated with Reduced Natural Killer Cytotoxicity. *Breast Cancer Res Treat,* 7**,** 187-192.

Sung, Y. J., Cheng, C. L., Chen, C. S., Huang, H. B., Huang, F. L., Wu, P. C., Shiao, M. S. & Tsay, H. J. 2003. Distinct Mechanisms Account for Beta-Amyloid Toxicity in PC12 and Differentiated PC12 Neuronal Cells. *J Biomed Sci,* 10**,** 379-88.

Surh, C. D. & Sprent, J. 2008. Homeostasis of Naive and Memory T Cells. *Immunity,* 29**,** 848-862.

Svanborg, C., Agerstam, H., Aronson, A., Bjerkvig, R., Duringer, C., Fischer, W., Gustafsson, L., Hallgren, O., Leijonhuvud, I., Linse, S., Mossberg, A. K., Nilsson, H., Pettersson, J. & Svensson, M. 2003. HAMLET Kills Tumor Cells by an Apoptosis-Like Mechanism--Cellular, Molecular, and Therapeutic Aspects. *Adv Cancer Res,* 88**,** 1-29.

Svensson, M., Hakansson, A., Mossberg, A. K., Linse, S. & Svanborg, C. 2000. Conversion of Alpha-Lactalbumin to A Protein Inducing Apoptosis. *Proc Natl Acad Sci U S A,* 97**,** 4221-6.

Svensson, M., Fast, J., Mossberg, A.-K., Düringer, C., Gustafsson, L., Hallgren, O., Brooks, C. L., Berliner, L., Linse, S. & Svanborg, C. 2003a. α-Lactalbumin Unfolding is not Sufficient to Cause Apoptosis, but is Required for the Conversion to HAMLET (Human α-Lactalbumin Made Lethal to Tumor Cells). *Protein Sci,* 12, 2794-2804.

Svensson, M., Mossberg, A.-K., Pettersson, J., Linse, S. & Svanborg, C. 2003b. Lipids As Cofactors in Protein Folding: Stereo-Specific Lipid–Protein Interactions are Required to Form HAMLET (Human α-Lactalbumin Made Lethal to Tumor Cells). *Protein Sci,* 12, 2805-2814.

Svensson, M., Sabharwal, H., Hakansson, A., Mossberg, A. K., Lipniunas, P., Leffler, H., Svanborg, C. & Linse, S. 1999. Molecular Characterization of Alpha-Lactalbumin Folding Variants that Induce Apoptosis in Tumor Cells. *J Biol Chem,* 274, 6388-96.

Szilágyi, A., Kardos, J., Osváth, S., Barna, L. & Závodszky, P. 2007. Protein Folding. *In:* Lajtha, A. & Banik, N. (Eds.) *Handbook of Neurochemistry and Molecular Neurobiology.* Springer Us.

Taga, K. & Tosato, G. 1992. IL-10 Inhibits Human T Cell Proliferation and IL-2 Production. *J Immunol.,* 148, 1143-8.

Takeda, K. & Akira, S. 2005. Toll-Like Receptors in Innate Immunity. *Int Immunol,* 17, 1-14.

Taketani, S. 2005. Aquisition, Mobilization and Utilization of Cellular Iron and Heme: Endless Findings and Growing Evidence of Tight Regulation. *Tohoku J Exp Med,* 205, 297-318.

Talmadge, J. E., Phillips, H., Schneider, M., Rowe, T., Pennington, R., Bowersox, O. & Lenz, B. 1988. Immunomodulatory Properties of Recombinant Murine and Human Tumor Necrosis Factor. *Cancer Res.,* 48, 544-50.

Terrault, N. A. 2009. Benefits and Risks of Combination Therapy for Hepatitis B. *Hepatology,* 49, S122-8.

Thies, W. & Bleiler, L. 2013. 2013 Alzheimer's Disease Facts and Figures. *Alzheimers Dement,* 9, 208-45.

Tolin, S., De Franceschi, G., Spolaore, B., Frare, E., Canton, M., Polverino De Laureto, P. & Fontana, A. 2010. The Oleic Acid Complexes of Proteolytic Fragments of Alpha-Lactalbumin Display Apoptotic Activity. *FEBS J,* 277, 163-73.

Tompa, P. 2005. The Interplay Between Structure and Function in Intrinsically Unstructured Proteins. *FEBS Lett,* 579, 3346-54.

Trifari, S., Kaplan, C. D., Tran, E. H., Crellin, N. K. & Spits, H. 2009. Identification of a Human Helper T Cell Population that has Abundant Production of Interleukin 22 and is Distinct from Th-17, Th1 and Th2 Cells. *Nat Immunol.,* 10, 864-871.

True, H. L. & Lindquist, S. L. 2000. A Yeast Prion Provides A Mechanism for Genetic Variation and Phenotypic Diversity. *Nature,* 407, 477-83.

Trulsson, M., Yu, H., Gisselsson, L., Chao, Y., Urbano, A., Aits, S., Mossberg, A.-K. & Svanborg, C. 2011. HAMLET Binding to α-Actinin Facilitates Tumor Cell Detachment. *PloS One,* 6, E17179.

Tsan, M. F. & Gao, B. 2009. Heat Shock Proteins and Immune System. *J Leukoc Biol,* 85, 905-10.

Tsiftsoglou, A. S., Tsamadou, A. I. & Papadopoulou, L. C. 2006. Heme as Key Regulator of Major Mammalian Cellular Functions: Molecular, Cellular, and Pharmacological Aspects. *Pharmacol Ther,* 111, 327-45.

Tycko, R. 2003. Insights into the Amyloid Folding Problem from Solid-State NMR. *Biochemistry,* 42, 3151-9.

Uversky, V. N. & Dunker, A. K. 2010. Understanding Protein Non-Folding. *Biochim Biophys Acta.* 1804(6):1231-64.

Uversky, V. N. & Ptitsyn, O. B. 1994. "Partly Folded" State, a New Equilibrium State of Protein Molecules: Four-State Guanidinium Chloride-Induced Unfolding of Beta-Lactamase at Low Temperature. *Biochemistry,* 33**,** 2782-2791.

Van Cruchten, S. & Van Den Broeck, W. 2002. Morphological and Biochemical Aspects of Apoptosis, Oncosis and Necrosis. *Anat Histol Embryol,* 31**,** 214-23.

Van, L. P., Bardel, E., Gregoire, S., Vanoirbeek, J., Schneider, E., Dy, M. & Thieblemont, N. 2011. Treatment with the TLR7 Agonist R848 Induces Regulatory T-Cell-Mediated Suppression of Established Asthma Symptoms. *Eur J Immunol,* 41**,** 1992-9.

Vassilenko, K. S. & Uversky, V. N. 2002. Native-Like Secondary Structure of Molten Globules. *Biochim Biophys Acta,* 1594**,** 168-77.

Veiopoulou, C., Kogopoulou, O., Tzakos, E., Mavrothalassitis, G., Mitsias, D., Karafoulidou, A., Paliogianni, F., Moutsopoulos, H. M. & Thyphronitis, G. 2004. IL-2 and IL-10 Production by Human $CD4^{+}$T Cells is Differentially Regulated by p38: Mode of Stimulation-Dependent Regulation of Il-2. *Neuroimmunomodulation,* 11**,** 199-208.

Velho, T. R. 2012. Metastatic Melanoma - A Review of Current and Future Drugs. *Drugs Context,* 2012**,** 19;212242.

Vieira, M. N. N., Forny-Germano, L., Saraiva, L. M., Sebollela, A., Martinez, A. M. B., Houzel, J.-C., De Felice, F. G. & Ferreira, S. T. 2007. Soluble Oligomers from a Non-Disease Related Protein Mimic Aβ-Induced Tau Hyperphosphorylation and Neurodegeneration. *J Neurochem.,* 103**,** 736-748.

Volpicelli-Daley, L. A., Luk, K. C. & Lee, V. M. Y. 2014. Addition of Exogenous A-Synuclein Preformed Fibrils to Primary Neuronal Cultures to Seed Recruitment of Endogenous α-Synuclein to Lewy Body and Lewy Neurite–Like Aggregates. *Nat Protocols,* 9**,** 2135-2146.

Vorum, H., Brodersen, R., Kragh-Hansen, U. & Pedersen, A. O. 1992. Solubility of Long-Chain Fatty Acids in Phosphate Buffer At pH 7.4. *Biochim Biophys Acta,* 1126**,** 135-42.

Vukojević, V., Bowen, A. M., Wilhelm, K., Ming, Y., Ce, Z., Schleucher, J. R., Hore, P. J., Terenius, L. & Morozova-Roche, L. A. 2010. Lipoprotein Complex of Equine Lysozyme with Oleic Acid (ELOA) Interactions with the Plasma Membrane of Live Cells. *Langmuir,* 26, 14782-14787.

Walker, G. J., Flores, J. F., Glendening, J. M., Lin, A., Markl, I. D. C. & Fountain, J. W. 1998. Virtually 100% of Melanoma Cell Lines Harbor Alterations at the DNA Level Within CDKN2A, CDKN2B, Or One of their Downstream Targets. *Genes Chromosomes Cancer,* 22, 157-163.

Walsh, D. M. & Selkoe, D. J. 2007. Aβ Oligomers – A Decade of Discovery. *J Neurochem.,* 101, 1172-1184.

Walsh, D. M., Klyubin, I., Fadeeva, J. V., Cullen, W. K., Anwyl, R., Wolfe, M. S., Rowan, M. J. & Selkoe, D. J. 2002. Naturally Secreted Oligomers of Amyloid Beta Protein Potently Inhibit Hippocampal Long-Term Potentiation *in vivo*. *Nature,* 416, 535-9.

Walsh, D. M., Townsend, M., Podlisny, M. B., Shankar, G. M., Fadeeva, J. V., El Agnaf, O., Hartley, D. M. & Selkoe, D. J. 2005. Certain Inhibitors of Synthetic Amyloid Beta-Peptide (Abeta) Fibrillogenesis Block Oligomerization of Natural Abeta and Thereby Rescue Long-Term Potentiation. *J Neurosci,* 25, 2455-62.

Wang, D., Cui, Z., Zeng, Q., Kuang, H., Wang, L. P., Tsien, J. Z. & Cao, X. 2009. Genetic Enhancement of Memory and Long-Term Potentiation but not CA1 Long-Term Depression in NR2B Transgenic Rats. *PloS One,* 4, E7486.

Wang, H. W., Pasternak, J. F., Kuo, H., Ristic, H., Lambert, M. P., Chromy, B., Viola, K. L., Klein, W. L., Stine, W. B., Krafft, G. A. & Trommer, B. L. 2002. Soluble Oligomers of Beta Amyloid (1-42) Inhibit Long-Term Potentiation but not Long-Term Depression in Rat Dentate Gyrus. *Brain Res,* 924, 133-40.

Watanabe, N. & Yamada, S. 1996. Activation of 20s Proteasomes from Spinach Leaves by Fatty Acids. *Plant Cell Physiol,* 37, 147-51.

Watson, H. C., Walker, N. P., Shaw, P. J., Bryant, T. N., Wendell, P. L., Fothergill, L. A., Perkins, R. E., Conroy, S. C., Dobson, M. J., Tuite, M. F.. 1982. Sequence and Structure of Yeast Phosphoglycerate Kinase. *Embo J,* 1**,** 1635-40.

Wenzel, T. & Baumeister, W. 1995. Conformational Constraints in Protein Degradation by the 20S Proteasome. *Nat Struct Mol Biol,* 2**,** 199-204.

Wetzel, R. 2002. Ideas of Order for Amyloid Fibril Structure. *Structure,* 10**,** 1031-1036.

Whiteside, T. L. 2009. Tricks Tumors use to Escape from Immune Control. *Oral Oncol,* 45**,** E119-23.

Whiteside, T. L. 2010. Immune Responses to Malignancies. *J Allergy Clin Immunol,* 125**,** S272-S283.

Wilhelm, K., Darinskas, A., Noppe, W., Duchardt, E., Mok, K. H., Vukojevic, V., Schleucher, J. & Morozova-Roche, L. A. 2009. Protein Oligomerization Induced by Oleic Acid at the Solid-Liquid Interface--Equine Lysozyme Cytotoxic Complexes. *FEBS J,* 276**,** 3975-89.

Williams, A. D., Sega, M., Chen, M., Kheterpal, I., Geva, M., Berthelier, V., Kaleta, D. T., Cook, K. D. & Wetzel, R. 2005. Structural Properties of Aβ Protofibrils Stabilized by A Small Molecule. *Proc. Natl. Acad. Sci. U. S. A.,* 102**,** 7115-7120.

Wimo, A., Jönsson, L., Bond, J., Prince, M. & Winblad, B. 2013. The Worldwide Economic Impact of Dementia 2010. *Alzheimer's Dement,* 9**,** 1-11.E3.

Wittenberg, J. B. & Wittenberg, B. A. 2003. Myoglobin Function Reassessed. *J Exp Biol,* 206**,** 2011-20.

Wong, K. P. & Tanford, C. 1973. Denaturation of Bovine Carbonic Anhydrase B by Guanidine Hydrochloride. A Process Involving Separable Sequential Conformational Transitions. *J Biol Chem,* 248**,** 8518-23.

Xiao, Z., Mak, A., Koch, K. & Moore, R. B. 2013. A Molecular Complex of Bovine Milk Protein and Oleic Acid Selectively Kills Cancer Cells *in vitro* and Inhibits Tumour Growth in an Orthotopic Rat Bladder Tumour Model. *BJU Int.,* 112**,** E201-10.

Xie, Y., Min, S., Harte, N. P., Kirk, H., O'brien, J. E., Voorheis, H. P., Svanborg, C. & Hun Mok, K. 2013. Electrostatic Interactions Play an Essential Role in the Binding of Oleic Acid with Alpha-Lactalbumin in the HAMLET-Like Complex: A Study Using Charge-Specific Chemical Modifications. *Proteins,* 81**,** 1-17.

Xu, M., Shashilov, V. A., Ermolenkov, V. V., Fredriksen, L., Zagorevski, D. & Lednev, I. K. 2007. The First Step of Hen Egg White Lysozyme Fibrillation, Irreversible Partial Unfolding, is a Two-State Transition. *Protein Sci.,* 16**,** 815-32.

Xue, W. F., Hellewell, A. L., Gosal, W. S., Homans, S. W., Hewitt, E. W. & Radford, S. E. 2009. Fibril Fragmentation Enhances Amyloid Cytotoxicity. *J Biol Chem,* 284**,** 34272-82.

Xue, W. F., Hellewell, A. L., Hewitt, E. W. & Radford, S. E. 2010. Fibril Fragmentation in Amyloid Assembly and Cytotoxicity: When Size Matters. *Prion,* 4**,** 20-5.

Yang, J., Liu, X., Bhalla, K., Kim, C. N., Ibrado, A. M., Cai, J., Peng, T. I., Jones, D. P. & Wang, X. 1997. Prevention of Apoptosis by Bcl-2: Release of Cytochrome *c* from Mitochondria Blocked. *Science,* 275**,** 1129-32.

Yankner, B. A. & Shooter, E. M. 1979. Nerve Growth Factor in the Nucleus: Interaction with Receptors on the Nuclear Membrane. *Proc Natl Acad Sci U S A,* 76**,** 1269-73.

Yankner, B. A., Duffy, L. K. & Kirschner, D. A. 1990. Neurotrophic and Neurotoxic Effects of Amyloid Beta Protein: Reversal by Tachykinin Neuropeptides. *Science,* 250**,** 279-82.

Ye, Z. J., Zhou, Q., Yuan, M. L., Du, R. H., Yang, W. B., Xiong, X. Z., Huang, B. & Shi, H. Z. 2012. Differentiation and Recruitment of Il-22-Producing Helper T Cells Stimulated by Pleural Mesothelial Cells in Tuberculous Pleurisy. *Am. J Respir Crit Care Med,* 185**,** 660-9.

Yewdell, J. W. 2005. Serendipity Strikes Twice: The Discovery and Rediscovery of Defective Ribosomal Products (DRIPS). *Cell Mol Biol (Noisy-Le-Grand),* 51**,** 635-41.

Yoshiike, Y., Akagi, T. & Takashima, A. 2007. Surface Structure of Amyloid-β Fibrils Contributes to Cytotoxicity. *Biochemistry,* 46, 9805-9812.

Young, H. A. & Hardy, K. J. 1995. Role of Interferon-Gamma in Immune Cell Regulation. *J Leukoc.Biol,* 58, 373-81.

Zahm, J. M., Kaplan, H., Herard, A. L., Doriot, F., Pierrot, D., Somelette, P. & Puchelle, E. 1997. Cell Migration and Proliferation During the *in vitro* Wound Repair of the Respiratory Epithelium. *Cell Motil Cytoskeleton,* 37, 33-43.

Zahorowska, B., Crowe, P. J. & Yang, J. L. 2009. Combined Therapies for Cancer: A Review of EGFR-Targeted Monotherapy and Combination Treatment with Other Drugs. *J Cancer Res Clin Oncol,* 135, 1137-48.

Zhu, N., Eves, P. C., Katerinaki, E., Szabo, M., Morandini, R., Ghanem, G., Lorigan, P., Macneil, S. & Haycock, J. W. 2002. Melanoma Cell Attachment, Invasion, and Integrin Expression is Upregulated by Tumor Necrosis Factor [Alpha] and Suppressed by [Alpha] Melanocyte Stimulating Hormone. *J Invest Dermatol*, 119, 1165-1171.

Zhu, Y., Schwarz, S., Ahlemeyer, B., Grzeschik, S., Klumpp, S. & Krieglstein, J. 2005. Oleic Acid Causes Apoptosis and Dephosphorylates Bad. *Neurochem Int,* 46, 127-35.

Zhuravlev, P. I. & Papoian, G. A. 2010. Protein Functional Landscapes, Dynamics, Allostery: A Tortuous Path Towards A Universal Theoretical Framework. *Q Rev Biophys,* 43, 295-332.

Zou, W. & Restifo, N. P. 2010. Th17 Cells in Tumour Immunity and Immunotherapy. *Nat Rev Immunol,* 10, 248-256.

Zwanzig, R., Szabo, A. & Bagchi, B. 1992. Levinthal's Paradox. *Proc Natl Acad Sci U S A,* 89, 20-22.